

AUGUST · 1953

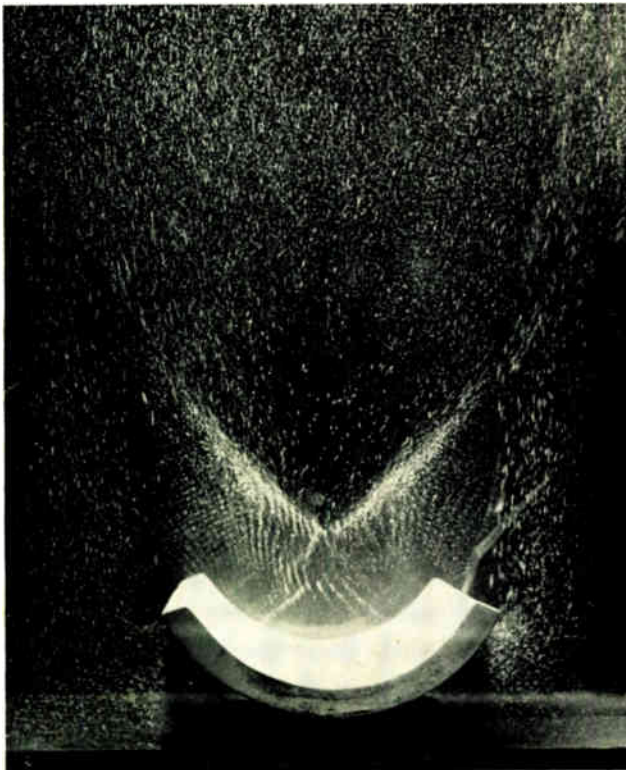
# Proceedings



of the I · R · E

## A Journal of Communications and Electronic Engineering

FOCUSING ULTRASONICS TRANSDUCER



*Brush Electronics Company*

This impressive wave pattern portrayed by thousands of bubbles is being produced by the tremendous energy radiated from a barium titanate ceramic transducer submerged in water.

Volume 41

Number 8

### IN THIS ISSUE

IRE Professional Group Plan  
Complexity of Military Electronics  
Reduction of VHF Transmission Loss  
Study of Synchronous Detection (Abstract)  
Unipolar "Field-Effect" Transistor  
Color Synchronization Performance  
Measurement of Transistor Parameters  
Analysis of Vacuum Tube and Transistor Circuits  
Magnetic Shift Register Operation  
Debunching of Electron Beams  
Graphical Analysis of Waveguide Junction  
The Gyrator as 3-Terminal Element  
Improving Read-Around Ratio in CR Storage Tubes  
Loop Antennas for Low-Frequency Reception  
Amplitude Stability in Oscillating Systems  
Equation for Atmospheric Refractive Index  
Reduction of Forced Error in Closed-Loop Systems  
Theory of AFC Synchronization  
Current and Voltage Distribution on Antennas  
Wide-Band Phase-Delay Circuit  
Feedback Coding Methods  
Abstracts and References

TABLE OF CONTENTS INDICATED BY BLACK-AND-WHITE MARGIN, FOLLOWS PAGE 64A

# The Institute of Radio Engineers



# NEW "M" TYPE TOROIDS Maximum Q Minimum Size

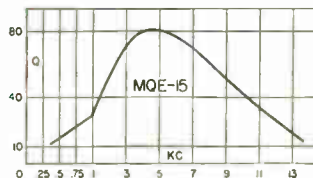
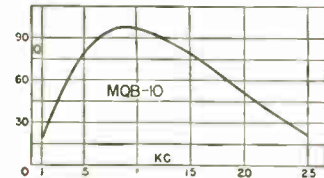
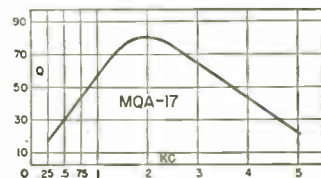
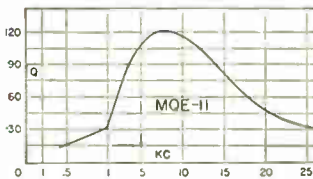
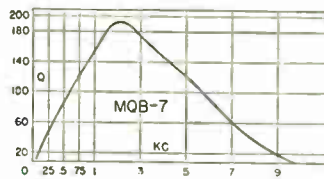
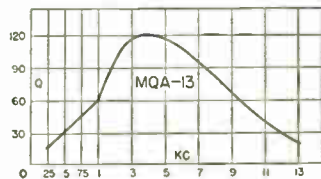
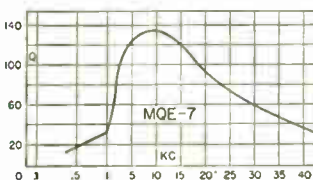
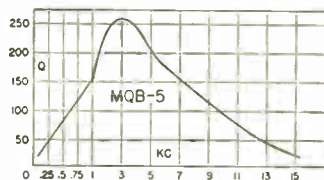
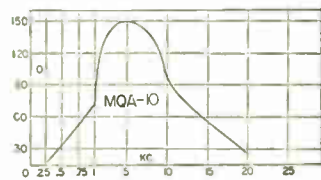
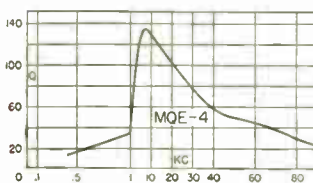
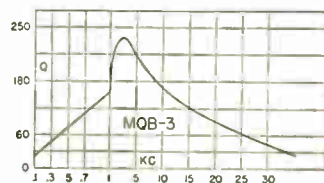
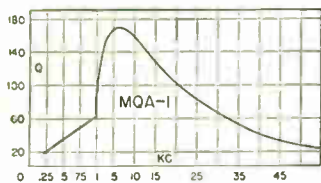
UTC Permalloy Dust Toroids have been the standard of the industry for over 15 years. The MQ series of coils provide the highest Q factor in their class (see curves below), with miniaturized dimensions. All units are hermetically sealed in MIL-T-27 Specifications.

The stability is excellent. For the MQE-7 the inductance change is less than 1% for voltages from .1 to 3 volts. The MQA-13 change is less than 1% for applied voltages from .1 to 20 volts. The MQB-1 change is less than 1% for applied voltages from .1 to 50 volts. DC is permissible through the coil (values listed below). Inductance is virtually independent of frequency, temperature and vibration.

Hum pickup is extremely low due to the toroidal winding structure, with windings uniformly spread over the core. The case is of high permeability, affording additional shielding such that close spacing of units can be effected, the coupling attenuation being approximately 80 DB.

Other values of inductance than those listed are available on special order at the price of the next higher listed value.

## TYPICAL Q CURVES



### MQA TYPES

Type No.	Inductance	*DC Max.
MQA-1	7 mhy.	250
MQA-2	12 mhy.	200
MQA-3	20 mhy.	150
MQA-4	30 mhy.	125
MQA-5	50 mhy.	100
MQA-6	70 mhy.	80
MQA-7	120 mhy.	60
MQA-8	.2 hy.	50
MQA-9	.3 hy.	40
MQA-10	.5 hy.	30
MQA-11	.7 hy.	25
MQA-12	1 hy.	20
MQA-13	1.5 hy.	17
MQA-14	2.5 hy.	13
MQA-15	4 hy.	10
MQA-16	6 hy.	9
MQA-17	10 hy.	7
MQA-18	15 hy.	5
MQA-19	22 hy.	4

### MQB TYPES

Type No.	Inductance	*DC Max.
MQB-1	10 mhy.	400
MQB-2	30 mhy.	250
MQB-3	70 mhy.	170
MQB-4	120 mhy.	120
MQB-5	.5 hy.	60
MQB-6	1 hy.	40
MQB-7	2 hy.	30
MQB-8	3.5 hy.	22
MQB-9	7.5 hy.	16
MQB-10	12 hy.	11
MQB-11	18 hy.	9
MQB-12	25 hy.	8

### MQE TYPES

Type No.	Inductance	*DC Max.
MQE-1	7 mhy.	135
MQE-2	12 mhy.	100
MQE-3	20 mhy.	80
MQE-4	30 mhy.	65
MQE-5	50 mhy.	50
MQE-6	70 mhy.	40
MQE-7	100 mhy.	35
MQE-8	150 mhy.	30
MQE-9	.25 hy.	22
MQE-10	.4 hy.	17
MQE-11	.6 hy.	14
MQE-12	.9 hy.	12
MQE-13	1.5 hy.	9
MQE-14	2 hy.	8
MQE-15	2.8 hy.	7.2



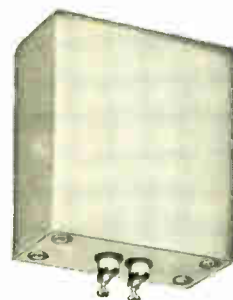
MQE CASE

Length ..... 1 1/16"  
Width ..... 1/2"  
Height ..... 17/32"  
Unit Weight ..... 1.5 oz.



MQA CASE

Length ..... 1 9/32"  
Width ..... 1 1/16"  
Height ..... 1 23/32"  
Unit Weight ..... 4 oz.



MQB CASE

Length ..... 2 9/16"  
Width ..... 1 13/16"  
Height ..... 2 13/16"  
Unit Weight ..... 14 oz.

\*This value of D.C. (MA) will drop the coil inductance 5%. Values of D.C. below this will show proportionately (linear) less inductance drop. For example, MQE-1 will drop 1/2% in L with 13.5 MA.

*United Transformer Co.*  
150 VARICK STREET NEW YORK 13, N. Y.

EXPORT DIVISION: 13 EAST 40th STREET, NEW YORK 16, N. Y. CABLES: "ARLAB"

BOARD OF DIRECTORS, 1953

J. W. McRae  
*President*

S. R. Kantebet  
*Vice-President*

W. R. G. Baker  
*Treasurer*

Haraden Pratt  
*Secretary*

Alfred N. Goldsmith  
*Editor*

I. S. Coggeshall  
*Senior Past President*

D. B. Sinclair  
*Junior Past President*

1953

R. D. Bennett  
G. H. Browning (R1)  
W. H. Doherty  
A. W. Graf (R5)  
W. R. Hewlett  
A. V. Loughren  
R. L. Sink (R7)  
G. R. Town  
Irving Wolff (R3)

1953-1954

J. T. Henderson (R8)  
C. A. Priest (R4)  
J. R. Ragazzini (R2)  
J. D. Ryder  
A. W. Straiton (R6)  
Ernst Weber

1953-1955

S. L. Bailey  
B. E. Shackelford

Harold R. Zeamans  
*General Counsel*

George W. Bailey  
*Executive Secretary*

Laurence G. Cumming  
*Technical Secretary*

Changes of address (with advance notice of fifteen days) and communications regarding subscriptions and payments should be mailed to the Secretary of the Institute, at 450 Ahnaip St., Menasha, Wisconsin, or 1 East 79 Street, New York 21, N. Y.

All rights of publication, including translation into foreign languages, are reserved by the Institute. Abstracts of papers with mention of their source may be printed. Requests for republication privileges should be addressed to The Institute of Radio Engineers.

# PROCEEDINGS OF THE I.R.E.<sup>®</sup>

*Published Monthly by*

The Institute of Radio Engineers, Inc.

VOLUME 41

August, 1953

NUMBER 8

## PROCEEDINGS OF THE I.R.E.

Amor L. Lane, Chairman, Professional Group on Ultrasonics Engineering.....	962
Ultrasonics Engineering..... Amor L. Lane	963
4631. An Evaluation of the IRE Professional Group Plan..... W. R. Hewlett	964
4632. Is Complexity of Military Electronics Necessary?..... R. J. Nordlund	965
4633. Large Reductions of VHF Transmission Loss and Fading by the Presence of a Mountain Obstacle in Beyond-Line-of-Sight Paths..... F. H. Dickson, J. J. Egli, J. W. Herbstreit, and G. S. Wickizer	967
4634. Low Level Synchronous Mixing (Abstract)..... M. E. Brodwin, C. M. Johnson, and W. M. Waters	969
4635. Unipolar "Field-Effect" Transistor..... G. C. Dacey and I. M. Ross	970
4636. A Subjective Study of Color Synchronization Performance..... M. I. Burgett, Jr.	979
4637. Measurement of the Small Signal Parameters of Transistors..... Geoffrey Knight, Jr., Richard A. Johnson, and Roland B. Holt	983
4638. A Note on the Analysis of Vacuum Tube and Transistor Circuits..... L. A. Zadeh	989
4639. Correction to "Transistor Operation: Stabilization of Operating Points"..... Richard F. Shea	992
4640. An Analysis of Magnetic Shift Register Operation..... E. A. Sands	993
4641. Debunching of Electron Beams Constrained by Strong Magnetic Fields..... M. Chodorow, E. L. Ginzton, and E. J. Nalos	999
4642. A Simple Graphical Analysis of a Two-Port Waveguide Junction..... J. E. Storer, L. S. Sheingold, and S. Stein	1004
4643. The Gyrotator as a 3-Terminal Element..... Jacob Shekel	1014
4644. A Method for Improving the Read-Around-Ratio in Cathode-Ray Storage Tubes..... Josef Kates	1017
4645. Stagger-Tuned Loop Antennas for Wide-Band Low-Frequency Reception..... David K. Cheng and Ralph A. Galbraith	1024
4646. Amplitude Stability in Oscillating Systems..... Norman R. Scott	1031
4647. The Constants in the Equation for Atmospheric Refractive Index at Radio Frequencies..... Ernest K. Smith, Jr. and Stanley Weintraub	1035
4648. Reduction of Forced Error in Closed-Loop Systems..... L. H. King	1037
4649. Theory of AFC Synchronization..... Wolf J. Gruen	1043
4650. A New Solution for the Current and Voltage Distributions on Cylindrical, Elliptical, Conical or Other Axisymmetrical Antennas (Abstract)..... O. Zinke	1048
4651. Wide-Band Phase-Delay Circuit..... Harry Sohon	1050
4652. Coding by Feedback Methods..... B. D. Smith	1053
4653. Discussion on "Synthesis of Narrow-Band Direct-Coupled Filters" by H. J. Riblet..... J. Reed and H. J. Riblet	1058
Correspondence:	
4654. "A Note on Sommerfeld's 1909 Paper"..... Bob M. Farran	1059
4655. "Collector-Base Impedance of a Junction Transistor"..... R. L. Pritchard	1060
4656. "Remarks on the Neutrino Communication System"..... M. H. Shamos	1060
4657. "Response Characteristics"..... Leo Storch	1061
4658. "A Note on the Impedance Transformation Properties of the Folded Dipole"..... Moshe Zakhaim	1061
Contributors to PROCEEDINGS OF THE I.R.E.....	1062

### EDITORIAL DEPARTMENT

Alfred N. Goldsmith  
*Editor*

E. K. Gannett  
*Administrative Editor*

Marita D. Sands  
*Assistant Editor*

### ADVERTISING DEPARTMENT

William C. Copp  
*Advertising Manager*

Lillian Petranek  
*Assistant Advertising Manager*

### BOARD OF EDITORS

Alfred N. Goldsmith  
*Chairman*

### PAPERS REVIEW COMMITTEE

George F. Metcalf  
*Chairman*

### ADMINISTRATIVE COMMITTEE OF THE BOARD OF EDITORS

Alfred N. Goldsmith  
*Chairman*



Reg. U. S. Pat. Off.

Responsibility for the contents of papers published in the PROCEEDINGS OF THE I.R.E. rests upon the authors. Statements made in papers are not binding on the Institute or its members.



### INSTITUTE NEWS AND RADIO NOTES SECTION

Foreign Members Use UNESCO.....	1066
Professional Group News.....	1068
Technical Committee Notes.....	1069
Western Electronic Show and Convention Program.....	1069
IRE People.....	1071
4659. Abstracts and References.....	1074
Meetings with Exhibits..... 2A Student Branch Meetings.....	80A
News—New Products..... 20A Membership.....	89A
Industrial Engineering Notes..... 66A Positions Open.....	128A
Section Meetings..... 72A Positions Wanted.....	134A
Advertising Index.....	150A

Copyright, 1953 by The Institute of Radio Engineers, Inc.





## Amor L. Lane

CHAIRMAN, 1953

PROFESSIONAL GROUP ON ULTRASONICS ENGINEERING

Amor L. Lane, first chairman of the new Professional Group on Ultrasonics Engineering, was born on February 16, 1926, in the state of Pennsylvania. He received the B.S. degree in electrical engineering from the University of Pennsylvania in 1949.

From 1947 to 1949 Mr. Lane served in the United States Navy as an electronic technician's mate, interrupting his college studies.

Mr. Lane joined the electronic guidance section of the Guided Missiles Division of the Naval Ordnance Laboratory in 1949. In 1950 he transferred to the ultrasonic transducers section in the Underwater Ordnance Department. He became a group head in 1951 and section chief in 1953. This section is responsible for applied research, design, development, construction, and evaluation of electroacoustic transducers, with emphasis on polycrystalline ceramics.

For his work in underwater sound Mr. Lane received the Navy Department's Civilian Meritorious Award last January.

Mr. Lane joined the Institute as an Associate in 1949. During the past year he has been instrumental in founding the Professional Group on Ultrasonics Engineering. He was elected its first chairman in May of this year.

Mr. Lane is a member of the Acoustical Society of America, Tau Beta Pi, Eta Kappa Nu, and Sigma Tau.

# Ultrasonics Engineering

A. L. LANE

As science and technology evolve, new and important fields of endeavor spring into being and assume their rightful place among their older brethren. What were little known of detailed principles become the bases of developed and expanded systems of thought which soon find their practical expression in humanly helpful engineering methods and equipment.

Ultrasonics in engineering is a striking example of this trend. Its development has been rapid and its applications many and increasingly valuable. It is therefore fitting that an IRE Professional Group on Ultrasonics Engineering should have been established, and that its interesting scope and encouraging plans should be described below by its Chairman, who is Section Chief, Ultrasonic Transducers Section, Underwater Ordnance Department of the Naval Ordnance Laboratories, White Oak, Maryland.—

*The Editor.*

Ultrasonics has been called correctly the science of a coming technology. Only a few years ago the scope of ultrasonics was limited and the applications comparatively few. However, if the tremendous advances that have recently been made in ultrasonics are used as a measuring stick, the future promises even more astounding developments. There can be little doubt that a potent and versatile tool is emerging, which, even now, is proving extremely useful to the scientist and engineer both in the laboratory and in industry.

At present the investigation and application of ultrasonics embraces many diverse fields. In the laboratory ultrasonic techniques are used for studying specific heats, molecular processes, shear viscosity, and elasticity of liquids, the elastic and dissipative properties of solids, thermal relaxation phenomena, velocity, and attenuation in gases. Marine applications include ultrasonic depth indicators, underwater object and fish locators. In the medical field ultrasonic diagnostic and therapeutic devices are being investigated and developed. These include diathermy instruments, tumor locators, dental caries locators, and even a device to replace the dentist's drill. In industry ultrasonics is finding applications in wide variety. Non-destructive testing of materials, acceleration of chemical reactions, emulsification, coagulation, sterilization are a few uses in this area. Ultrasonic delay lines and electromechanical filters are being used in radio, radar, and digital computers. There may one day be ultrasonic washing machines.

In view of these tremendous strides, there has been a large and spontaneous demand from widely divergent fields, interested in or utilizing the generation and effects of ultrasonics, for an organization representing their interest. In response to this widespread demand the Ultrasonics Engineering Professional Group of the IRE has been organized. This Group is now taking its place among the other Professional Groups of the IRE, according to the IRE policy of decentralization into smaller, more compact Groups formed on the basis of professional interest.

The newly formed Ultrasonics Engineering Group will benefit both the ultrasonic engineer and industry as a whole. This will result from an attempt to bring together the literature on ultrasonic applications and associated circuitry which heretofore has been dispersed in a wide variety of publications. Both the TRANSACTIONS of the Ultrasonics Engineering Group and the PROCEEDINGS OF THE I.R.E. may be used for this purpose. Moreover, the TRANSACTIONS often will enable more rapid publication of certain papers. In addition to the TRANSACTIONS, the Ultrasonics Engineering Group will sponsor symposia and local meetings which will provide ultrasonic engineers with their own outlet of expression. Industry will be helped, since the interchange of ultrasonics information will be available to the entire IRE membership of 30,000 engineers and scientists, as well as the additional thousands of readers of IRE literature.

# An Evaluation of the I.R.E. Professional Group Plan\*

W. R. HEWLETT†, FELLOW, IRE

**Summary**—The rapid growth during the past ten years of the radio engineering profession resulted in the initiation by the I.R.E. of the Professional Group Plan. The significant steps in the development of the Professional Groups are reviewed and the value of the Professional Group Plan to the Institute and to the Profession as a whole is evaluated. The importance of realistic consideration of problems arising from the group expansion program is stressed.

THE YEAR 1953 saw 40 of the 43 technical sessions at the National Convention sponsored by Professional Groups. This is indicative of a change that has been gradually taking place in the Institute since the Professional Group plan was first initiated. It is the purpose of this article to review briefly some of the factors that led up to the Professional Group system and to indicate the advantages that will accrue to the membership as a result.

A little less than five years ago the Professional Group plan was initiated within the I.R.E. This plan consists of a voluntary association of Institute members who are interested in seeing that their particular branch of the electronic industry is adequately covered by Institute activities. Upon approval of the Institute and after meeting certain formal requirements, a Professional Group may be set up to insure this aim. In this short five-year period, the plan has grown until there are now no less than 19 Professional Groups with a paid-up membership of approximately 12,500.

To go back a bit in history, the Institute was founded in 1913 by a small group of engineers and scientists who were interested in or directly concerned with the infant field of "radio engineering." It is interesting to look at the type of problems that concerned this early group. Selecting a few papers from the first two years of PROCEEDINGS publication, one finds articles by all three of our founders, two of whom we have honored today. These papers treated such subjects as: "Radio Operations of Steamship Companies," "The Seibt Direct Indicating Wave Meter," "The Heterodyne Receiving System," papers on "Experimental Tests of the Radiation Law of Antennas" by Michael Pupin, "The Daylight Effect in Radio Telegraphy" by Kennelly, "The Audion-Detector and Amplifier" by Lee deForest, and "Radio Traffic" by David Sarnoff.

Although the subject matter of any of these papers might make it the legitimate claim of a modern Professional Group, the basic difference is that these papers were of paramount interest to all "Radio Engineers" at that time, and not just a special group.

In contrast, these typical papers appeared in last year's PROCEEDINGS: "Network Synthesis by the Use of Potential Analogs," "The Binac," "A Homo-Polar Tachometer for Servo-mechanism Applica-

tions," "Transistor Forming Effects in N Type Germanium."

These papers were selected to represent the high degree of sophistication the art has assumed.

Several basic factors have contributed to the broadened scope of interest of the I.R.E. membership. About 1940, the profession of radio engineering was pretty well confined to the field of communications and the directly supporting activities. The war had a tremendous impact on the entire field, and electronics emerged from the war as a basic tool of industry as a whole and not just the bread and butter item of a small group of engineers in the field of communications. The extent of this expansion is perhaps best indicated by the fact that for the 12 years prior to 1940 the Institute membership had been almost constant at 6,000, but starting in 1940, the annual increase in membership has averaged close to 2,500 per year.

Dr. William Everitt<sup>1</sup> stressed electronics as interested primarily in extending man's senses, and proposed this definition:

"Electronics is the science and technology which deals primarily with the supplementing of man's senses and his brain power by devices which collect and process information, transmit it to the point needed, and there either control machines or present the processed information to human beings for their direct use."

An acceptance of this definition and a tacit assumption that the I.R.E. is the professional society primarily responsible for the field of electronics immediately indicates the enormous scope of the I.R.E.'s responsibility. The diversity of interests represented by this definition obviously offers a tremendous challenge to the Institute, a challenge that must be accepted if the Institute is to live up to its basic objectives as set forth so well in its constitution, here quoted.

"Its objectives shall be scientific, literary, and educational. Its aims shall include advancement of the theory and practice of radio and allied branches of engineering and of the related arts and sciences, their application to human needs, and the maintenance of a high professional standing among its members."

The Institute's answer to this challenge has been the Professional Group system. It is interesting to note that the author of the broad definition of electronics, Dr. Everitt, together with Dr. Raymond Heising, played a leading role in the establishment of the Professional Group system. As previously noted, the Professional Group plan was set up so that the impetus for the formation of a Group must come directly from the membership, not from some arbitrary wish on the part of Institute headquarters. Operating on this basis, it became evident by 1951 that, not only was the Professional

Group plan gaining rapid support from the membership, but also, that if the best interest of the profession were considered, even greater stimulation must be given to the movement. This step was taken by a strong statement of policy by the Board favoring decentralization and the adoption of a plan whereby publication of technical and specialized papers by the Professional Groups would be stimulated.

This plan provided that, on a one-time basis, the Institute would match, up to \$1,000, any sums raised by a group either through assessment or by the holding of symposia. This plan has since been expanded so that the Professional Groups may count on continued financial support from the Institute, with the funds to be furnished on a matching basis subject to certain restrictions as to maximum amount. The result of the encouragement given the Professional Groups by the Institute, both financial and moral, resulted in a noticeable strengthening of the Group plan. In 1952, for example, 22 separate TRANSACTIONS were published by Professional Groups. It is interesting to note that, although responsibility for obtaining subject material for these TRANSACTIONS rests primarily with these groups, a very considerable support is furnished by the Editorial Staff of the Institute. The increased vigor of the Professional Groups is not only indicated in their publications but also in the symposia they sponsor. Last year there were about 12 specialized symposia held throughout the country that were either sponsored or co-sponsored by Professional Groups.

The flow of assistance, however, has not been a one-sided proposition. More and more the Institute is looking to the Professional Groups for aid. In the case of publications this help has been two-fold—one direct and one indirect. The Editorial Department looks to a Professional Group for definitive papers in the particular field of interest of that Group and has so streamlined its editorial procedure that papers recommended by the Professional Groups now receive preferential treatment. The indirect benefit has been that the PROCEEDINGS is relieved of the very considerable pressure to publish detailed and often specialized papers in various fields now covered by Professional Groups. In many instances these papers can be more satisfactorily handled through Group TRANSACTIONS. This permits the PROCEEDINGS to concentrate on papers of a more basic nature and of greater general interest to the Institute as a whole.

In the national conventions the Groups are playing an ever increasing role, as witnessed by this year's national convention. The same thing to a lesser extent is true of conventions held elsewhere in the United States. For example, at the West Coast Convention held in Long Beach last year 14 groups sponsored technical sessions. Even the Sections themselves are finding the local

\* Decimal classification: R060. Original manuscript received by the Institute April 24, 1953. Presented, annual meeting of the Institute, I.R.E. National Convention, New York, N. Y.; March 25, 1953.  
† Hewlett-Packard Co., Palo Alto, California.

<sup>1</sup> W. L. Everitt, "Let us re-define electronics," Proc. I.R.E., vol. 40, p. 899; August, 1952.

Professional Group Chapters of assistance and often will request that a Group Chapter sponsor one or more meetings during the year for the general membership.

We are now in a position to stand back and evaluate our Professional Group system. Most significant, of course, has been the recognition by the Institute that if the best interests of its members and the profession as a whole are to be preserved it must adopt some sort of division along professional lines. The requirement for a division of this type indicates the profession has become sufficiently complex that it can no longer be served properly by media common to all members. Although there are large fields of common interests which still should and will be handled by the present media, the specialist must be provided with means for the direct and rapid interchange of information within his own field. These means could not be provided on an economical basis by the previously existing publications, conventions and meetings.

A less obvious benefit of the Group system has been to broaden the base of membership participation. This in itself is a fact of no mean significance. Examples of this are to be seen in the greater opportunity among our membership for experience in organization and leadership. Many of the men so trained will eventually work into Institute management where their reservoir of experience will be of great value. Additional opportunities have been offered in the field of publication and rapid dissemination of technical papers and again this will be of value to the Institute. Through the ever

increasing number of conferences and symposia in which the Professional Groups are playing a leading role, the membership of the Institute as a whole will derive great benefit. In addition, many interesting experiments on how to organize and run a conference are being tried by the groups. Some of the more successful will undoubtedly have a direct effect on our national convention.

In many ways the Institute might be likened to a parent with 19 vigorous and growing children. Most of these children have been carried through their first few critical years and have survived the usual childhood diseases of a very young organization. Most of the Groups are now sturdy children rapidly approaching maturity. Already the Institute is leaning heavily on them. There are, however, critical periods ahead, both for the Institute and for the Professional Groups themselves. New organizations are usually started by a few energetic people who through their enthusiasm and drive establish the organization as a going concern. However, in many cases the interest of these people is transitory, either because they look for new worlds to conquer or through general lack of interest once the basic problems of organization have been surmounted. It is, therefore, imperative that the Professional Groups insure that young and vigorous personnel are attracted into the management and guidance of the Group. When the time comes for the original organizers to step aside there will be a well-trained and capable team to insure the continued good management of the Group. On the other hand, the Institute

itself must furnish intelligent leadership to its Professional Group children. It will not be long before these Groups are fully grown adults and as such will ask and must be given an important role in the running of the Institute. Institute leadership must be such that the first allegiance of the Professional Group will be to the Institute as a whole.

We are probably entering one of the most critical phases in the development of our Group system. We have gone too far to turn back, and must make the system work or see the Institute shatter into small pieces, the total of which would never be as strong as the whole, nor as capable of serving the interests of the profession.

The Groups have become large enough and sufficiently well defined that basic questions are arising with respect to the relation of Groups to each other and of Groups to the Institute itself. It is imperative that these and similar problems as they arise be faced squarely and considered honestly by the Professional Groups and the Institute alike. On the soundness of these decisions rests the long range success or failure of the Professional Group plan. The basic yardstick must be "What is best for the Institute and the profession as a whole?" If this yardstick is conscientiously used, our Professional Groups will thrive, membership in the Institute will continue to rise, the service performed to our members and profession will grow better, and the Institute of Radio Engineers and its Professional Group system will be a model of how a professional society can meet the demanding requirements of an ever-increasing technical field.

## Is Complexity of Military Electronics Necessary?\*

R. J. NORDLUND†, SENIOR MEMBER, IRE

Until recent years, adequate attention had not been paid to the engineering of systems embodying both complex electronic mechanisms and the human operator of such mechanisms. When such composite systems are thoughtfully designed, they often turn out to be highly complex. Complexity may bring unreliability in its train. However, painstaking planning and pretesting of such systems may restore reliability. The following paper comprehensively analyzes these situations and is accordingly a useful guide to engineers attacking such problems.—*The Editor.*

**Summary**—An analysis is made of the reasons for the trend of military electronics toward more system complexity. Some interesting aspects of the relation of complexity to unreliability are investigated, and a distinction is established between circuit complexity and operation complexity. The soundness of the choice of complexity is established by curves of a general "trend" nature. Systems engineering is proposed as a solution to the complexity versus reliability problem, and as a challenge to the young engineer.

**M**ANY PEOPLE believe that the military departments have "gone off the deep end" in the matter of system complexity. Statements have been made, in the press and elsewhere, to the effect that we are soon going to attain "push-button" warfare. This seems to imply the

replacement of the human as part of the basic system. Certain of the more intricate circuits of the computation type are rather thoughtlessly called a "brain."

I think you will agree that the most important contribution of the human in a servo loop, in a dynamic situation, is his ability to reason and correct a wrong trend or event if and when it occurs. With most humans, this is true only so long as events occur at a reasonable rate, so that confusion does not ensue, and emotional stability is not upset. On the other hand, electronic instrumentation can be devised which can perform certain functions at an extremely rapid rate, without confusion. Even a perfunctory analysis of almost any branch of air warfare immediately shows that one of the inherent ingredients of any such battle is an ever-changing situation to which reasoning power can be profitably applied. It immediately

becomes apparent that an optimum combination of human and instrumentation must exist for the most precise solution of any given dynamic problem. The faster and higher an airplane flies, the more necessary this becomes; in fact automaticity, and hence, complexity, will *have* to increase in proportion to the rate of increase of speed and altitude.

World War II saw the first application of complex electronic gear to the air battle (as well as to sea and land warfare). The introduction of radar to extend human capabilities in detection and ranging for fire control and bombing was certainly a milestone both in the military field and in the electronic industry. While it is undoubtedly true that this development contributed greatly to the achievement of mastery over the enemy, it is also true that specific results fell far, far short of the goals envisaged by

\* Decimal classification: R560. Original manuscript received by the Institute, April 2, 1953.

† Bombing Consultant, Armanent Laboratory, Wright Air Development Center, Dayton, Ohio.

equipment designer and manufacturer. Two basic reasons for this are unreliability and complexity of operation.

In retrospect, it is apparent that this unreliability was inevitable, considering the astonishingly short period given to development and design. But the greatest reason for its unreliability was the revolutionary nature of the impact of such complex gear, introduced in such a short time, upon the maintenance organizations of the services. This was like asking a building construction electrician to repair a television set and withholding the circuit diagram. Looking back, it seems a wonder that any effectiveness was achieved at all, and much credit must be given to the electronics industry and the cooperative spirit and understanding of its technical representatives in the field.

The other reason was termed "complexity of operation." It will be shown that this is an entirely different thing than circuit complexity, and this is very important. Complexity of operation brings in the human who uses the equipment. The electronic equipment used in the Air Force in World War II simply required of the user so many parallel actions and this at a time of great emotional strain, being under attack, that his ability to reason and rationalize was destroyed. The result was a great plague of gross errors—in the case of bombing—which was difficult for the designer of the equipment to understand or explain. These gross errors were the result of the operator actually forgetting to perform some important calculation, or actually making an erroneous calculation, or failing to apply reason to a sudden turn of events.

In the developmental evolution of Air Force electronic equipment, during and immediately following World War II, analysis clearly showed what the limitations of the user were. An important decision had to be made. This decision was to accept the limitations of the human and to stay within these limitations by complex instrumentation which accomplished many of the tasks and computations automatically. The aim was to achieve maximum utilization of the reasoning capability of the human, which cannot be instrumented, by removing the confusion factor caused by overloading him. The penalties to be incurred by circuit complexity in the form of unreliability and difficult maintenance were clearly understood and considered in the decision.

There seems to exist a certain amount of confusion between the terms circuit complexity, operating complexity and reliability. It is obvious that circuit complexity and reliability are basic problems facing the equipment designer. The problem is to accept the fact that circuit complexity is necessary and to go about the business of achieving reliability in spite of complexity. A certain amount of introspection can convince one that, in the eyes of the user, circuit complexity and unreliability are synonymous. If a black box performs its function day after day, never requiring disassembly or attention, to the user it is a simple gadget regardless of the wondrous jumble of tubes, capacitors, resistors and whatnot which may be hidden inside.

The goal of the designer, then, is to make the user believe that a complex equipment is really simple. We have many examples of this in our homes. Almost every home in the

country has a telephone. To millions of persons this is assuredly a simple device, since it never fails and is easy to operate. To those who spent thousands of hours designing, testing, redesigning and retesting to achieve this almost perfect reliability, it was hardly a simple task, nor is the welter of electronic instruments in the modern automatic exchange to be considered simple. The telephone system, incidentally, also illustrates to some extent the earlier contention that *from the system standpoint*, in both the economical and accuracy aspects, optimum utilization should be made of the human being and electronic instrumentation. The telephone system still utilizes people to apply reasoning power to sort out the weird questions which we can pose from the other end of the line, but has removed from the human the mechanical tasks of making proper connections to connect us to the right party. Many other examples in daily life need not be mentioned here.

the "operational reliability" curve. "Instrument Accuracy" was also degraded because of the coarser nature of the radar-data inputs and of the lesser accuracy of the electronic solution versus the previous mechanical computation. These curves improved slightly between 1944 and 1946 reflecting increasing capability in maintenance and adjustment and admirable support of the Air Force by the electronics industry.

The first radical change in these curves coincides with the introduction of the new equipment designed to most effectively use the human operator. The "operator's task" curve goes rapidly from complex to relatively easy, and at the same time the "operational reliability" curve rapidly falls to a dangerously low level. The double low spot in the "operational reliability" curve resulted from the introduction, about a year apart, of two different configurations of this new concept, the second more elaborate in capability and complexity than the first. The

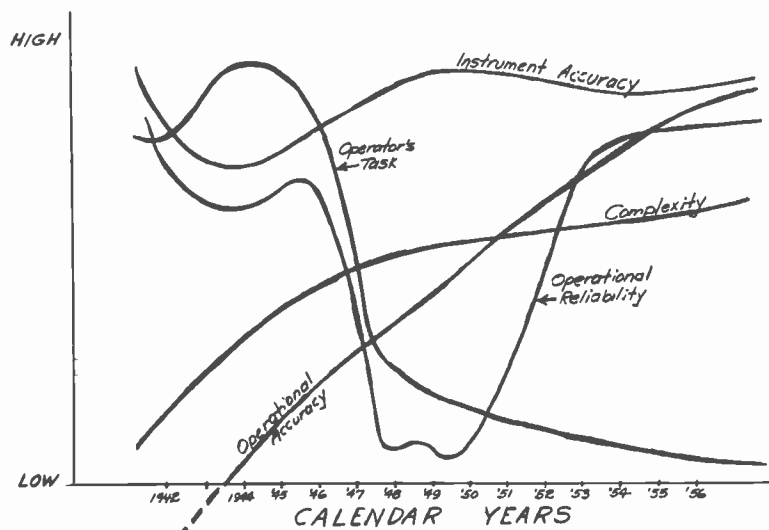


Fig. 1—USAF system concepts.

An attempt will now be made to demonstrate by means of some simple curves that the decision to try to achieve proper balance between human and instrumentation, at the cost of circuit complexity, was a most wise choice on the part of the Air Force.

Fig. 1 contains five curves based on factual data concerning one particular type of Air Force weapon system. Because of this factual nature, the figure is lacking in a quantitative sense, since these data are classified information. Nevertheless, much can be learned from a study of these curves. The curve entitled "Instrument Accuracy" is included because precision of computational accuracy does have a bearing on complexity and reliability, and the disparity between instrumental and operational accuracy is explained by the other three curves. It should be noted that a high order of instrumental accuracy was available even at the beginning of World War II. However, the disparity between this and actual operational accuracy was enormous due to large demands upon the human at the wrong time.

Introduction of radar increased the operator's capability but complicated his task to a great degree so we have the "operator's task" curve rising to a broad peak around 1944, with a corresponding degradation in

climb back to respectability of the "reliability" curve was achieved by an agonizing and very expensive "bootstrap" operation in which basic mistakes of installation which adversely affected the equipment environment were corrected, the usual two year gap between engineering knowledge of deficiency and actual production-line quality was overcome, and the capability of the using organization made a surprising improvement. This was a period during which the Air Force was learning to live with circuit complexity. That this was possible is demonstrated by the rapid rise of the "reliability" curve during 1949 to 1953.

The "complexity" curve is a rather arbitrary one, since this is hard to measure in chart numbers. It does illustrate the revolutionary nature of what took place between 1942 and 1948 in this matter so important to the members of the Institute.

The significant thing about this figure is, of course, the "operational accuracy" curve. The fact that it shows a steady rise during all the gyrations of the other curves is of tremendous importance to the nation and, it is believed, proves that the decision in favor of circuit complexity was sound.

The fact remains, unfortunately, that reliability is at present far from acceptable,



and while learning to live with electronic-equipment complexity we have continuously had present that ugly unwanted bed-fellow "unreliability." We know now that we have capability, but for it we are paying far too high a price in maintenance, attrition and mission failures. The challenge obviously is to learn how to build reliability into complex electronic equipment. The Air Force has not the slightest doubt that the electronics industry will be able to achieve this. We are, of course, interested in how soon, not only because of cost considerations, but also because the quality of the nation's security is inextricably involved.

The Air Force technical personnel have recently come to recognize that the only way to achieve a position where our customers, the operating Air Forces, can be led to believe that complex electronic equipment is in fact simple and reliable is by approaching the problem from the complete "systems" viewpoint. This is how a "simple" black-rubber telephone instrument was achieved.

A modern weapon system is an extremely complicated thing and the problems of adequate technical administration of such a project are enough to stagger the imagination. The galaxy of specialized talent which must work together on such a project includes representation from all fields of the aerodynamic, mechanical, optical, geodetic and electronic arts, as well as human re-

sources research, basic materials research, aeromedical research, not to mention the basic military sciences. The Air Forces' technical administration is keenly and humbly aware of the enormity of the task and looks to the industry for a large measure of the necessary aid.

The author believes that it is in systems engineering in complex electronics-systems work that the real challenge to the present day young engineer lies. It is work that does not appeal to the type of person who desires to specialize and acquire a great store of knowledge about some distinct and unique portion of the field. Nor does it continue for long to appeal to the type of individual who likes his days to be serene and his nights untroubled. It is difficult work, but unbelievably rewarding in the sense of real accomplishment and service. The young man who is fortunate enough to get in on the conception of a systems project, and can stay with it through the many years required for development of such a project, emerges with a mature sense of his own capabilities and is usually then equipped to engage in technical administration work. Systems engineering work is the most broadening of any phase of the profession and is a liberal education in itself.

In general, the Air Force has enjoyed the best of relations with the electronics industry, and is deeply appreciative of the spirit of understanding and cooperation

that has existed. Air warfare is young and dynamic, and consequently subject to continuing change based on experience and technological advancement. Its technical programs are full of unique problems—unique because the environment in which airborne electronic equipment "lives" is certainly unique, and this is one of the most difficult problems to overcome in the struggle to achieve reliability in spite of complexity. These special problems are of the type which require the most thorough cooperation between the industry and the military departments.

#### Concluding points:

- (a) Modern military equipment, to achieve the most precise solution to dynamic problems, must rely on complex instrumentation to permit optimum use of the human being.
- (b) To the user, complexity of itself is of no real significance except as it affects reliability.
- (c) The "systems" concept in engineering administration and technical control is essential to insure success in achieving reliability.
- (d) Systems engineering is the new frontier in the engineering profession.
- (e) Our goal must be to achieve reliability in spite of complexity.

## Large Reductions of VHF Transmission Loss and Fading by the Presence of a Mountain Obstacle in Beyond-Line-of-Sight Paths\*

F. H. DICKSON†, J. J. EGLI‡, ASSOCIATE, IRE, J. W. HERBSTREIT§, SENIOR MEMBER, IRE, AND G. S. WICKIZER||, SENIOR MEMBER, IRE

**Summary**—A detailed investigation of the probable mode of propagation in vhf operation over mountain obstacles has been made. Theory indicates that tremendous gains in received signal strength—above those obtained over a smooth spherical earth—may be expected from diffraction over an appropriate knife edge located in the path. Experimental verification of the principles involved is reported. In addition, the fading was found to be small and even essentially nonexistent on certain very long obstructed paths.

VERY SUCCESSFUL VHF communications have been reported with essentially no fading over very long paths across mountainous terrain. The authors have just completed a detailed examination of these reports and visited engineers and scientists of the Mutual Telephone Company of Hawaii; the Electrical Communication Laboratory, Ministry of Communications, Tokyo, Japan (similar to the Bell Telephone

Laboratories in the U. S. A.); the Radio Research Laboratories, Ministry of Postal Services, Tokyo, Japan (similar to Central Radio Propagation Laboratory in the U. S. A.); and the Civil Aeronautics Administration in Alaska.

In a preliminary study prepared in the Office of the Chief Signal Officer, Lt. Col. H. V. Cottony, USAR, on military leave of absence from the National Bureau of Standards, pointed out that a considerable increase in received signal strength would result when a large knife-edge obstacle is located at the midpoint of an 85-mc, 100-mile path. Japanese scientists have made similar theoretical investigations and have substantiated their findings by experiments.<sup>1</sup>

Fig. 1 shows the results of using the four-ray method of Schelleng, Burrows and Ferrell<sup>2</sup> for computing diffraction across a knife edge at radio frequencies. This

\* Decimal classification: R115.5. Original manuscript received by the Institute May 1, 1953. Presented at the joint meeting of the URSI National Committee and the I.R.E. Professional Group on Antennas and Propagation, Washington, D. C., April 27-30, 1953.

† Office of the Chief Signal Officer, Washington, D. C.

‡ Signal Corps Engineering Laboratories, Fort Monmouth, N. J.

§ National Bureau of Standards, Boulder, Colo.

|| RCA Laboratories, Riverhead, N. Y.

<sup>1</sup> S. Matsuo, "The Method of Calculating VHF Field Intensity and Research on Its Variation," Report of the Electrical Communication Laboratory 621.39.001.6(047.3), Ministry of Telecommunications, Tokyo, Japan; August, 1950.

<sup>2</sup> J. C. Schelleng, C. R. Burrows and E. B. Ferrell, "Ultra short-wave propagation," *Proc. I.R.E.*, vol. 21, pp. 427-463; March, 1933.

figure shows the expected basic transmission loss<sup>3</sup> at 100 mc over transmission-path distances of 50 and 150 miles. The basic transmission loss is defined to be the ratio, expressed in decibels, between the power delivered to an isotropic transmitting antenna divided by the received signal power available from an isotropic receiving antenna. The actual transmission loss on a circuit may thus be obtained simply by subtracting the effective transmitting and receiving antenna gains, expressed in decibels related to an isotropic antenna, from the basic transmission loss shown in Fig. 1.

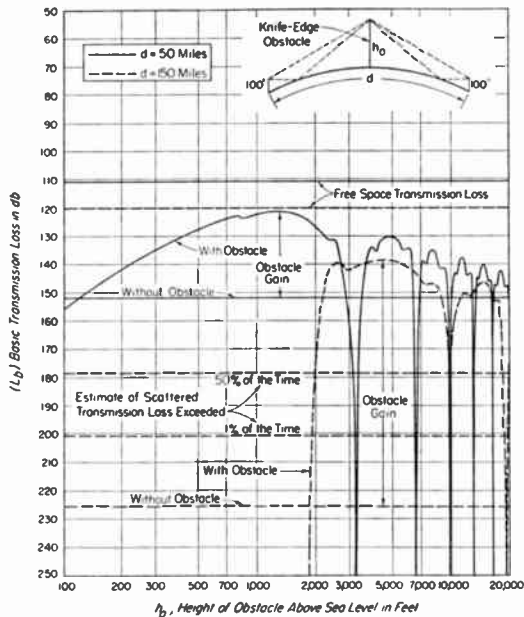


Fig. 1—Theoretical obstacle gains at 100 mc, assuming four-ray knife-edge diffraction theory. Transmitting and receiving antenna heights each 100 feet above the surface.

To simplify calculations, the ground-reflection coefficient has been assumed to be  $(-1)$ , thus neglecting the small phase and amplitude changes expected for an actual earth, as well as the divergence of the energy reflected from the curved earth's surface. With this approximation, the height of the obstruction must be greater than the elevation of the common horizon to have an "obstacle gain"—as the computed transmission loss is infinite at this point, e.g., 1,850 feet for a 150-mile path. It may be seen from Fig. 1 that for particular combinations of antenna heights, obstacle heights, and frequency, tremendous "obstacle gains" in received field strength are to be expected. The "obstacle gain" is defined, as shown in Fig. 1, to be the ratio of the received signal power expected with and without the obstacle. Experimental evidence has been obtained of the existence of these very large predicted "obstacle gains" in field strength. These hitherto unexpected gains are being used in obtaining very satisfactory vhf radio communication over severely obstructed transmission paths in mountainous regions.

An example of the use of "obstacle gain" examined in detail can be found in the 38-mc 160-mile transmission

circuit tested by the Civil Aeronautics Administration between Yakutat and Gustavous, Alaska. This path passes over the 8,000-foot level of Mt. Fairweather from two low terminals (approximately 200 feet) at the transmitting and receiving locations. The profile of this path, together with a typical sample signal-strength recording made by the Civil Aeronautics Administration on this circuit, is shown in Fig. 2.

On the basis of smooth-earth diffraction theory with the mountain removed, the calculated transmission loss for the 38-mc circuit would have been 207 db; however, on the assumption that Mt. Fairweather acts as a single 8,775-foot knife-edge ridge, calculations using the four-ray diffraction theory indicate that only 127-db transmission loss would be expected. The observed transmission loss was approximately 134 db, or within 7 db of the value indicated by the knife-edge diffraction calculations. These values correspond to a calculated "obstacle gain" of 80 db and a measured "obstacle gain" of 73 db greater than the field strength to be expected over a smooth spherical earth. Thus it appears that the mountain behaves effectively like a knife edge. Effective transmitting and receiving antenna heights of 50 feet and gains of 8 db over an isotropic antenna have been assumed in the above calculations, together with an allowance of 4 db for transmission-line losses.

Over a smooth spherical earth, signals arrive well below the radio horizon not only by the normal diffraction process around the curved surface of the earth but by scattering from the turbulent atmosphere. This turbulence is greatest near the surface of the earth. It is the turbulence of that portion of the higher atmosphere which is within line of sight of both transmitting and receiving antennas that is considered responsible for the relatively weak scattered, fading signal normally observed at distances beyond the horizon.<sup>4</sup> An estimate of the scattered-signal basic-transmission loss exceeded, for 1 per cent and 50 per cent of the time at 150 miles on 100 mc over a smooth spherical earth, is also shown in Fig. 1. This estimate was obtained by extrapolating the NBS Cheyenne Mountain data<sup>4</sup> so as to correspond to the 100-foot transmitting and receiving antenna heights of this example. It may be noted that the calculated "obstacle gain" of the properly situated knife-edge ridge reduces the transmission loss to such an extent that the received signal strength will far exceed the signal received by way of atmospheric scattering process, effectively eliminating fading arising from this scattering.

In addition, when an obstruction is situated at the proper location, and extending well above the horizon of both the transmitting and receiving antennas, the radio transmissions travel through the most turbulent and disturbed region of the atmosphere, close to the surface of the earth at a relatively large grazing angle. This large grazing angle reduces the possibility of the existence of numerous additional variable-transmission paths from the highly turbulent lower portions of the

<sup>3</sup> K. A. Norton, "Transmission loss in radio propagation," Proc. I.R.E., vol. 41, pp. 146-152; January, 1953.

<sup>4</sup> J. W. Herbstreit, K. A. Norton, P. L. Rice and G. R. Shafer, "Radiowave Scattering in Tropospheric Propagation," I.R.E. 1953 Convention Record.

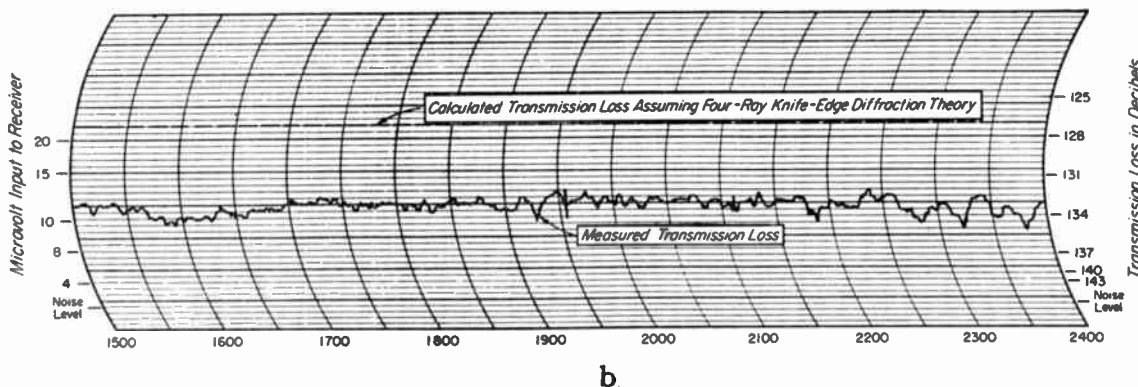
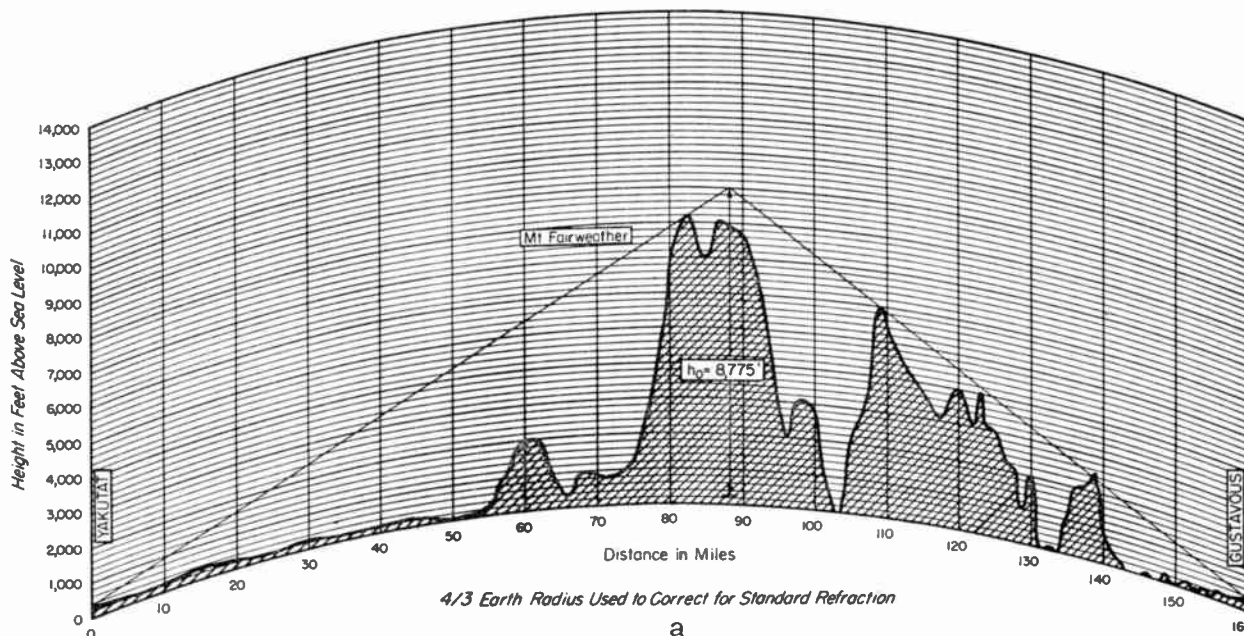


Fig. 2—(a) Profile of path from Yakutat to Gustavus, Alaska;  $h_t = h_r = 50$  feet;  $f = 38$  mc. (b) Typical sample recording on the above path; 50-watt transmitter power;  $h_t = h_r = 50$  feet. Local Alaska time, June 16, 1948.

atmosphere. In this way, the principal cause of tropospheric fading is effectively eliminated. The absence of severe tropospheric fading on a long-obstructed vhf transmission circuit is strikingly illustrated by the typical recording in Fig. 2. Over a period of 30 days' recordings on this path, the instantaneous transmission loss was found to vary from its mean value by less than  $\pm 2$  db.

It is concluded that the hitherto considered disadvantageous high-mountain ridges in vhf transmission paths can, in fact, be of tremendous advantage in reducing both transmission loss and tropospheric fading. Future vhf siting practices in mountainous regions should be modified to take advantage of "obstacle gains" in accordance with the principles outlined above.

## Low Level Synchronous Mixing\*

M. E. BRODWIN†, ASSOCIATE, IRE, C. M. JOHNSON†, AND W. M. WATERS†

### ABSTRACT

**A** SYNCHRONOUS DETECTION SYSTEM using same oscillator to furnish power for two signal channels has been used to obtain sensitivities on order of 110 dbm at 100 kc, 9 kmc, and 33 kmc.

\* Decimal classification: R361.2. Abstract of original manuscript received by the Institute, June 11, 1952; abstract received March 5, 1953.

† The Johns Hopkins University Radiation Laboratory, Baltimore, Md.

The system operates by channeling the energy from an unmodulated RF source into two isolated paths. A portion of the energy is phase or amplitude modulated in one path termed the "signal channel." The remainder of unmodulated carrier is directed through the other channel, the "reference channel." The amplitude and phase of the energy in the reference channel is carefully controlled. The power output of each chan-

nel is mixed in a detecting element, and the modulation component is amplified and metered.

The behavior of synchronous mixing with amplitude modulation is predicted from a mathematical analysis based on a series expansion of the volt-ampere characteristic of the nonlinear detecting element. This analysis shows that the modulation component appearing at the output depends

upon the product of the reference power and the signal power. In addition, the modulation component is a linear function of the signal power. Further analysis with the series expansion was carried out for the case where the signal power is harmonically related to the reference power. In this situation, the theoretical sensitivity is less than in the fundamental case but is still appreciable.

When the signal channel is phase modulated, a simpler analysis is employed based upon the Fourier series expansion of the transconductance of the detector. This analysis leads to the same results as the amplitude-modulated case except that the second harmonic of the modulating frequency may be optimized in the output by properly adjusting the phase difference between the two channels.

The results of the theoretical analysis have been verified experimentally at three different frequencies. A low frequency, 100 kc, was chosen to obtain information on harmonically related energy and to verify the results of the phase modulated case. At this frequency it is possible to obtain phase modulation with very little accompanying amplitude modulation. A high frequency, 33 kmc, was employed primarily to examine the possible use of low-level synchronous detection for use in detecting 99-kmc power.

The experimental results showed that the sensitivity of the synchronous detector as compared to the crystal-video detector was approximately 30 db greater. Furthermore, the experiments demonstrated that the "law" of the detector was a linear function of signal power. For maximum sensi-

tivity a pronounced optimum reference power,  $-20$  dbm at 9 kmc and  $-40$  dbm at 24 kmc was observed. Harmonic detection of 3-mm waves with 6-mm energy in the reference channel exhibited a 10-db increase in sensitivity as compared to crystal-video detection. Experiments were also made to examine the relationship between sensitivity and the modulating frequency.

The principal advantages of synchronous mixing are the sensitivity and dynamic range which can be attained with a minimum of electronic equipment. A sensitivity comparable to that of a superheterodyne receiver and a dynamic range greater than 60 db was easily attained. The disadvantage of synchronous mixing lies in the need for a reference-power connection between the source and the detector.

## Unipolar "Field-Effect" Transistor\*

G. C. DACEY† AND I. M. ROSS†

**Summary**—Unipolar "field-effect" transistors of a type suggested by W. Shockley have been constructed and tested. The idealized theory of Shockley has been extended to cover the actual geometries involved, and design nomographs are presented. It is found that these structures can be designed in such a way as to yield a negative resistance at the input terminals. The characteristics of several units are presented and analyzed. It is shown that these characteristics are in substantial agreement with the extended theory. Finally a speculative evaluation of the possible future applications of field effect transistors is made.

### PART I, THEORY AND DESIGN

#### 1. Introduction

THE "FIELD-EFFECT" transistor was first proposed by W. Shockley, and experiments of G. L. Pearson and W. T. Read gave some hope for ultimate success. Since that time, certain structural modifications have been proposed and the theory has been considerably enlarged. A detailed theoretical exposition has been prepared by Shockley.<sup>1</sup> We shall borrow liberally from this paper.

It has now become possible, through the advance of technique, to make units which are structurally similar to the ideal model of the theory, and to obtain a quantitative verification of the theory. In this paper we shall first review the ideal theory from a physical viewpoint giving plausibility arguments rather than proofs. We shall then consider certain modifications of the ideal theory suggested by the experiments and shall obtain design charts. The experimental verification of the theory will be given in some detail and finally relative merits of "field-effect" structures will be discussed.

#### 2. Shockley's Ideal Theory

In essence, a field-effect transistor can be regarded as a structure containing a semiconducting current path, the conductivity of which is modulated by the application of a transverse electric field. In particular, we shall consider the structure shown in Fig. 1. To fix our ideas, let us suppose that the central portion of the unit is made of  $n$ -type germanium and that two  $p$ -type regions are centrally located as shown in the figure. We shall call these regions the *gate* for reasons which will presently become clear. In addition we suppose that ohmic contacts have been made at both ends. The contact at which the carriers flow into the germanium is called the *source* and the contact at which they flow out is called the *drain*.

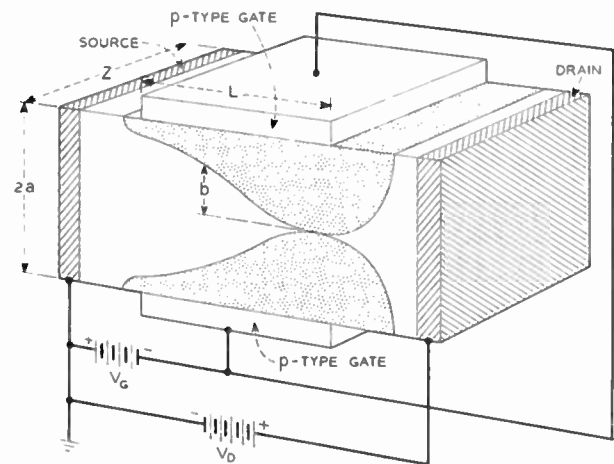


Fig. 1—Schematic diagram of field-effect transistor.

Now suppose that the gate is connected to the grounded source and that the drain is made slightly positive. Under these conditions current will flow from drain to source. This current consists of electrons flow-

\* Decimal classification: R282.12. Original manuscript received by the Institute, January 20, 1953; revised manuscript received May 7, 1953.

† Bell Telephone Laboratories, Inc., Murray Hill, New Jersey.  
<sup>1</sup> W. Shockley, "A unipolar field effect transistor," *Proc. I.R.E.*, vol. 40, pp. 1365-1376; November 1952.



ing through the *n*-type channel from source to drain. For small applied voltages the resistance  $R_0$  of this channel is

$$R_0 = L/2aZ\sigma \tag{1}$$

where  $\sigma$  is the conductivity of the *n*-type germanium,  $L$  is the length of the channel,  $2a$  its thickness and  $Z$  its width. As the drain voltage is raised, more current flows in the channel, and the  $IR$  drop along the channel makes it more positive the greater the distance from the source. This means that those portions of the gate *p-n* junction which are most distant from the source will be biased most strongly in the reverse direction and a wedge shaped space-charge barrier will result. This space charge region is shown by the dotted areas of Fig. 1. The current flow is confined to the neutral channel (shown white in the figure). When the drain voltage reaches a critical limiting value,  $W_0$ , the channel is completely *pinched off* at its drain end. Virtually no further increases of drain current will result when the drain voltage is raised above  $W_0$ , the only effect of this voltage being to change the channel shape at constant current. The value of this *pinch-off voltage* is given by

$$W_0 = \rho_0 a^2 / 2K = \sigma a^2 / 2\mu K = qNa^2 / 2K \tag{2}$$

where  $a$  is the half-thickness of the channel,  $\rho_0 = qN$  is the magnitude of the fixed donor charge density in the space-charge region, and  $K$  is the dielectric constant. For germanium

$$K = 1.42 \times 10^{-12} \text{ farads/cm.}$$

The use of  $K$  in farads/cm rather than  $\kappa\epsilon_0$  in farads/m can be justified as indicated in ref. 1, page 1367.

Now suppose that the gate is biased negatively with respect to the source. Under these conditions the magnitude of the  $IR$  drop necessary to produce pinch-off will be smaller, since part of this voltage is already supplied by the bias, and saturation will accordingly occur at a lower value of drain voltage and current. Shockley has shown that, if the wedge-shaped channel referred to above narrows sufficiently slowly, then, for drain voltages less than the saturation value of  $V_D$ , the current (per unit length in the  $Z$  direction) is given by<sup>2</sup>

$$I_D = (1/L)[J(V_D - V_G) - J(V_S - V_G)] \tag{3}$$

where the function  $J$  is given by

$$\begin{aligned} J(x) &= 2\sigma a x [1 - (2/3)(2xK/\rho_0 a^2)^{1/2}] \\ &= g_0 x [1 - (2/3)(x/W_0)^{1/2}]. \end{aligned} \tag{4}$$

Above the saturation value of  $V_D$  the current is substantially constant.

It will be convenient to introduce certain natural parameters defined as follows:

$$\begin{aligned} W_0 &= \rho_0 a^2 / 2K \\ E_0 &= \rho_0 a / K = 2W_0 / a \end{aligned}$$

<sup>2</sup> W. Shockley has discussed the case of a *p*-type channel. For the *n*-type channel appropriate changes of sign must be made.

$$g_0 = 2\rho_0\mu_0 a = 2\sigma a$$

$$I_0 = g_0 E_0 = 2\rho_0^2 \mu a^2 / K$$

$$\tau_0 = a / \mu_0 E_0 = K / \mu_0 \rho_0 = K / \sigma.$$

In Fig. 2 we have shown the drain voltage-current characteristics as obtained from (3) and (4). It can be seen from the form of (3) that different values of  $V_G$  translate the curve in both the  $I_D$  and  $V_D$  directions. As a consequence of this, the curve joining the saturation points of the characteristics (shown dotted) is simply the  $V_G = 0$  curve rotated through  $180^\circ$ .

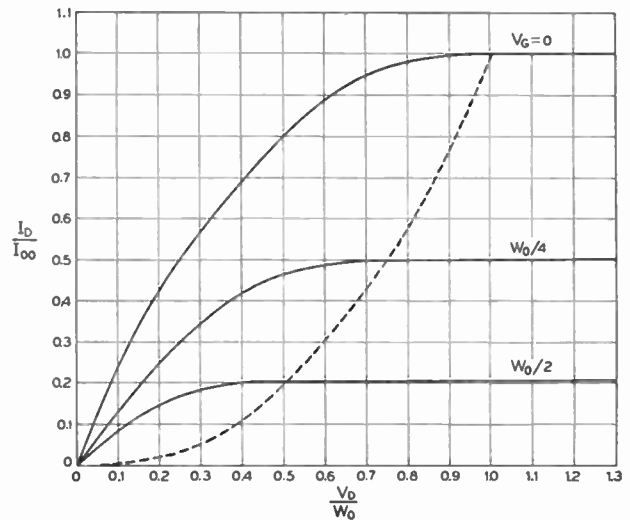


Fig. 2—Normalized drain characteristics with source at zero potential. The dashed curve shows the locus of the pinch-off points (see text).

Comparisons of these theoretical curves with those experimentally determined will be made in Part II. The gate currents, in general, will be the reverse saturation current of the gate *p-n* junction and can be neglected.

We are now in a position to calculate the transconductance of the device. From (3) and (4) we obtain

$$\begin{aligned} g_m &= \left. \frac{\partial I_D}{\partial V_G} \right|_{V_D = \text{const}} \\ &= (2\sigma a / LW_0^{1/2}) [(V_D - V_G)^{1/2} - (V_S - V_G)^{1/2}]. \end{aligned} \tag{5}$$

Now if in particular we take  $V_S = 0$  and  $(V_D - V_G) = W_0$  corresponding to grounded source and operation in the pinch-off region, this reduces to

$$\begin{aligned} g_{mG} &= (2\sigma a / L) [1 - (-V_G/W_0)^{1/2}] \\ &= g_{m0} [1 - (-V_G/W_0)^{1/2}] \end{aligned} \tag{6}$$

where we have introduced

$$g_{m0} = \frac{2\sigma a}{L} \tag{7}$$

the maximum transconductance. This quantity can be obtained from the nomograph of Fig. 4.

The saturation drain current  $I_{D0}$  which flows for any gate voltage can be obtained from (3) and (4) by setting  $V_S = 0$ ;  $(V_D - V_G) = W_0$ . This yields

$$I_{D0} = (g_{m0} W_0 / 3) [1 + (V_G/W_0)(3 - 2\sqrt{-V_G/W_0})]. \tag{8}$$

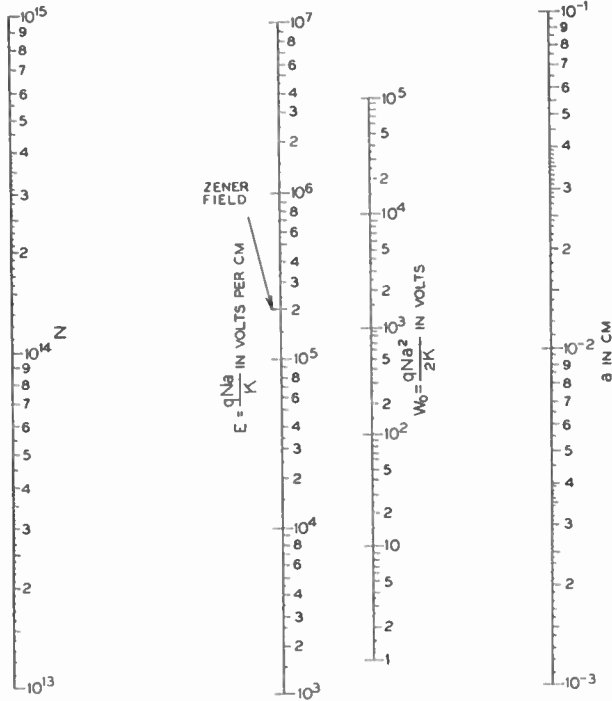


Fig. 3—Pinch-off nomograph.

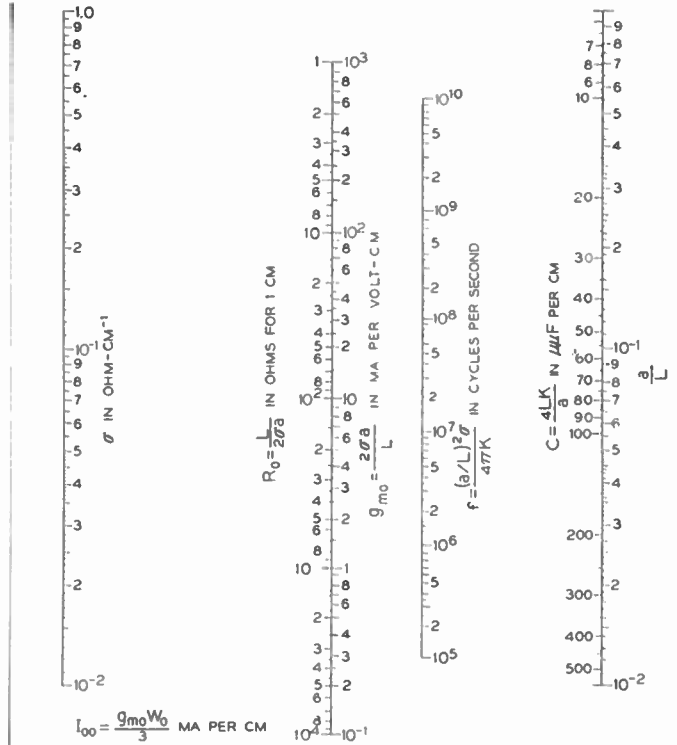


Fig. 4—Field-effect transistor nomograph.

We see from this that the current is completely cutoff for a gate voltage of  $V_G = -W_0$ . Maximum current is

$$I_{D0} = g_{m0}W_0/3 \tag{9}$$

obtained for zero bias on the gate.

The frequency response of the device can be estimated by the following simple argument. In order to change the gate voltage the capacity of its *p-n* junctions must be charged through the resistance of the channel. This process has an associated time constant which limits the frequency response. Let us assume a wedge-shaped channel, completely pinched off at the drain end and completely open at the source end (that is  $V_G = V_S = 0$ ). The capacity for unit length in the *Z* direction is approximately

$$C \simeq 4KL/a. \tag{10}$$

The factor 4 arises because the average width of the space-charge region is approximately  $a/2$  and because there are two such regions, one on either side. This capacity on the average charges through half the resistance of the channel, i.e.

$$R = L/2a\sigma. \tag{11}$$

We would accordingly expect a limiting frequency *f* given by

$$f = 1/2\pi RC = a^2\sigma/4\pi L^2K. \tag{12}$$

These relationships are also shown on the nomograph of Fig. 4.

### 3. Modifications of the Ideal Theory

The theory presented in Section 2 deals with an ideal structure. In practice we shall find it necessary to modify

the theory somewhat to take account of special experimental conditions. In particular we shall discuss the following effects:

- A. Series resistance of semiconducting paths at the source and/or drain contacts.
- B. Depletion of thermally generated carriers in units having conductivity close to intrinsic.
- C. Negative resistance effects due to hole current flow into the gate.
- D. Temperature effects.

A. *Series Resistance.* In Section 2 we have considered that source and drain connect directly onto the channel between the gates. It has been found necessary in the fabrication of these units, however, to allow a small bridge of semiconductor between the actual contact and the gate, an example of which is shown in Fig. 5. This means that a series resistance appears between the electrodes to which voltages are applied and the working part of the structure. It is possible to take account of these resistances by simple circuit theory.

For the calculation of  $g_m$  one must recognize two differences. Firstly, the voltages which must be inserted into (5) to obtain the transconductance of the working part of the structure must be changed as follows:

$$V_G \rightarrow V_G, V_S \rightarrow -IR_S, V_D \rightarrow (V_D - IR_D) \tag{13}$$

where  $R_S$  and  $R_D$  are the values of the source and drain resistances. Secondly, the degeneration of the source resistor must be taken into account. If the apparent transconductance is denoted by  $g_m'$ , we must write

$$g_m' = g_m/(1 + R_Sg_m) \tag{14}$$

which takes account of the fact that a fraction of any increase in gate voltage appears as an increased drop

across the source resistor. In (14), of course,  $g_m$  must be calculated considering the modifications (13).

It is clear from (14) that if  $g_m R_s \gg 1$ , then the transconductance  $g_m'$  is simply given by  $1/R_s$ . If then we are to obtain the potentially high transconductance of the device, we must keep the source resistance small. The drain resistance does not have as serious consequences, the chief disadvantages being, (a) the necessity of having a higher supply voltage, and (b)  $I_D^2 R_D$  heat which must be dissipated.

The source resistance also alters the frequency response. One must add  $R_s$  to the  $R$  of (12) in obtaining the limiting frequency.

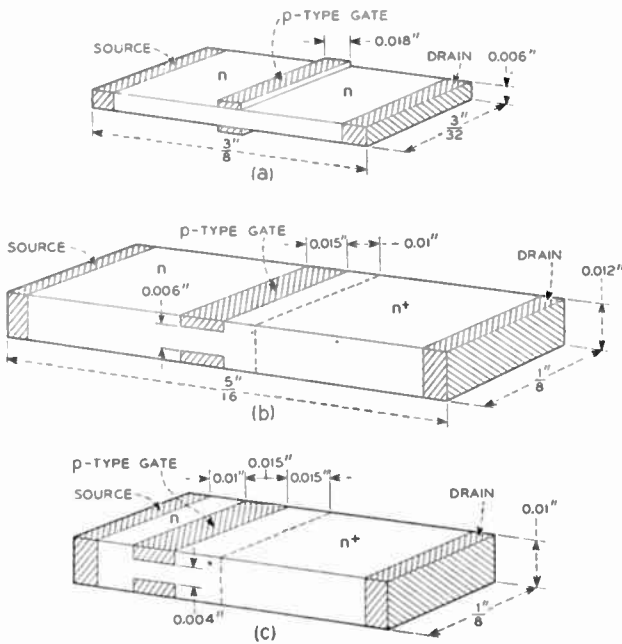


Fig. 5—Schematic diagrams of experimental units.

**B. Carrier Depletion.** Suppose, as in Fig. 5(b), that at the drain end the germanium is made strongly  $n$ -type (designated  $n^+$ ). Such a  $n$ - $n^+$  junction will not act as a source of holes. Now the direction of current flow is such that electrons tend to flow into the drain, and holes into the source. These holes must largely arise by generation processes within the volume of the semiconductor or at the free surfaces, and these holes will tend to be depleted. In order to maintain electrical neutrality within the body of the crystal an equal density of electrons must also be depleted. In the limit of strong applied fields, such that carriers are swept out in a small fraction of a mean lifetime, virtually all of the holes will be swept out and the only remaining carriers will be electrons equal in density to the excess donor density. In material which is close to intrinsic conductivity this means the apparent conductivity will go down. In fact

$$\sigma = q\mu_n N$$

instead of

$$\sigma_i = q\mu_n n_i (1 + 1/b)$$

so that the conductivity has changed in the ratio

$$\sigma/\sigma_i = (Nb/n_i)/(1 + b) \approx 2N/3n_i \quad (15)$$

**C. Negative Gate Resistance.** It is possible, in units with no  $n$ - $n^+$  junction where an appreciable fraction of the current is carried by holes, to obtain a negative gate resistance. This effect arises as follows: Suppose that the gate is made more positive so that it opens somewhat and allows additional electron current to flow in the channel. This additional electron current is accompanied by an increased hole current on the drain side of the gate, since electrical neutrality must be maintained. If the unit is operating in the pinched-off region, however, these holes will not flow through the channel but will instead flow to the gate. This is the case because, while the electric field in the pinched-off space-charge region near the drain is directed away from the axis of the channel and is thus focussing for electrons, it tends to pull holes into the gate. From this argument we see that a positive change of gate voltage results in an increased flow of holes to the gate and thus in a negative change in the current flowing into the gate. Hence the gate terminal presents a negative resistance.

The holes referred to in the argument above may arise from three sources: (a) They may be thermally generated in the body of the semiconductor; (b) they may be generated at low life time areas on the surface; or (c) they may be injected at the contacts. It might be desirable to make a device in which the drain contact was intentionally made hole-injecting (say by the use of a  $p$ - $n$  junction) and in which the negative resistance effects would thus be greater.

**D. Temperature Effects.** As can be seen from the nomographs, the unipolar field effect transistor is a relatively high power device. Furthermore, most of the power dissipation takes place in the space-charge region of the drain. Therefore the removal of heat will be a major problem. These devices should probably not prove as temperature sensitive as the  $n$ - $p$ - $n$  transistor. The chief effect of heating is to increase the gate saturation current by increasing the number of thermally generated hole-electron pairs. It is true that the mobility also varies as  $T^{-3/2}$  but this variation is fairly slow and only serves to vary  $\sigma$  which enters the theory linearly. In Part II experiments are described which were performed at liquid air temperatures. Here, of course, the mobility has increased by a factor of about 8 times and major differences arise.

4. Design Considerations

The theory of the preceding sections has been summarized in the form of nomographs which are given in Fig. 3 and Fig. 4. In Fig. 3 we have given a nomograph for the calculation of the pinch-off voltage  $W_0$ . If a straight line is drawn between the value of  $N$  on the left scale and the value of  $a$  on the right scale, it intersects the center scales at  $W_0$  and at  $E$ , the maximum value of the electric field in the space charge region. Fig. 4 shows simultaneously the consistent field-effect parameters,  $a/L$ ,  $\sigma$ ,  $g_{m0}$ ,  $R_0$ ,  $f$  and  $C$ . A straight line drawn

across the chart intersects the various scales in a set of values which are consistent with a given design. The one remaining parameter of interest, the current, is easily obtained from (9).

It is clear from an inspection of the nomographs that the choice of material and dimensions is not completely arbitrary. It is desirable to have the pinch-off voltage reasonably low both in order to avoid heating and to avoid nonlinear mobility effects which set in at high electric fields and which would limit the transconductance. A low pinch-off voltage implies small spacing and/or small donor concentration. Small donor concentrations are undesirable however because of depletion effects and because both  $f$  and  $g_m$  are proportional to  $\sigma$ . The best compromise therefore is to make  $a$  and  $L/a$  as small as is mechanically feasible and then to choose  $N$  in order to make  $W_0$  reasonably small.

A typical design example is shown below

$$\begin{aligned} N &= 10^{14} \\ \sigma &= .059 \text{ mho/cm} \\ a &= 3 \times 10^{-3} \text{ cm} \\ W_0 &= 50 \text{ volts} \\ a/L &= .2 \\ g_{m0} &= 24 \text{ ma/volt cm} \\ f &= 140 \text{ Mc/S} \end{aligned}$$

## PART II, EXPERIMENTAL RESULTS

### 1. Introduction

This part contains a description of the experimental work that was done in order to test the theory of unipolar "field-effect" transistors. As discussed in Part I, section 4, a suitable choice of resistivity for the channel material would be about 20 ohm-cm. However, in order to have a pinch-off voltage of about 10 volts with such material, the channel width would have to be about  $10^{-3}$  cm and such a structure would be difficult to make. If higher resistivity material, say 50 ohm-cm, were used, the channel width for 10 volts pinch-off would be of the order of  $4 \times 10^{-3}$  cm and preparation would be much simpler. However, with such material, the effects of depletion of carriers would be appreciable and there would be a consequent loss of transconductance and frequency response. It was decided that, for the purposes of verifying the theory, performance characteristics could be sacrificed to ease of preparation and 47 ohm-cm  $n$ -type germanium was chosen.

Units were made with the three geometries shown in Fig. 5(a), (b) and (c). For clarity, the diagrams show the gates as being only on the top and bottom surfaces of the germanium blank. In practice, the gates extended over the sides of the blank to make a continuous loop. This was done in order to insure that none of the channel current flowed along the surfaces of the germanium. Pearson and Read had found that free surfaces in the channel region resulted in instability in the characteristics of their specimens. No special means were provided for removing heat generated in the specimens.

This would have required attaching cooling fins or a heat sink of some form to one of the three contacts. It was decided that the added complication was not justified in a preliminary survey of properties of the device.

In all, six specimens were made and tested. This part will include a discussion of three of these which exhibited all the salient features of the others.

### 2. Specimen PF 66 #2

The dimensions of the specimen are shown in Fig. 5(a). This was the first specimen to be made and was designed for ease of fabrication. Ohmic contacts for the source and drain were made at the ends of the germanium blank and the gates were situated approximately half way between source and drain. The theoretical pinch-off voltage, as obtained from the nomograph of Fig. 3, for a channel half-width of 0.003" in 47 ohm-cm  $n$ -type material is 32 volts.

With the specimen at 25°C and at 0°C, the static characteristics were measured and are reproduced in Figs. 6 and 7. Fig. 6 shows the  $I_D - V_D$  curves with  $V_G$  as parameter. The curves have the same form as the theoretical curves of Fig. 2. The experimental values of pinch-off voltage and transconductance at 25°C can be compared with the theoretical values as follows:

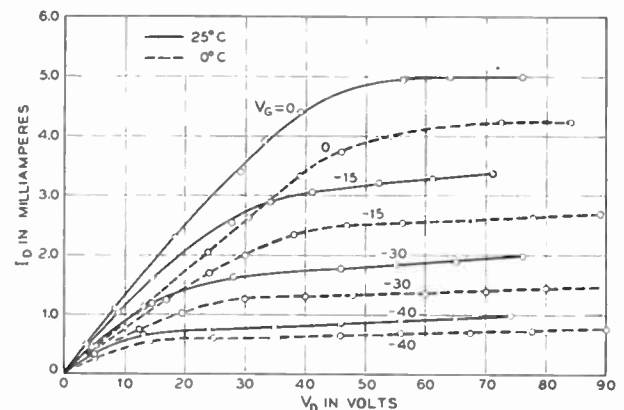


Fig. 6—Drain characteristics of unit PF66 #2. The solid curves are for 25°C and the dashed curves for 0°C.

It is first necessary to know the values of the source and drain resistances,  $R_S$  and  $R_D$ . The method of preparation of the specimen did not permit of accurate measurements of the source-to-gate and gate-to-drain distances and it is therefore impossible to calculate  $R_S$  and  $R_D$  directly. However, if  $V_G$  is zero and  $V_D$  small compared to  $W_0$ , the resistance between source and drain will be essentially the sum of  $R_S$ ,  $R_D$  and  $R_0$ . Hence this sum can be determined from the initial gradient of the  $I_D - V_D$  curve for  $V_G = 0$ . From this initial slope

$$R_S + R_D + R_0 = 7.8 \text{ K}\Omega.$$

From the nomograph of Fig. 4

$$R_0 = 400 \Omega$$

$$\therefore R_S + R_D = 7.4 \text{ K}\Omega.$$

Since the gate was half way between source and drain it is reasonable to take

$$R_S = R_D = 3.7 \text{ K}\Omega.$$



Now, for  $V_G=0$ ,  $I_D$  saturated at  $5mA$  with a drain voltage of 55 volts. The  $IR$  drop in  $R_D$  was then 18.5 volts. Hence

$$W_0 = 55 - 18.5 = 36.5 \text{ volts.}$$

This value is in fair agreement with the theoretical value of 32 volts. The transconductance of the channel for  $V_G=0$  can be determined from (5)

$$g_m = \frac{2\sigma a}{L} \left[ \frac{(V_D - V_G)^{1/2} - (V_S - V_G)^{1/2}}{(W_0)^{1/2}} \right] \quad (5)$$

by putting  $2\sigma a/L = g_{m0}$ ,  $V_G=0$  and  $V_D - V_G = W_0$  giving

$$g_{mS} = g_{m0} \left[ 1 - \left( \frac{V_S}{W_0} \right)^{1/2} \right].$$

In this case  $g_{m0}$  as determined from Fig. 4 is  $1.67 \text{ mA/V}$ ,  $W_0 = 36.5V$ ;  $V_S = R_S(I_D - I_G) = 3.7(5 - 1.5) = 13V$   
 $\therefore g_{mS} = 0.67 \text{ mA/V}$ .

The effective transconductance  $g_m'$ , for  $V_G=0$ , is then obtained from (14)

$$g_m' = \frac{g_m}{1 + R_S g_m} = 0.19 \text{ mA/V.}$$

From Fig. 6 the average transconductance over a range of  $V_G$  from 0 to  $-15$  volts is found to be  $0.12 \text{ mA/V}$ . This value is smaller than the calculated value for  $V_G=0$  as would be expected since (6) shows that the transconductance decreases as  $V_G$  becomes more negative. A more useful comparison could be made with the calculated value of  $g_m'$  for  $V_G = -7.5$  volts. For these conditions (5) and (14) give  $g_m' = 0.16 \text{ mA/V}$ . The agreement between this and observed value of  $0.12 \text{ mA/V}$  is within the accuracy of the calculations.

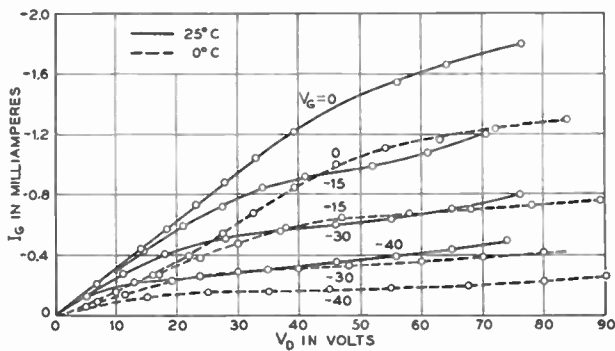


Fig. 7—Gate current versus drain voltage for specimen PF66 #2.

Fig. 7 shows the  $I_G - V_D$  curves with  $V_G$  as parameter. As discussed in Part I, section 3, the gate current consists of holes which could arise in three ways: thermal generation in the germanium between gate and drain, generation at a surface of the germanium, and injection at the drain. For this specimen, the gate currents obtained from the first two causes would be of the order of  $100\mu A$  and would be very temperature dependent. Fig. 7 shows that the gate current was as high as  $2mA$  and that a temperature change of  $25^\circ C$  produced

only 30 per cent change in  $I_G$ . This suggests that the gate current arose predominantly from hole injection at the drain. If this were the case, then the gate current and drain current at any particular values of  $V_D$  and  $V_G$  should be related by the equation

$$\frac{I_D}{I_G} = \frac{n_0\mu_n E + p_0\mu_p E}{p_0\mu_p E} = \frac{n_0\mu_n + p_0\mu_p}{p_0\mu_p}$$

where  $n_0$  and  $p_0$  are the equilibrium densities of electrons and holes,  $\mu_n$  and  $\mu_p$  their mobilities, and  $E$  the electric field at the drain contact.

For this material

$$\begin{aligned} n_0 &= 3 \times 10^{13}/\text{cm}^3 \\ p_0 &= 2 \times 10^{13}/\text{cm}^3 \\ \mu_n &= 3600 \text{ cm}^2/\text{volt-sec} \\ \mu_p &= 1700 \text{ cm}^2/\text{volt-sec} \\ \therefore \frac{I_D}{I_G} &= 4.08 \end{aligned}$$

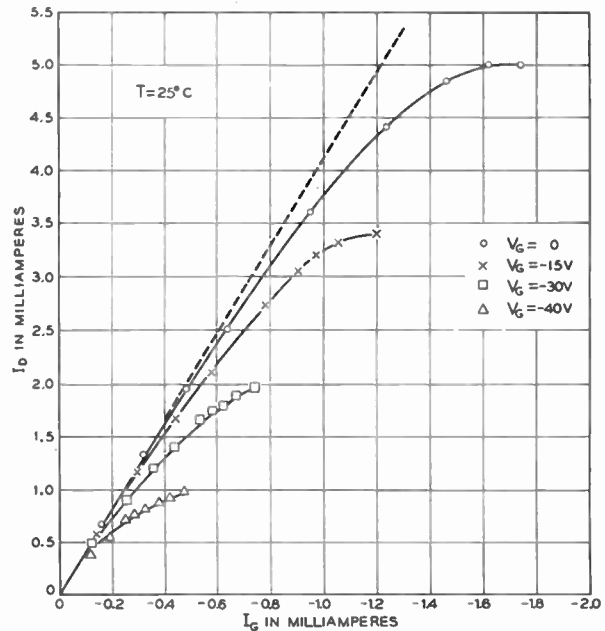


Fig. 7(a)—Drain current versus gate current with gate voltage as parameter for specimen PF66 #2. The theoretical relationship is shown in the dashed curve.

Fig. 7(a) gives a plot of  $I_D$  vs.  $I_G$  with  $V_G$  as parameter, the progression towards higher currents on each curve corresponding to increasing values of  $V_D$ . The broken line is the theoretical relationship. It is seen that initially the experimental curves follow the theoretical one but that at higher currents the gate current increases more rapidly. This deviation of gate current is of the order of magnitude that would be obtained from holes generated in the body and at the surfaces of the germanium. It may be concluded that the gate current arose from all three causes but that injection at the drain was the predominant effect.

In Fig. 8 the data of Fig. 7 has been replotted to give the gate characteristic. The figure shows that the gate exhibits negative resistance, as predicted by the theory of Part I, section 3, and that its magnitude varies from  $30 \text{ K}\Omega$  at  $V_D=60$  volts to very large values at  $V_D=10$

volts. It should therefore be possible to make the unit oscillate by putting an  $L-C$  resonant-circuit in series with the gate. This was done with the specimen operating at  $V_D=60$  volts and  $V_G=0$  and oscillations were produced up to a frequency of 100 kc. It was found that the oscillations were killed by shunting the resonant circuit with a resistance of less than about 30 K $\Omega$  which is the magnitude of the negative resistance at these operating conditions.

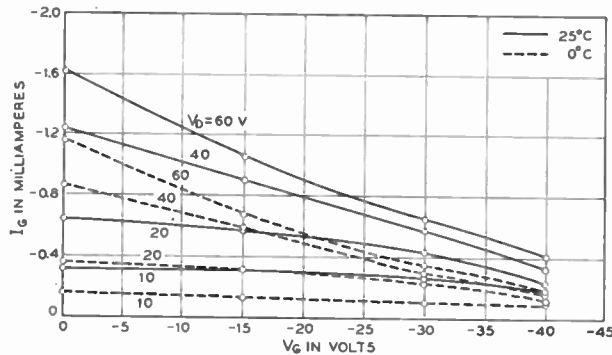


Fig. 8—Gate characteristic for specimen PF66 #2. The solid lines refer to 25°C and the dashed lines to 0°C.

The measurements on this specimen showed that this form of structure would result in an amplifying transistor in agreement with the theory and that emission of holes from the drain caused the gate to have a negative resistance. If a unit were required as a negative-resistance oscillator, then it would be desirable to enhance the emission of holes from the drain. This could be achieved by using a  $p-n$  junction as the drain contact. However, for an amplifying transistor, this negative gate-resistance and the high values of gate current associated with it would both be undesirable. For this application, emission of holes from the drain should be reduced to a minimum. This could be achieved by using an  $n-n^+$  junction for the drain contact. The next specimen to be described, PF 70 #7, was made this way.

### 3. Specimen PF 70 #7

The dimensions of the specimen are shown in Fig. 5(b). The resistivity of the  $n$  material was 47 ohm-cms, and the resistivity of the  $n^+$  material was less than 1 ohm-cm. To reduce the value of  $R_D$  the gate was placed as close as possible to the drain (approximately .01").

As discussed in Part I, section 3, virtually all the holes will be swept out of the structure if the transit time for holes is small compared to the lifetime. For this specimen the transit time for holes across the distance  $l$  from drain to source will be approximately

$$l^2 = \frac{\left(\frac{5}{32}\right)^2}{\mu_p V_D} = \frac{15}{V_D} \times 10^{-6} \text{ secs.}$$

Therefore, if  $V_D=1$  volt, the transit time will be of the order of  $15\mu$  secs which was small compared to the lifetime of the material. It is thus reasonable to assume that, at all normal operating conditions, the material will be swept free of holes. Conductivity will then be

maintained by the remaining electrons which are just those required to neutralize the excess charge-density of the excess donors, in this case  $10^{13}/\text{cc}$ . The effective conductivity will therefore be

$$10^{13} \times 1.6 \times 10^{-19} \times 3600 = 5.8 \times 10^{-3} \text{ mho/cm.}$$

The estimated pinch-off voltage from Fig. 3 is 32 volts.

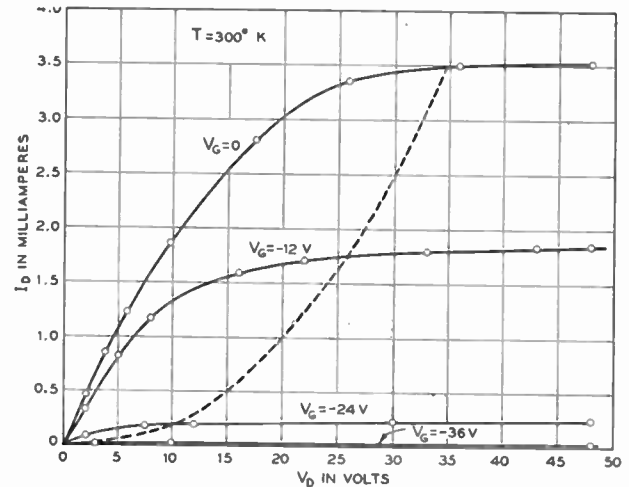


Fig. 9—Drain characteristic at 300°K for PF20 #7. The dashed line is the same shape as the  $V_G=0$  line but is rotated through 180°. Note this curve is approximately the locus of pinch-off points.

With the specimen at 300°K and at 77°K, the static characteristics were measured and are reproduced in Figs. 9–12. Fig. 9 shows the  $I_D-V_D$  curve with  $V_G$  as parameter and the specimen at 300°K. The theoretical values of pinch-off voltage and transconductance can be estimated as for the previous specimen. In this case, the magnitude of  $R_D$  is sufficiently small so that the  $IR$  drop in it can be neglected and, hence, the value of  $V_D$  at saturation is equal to  $W_0$ . The observed value of  $W_0$  is then about 35 volts and the theoretical value 32 volts. The observed value of  $g_m'$  over a range of  $V_G$  from 0 to  $-12$  volts is  $0.14 \text{ mA/V}$  while the calculated value at  $V_G=-6$  volts is  $0.19 \text{ mA/V}$ . Hence, the theory and experiment are in reasonable agreement.

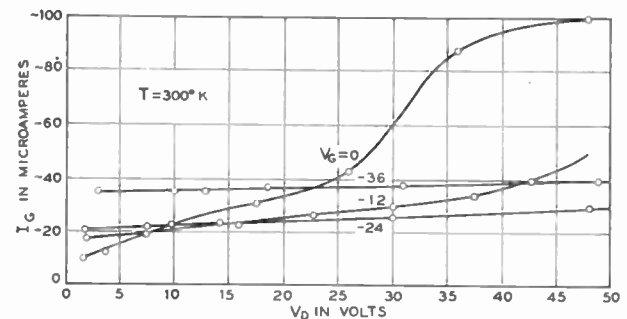


Fig. 10—Gate current versus drain voltage for specimen PF70 #7 at 300°K.

Fig. 10 shows the plot of  $I_G-V_D$  with  $V_G$  as parameter. It is seen that the gate current is now less than 100  $\mu\text{A}$ . Injection of holes at the drain had therefore been greatly reduced or eliminated. Also  $I_G$  increased most rapidly with  $V_D$  under conditions where  $V_D$  was large and  $V_G$  small. Since these are the conditions under

which the power dissipated in the unit was greatest and hence the temperature highest, the evidence suggests that the source of current was thermal generation of holes. The data of Fig. 10 have been replotted in Fig. 11 to give the gate characteristic. When the power dissipation was greatest the gate exhibited negative resistance. This is in qualitative agreement with theory since under these conditions the temperature, and therefore rate of generation of holes, is highest and therefore the proportion of current carried by holes is greatest.

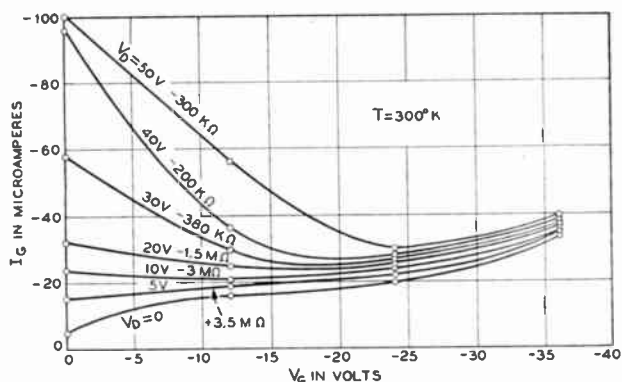


Fig. 11—Gate characteristic of specimen PF70 #7 at 300°K.

As shown in Part I, section 3, negative resistance can occur under such conditions. When the power dissipated and hence the temperature and rate of hole generation was lowest, the gate exhibited positive resistance. The negative resistance of the gate was always greater than 200 KΩ and therefore the specimen should be stable, provided the impedance in the external circuit to the gate is less than this value. The specimen could therefore be conveniently used as an amplifier. Furthermore, if means were provided to take away the heat generated in the unit, as by attaching cooling fins, negative resistance of the gate could be further increased.

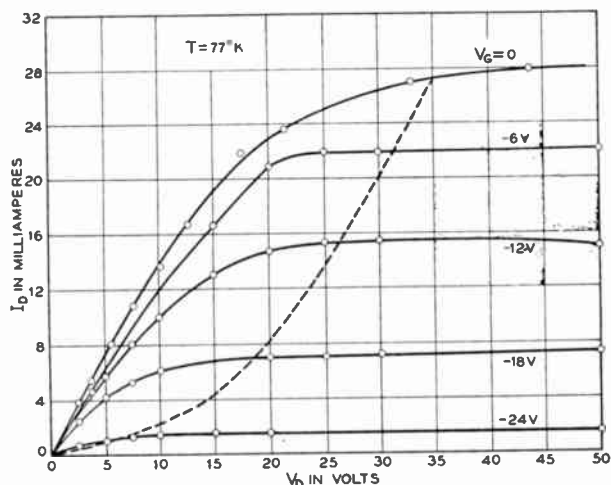


Fig. 12—Drain characteristic of specimen PF70 #7 at 77°K. Note reversed  $V_G=0$  curve shown dashed.

Fig. 12 shows the  $I_D - V_D$  curves with the specimen at 77°K. The observed value of  $W_0$  is 35 volts compared to a theoretical value of 32 volts. The observed value of  $g_m'$  over a range of  $V_G$  from 0 to -6 volts is  $1 \text{ mA/V}$

while the calculated value at  $V_G = -3$  volts is  $0.95 \text{ mA/V}$ . The gate current was found to be always less than  $1 \mu\text{A}$ . At this temperature the thermal generation of holes should have been very small. Therefore, so must the injection of holes at the drain.

#### 4. Specimen PF 73 #10

The dimensions of the specimen are shown in Fig. 5(c). The source-to-gate distance was made as small as possible in order to decrease the value of  $R_S$  and hence increase the effective transconductance. The width of the channel was decreased in an attempt to achieve a lower value of pinch-off voltage.

With the specimen at 300°K and at 77°K, the static characteristics were measured and are reproduced in Figs. 13 to 16. Fig. 13 shows that  $I_D - V_D$  curve with  $V_G$  as parameter and the specimen at 300°K. The resistance as calculated from the initial slope of the  $V_G = 0$  curves is  $2.2 \text{ K}\Omega$  while the channel resistance,  $R_0$ , as determined from Fig. 4 is also  $2.2 \text{ K}\Omega$ . It may therefore be concluded that effectively all the resistance occurred in the channel and that both  $R_S$  and  $R_D$  may be neglected. The calculated pinch-off voltage is 14 volts while the observed value was about 12 volts. The observed transconductance over a range of  $V_G$  from 0 to -3 volts was  $0.32 \text{ mA/V}$  while the calculated value at  $V_G = -1.5$  volts is  $0.30 \text{ mA/V}$ . Figs. 14 and 15 show the  $I_G$  characteristics which are similar in form to those for specimen PF 70 #7. The frequency response of the specimen was estimated by connecting it as a tuned-drain feedback oscillator and determining the maximum frequency at which it was possible to excite oscillation. The specimen was made to oscillate up to frequencies of  $4 \text{ mc/s}$ . This is in reasonable agreement with the theoretical maximum, as determined from Fig. 4, of  $6 \text{ mc/s}$ .

Fig. 16 shows the  $I_D - V_D$  curves for the specimen at 77°K. The observed pinch-off voltage was 12 volts compared to the theoretical value of 14 volts. The transconductance over a range of  $V_G$  from 0 to -3 volts was  $1.15 \text{ mA/V}$  as compared to the calculated value at  $V_G = -1.5$  volts of  $2.8 \text{ mA/V}$ . The observed value of transconductance was therefore much less than the calculated value and the discrepancy is too large to be attributed to experimental error. A possible explanation would be that the field in the channel is so high that the mobility is no longer independent of field. Ryder has shown<sup>3</sup> that, above a certain critical value of field, the mobility is proportional to  $1/E^{1/2}$  and that, for the  $n$ -type germanium at 77°K, the critical value is about 140 volts/cm. In this specimen, virtually all the potential drop of 12 volts would occur in the channel region. The average field in the channel was therefore  $12 \times 1000 / 15 \times 2.54 = 310$  volts/cm which is greater than the critical field. Since the field at the drain end of the channel is greater than the average field, at least part of the channel had a field greater than critical.

<sup>3</sup> E. W. Ryder, to be submitted to Phys. Rev. See also: W. Shockley, "Hot electrons in germanium and Ohm's law," *Bell System Tech. Jour.*, vol. 30, pp. 990-1034; October, 1951.

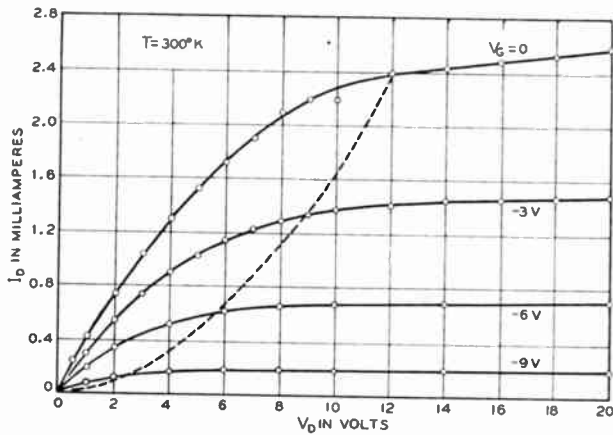


Fig. 13—Drain characteristic of specimen PF73 #10 at 300°K. Note locus of pinch-off points.

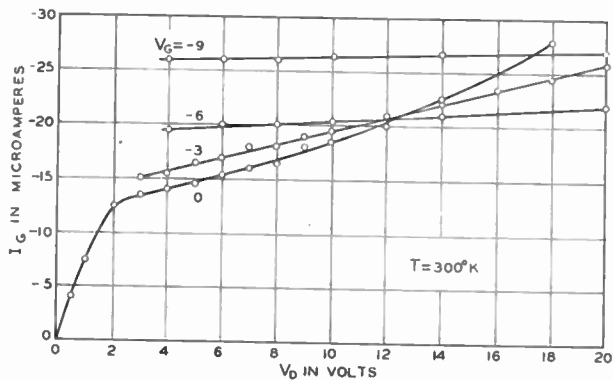


Fig. 14—Gate current versus drain voltage for specimen PF73 #10 at 300°K.

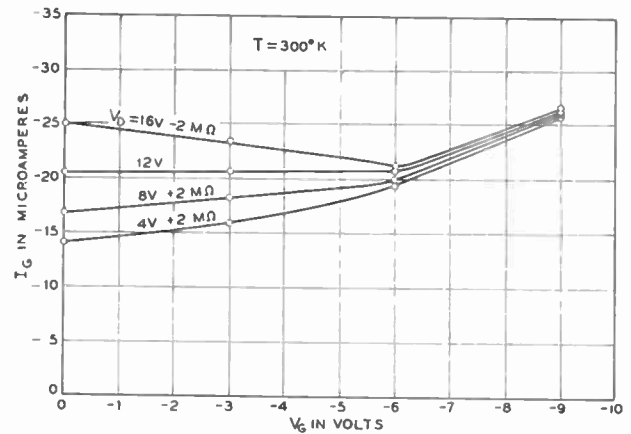


Fig. 15—Gate characteristic for specimen PF73 #10 at 300°K.

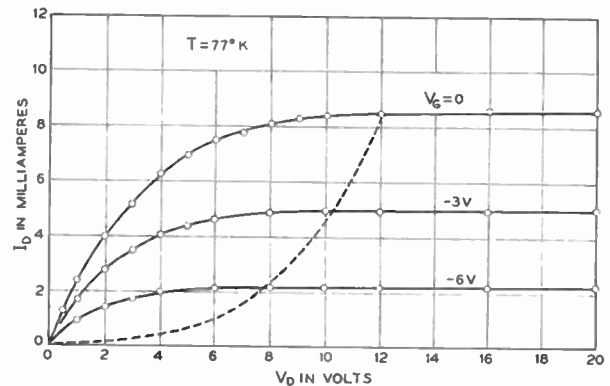


Fig. 16—Drain characteristic for PF73 #10 at 77°K.

Hence the effective conductivity and therefore the transconductance would be less than that calculated on the assumption of constant mobility. At 300°K the value of the critical field is about 900 volts/cm which is much greater than the maximum field present in the specimen. Hence at 300°K the theoretical and experimental values of transconductance should agree. The variation of mobility therefore seems capable of explaining the observed results.

### 5. Stability and Noise

The *D-C* characteristics of all the specimens were found to be stable with time. The characteristics were repeatable to a high accuracy. The specimens could be subjected to fairly high temperatures without changing the characteristics at room temperature. For example, the power dissipation in one specimen was on one occasion so great that the soldered gate connection melted. New leads were soldered on, the specimen re-etched and the characteristics found to be unchanged.

The noise properties of specimen PF 73 #10 were examined by H. C. Montgomery.<sup>4</sup> With the specimen at 300°K,  $V_D = 17.5$  volts,  $V_G = -3$  volts and a power gain of 19.6 *db*, the noise figure at 1000 c/S was 68 *db*. This is large compared to the noise figure for an average *n-p-n* of about 10-15 *db*. At 77°K, with  $V_D = 12.5$  volts,  $V_G = -4.7$  volts and a power gain of 30.2 *db*, the noise figure was about 35 *db*. By varying the bias conditions

<sup>4</sup> H. C. Montgomery, personal communication.

a minimum noise figure of 25 *db* was measured. The most significant change in the characteristics of the specimen in going from 77°K to 300°K is the increase in gate current. It may then be that the difference in noise figure can be attributed to the gate current. If this is the case, suppression of gate current at 300°K would lead to a unit having a noise figure comparable to an *n-p-n* transistor.

### PART III, CONCLUSIONS

The experimental results of Part II are substantially in agreement with the extended theory. Transistors have been made which at room temperature had transconductances as high as 0.3 ma/volt, and whose characteristics were very stable. A flat frequency response has been obtained up to about 3 mc/sec. In addition a new feature has been observed, namely negative gate resistance. The gate resistance can be made either positive or negative depending on the nature of the drain contact.

There is reason for confidence, based on the agreement with theory which has already been obtained, that the theory can be used to design transistors for higher transconductances and frequency response. Such a design was discussed in Part I sec. 4 where it was shown that using 17 ohm-cm germanium a transconductance of 24 ma/volt and an upper frequency limit of 140 mc/sec could be obtained. This does not necessarily represent a limiting design but should be well within the scope of present fabrication techniques.



The chief virtue of this new form of transistor is its high frequency response. To obtain similar frequency response with point contact or junction transistors would require structures with much smaller critical dimensions. This is a consequence of the unipolar nature of the device, that is, that essentially only the majority carriers are involved in its operation. Another important feature of field-effect transistors is their high input and output impedance together with high transconductance. In this respect they resemble pentodes. They are more efficient than pentodes, however, in that they do not require cathode heating power.

While, as stated above, it is possible to achieve high transconductance and frequency response, this can only be done at the expense of high current and power dissipation. Since, in addition, these units have a relatively high noise figure, it appears that they will not be suitable for low power applications. Units have been made of silicon<sup>5</sup> which have much lower noise figure but these have lower transconductance and frequency response.

#### Acknowledgments

The authors wish to acknowledge the help of P. W. Foy and W. Wiegmann in the fabrication of the units and of W. W. Bradley who supplied the germanium. They are also indebted to W. Shockley for advice and encouragement.

#### Symbols

$a$ —half thickness of channel  
 $b$ — $\mu_n/\mu_p$

<sup>5</sup> G. L. Pearson, *Phys. Rev.*, vol. 90, p. 336; 1953.

$C$ —capacitance  
 $E$ —maximum value of electric field in space-charge region  
 $E_0$ — $2W_0/a$   
 $f$ —frequency  
 $g$ —conductance  
 $g_0$ — $2\rho_0\mu a$   
 $g_m$ —transconductance  
 $I_D$ —current into drain  
 $I_G$ —current into gate  
 $I_S$ —current into source  
 $I_0$ — $g_0E_0$   
 $K$ —dielectric constant  
 $L$ —length of channel  
 $N$ —excess impurity concentration  
 $N_d, N_a$ —density of donors, acceptors  
 $q$ —electronic charge  
 $R$ —resistance of channel  
 $R_D$ —resistance of drain contact  
 $R_S$ —resistance of source contact  
 $R_0$ —resistance of channel at zero bias  
 $\tau_0$ — $K/\sigma$   
 $V_D$ —potential on drain  
 $V_G$ —potential on gate  
 $V_S$ —potential on source  
 $W$ —potential between channel and gate  
 $W_0$ —value of  $W$  for pinch-off  
 $Z$ —width of channel  
 $\rho_0$ —fixed charge density  
 $\sigma$ —conductivity  
 $\sigma_i$ —intrinsic conductivity  
 $\mu_n, \mu_p$ —mobility of electrons, holes

## A Subjective Study of Color Synchronization Performance\*

M. I. BURGETT, JR.†, SENIOR MEMBER, IRE

**Summary**—The NTSC color-synchronization signal is reviewed to determine its operational quality. A subjective testing system is then described which dissects various receiver functions such that the thermal-noise impairment in each function may be evaluated. Results of these subjective tests show that color-synchronization performance is completely adequate under conditions of thermal-noise interference. The tests also show that the limiting factors of performance are primarily those functions which are common to monochrome transmission.

**T**HE HIGH QUALITY of the NTSC color television<sup>1,2</sup> system is primarily obtained by the transmission of a greater amount of useful information

through the conventional television channel. This increase has been accomplished by utilization of the vacant frequency spectrum of monochrome television and by quadrature modulation of the color information upon a 3.898125 mc subcarrier. Realization of the extra information at the receiver, however, requires the presence of an unmodulated reference signal of the same frequency and of known phase relative to one of the modulation components of the subcarrier. Thus, an extra synchronizing function is necessary in the system to provide the information required to generate the color-reference signal.

In choosing the form of the color-synchronizing signal, it is obvious that several requirements must be met. First, the signal must contain sufficient energy so that adequate-noise performance may be obtained at noise levels so high that the picture is no longer useful.

\* Decimal classification: R583.13. Original manuscript received by the Institute, September 5, 1952; revised manuscript received April 13, 1953.

† Project Engineer, Philco Corporation, Philadelphia, Pa.

<sup>1</sup> B. D. Loughlin, "Recent improvements in band-shared simultaneous color television," *Proc. I.R.E.*; October, 1951.

<sup>2</sup> C. J. Hirsh, W. F. Bailey, and B. D. Loughlin, "Principles of NTSC compatible color television," *Electronics*; February, 1952.

Quantitatively, this energy level depends upon the required accuracy of the signal, which in the NTSC system is plus or minus 10 to 20°. The signal also must be of such a type that the phase relative to the color-carrier components is maintained under conditions of receiver tuning or drift. Since the phase characteristics of receivers are generally nonlinear in the vicinity of the chroma carrier, compensation for tuning or drift is most simply carried out by using a color-synchronization signal that has the same frequency as the color carrier so that the relative phase shift will remain constant. This argument may be extended to multipath considerations, as well, since small echoes cause the phase of the sync and chroma information to be shifted by the same amount when the frequency of each is identical, so that the relative phase is unchanged. In addition the signal should be such that compatibility is maintained in existing monochrome receivers.

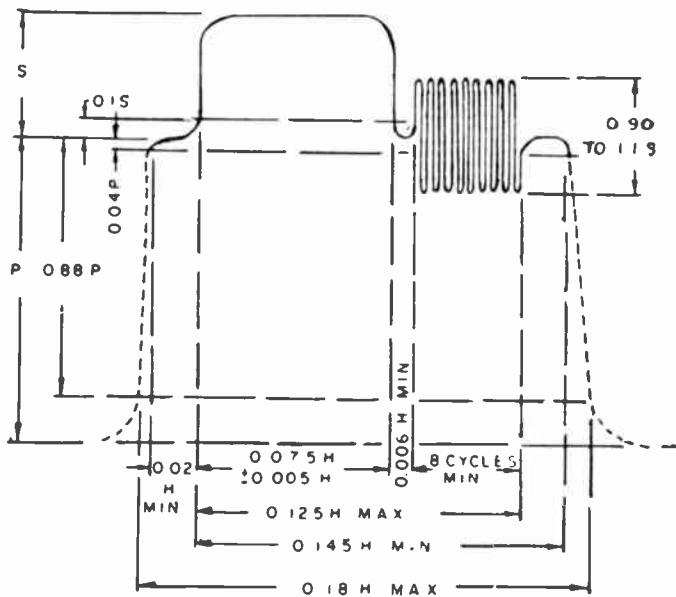


Fig. 1—NTSC compatible color television.

The NTSC specification for the color-sync signal was that adopted by NTSC Panel 14 on May 20, 1952 as shown in Fig. 1 in which a nine-cycle burst of color carrier is inserted upon the back porch of the horizontal-synchronizing signal. At the receiver the burst may be used to create the CW color-reference signal by means of narrow-band filters, locked oscillators, or APC circuits. Since the burst is synchronous in frequency with the color carrier, changes in tuning of the receiver or drift have no effect. This is also true of small echoes as explained previously. It is the purpose of this paper to show the adequacy of the burst method of color synchronization under noise conditions.

Since the merit of a function depends upon how well the intended purpose is accomplished, evaluation of the merit should be made in terms of that purpose. Application of this logic to synchronization in compatible color television suggests that the adequacy of color-syn-

chronization performance should be measured in terms of the basic terminal of the system which is the eye. This may best be accomplished by subjective tests.

Results of such tests depend upon the equipment and operational details; accordingly, these details should be known. The first factor to be considered is restriction of observer reaction to the factor of interest such as the color synchronization. Obviously, a presentation of a noisy signal on a color receiver would show impairment caused by noise in the picture information and deflection synchronizing as well as color synchronization. Thus, noise should be controllable in each of these channels so that impairment may be isolated to a particular function. With this general technique, impairment may be measured for each function of the color system individually so that the separate impairments may be related to each other to determine both absolute and relative subjective performance to a high order of accuracy.

In order to obtain greater dependability and accuracy in the test equipment, the tests were performed by noise matrixing with the composite color video. Fig. 2 illustrates the arrangement of the test equipment in block diagram form.<sup>3</sup> A composite-color video signal was fed to the input of six combiners whose outputs acted as signal sources for the picture-luminosity information, picture-chroma information, deflection synchronization, frame synchronization, and color synchronization for a color receiver, and for a complete monochrome receiver. Noise was introduced into each of the combiners either independently or in combination in such a manner that the operator conducting the test could vary the effective signal-to-noise ratio in a particular channel or channels at will. This allowed the observer to have the noise varied in one or more channels until the impairment corresponded to a particular comment which described his subjective reaction to the impairment caused by the function or functions in relationship to the signal-to-noise ratio.

The noise generator was a modified IF and RF section of a television receiver in which the antenna lead had been replaced by a dummy load and the whole unit well shielded. Normally this type of system would generate thermal noise with a triangular frequency spectrum. However, by increasing the bandwidth slightly and by proper video peaking, the noise spectrum may be made substantially flat throughout the normal television band. After giving effect to these changes, a check of the frequency spectrum of the noise showed it to be flat within 1.5 db of the average level as illustrated in Fig. 3. The chain which handled the noise also was checked so that the uniform spectrum was actually maintained through the combiners. The video and noise levels were set so that when the attenuators were set at minimum the effective signal-to-noise ratio at the output of the

<sup>3</sup> The technique presented here was originally developed to evaluate the merits of an earlier color system. Results of those tests were described in a paper by E. M. Creamer and M. I. Burgett, Jr., "Performance of Carrier Synchronizing Circuits for Color Television Signals," presented at the March, 1951 IRE Convention.

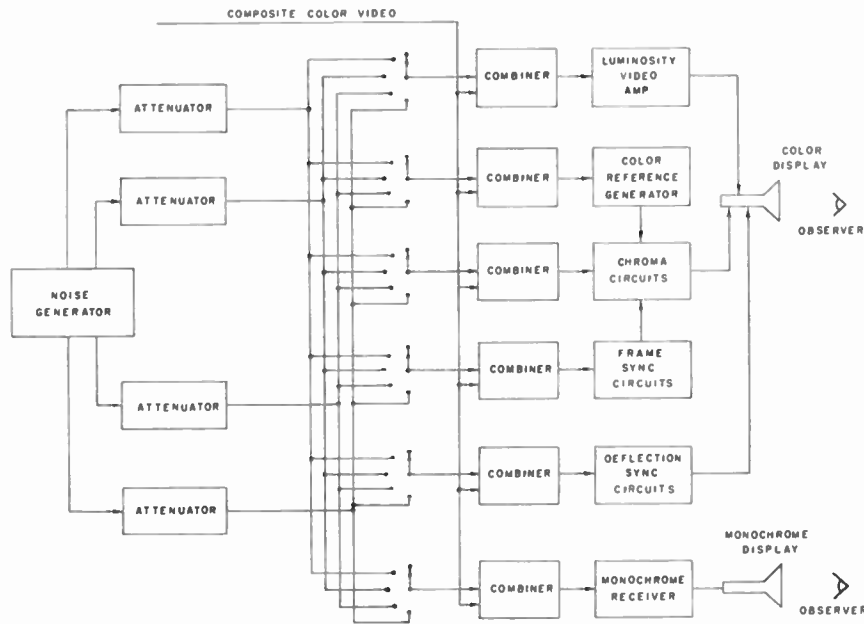


Fig. 2—Block diagram of noise and signal matrixing.

combiners was  $-2$  db. Thus, variation of the calibrated attenuator setting could vary the signal-to-noise ratio of a channel in steps of 1 db over the range minus 2 to 60 db. As defined in these tests, signal-to-noise ratio is the ratio of the peak video measured at the sync tips

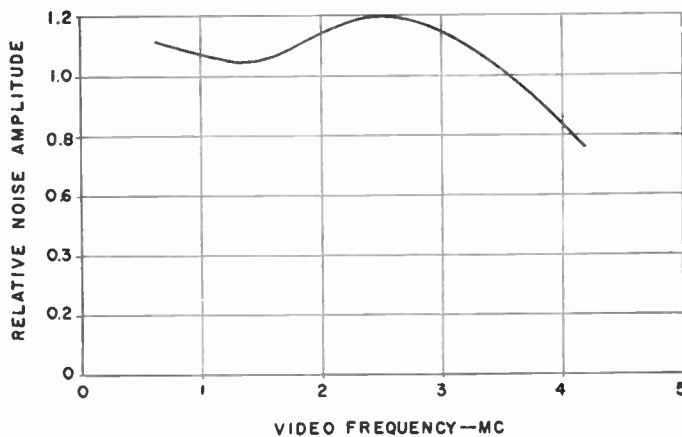


Fig. 3—Relative spectrum of noise generator.

and referenced against white to the RMS value of the noise. It should be noted that this definition gives a signal-to-noise ratio which is pessimistic by a voltage factor of approximately four in comparison with the definition frequently used in which both video and noise are measured as peak-voltage ratios.

The signal used during the tests was a standard NTSC color transmission, as specified in the NTSC press release of November 26, 1951, of two of the NTSC reference test slides which showed a girl's face next to a sunflower set against a blue-sky background and a vase of roses set against a black-and-white background containing considerable detail. The color sync contained nine cycles of color carrier whose peak-to-peak height was 90 per cent of the deflection-sync height.

A trinescope adjusted for a highlight brightness of 35 foot-lamberts was used for the display of the composite picture. To avoid bias by the observer in rating the picture, the functions of the various controls and their calibration was disguised so that observer comment was restricted to the picture itself.

Studies by Mertz, Fowler, and Christopher<sup>4</sup> have shown that certain standard comments have an approximately linear relationship to psychological or liminal units. Accordingly, their recommended comments were used in the tests as rating factors, i.e., the observers were asked to adjust the controls until a particular comment was obtained. These impairment rating comments were:

1. Not perceptible.
2. Just perceptible.
3. Definitely perceptible, but only slight impairment to picture.
4. Impairment to picture but not objectionable.
5. Somewhat objectionable.
6. Definitely objectionable.
7. Not usable.

Ten observers at a viewing distance of four times the picture height used these comments to rate the thermal-noise performance of the picture, brightness information, the picture-chroma information, deflection synchronization, frame synchronization, and color synchronization of the color receiver on two different pictures. In addition, noise was injected into all channels of a color and of a monochrome receiver to show total picture impairment under the same noise conditions.

The averages of the noise settings at each impairment rating are plotted in Fig. 4 for individual functions and

<sup>4</sup> Pierre Mertz, A. D. Fowler, and H. N. Christopher, "Quality rating of television images," *Proc. I.R.E.*; November, 1950.

in Fig. 5 for total performance and for color synchronization. Fig. 4 shows that the limiting factor in the noise performance of the color signal is the luminosity information at all noise levels. Second-order limitation is primarily the deflection synchronization though the chroma-picture information has about the same noise performance. Thus, it may be seen that the controlling factors in the color-system performance are exactly the same as those met in the basic monochrome signal.

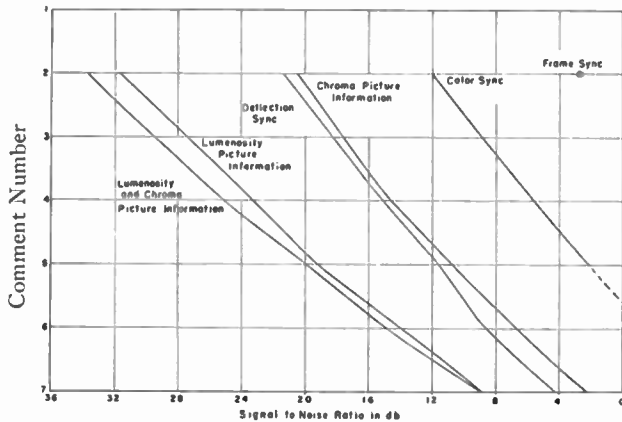


Fig. 4—Subjective response to noise in color receiver functions.

The chroma-picture information showed about the same impairment as deflection synchronization at low noise levels, but deflection synchronization caused appreciably more impairment under high noise conditions. It is interesting to note the noise-performance differential that exists between the picture luminosity and

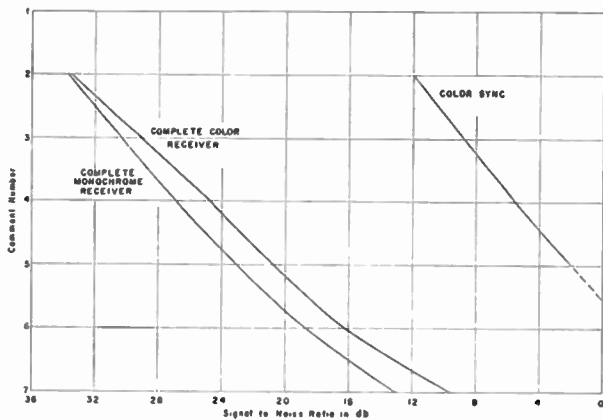


Fig. 5—Subjective response to noise in color and monochrome receivers.

chroma information which demonstrates the noise advantages obtained by the constant-luminance features of the NTSC system.

The impairment caused by color synchronization was far lower than that caused by the picture information and deflection synchronization. In fact, the picture information had reached a point where it was classified as definitely objectionable before the color-sync impairment became just perceptible. When the picture information has reached a not usable classification the color-sync degradation is still so low that the picture

would be entirely satisfactory even with a noise-free picture. The impairment that is obtained could not be distinguished under normal circumstances where noise is applied to all receiver functions simultaneously. The technique used in testing in effect acts as a magnifier upon impairment.

Several reasons exist for the excellent performance of the color-sync circuits. Most important is the high-energy content of the burst, the ease with which it may be separated from general-noise disturbances at frequencies, times, or amplitudes other than those corresponding to the burst period, frequency and amplitude range, and the fact that little information is required to operate the circuits permitting the use of stiff memory-protective circuits. Second, the NTSC color system inherently minimizes disturbances in the color functions including color synchronization by use of constant-luminance transmission. This means that any fluctuation of the color-reference signal that may exist will have no effect upon luminance, but only hue or saturation to which the eye is relatively insensitive for short-time disturbances as is shown in the noise-performance differential between luminosity and chromaticity in Fig. 4.

Furthermore, the color-sync circuit used was by no means representative of ultimate performance. It is believed to be representative of ordinary low-cost AFC circuits using a conventional LC oscillator and utilizing a total of three tubes which includes the burst-separator tube. The unit had a lock-in range of plus or minus 5,000 cycles about the color-carrier frequency, which was maintained with ten-to-one changes of circuit-input levels. Lock-in time was less than one-tenth second from a frequency of 2,000 cycles off the reference. The maximum-phase shift from the nominal-center value was  $6^\circ$  which corresponded to a free-running oscillator frequency 500 cycles off the nominal value.

The nature of the disturbance in the picture caused by high noise in the color synchronization is a slight fluctuation or flutter of the instantaneous hue and saturation. Since the noise is random, the disturbance tends to average out so that little apparent change is observable. In particular, the disturbance has little subjective weight in comparison with a function such as deflection synchronization.

In Fig. 5 it may be noted that the subjective response to an over-all color receiver was more tolerant under thermal-noise interference than to the monochrome receiver. In general, this should be expected since the color receiver provides far more useful information; yet, as Fig. 4 shows, the impairment exists primarily in only the monochrome functions, leaving the added information relatively unimpaired. Again, this performance differential shows that the color functions, including color sync, are relatively unaffected by noise.

To find the influence of amplitude variations upon color-synchronizing performance, subjective tests were run with varied burst amplitude in the transmitted signal as a function of the video signal-to-noise ratio. This condition could be encountered when the effective



antenna selectivity is great enough to reduce the higher-video frequencies. As shown in Fig. 6, the operation is still adequate down to quite low-burst amplitudes. In general, the same type of curve is obtained when fewer burst cycles are transmitted—not becoming objectionable until the burst contains less than 2 cycles and the signal-to-noise ratio lower than 2 to 3 db.

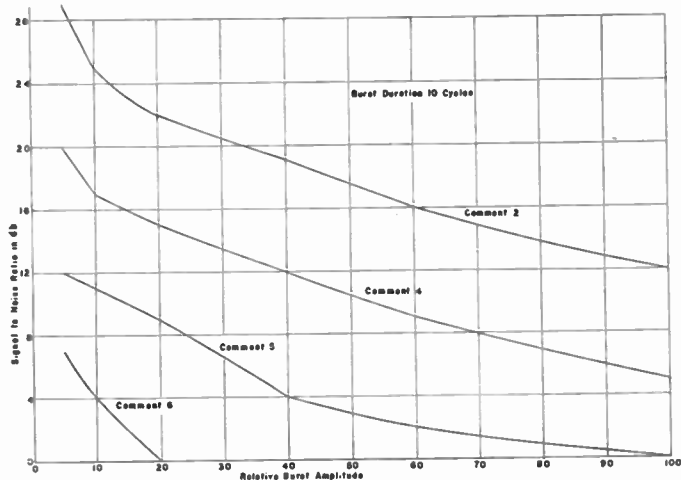


Fig. 6—Influence of burst amplitude on color synchronizing performance.

It is also found that high noise conditions in the picture information cause the eye to be even more tolerant of changes in the color-reference phase. This effect is shown in Fig. 7, which is a plot of the range of allowable phase variation of the color-reference signal for a given signal-to-noise ratio. Apparently, the noise disturbance in the picture obscures the hue disturbance sufficiently so that the eye is relatively unaware of the error.

The results shown here are probably somewhat pessimistic since the tests used slides for program material. In practice, changing program content and dramatic interest may decrease the observer's ability to detect given amounts of noise impairment. Although the subjective judgment of only ten observers does not give a

universal result, it is believed that these studies show that the NTSC color-synchronization system is adequate from the standpoint of thermal-noise performance. Extensive field experience in NTSC and Philco tests with weak-signal performance have further strengthened these conclusions. Field experience with severe

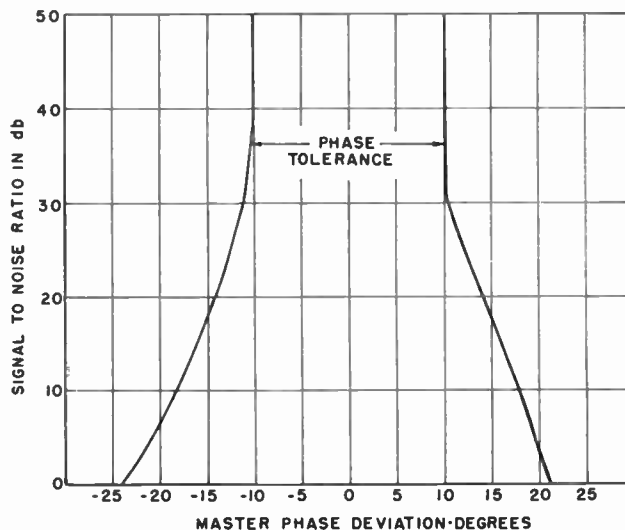


Fig. 7—Influence of picture noise on phase tolerances.

impulse noise has shown no signs of deterioration other than deflection-synchronizing functions, and therefore, the effect is relatively unimportant in color-synchronizing considerations. Furthermore, theoretical considerations<sup>5</sup> agree closely with the experimental results, indicating that the NTSC color-synchronizing specifications are completely satisfactory and adequate. Indeed, the studies as shown in Figs. 4 and 5 indicate that the problem of noise in the NTSC color system is primarily the same as in monochrome-improving receiver noise figures and noise immunity of deflection-synchronization circuits.

<sup>5</sup> T. S. George, "Performance of carrier synchronizing systems," *Proc. IRE*; February, 1951.

## Measurement of the Small Signal Parameters of Transistors\*

GEOFFREY KNIGHT, JR.†, RICHARD A. JOHNSON†,  
AND ROLAND B. HOLT†, SENIOR MEMBER, IRE

**Summary**—A theoretical study of various small signal parameters of transistors shows that the set of parameters which is most appropriate for the description of the circuit operation of junction transistors differs from the set which is customarily measured for point contact transistors. A uniform method for measuring both sets of parameters is described in detail and the sources of error inherent in this method are discussed.

\* Decimal classification: R282.12. Original manuscript received by the Institute, September 23, 1952; revised manuscript received April 3, 1953.

† Transistor Products, Inc., Brighton, Massachusetts.

### INTRODUCTION

IN THE DESIGN of vacuum tube amplifiers and related circuits it is customary to represent the tube by an equivalent circuit, the components of which include such differential properties of the tube as its transconductance, its amplification factor, and its plate resistance. This makes it possible to treat the tube as a network of linear circuit elements which greatly simplifies the analysis of circuits in the region of

the tube operation where the linear approximation is valid. Similarly, in the design of many kinds of transistor circuits it is appropriate and convenient to represent the transistor by an equivalent circuit composed of linear elements, the values of which are related to the differential properties of the transistor.

The term differential property refers to the rate at which a dependent variable changes as one of the independent variables is changed while the other independent variable is held constant. These differential properties are often called small-signal parameters. One of the most significant of the transistor parameters is the short-circuit current gain, denoted by  $\alpha$ , which corresponds in some ways to the open-circuit voltage gain,  $\mu$ , of a vacuum tube. Another parameter of interest,  $r_{22}$ , is very similar to the plate resistance of a tube. On the other hand, the transconductance of a transistor is not a particularly interesting parameter whereas its transresistance is important. This difference stems from the fact that a transistor is essentially a current operated device while a vacuum tube is a voltage operated device. For a vacuum tube triode with a negative grid-to-cathode voltage there are only three variables, two independent and one dependent, since the grid current is always zero. As a result only two of the three triode parameters are independent, anyone of them being expressible as a product or ratio of the other two. For a transistor, however, there are always four variables, two independent and two dependent, and as a result four independent parameters must be determined in order to completely specify the response of a transistor as a linear circuit element. It is the purpose of this paper to define and discuss the parameters of interest for transistor circuit analysis and to describe a particular method of measuring them.

DISCUSSION OF THE SMALL-SIGNAL PARAMETERS

1.  $r_{11}$ ,  $r_{12}$ ,  $r_{21}$ ,  $r_{22}$ .

For purposes of circuit analysis a transistor can be considered to be an active four terminal network.<sup>1</sup> For any such network the voltages across any two pairs of terminals and the currents flowing at those pairs of terminals are functionally related and these functions completely characterize the performance of the network. One of six possible ways to express this functional relationship is shown in (1) and (2) where capital letters designate constant values of voltage and current.

$$V_1 = V_1(I_1, I_2) \tag{1}$$

$$V_2 = V_2(I_1, I_2). \tag{2}$$

The curves obtained by plotting these functions with one current as the independent variable and the other as a parameter are known as characteristic curves of the network.

<sup>1</sup> R. M. Ryder and R. J. Kircher, "Some circuit aspects of the transistor," *Bell System Tech. Jour.*, vol. 28, pp. 367-401; July, 1949.

If the currents  $I_1$  and  $I_2$  make low frequency excursions about some bias values  $I_{10}$  and  $I_{20}$  as they do when a low frequency alternating signal is applied to the network, the functions  $V_1$  and  $V_2$  both have the form

$$V(t) = V_0 + v(t) = V[I_{10} + i_1(t), I_{20} + i_2(t)] \tag{3}$$

where  $V_0 \equiv V(I_{10}, I_{20})$  and  $v(t)$  and  $i(t)$  are the instantaneous values of the voltage and current excursions. This function can be expanded in a Taylor's series as

$$\begin{aligned} V(t) &= V_0 + v(t) \\ &= V(I_{10}, I_{20}) + \frac{\partial V}{\partial I_1} \cdot i_1(t) + \frac{\partial V}{\partial I_2} \cdot i_2(t) \\ &\quad + \frac{1}{2} \left[ \frac{\partial^2 V}{\partial I_1^2} \cdot i_1^2(t) + \frac{\partial^2 V}{\partial I_2^2} \cdot i_2^2(t) \right. \\ &\quad \left. + 2 \frac{\partial^2 V}{\partial I_1 \partial I_2} \cdot i_1(t) i_2(t) \right] + \dots \end{aligned} \tag{4}$$

where the partial derivatives are evaluated at  $I_1 = I_{10}$  and  $I_2 = I_{20}$ .

If the current excursions  $i_1(t)$  and  $i_2(t)$  are so small that all the terms of this expansion of higher order than the first can be neglected, it reduces to the form:

$$v_1(t) = r_{11}i_1(t) + r_{12}i_2(t) \tag{5}$$

$$v_2(t) = r_{21}i_1(t) + r_{22}i_2(t) \tag{6}$$

where

$$\begin{aligned} r_{11} &\equiv \left[ \frac{\partial V_1}{\partial I_1} \right]_{I_2 = \text{const.}} & r_{12} &\equiv \left[ \frac{\partial V_1}{\partial I_2} \right]_{I_1 = \text{const.}} \\ r_{21} &\equiv \left[ \frac{\partial V_2}{\partial I_1} \right]_{I_2 = \text{const.}} & r_{22} &\equiv \left[ \frac{\partial V_2}{\partial I_2} \right]_{I_1 = \text{const.}} \end{aligned} \tag{7}$$

are the slopes of the set of characteristic curves implicit in (1) and (2).

The linear equations (5) and (6) correspond to the circuit shown in Fig. 1. It is apparent from this figure that  $r_{11}$  is the open circuit (*i.e.*  $i_2 = 0$ ) input resistance and that  $r_{22}$  is the open circuit (*i.e.*  $i_1 = 0$ ) output re-

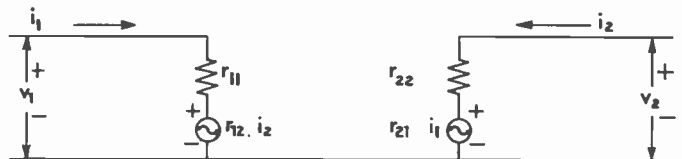


Fig. 1—Equivalent circuit of the network described by equations (5) and (6).

sistance of the network. It is also apparent that  $r_{12}$  is a feedback resistance whereby a current  $i_2$  flowing in the output circuit generates a voltage  $r_{12}i_2$  in the input circuit, and the  $r_{21}$  is a forward transfer resistance whereby a current  $i_1$  flowing in the input circuit generates a voltage  $r_{21}i_1$  in the output circuit.

2.  $g_{11}$ ,  $\gamma$ ,  $\alpha$ ,  $r_{22}$ .

In the previous discussion we have considered the input and output currents to be the natural independent variables of the network. However, in some ways it is more appropriate to the nature of a transistor to consider the input current and the output voltage to be the independent variables in the usual circuit connections. This is true from the point of view of the physics of the transistor because the parameter which is the most direct measure of transistor action, namely the current gain, is defined in terms of an input current signal and a constant output voltage. It is also true from the point of view of measurement and of circuit operation because the transistor is inherently a low input resistance, high output resistance device in the most useful circuit connections. In fact, the input resistance of a transistor may be so low that the input voltage cannot be conveniently controlled whereas the output resistance may be so high that the output current cannot be conveniently controlled. As an example we may consider the measurement of  $r_{11}$ ,  $r_{12}$ ,  $r_{21}$ , and  $r_{22}$  by the method to be discussed later in this paper. In each case the dynamic resistance of the collector dc supply must be very much greater than  $r_{22}$  if the measurement is to be accurate. However, the value of  $r_{22}$  for a junction transistor may be many megohms so the resistance of the supply would have to be of the order of hundreds of megohms, which is impossible to achieve at any reasonable measuring frequency because of the effects of distributed capacity.

When  $I_1$  and  $V_2$  are taken to be the independent variables, the functional relationship between the network voltages and currents may be written:

$$V_1 = V_1(I_1, V_2) \tag{8}$$

$$I_2 = I_2(I_1, V_2). \tag{9}$$

If the current  $I_1$  and the voltage  $V_2$  make sufficiently small excursions about some bias values, the Taylor's series expansions of these equations reduce to the linear relations:

$$v_1 = \frac{1}{g_{11}} i_1 + \gamma v_2 \tag{10}$$

$$i_2 = -\alpha i_1 + \frac{1}{r_{22}} v_2 \tag{11}$$

where

$$\frac{1}{g_{11}} \equiv \left[ \frac{\partial V_1}{\partial I_1} \right]_{V_2=\text{const.}} \quad \gamma \equiv \left[ \frac{\partial V_1}{\partial V_2} \right]_{I_1=\text{const.}} \tag{12}$$

$$\alpha \equiv - \left[ \frac{\partial I_2}{\partial I_1} \right]_{V_2=\text{const.}} \quad \frac{1}{r_{22}} \equiv \left[ \frac{\partial I_2}{\partial V_2} \right]_{I_1=\text{const.}}$$

Thus  $g_{11}$ ,  $\gamma$ ,  $\alpha$ , and  $r_{22}$  are the natural parameters when  $I_1$  and  $V_2$  are the independent variables. This set of parameters has recently been adopted by Bell Telephone

Laboratories and Western Electric Company for the specifications of their junction transistors. (Private communication.) Also, these parameters are measured for junction transistors by a test set manufactured by Transistor Products, Inc.

The linear equations (10) and (11) correspond to the circuit shown in Fig. 2. Examination of this circuit shows that  $g_{11}$  is the short circuit ( $v_2=0$ ) input conductance and that  $r_{22}$  is the open circuit ( $i_1=0$ ) output re-

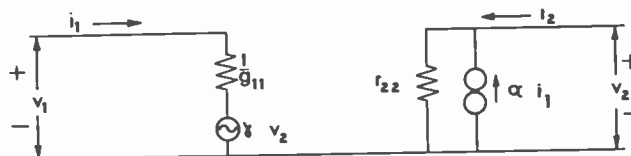


Fig. 2—Equivalent circuit of the network described by (10) and (11).

sistance. It is also apparent that  $\gamma$  is a voltage feedback ratio such that if a voltage  $v_2$  appears across the output terminals, a voltage generator of magnitude  $\gamma v_2$  appears in the input circuit. The final parameter,  $\alpha$ , is seen to be the short circuit ( $v_2=0$ ) current gain of the network such that if a current  $i_1$  flows in the input circuit a current generator  $-\alpha i_1$  appears in the output circuit. The parameters  $g_{11}$ ,  $\gamma$ , and  $\alpha$  are related to  $r_{11}$ ,  $r_{12}$ ,  $r_{21}$ , and  $r_{22}$  by the expressions

$$1/g_{11} = r_{11} - \alpha r_{12}, \quad \gamma = r_{12}/r_{22}, \quad \text{and} \quad \alpha = r_{21}/r_{22}.$$

The values of  $r_{11}$ ,  $r_{12}$ ,  $r_{21}$ , and  $r_{22}$  and of  $g_{11}$ ,  $\alpha$ , and  $\gamma$  for a given transistor depend upon which lead of the transistor is taken to be the common terminal (usually called the ground terminal) for the voltages  $v_1$  and  $v_2$ . In this paper we shall only find it necessary to consider parameters which are associated with the grounded base connection.

In general the characteristic curves of a transistor are nonlinear so the values of the parameters must be determined as functions of the operating point, e.g.  $r_{11}(I_{10}, I_{20})$  and  $\alpha(I_{10}, V_{20})$ , if the small signal response of the transistor at low frequencies is to be completely specified.

As the signal frequency increases, capacitative and transit time effects in the transistor become more important so that it becomes necessary to consider impedances and admittances rather than resistances and conductances. However, in all the measurements described here, signal frequency will be assumed to be so low that frequency dependent effects can be ignored.

MEASUREMENT OF THE SMALL SIGNAL PARAMETERS

A standard method of measuring the parameters  $r_{11}$ ,  $r_{12}$ ,  $r_{21}$ , and  $r_{22}$  is based on (5) and (6).<sup>1,2</sup> They may be

<sup>1</sup> K. Lehovc, "Testing transistors," *Electronics*, vol. 22, pp. 88-89; June, 1949.

rewritten for the grounded base connection:

$$v_{eb} = r_{11b}i_e + r_{12b}i_c \quad (13)$$

$$v_{cb} = r_{21b}i_e + r_{22b}i_c \quad (14)$$

where  $v_{eb}$  and  $v_{cb}$  are the signal voltages between emitter and base and collector and base respectively and  $i_e$  and  $i_c$  are the signal currents into emitter and collector.

As an example, let us consider the case of  $r_{11b}$ . Solution of (13) for  $r_{11b}$  gives

$$r_{11b} = \frac{v_{eb}}{i_e} - r_{12b} \frac{i_c}{i_e} \quad (15)$$

Thus  $r_{11b}$  equals the ratio  $v_{eb}/i_e$  if the second term is so small compared with the first that it can be neglected. This will be the case if

$$i_c \ll -\frac{r_{11b}}{r_{12b}} i_e,$$

that is, if the magnitude of the collector current is very small compared with the emitter current. Now if a load resistance  $r_L$  is connected between collector and base so that  $V_{cb} = -r_L i_c$ , we have (from (14))

$$i_c = \frac{-r_{21b}}{r_{22b} + r_L} i_e$$

so if

$$\frac{r_{21b}}{r_{22b} + r_L} \ll \frac{r_{11b}}{r_{12b}},$$

i.e. if

$$r_L \gg \frac{r_{12b}}{r_{11b}} r_{21b},$$

the required condition will be established.

Similar relations can be derived for  $r_{12b}$ ,  $r_{21b}$ , and  $r_{22b}$ . The method, then, consists of introducing a small alternating signal current  $i_e$  or  $i_c$ ; establishing a condition,  $i_c = 0$  or  $i_e = 0$  by means of an external resistance; and measuring a small signal voltage. The value of the parameter is given by the ratio of the output voltage to the input current. Therefore, if the input current is made equal to unity, the value of the parameter is numerically equal to the output voltage.

This method can also be used to measure  $1/g_{11b}$ ,  $\gamma_b$ ,  $\alpha_b$ ,  $1 - \alpha_b$ ,<sup>3</sup> and  $1/r_{22b}$ . The basic equations, obtained by rewriting (10) and (11) for the grounded base connection and by using the relation  $i_b = -(i_e + i_c)$ , are:

$$v_{eb} = \frac{1}{g_{11b}} i_e + \gamma_b v_{cb} \quad (16)$$

$$i_c = -\alpha_b i_e + \frac{1}{r_{22b}} v_{cb} \quad (17)$$

$$i_b = -(1 - \alpha_b) i_e - \frac{1}{r_{22b}} v_{cb} \quad (18)$$

These equations can be solved so as to express each of the parameters in terms of a ratio of output signal to input signal plus a term which can be made negligibly small by a suitable resistance in the external circuit.

A summary of the type of signal required, the type of measurement to be made, the condition to be established, and the necessary values of external resistance for each of the desired parameters is given in Table I.

Because the required signals, conditions, and measurements are similar for all of the parameters, the appropriate measuring circuits all have similar components. In each case there must be a source of signal current or voltage, a source of dc current for the emitter, a source of dc current or voltage for the collector, and an ac millivoltmeter or milliammeter. The arrangements of these components which are required for the measurement of the parameters discussed in this paper are shown schematically in Figs. 3, 4, and 5.

In these circuits the symbols  $r_s$ ,  $r_k$ ,  $r_L$ ,  $r_m$ , and  $r_n$  represent the dynamic resistances of the signal source, of the emitter dc supply, of the collector dc supply, of the millivoltmeter, and milliammeter respectively.

#### SOURCES OF ERROR

There are inherent in this method of evaluating small signal parameters a number of sources of error which affect the accuracy of measurement.

First we may consider the error due to the nonlinearity of the characteristic curves which results when a finite rather than an infinitesimal signal is used to measure the slope. Let us take the case of  $r_{11}$  as an example. If the input signal current is a pure sine wave,  $i_1(t) = i_{10} \sin \omega t$ , while the other current,  $i_2(t)$ , equals zero; (4) becomes:

$$v_1(t) = \frac{\partial V_1}{\partial I_1} i_{10} \sin \omega t + \frac{1}{2} \frac{\partial^2 V_1}{\partial I_1^2} i_{10}^2 \sin^2 \omega t + \frac{1}{6} \frac{\partial^3 V_1}{\partial I_1^3} i_{10}^3 \sin^3 \omega t + \dots \quad (19)$$

where the second, third, and higher terms vanish compared with the first only if  $i_{10}$  is infinitesimal or if  $V_1$  is a linear function of  $I_1$ .

In order to determine the order of magnitude of the error introduced by these additional terms it is necessary to consider the nature of the measurement of  $v_1(t)$ . If the signal voltage to be measured passes through an amplifier which is sharply tuned to the measuring frequency before it reaches the voltmeter, the second harmonic of the signal frequency will be greatly attenuated and higher order harmonics will be effectively eliminated

<sup>3</sup> In the case of junction transistors the value of  $\alpha_b$  may be so close to unity that it is desirable to measure  $1 - \alpha_b$ .

TABLE I

SUMMARY OF THE REQUIREMENTS FOR THE MEASUREMENT OF TRANSISTOR PARAMETERS BY THE METHOD DESCRIBED IN THE TEXT

Parameter	Signal	Measurement	Condition	Required Values of Internal Resistance			
				Signal Source	Emitter DC Supply	Collector DC Supply	Circuit Diagram
$r_{11b} = \frac{v_{ob}}{i_o} - r_{12b} \frac{i_c}{i_o}$	$i_o$	$v_{ob}$	$i_c \ll \frac{r_{11b}}{r_{12b}} i_o$	$r_s \gg r_{11b}$	$r_k \gg r_{11b}$	$r_L \gg \frac{r_{12b}}{r_{11b}} r_{21b}$	3
$\frac{1}{g_{11b}} = \frac{v_{ob}}{i_o} - \gamma_b \frac{v_{cb}}{i_o}$	$i_o$	$v_{ob}$	$v_{cb} \ll \frac{i_o}{\gamma_b g_{11b}}$	$r_s \gg \frac{1}{g_{11b}}$	$r_k \gg \frac{1}{g_{11b}}$	$r_L \ll \frac{1}{\alpha_b \gamma_b g_{11b}}$	3
$r_{12b} = \frac{v_{ob}}{i_c} - r_{11b} \frac{i_o}{i_c}$	$i_c$	$v_{ob}$	$i_o \ll \frac{r_{12b}}{r_{11b}} i_c$	$r_s \gg r_{22b}$ $r_s \gg r_{11b}$	$r_k \gg r_{11b}$ $r_k \gg r_{11b}$	$r_L \gg r_{22b}$ $r_L \gg r_{22b}$	3 3
$r_{21b} = \frac{v_{cb}}{i_o} - r_{22b} \frac{i_c}{i_o}$	$i_o$	$v_{cb}$	$i_c \ll \alpha_b i_o$	$r_s \gg r_{22b}$	$r_k \gg \alpha_b r_{12b}$	$r_L \gg r_{22b}$	3
$r_{22b} = \frac{v_{cb}}{i_c} - r_{21b} \frac{i_o}{i_c}$	$i_c$	$v_{cb}$	$i_o \ll \frac{1}{\alpha_b} i_c$	$r_s \gg \frac{1}{g_{11b}}$	$r_k \gg \frac{1}{g_{11b}}$	$r_L + r_n \ll r_{22b}$	4
$\alpha_b = \frac{i_c}{i_o} + \frac{1}{r_{22b}} \frac{v_{cb}}{i_o}$	$i_o$	$i_c$	$v_{cb} \ll r_{21b} i_o$	$r_s \gg \frac{1}{g_{11b}}$	$r_k \gg \frac{1}{g_{11b}}$	$r_L - \frac{1 - \alpha_b}{\alpha_b} r_n$	4
$1 - \alpha_b = \frac{i_b}{i_o} + \frac{1}{r_{22b}} \frac{v_{cb}}{i_o}$	$i_o$	$i_b$	$v_{cb} \ll (1 - \alpha_b) r_{22b} i_o$			$\ll \frac{1 - \alpha_b}{\alpha_b} r_{22b}$	
$\gamma_b = \frac{v_{ob}}{v_{cb}} - \frac{1}{g_{11b}} \frac{i_o}{v_{cb}}$	$v_{cb}$	$v_{ob}$	$i_o \ll g_{11b} \gamma_b v_{cb}$	$r_s \ll r_{22b}$	$r_k \gg \frac{1}{g_{11b}}$		5
$\frac{1}{r_{22b}} = \frac{i_c}{v_{cb}} + \alpha_b \frac{i_o}{v_{cb}}$	$v_{cb}$	$i_c$	$i_o \ll \frac{v_{cb}}{\alpha_b r_{22b}}$	$r_s + r_n \ll r_{22b}$	$r_k \ll \alpha_b \gamma_b r_{22b}$		5

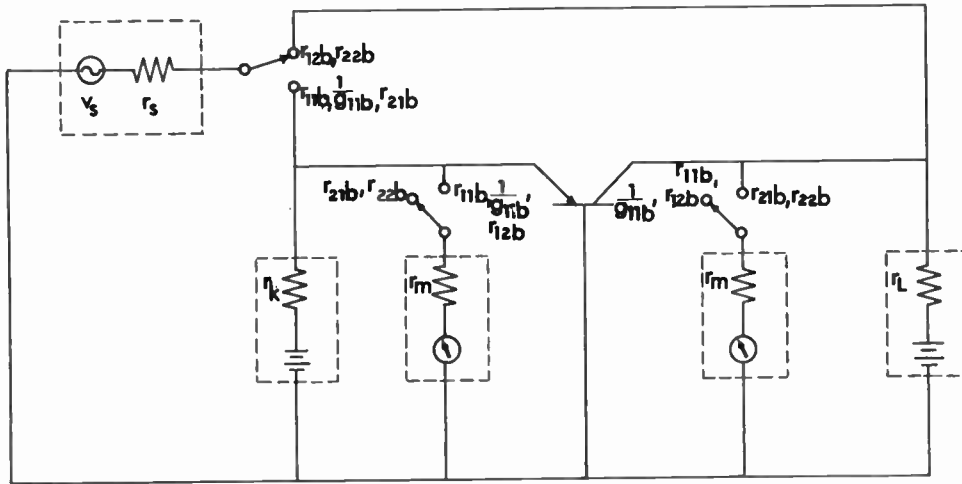


Fig. 3—Prototype circuit for the measurement of the parameters  $r_{11b}$ ,  $1/g_{11b}$ ,  $r_{12b}$ ,  $r_{21b}$ ,  $r_{22b}$ .

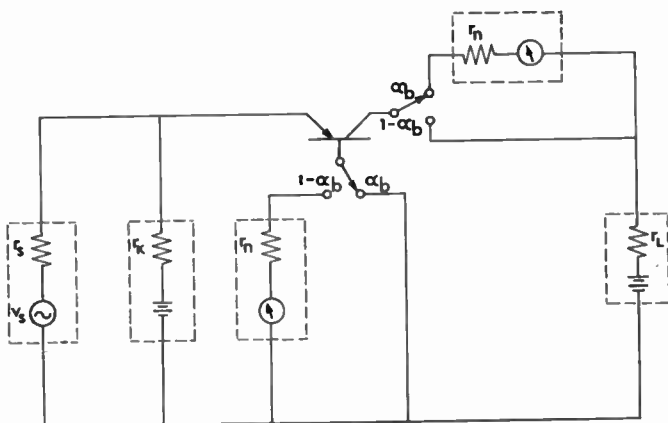


Fig. 4—Prototype circuit for measurement of parameters  $\alpha_b$ ,  $1 - \alpha_b$ .

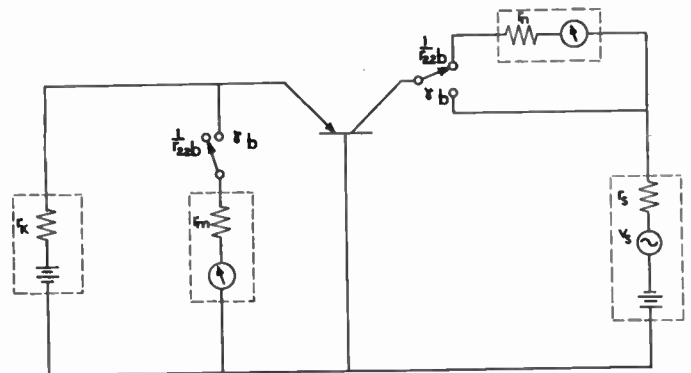


Fig. 5—Prototype circuit for measurement of parameters  $1/r_{22b}$ ,  $\gamma_b$ .



Thus if the input to the amplifier is

$$v_1(t) = \left( \frac{\partial V_1}{\partial I_1} i_{10} + \frac{1}{8} \frac{\partial^2 V_1}{\partial I_1^2} i_{10}^2 + \dots \right) \sin \omega t \\ + \frac{1}{4} \frac{\partial^2 V_1}{\partial I_1^2} i_{10}^2 \cdot (1 - \cos 2\omega t) \\ - \frac{1}{24} \frac{\partial^3 V_1}{\partial I_1^3} i_{10}^3 \sin 3\omega t + \dots \quad (20)$$

(which can be obtained from (19) by trigonometric identity), the output from the amplifier is proportional to

$$\left( \frac{\partial V_1}{\partial I_1} i_{10} + \frac{1}{8} \frac{\partial^2 V_1}{\partial I_1^2} i_{10}^2 + \dots \right) \sin \omega t \quad (21)$$

plus a small second harmonic term which is further reduced by the averaging action of the meter. If the signal is infinitesimal,  $i_{10}$  being so small that the second term of this expression is completely negligible compared with the first, the correct value,  $r_{11} = \partial V_1 / \partial I_1$ , is obtained. When a finite signal is used, the second term may not be negligible if the rate of change of curvature of the characteristic,  $\partial^3 V_1 / \partial I_1^3 = \partial^2 r_{11} / \partial I_1^2$ , is appreciable. The fractional error in the measurement of  $r_{11}$  due to the combined effects of finite signal size and curvature of the characteristic is to an excellent approximation the ratio of the second (error) term of (21) to the first (correct) term, i.e.

$$\frac{1}{8} \frac{1}{r_{11}} \frac{\partial^2 r_{11}}{\partial I_1^2} i_{10}^2 \quad (22)$$

where  $i_{10}$  is the amplitude of the input signal current. An expression similar to (21) can be derived for each of the other parameters so in each case the fractional error is similar in form to (22). The general expression for the fractional error in the measured value,  $p$ , of a parameter is either

$$\frac{1}{8} \frac{1}{p} \frac{\partial^2 p}{\partial I_s^2} i_{s0}^2 \quad \text{or} \quad \frac{1}{8} \frac{1}{p} \frac{\partial^2 p}{\partial V_s^2} v_{s0}^2, \quad (23)$$

depending on whether the signal is a current  $i_s$  or a voltage  $v_s$ .

It is apparent that this error can be made negligibly small by making  $i_{s0}$  or  $v_{s0}$  sufficiently small. However, the presence of transistor and thermal noise establishes a lower limit to the useful size of the signal. Since transistors are relatively noisy, this may be an important consideration.

A second source of error associated with the signal current results from the finite internal resistance of the signal source. In measuring any of the parameters the magnitude of the input signal is assumed to be independent of the resistance of the transistor, but this will only be true if the source resistance is either very much

greater or very much less than the input resistance of the transistor. The order of magnitude of the fractional error in the measured value of a parameter is either the ratio of the input resistance of the transistor to the internal resistance of the source or its reciprocal, depending on whether a current source or a voltage source is required.

A third source of error associated with the signal current results from the shunting of the signal through the voltmeter and through the dc supply which is in parallel with the signal source since the part of the input signal which bypasses the transistor in this way cannot contribute to the output signal. In practice the resistance of the voltmeter can be made so large that its shunting effect can be neglected. The order of magnitude of the fractional error due to the shunting of the dc supply is the ratio of the input resistance of the transistor to the dynamic resistance of the dc supply.

The error associated with establishing the necessary condition can be illustrated by the case of  $r_{11b}$ . The magnitude of the resistance  $r_L$  required to make the second term of (15) negligible can be determined in the following way: The equations for the flow of collector current in the circuit are:

$$v_{cb} = r_{21b} i_e + r_{22b} i_c = -r_L i_c \quad (24)$$

so that

$$\frac{i_c}{i_e} = -\frac{r_{21b}}{r_L + r_{22b}} \cong -\frac{r_{21b}}{r_L} \quad (25)$$

if  $r_L \ll r_{22b}$ . Substitution of this result into (15) gives:

$$r_{11b} = \frac{v_{eb}}{i_e} + r_{12b} \frac{r_{21b}}{r_L} \quad (26)$$

The fractional error which results if the second term is neglected in the computation of  $r_{11b}$  is

$$\frac{r_{12b} r_{21b}}{r_{11b} r_L}$$

Therefore, for this error to be small,  $r_L$  must be many times greater than

$$\frac{r_{12b}}{r_{11b}} r_{21b}$$

For example, for a point contact transistor with  $r_{21b} = \alpha_b r_c = 50K$  and  $r_{12b}/r_{11b} = \frac{1}{2}$  this error will be  $<1\%$  only if  $r_L > 2.5$  megohms. Similar expressions giving the error involved in the assumption that a parameter equals the ratio of the output signal to the input signal can be derived in each case.

The values of  $r_s$ ,  $r_k$ , and  $r_L$  which are required if these errors are to be kept small are given in Table I for each parameter. The approximate values of the fractional error in the measurement of a given parameter



for the vacuum tube and the transistor, and its application requires a minimum of thought and labor.

Although the basic idea underlying the method is well known,<sup>1-3</sup> it appears that a description incorporating tables of admittance and impedance coefficients for the vacuum tube and the transistor (regarded as three-terminal elements) has not been given in the literature. Since experience with the method indicates it is considerably more effective than the conventional method, a brief exposition might be worthwhile.

II. DESCRIPTION OF METHOD

For simplicity, the discussion will be limited to triodes and three-terminal transistors. Furthermore, only the node method of analysis will be considered in detail.

The method described here is illustrated in Fig. 1, which shows (a) a network *N* containing a three-ter-

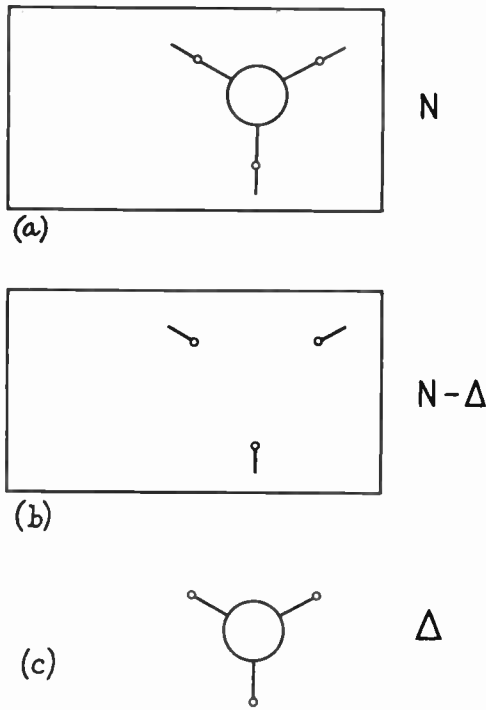


Fig. 1—(a) Active network *N* containing an active three-terminal element  $\Delta$ . (b) Network *N* with  $\Delta$  removed. (c) Active element  $\Delta$ .

minal network  $\Delta$ ; (b) the network  $N-\Delta$ , which results from removing  $\Delta$  from *N*; and (c) the network  $\Delta$ . It is assumed that  $\Delta$  is not inductively coupled to  $N-\Delta$ .

Let  $Y_{\nu\mu(N)}$ ,  $Y_{\nu\mu(N-\Delta)}$  and  $Y_{\nu\mu(\Delta)}$  ( $\nu, \mu = 1, 2, 3, \dots, n$ ) be the admittance coefficients for *N*,  $N-\Delta$  and  $\Delta$ , re-

spectively. From the definitions<sup>4</sup> of these admittances it follows at once that

$$Y_{\nu\mu(N)} = Y_{\nu\mu(N-\Delta)} + Y_{\nu\mu(\Delta)} \tag{2}$$

with the understanding that  $Y_{\nu\mu(\Delta)}$  is zero for all  $\nu$  and  $\mu$  which are not associated with the terminals of  $\Delta$ .

Equation (2) may be used to reduce the determination of the  $Y_{\nu\mu(N)}$  to two simpler problems, namely, the calculation of the  $Y_{\nu\mu(N-\Delta)}$  and the calculation of the  $Y_{\nu\mu(\Delta)}$ . In general there is little or no advantage in using this reduction. However, when  $\Delta$  is a standard network such as a vacuum tube or a transistor, the  $Y_{\nu\mu(\Delta)}$  may be obtained from a table of admittance coefficients for  $\Delta$ . In this way, the setting up of node equations for a network *N* containing one or more active elements  $\Delta_1, \Delta_2, \dots, \Delta_m$ , is reduced essentially to determining the admittance coefficients for the passive network  $N-\Delta_1-\Delta_2-\dots-\Delta_m$  (resulting from removing  $\Delta_1, \Delta_2, \dots, \Delta_m$  from *N*) and adding to these the corresponding admittance coefficients for  $\Delta_1, \Delta_2, \dots, \Delta_m$ , the latter being obtained from tables such as those given below.

TABLE I

ADMITTANCE COEFFICIENTS TABLE FOR THE VACUUM TUBE

$Y_{gg} = 0$	$Y_{gp} = 0$	$Y_{gk} = 0$
$Y_{pp} = g_m$	$Y_{pp} = g_p$	$Y_{pk} = -g_p - g_m$
$Y_{kp} = -g_m$	$Y_{kp} = -g_p$	$Y_{kk} = g_p + g_m$

where *g*, *p* and *k* represent the grid, plate and cathode terminals, respectively;  $g_m$  is the transconductance and  $g_p = 1/r_p$  = plate conductance.

TABLE II

ADMITTANCE COEFFICIENTS TABLE FOR THE TRANSISTOR

$Y_{ee} = \frac{r_b + r_c}{r_e(r_b + r_c) + (1-\alpha)r_b r_c}$	$Y_{ec} = \frac{-r_b}{r_e(r_b + r_c) + (1-\alpha)r_b r_c}$	$Y_{eb} = \frac{-r_c}{r_e(r_b + r_c) + (1-\alpha)r_b r_c}$
$Y_{ce} = \frac{-r_b - \alpha r_c}{r_e(r_b + r_c) + (1-\alpha)r_b r_c}$	$Y_{cc} = \frac{r_b + r_e}{r_e(r_b + r_c) + (1-\alpha)r_b r_c}$	$Y_{cb} = \frac{\alpha r_c - r_e}{r_e(r_b + r_c) + (1-\alpha)r_b r_c}$
$Y_{be} = \frac{-r_c(1-\alpha)}{r_e(r_b + r_c) + (1-\alpha)r_b r_c}$	$Y_{bc} = \frac{-r_e}{r_e(r_b + r_c) + (1-\alpha)r_b r_c}$	$Y_{bb} = \frac{r_e + (1-\alpha)r_c}{r_e(r_b + r_c) + (1-\alpha)r_b r_c}$

<sup>4</sup>  $Y_{\nu\mu}$  is numerically equal to the current flowing toward the  $\nu$ th node through a short circuit between the  $\mu$ th node and ground when (a) all current sources are open-circuited, (b) all nodes except the  $\mu$ th node are connected to ground, and (c) a potential of one volt is impressed upon the  $\mu$ th node. In the case of a passive network which does not contain coupled coils,  $Y_{\nu\mu}$  ( $\nu \neq \mu$ ) is equal to the negative of the admittance of the branch connecting the nodes  $\nu$  and  $\mu$ ; and  $Y_{\nu\nu}$  is equal to the sum of the admittances of the branches connected to the  $\nu$ th node.

<sup>1</sup> G. Kron, "Tensor Analysis of Networks," John Wiley and Sons, Inc., New York, N. Y.; 1949. In particular, note pp. 389-390.

<sup>2</sup> S. R. Deards, "Matrix theory applied to thermionic valve circuits," *Electronic Eng.*, vol. 24, pp. 264-277; June, 1952. In this paper tables of admittance and impedance coefficients are given for several basic vacuum tube circuits (regarded as two terminal-pair elements).

<sup>3</sup> J. Shekel, "Matrix representation of transistor circuits," *Proc. I.R.E.*, vol. 40, pp. 1493-1497; November, 1952. The method given in this paper is closely related to that described in the present paper. However, the paper does not contain tables of impedance and admittance coefficients.

where  $\epsilon$ ,  $c$  and  $b$  represent the emitter, collector and base terminals respectively;  $r_\epsilon$ ,  $r_c$ , and  $r_b$  are the incremental emitter, collector and base resistances; and  $\alpha$  is the current amplification factor.

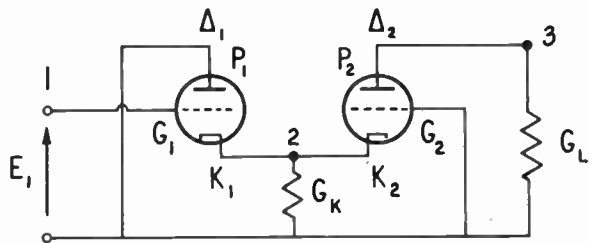


Fig. 2—Circuit analyzed in example 1.

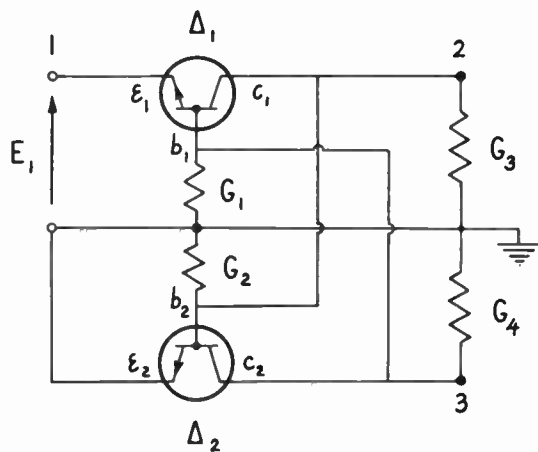


Fig. 3—Circuit analyzed in example 2.

As an illustration of the method, the node equations for the circuits shown in Figs. 2 and 3 will be set up. In the circuit shown in Fig. 2, the node voltage of node 1 is specified and hence the node equation for this node may be omitted. For nodes 2 and 3 the equations are of the form

$$0 = Y_{21}E_1 + Y_{22}V_2 + Y_{23}V_3 \tag{3}$$

$$0 = Y_{31}E_1 + Y_{32}V_2 + Y_{33}V_3. \tag{4}$$

The admittance coefficients in these equations are calculated in the following manner. Taking  $Y_{22}$ , for example, one has

$$Y_{22(N-\Delta_1-\Delta_2)} = G_k, \tag{5}$$

and from Table 1

$$Y_{22}(\Delta_1) = Y_{k_1k_1} = g_{p_1} + g_{m_1} \tag{6}$$

$$Y_{22}(\Delta_2) = Y_{k_2k_2} = g_{p_2} + g_{m_2}. \tag{7}$$

Thus

$$\begin{aligned} Y_{22(N)} &= Y_{22(N-\Delta_1-\Delta_2)} + Y_{22}(\Delta_1) + Y_{22}(\Delta_2) \\ &= G_k + g_{p_1} + g_{m_1} + g_{p_2} + g_{m_2}. \end{aligned} \tag{8}$$

Similar calculations for other coefficients yield the desired node equations

$$0 = -g_{m_1}E_1 + (G_k + g_{p_1} + g_{m_1} + g_{p_2} + g_{m_2})V_2 - g_{p_2}V_3 \tag{9}$$

$$0 = 0 - (g_{p_2} + g_{m_2})V_2 + (G_L + g_{p_2})V_3, \tag{10}$$

in which the lower case symbols represent quantities obtained from Table I.

Consider now the network shown in Fig. 3, which will be recognized as a simplified circuit of a negative-impedance converter. On inspecting the circuit diagram and making use of Table II, one readily obtains the following node equations

$$\begin{aligned} 0 &= -\frac{(r_b + \alpha r_c)E_1}{r_c(r_b + r_c) + (1 - \alpha)r_b r_c} \\ &+ \left[ G_2 + G_3 + \frac{2r_c + r_b + (1 - \alpha)r_c}{r_c(r_b + r_c) + (1 - \alpha)r_b r_c} \right] V_2 \\ &+ \frac{(\alpha r_c - 2r_c)V_3}{r_c(r_b + r_c) + (1 - \alpha)r_b r_c} \end{aligned} \tag{11}$$

$$\begin{aligned} 0 &= -\frac{r_c(1 - \alpha)E_1}{r_c(r_b + r_c) + (1 - \alpha)r_b r_c} \\ &+ \frac{(\alpha r_c - 2r_c)V_2}{r_c(r_b + r_c) + (1 - \alpha)r_b r_c} \\ &+ \left[ G_1 + G_4 + \frac{2r_c + r_b + (1 - \alpha)r_c}{r_c(r_b + r_c) + (1 - \alpha)r_b r_c} \right] V_3. \end{aligned} \tag{12}$$

For the sake of clarity, these equations are rewritten below in a form which places in evidence the terms obtained from the table.

$$\begin{aligned} 0 &= Y_{\epsilon_1\epsilon_1}E_1 + (G_2 + G_3 + Y_{b_2b_2} + Y_{\epsilon_1\epsilon_1})V_2 \\ &+ (Y_{\epsilon_1b_1} + Y_{b_2\epsilon_2})V_3 \end{aligned} \tag{13}$$

$$\begin{aligned} 0 &= Y_{b_1\epsilon_1}E_1 + (Y_{\epsilon_2\epsilon_2} + Y_{b_1\epsilon_1})V_2 \\ &+ (G_1 + G_4 + Y_{\epsilon_2\epsilon_2} + Y_{b_1b_1})V_3. \end{aligned} \tag{14}$$

It will be observed in this case, as in the preceding example, most of the terms in the admittance coefficients are obtained from the table.

When the circuit configuration is such that the mesh method of analysis is better suited than the node method, one may use the dual of the procedure outlined above in conjunction with appropriate tables of impedance coefficients.<sup>5</sup> In the case of the vacuum tube a

<sup>5</sup>  $Z_{\nu\mu}$  is numerically equal to the voltage drop induced in the  $\nu$ th mesh by a unit current in the  $\mu$ th mesh when all voltage sources are short-circuited and all meshes except the  $\mu$ th mesh are open-circuited. In the case of a passive network which does not contain coupled coils and in which all mesh currents have the same positive sense,  $Z_{\nu\nu}$  is equal to the sum of the impedances of the branches traversed by the  $\nu$ th mesh current, and  $Z_{\nu\mu}$  ( $\nu \neq \mu$ ) is equal to the negative of the impedance of the branch common to  $\nu$ th and  $\mu$ th meshes. It should be noted that when the mesh method of analysis is used, the network  $N-\Delta$  consists of  $N$  with  $\Delta$  replaced by a short circuit.

difficulty arises in that the impedance coefficients associated with the grid terminal are infinite. One way of circumventing this difficulty is to assume that the tube has a grid return. With this assumption and with the meshes numbered as in Fig. 4(a), the impedance coefficients table assumes the following form

TABLE III  
IMPEDANCE COEFFICIENTS TABLE FOR THE VACUUM TUBE WITH A GRID RETURN

$Z_{11} = R_g$	$Z_{12} = 0$	$Z_{13} = -R_g$
$Z_{21} = \mu R_g$	$Z_{22} = r_p$	$Z_{23} = -\mu R_g - r_p$
$Z_{31} = -(1 + \mu)R_g$	$Z_{32} = -r_p$	$Z_{33} = r_p + (1 + \mu)R_g$

where  $R_g$  is the grid return resistance,  $r_p$  is the plate resistance and  $\mu$  is the voltage amplification factor.

In the case of the transistor there are no such difficulties, and the impedance coefficients (with the meshes numbered as in Fig. 4(b)) read

TABLE IV  
IMPEDANCE COEFFICIENTS TABLE FOR THE TRANSISTOR

$Z_{11} = r_e + r_b$	$Z_{12} = -r_b$	$Z_{13} = -r_e$
$Z_{21} = -r_m - r_b$	$Z_{22} = r_b + r_c$	$Z_{23} = r_m - r_c$
$Z_{31} = r_m - r_e$	$Z_{32} = -r_c$	$Z_{33} = r_e + r_c - r_m$

where the symbols have the same meaning as in Table I, and  $r_m = \alpha r_c$ .

In conclusion, it will be noted that the method outlined here has a twofold advantage over the conventional method. First, its use does not require a redrawing of the circuit diagram, and second, the process of setting

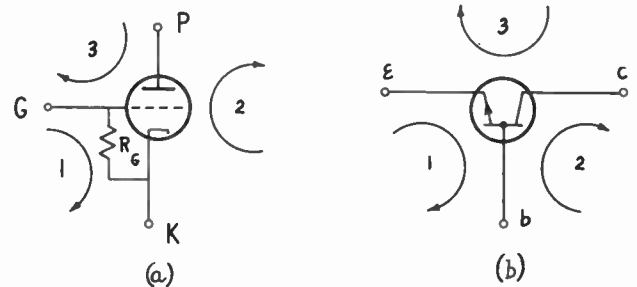


Fig. 4—(a) Vacuum tube with a grid return. (b) Transistor.

up the node (or mesh) equations is simplified considerably through the use of admittance or impedance coefficients tables. It will also be noted that the method can readily be extended to networks containing active elements other than three-terminal vacuum tubes and transistors, by constructing admittance or impedance coefficients tables for such elements.



CORRECTION

Richard F. Shea, author of the paper, "Transistor Operation: Stabilization of Operating Points," which appeared on pages 1435-1437 of the November, 1952, issue of the PROCEEDINGS OF THE I.R.E., has brought the following errors to the attention of the editors:

On page 1435, Equation (3),  $I_j = 0$  should read  $I_e = 0$ . Equation (9),  $R_{DC}$  should be  $P_{DC}$ .

On page 1436, the eleventh line below Fig. 2 should be  $P_{DC} = 10.8$  mw instead of 14.6 mw; two lines further, 8.6 mw should be 4.8 mw. Equation (14),  $S$  in denominator should be removed; third line below Fig. 3, 5 mw should be 1.4 mw.

# An Analysis of Magnetic Shift Register Operation\*

EUGENE A. SANDS†, ASSOCIATE, IRE

**Summary**—The purpose of this paper is to describe quantitatively the design of a magnetic shift register. The article is divided into 3 sections as follows:

- A. A qualitative description of magnetic shift register operation.
- B. The design of a magnetic shift register.
- C. The effects of leakage inductance on stability and maximum speed of operation of a magnetic shift register.

In section B, the equivalent impedance concept discussed in a previous article by the author<sup>1</sup> is used in the quantitative analysis of a magnetic shift register. Optimum design conditions are derived and variations from optimum design discussed.

In section C, the maximum and minimum allowable values of leakage inductance are found such that the shift register remains stable and information is reliably transferred from core to core.

## A. A QUALITATIVE DESCRIPTION OF MAGNETIC SHIFT REGISTER OPERATION

FIG. 1 SHOWS A TYPICAL SECTION of a magnetic shift register consisting of 4 magnetic cores. Information is put into the first core by means of the input driver, and then advanced to the second core by means of the A driver. Fig. 2 shows the relationship in time of the A driver current, the B driver current, and the input driver current. The information being put into the line in Fig. 2 is the binary

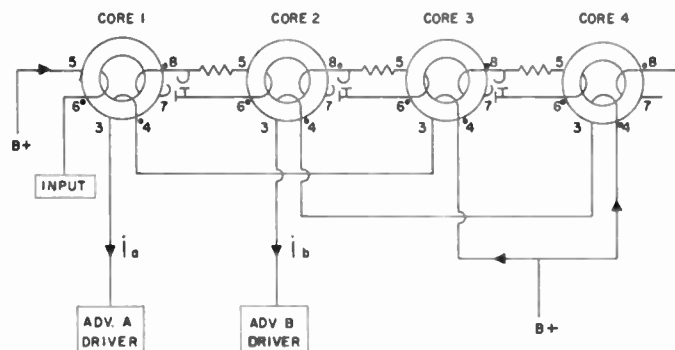


Fig. 1—Four-core magnetic-shift register. Advance winding 3-4. Input winding 5-6. Output winding 7-8.

number one zero. The input driver current is in such a direction as to drive the first core into positive saturation ( $B_M$ ). The A and B driver currents are in such a direction as to return the cores to a condition of negative saturation ( $-B_M$ ). The core material used has a rectangular hysteresis loop as shown in Fig. 3. When a core in the shift register is in the positive residual flux

density condition, it is defined as having a "one" stored in it, and when it is in the negative residual flux, it is defined as having a "zero" stored in it.

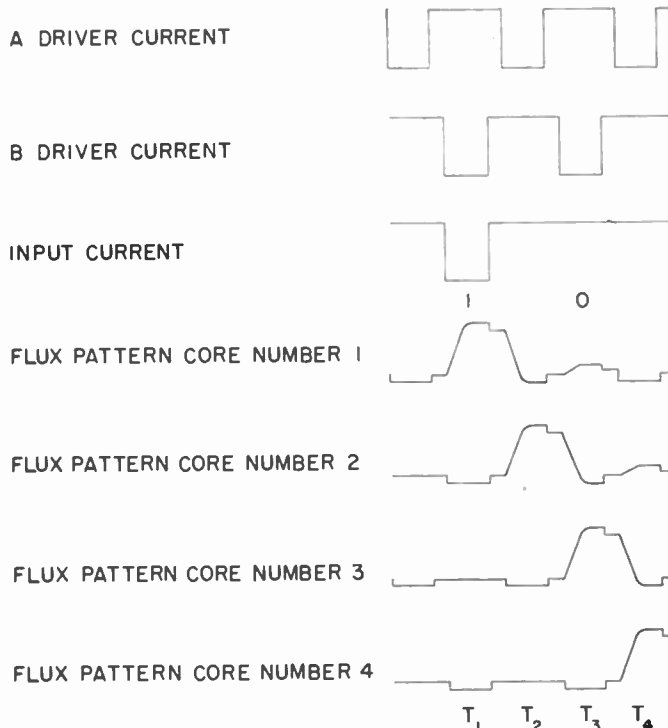


Fig. 2—Magnetic-shift register pulse pattern configuration.

The cycle of operation in putting the binary number one zero into the shift register will now be described. Let it be assumed that all four cores are initially in the "zero" state, i.e., they are at the value  $-B_R$  in Fig. 3. The input driver and the B driver are pulsed, and produce currents shown in Fig. 2. These are coincident in time. At time  $T_1$  (Fig. 2), the input current flows through the input winding in such a direction as to change the flux in core 1 to the condition  $B_M$ . The B-driver current flows through the advance windings of cores 2 and 4 in such a direction as to magnetize them to  $-B_M$ . The voltage pulse produced at the terminals of the output winding of core 1 as its flux changes from  $-B_R$  to  $B_M$  is in such a direction as to drive current through the back resistance of the series rectifier in the transfer loop between cores 1 and 2. Therefore, no appreciable demagnetizing current flows into core 2.

At the end of the input and B current pulses, core 1 is at a value of  $B_R$ , and all other cores are at a value  $-B_R$ . At time  $T_2$ , the A driver is pulsed. Its current produces a magnetizing force in such a direction as to return cores 1 and 3 to negative saturation. The change in flux in core 1 produces a voltage at its output-winding terminals of polarity to drive current through the forward conduction direction of the series rectifier and into

\* Decimal classification: 621.375.2. Original manuscript received by the Institute, September 6, 1951; revised manuscript received February 9, 1953.

† Magnetics Research Co., Chappaqua, N. Y.

<sup>1</sup> E. A. Sands, "The behavior of rectangular hysteresis loop magnetic materials under current pulse conditions," Proc. I.R.E., vol. 40, pp. 1246-50; October, 1952.



core 2. This current is in such a direction as to magnetize core 2 to the condition  $B_M$ . At time  $T_3$ , the  $B$  current pulse changes core 2 to "zero," and advances the information into core 3 in the same manner as described for the transfer from 1 to 2. The voltage appearing across the input terminals (5-6) of core 2 is in such a direction as to drive current into the output winding of core 1 through the forward conduction direction of the series rectifier. This effect, which is called "back flow of information," is manifested in the small positive bump occurring in the flux pattern of core 1 at time  $T_3$ , and the flux pattern of core 2 at time  $T_4$ .

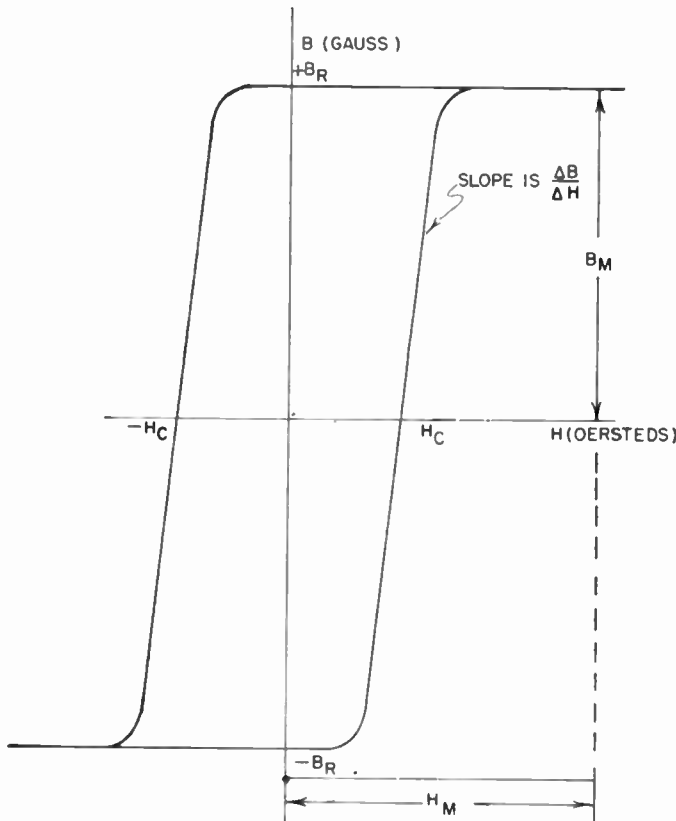


Fig. 3—Pertinent quantities on static B-H loop.

The back flow of information must be less than a certain value to maintain a good zero-to-one signal ratio, and to maintain stability. It is the function of the series resistor and shunt rectifier to cut down the amount of back flow of information. At time  $T_3$ , the voltage across the input terminals of core 2 is in such a direction as to make the shunt rectifier conduct. The series resistor is adjusted to cause a sufficient voltage drop across it that core 1 is not appreciably magnetized. At time  $T_4$ , the A driver current pulse changes core 3 to the "zero" state, and the information is transferred to core 4.

#### B. THE DESIGN OF A MAGNETIC SHIFT REGISTER

The design problem to be considered is that of reliably transferring a "one" from one core to another in a given time and using a minimum amount of input

energy. Since the magnetic shift register is an iterative structure, and the transfer is concerned with 3 cores, namely the core out of which the "1" is being read and the cores preceding and succeeding this core, for the purposes of analysis, cores 1, 2, and 3 of Fig. 1 will be considered as a typical set of 3 and the situation corresponding to the transfer of a "1" from core 2 to core 3 will be analyzed. In the previously cited article by the author<sup>1</sup> an expression was derived for the equivalent input resistance per turns squared ( $\bar{R}_0$ ) of a rectangular hysteresis loop magnetic material operating on its saturation hysteresis loop under current pulse conditions. This was

$$\bar{R}_0 = \frac{A(B_R + B_M) \times 1.26 \times 10^{-8}}{H_M T L} \quad (\text{ohms/turns squared})$$

where

$B_R$  = Residual flux density in gauss.

$B_M$  = Saturation flux density produced by  $H_M$  in gauss.

$H_M$  = Amplitude of the step function of applied field in oersteds.

$A$  = Cross-sectional area of the core in centimeters squared.

$L$  = Mean path length of the core in centimeters.

$T$  = The time it takes for the core to change its condition from  $-B_R$  to  $B_M$  with the application of  $H_M$  (measured in seconds).

Fig. 4 shows a typical switching time applied field-strength characteristic ( $H_M$  vs  $T$ ) for orthonik cores of 1.1 and 0.5 mil thickness. The product  $H_M T$  is approximately constant in the range 1 to 5 oersteds which means that  $\bar{R}_0$  is approximately constant and independent of applied field strength in this range.

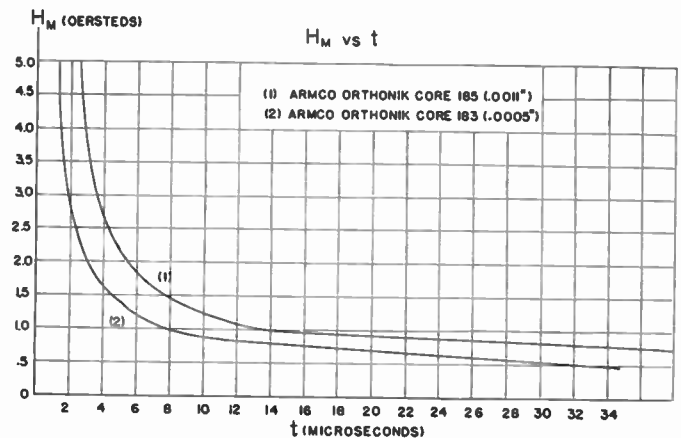


Fig. 4

Fig. 5 is the equivalent circuit corresponding to the condition of the transfer of a "1" from core 2 to core 3 of Fig. 1.  $N_3$ ,  $N_6$ ,  $N_7$  correspond respectively to the advance winding (3-4) the input winding (5-6), and the output winding (7-8). The series resistor in the transfer loop between cores is called  $R_1$ , and the forward resistance of the series and shunt rectifiers is called  $R$ ,

(assumed to be constant).  $N_5^2\bar{R}_0$  is the equivalent resistance of core 3 as viewed from its input winding.  $N_7^2\bar{R}_0$  is the equivalent resistance of core 1 as viewed from its output winding.  $N_3^2\bar{R}_0$  is the equivalent resistance of core 2 as viewed from its advance winding.

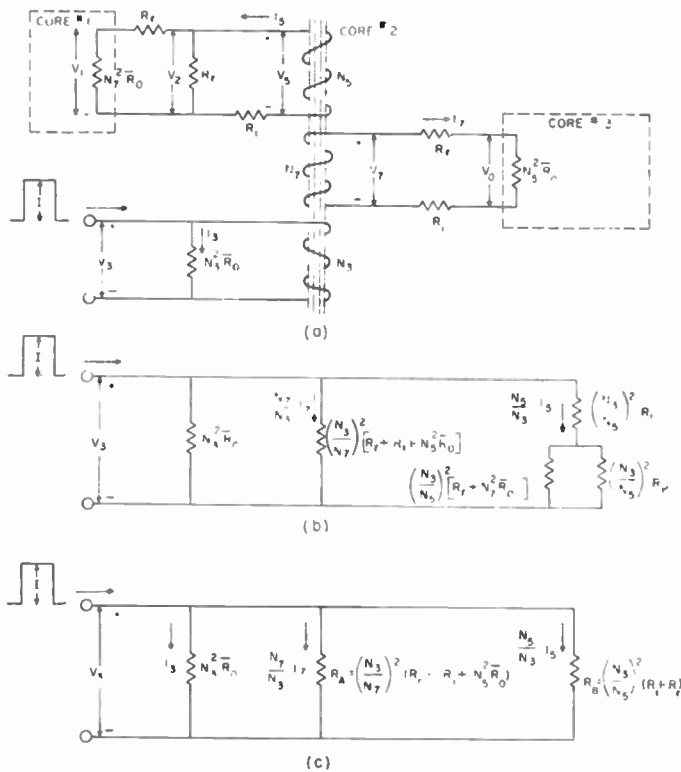


Fig. 5—Equivalent circuit for transfer of a one.

In the analysis, the following additional symbols will be used

- $T_3$  = Time taken by core 3 to change from "0" to "1" during transfer.
- $T_2$  = Time taken by core 2 to change from "1" to "0" during transfer.
- $F_{ij}$  = Fractional amount of total possible flux change  $((B_R + B_M)A)$  in core  $i$  ( $i = 1, 2, 3$ ) at time  $T_j$  ( $j = 2, 3$ ). By definition  $F_{ij} \leq 1$ .
- $R_{in}$  = Equivalent input resistance as seen at the advance winding terminals of core 2 during the time interval  $0 \leq t \leq T_3$ .

$$N = \frac{R_1 + R_r}{N_5^2\bar{R}_0}$$

$$\left(\frac{d\phi}{dt}\right)_i = \text{Rate of change of flux with time in core } i \quad (i = 1, 2, 3).$$

In what follows, these physical facts must always be borne in mind:

A. In a shift register in which information is being transferred reliably, the flux density change in going from "0" to "1," or from "1" to "0" is the same in all cores and is identically  $(B_R + B_M)$ .

B. A core out of which a "1" is being transferred (for example core 2) must change from "1" to "0" at a slower rate than the core which it is driving changes from "0" to "1." This follows from the fact that after the driving core saturates, no further energy can be transferred by transformer action to the driven core. Therefore,  $T_2 \geq T_3$ .

C. The input to the advance winding is a constant amplitude step-function of current lasting long enough to insure that all flux changes have been completed.

D. The cores are identically wound, have equal cross-sectional areas, and mean path lengths.

The relationship between  $N_7$  (the output winding) and  $N_5$  (the input winding) will now be considered. From Fig. 5(a), the voltage across the output winding of core 2 is

$$V_7 = N_7 \left(\frac{d\phi}{dt}\right)_2 \times 10^{-8} = \frac{N_7 F_{23} (B_R + B_M) A \times 10^{-8}}{T_3} \quad 0 \leq t \leq T_3. \quad (1)$$

(1) follows from the fact that the equivalent circuit is entirely resistive and the input is a constant amplitude pulse of current. Similarly, the voltage across the input winding of core 3 is

$$V_0 = \frac{N_5 (B_R + B_M) A \times 10^{-8}}{T_3} \quad 0 \leq t \leq T_3. \quad (2)$$

From the equivalent circuit

$$V_0 = \frac{V_7 N_5^2 \bar{R}_0}{R_1 + R_r + N_5^2 \bar{R}_0} = V_7 / 1 + N. \quad (3)$$

Equating (2) and (3) and substituting (1) in (3), the relationship between the number of turns on the output and input windings is found to be

$$N_5 = F_{23} N_7 / 1 + N. \quad (4)$$

Therefore, the output winding always has to have more turns than the input winding.

The flux change in core 1, when a "1" is being transferred from core 2 to core 3 will now be found. This is the back flow of information mentioned previously. For the equivalent representation of Fig. 5(a), the back flow of information is independent of  $T_2$  and  $T_3$ , so for simplicity, the case where  $F_{23} = 1$  will be discussed (core 2 and core 3 switch in the same time), and  $F_{12} = F_{13}$  found. This is the "0" to "1" ratio and should be less than 1 to 8. The total flux change in core 1 is

$$F_{12} (B_R + B_M) A = \frac{1}{N_7} \int_0^{T_2} V_{12} dt \times 10^{+8}. \quad (5)$$

From Fig. 5(a):

$$V_{12} = \frac{V_5 (N_7^2 \bar{R}_0 R_r)}{R_1 (2R_r + N_7^2 \bar{R}_0) + R_r (N_7^2 \bar{R}_0 + R_r)}. \quad (6)$$

In the usual case,  $N_7^2\bar{R}o$  is much greater than  $Rr$ . Making use of this in (6)

$$V_1 = V_5 \left( \frac{Rr}{R_1 + Rr} \right), \quad (7)$$

but

$$V_5 = \frac{N_5(B_R + B_M)A \times 10^{-8}}{T_2}. \quad (8)$$

Substituting (8) and (7) in (5)

$$F_{12} = \frac{N_5}{N_7} \frac{Rr}{R_1 + Rr}. \quad (9)$$

There are then, two ways to make the "0" to "1" ratio small. First,  $R_1$  can be made large with respect to  $Rr$ . Second, the number of turns on the output winding can be made great—relative to the number of turns on the input winding. However, the turns ratio is determined from minimum input energy considerations, and, as will be shown, stability obtained by increasing  $N_7/N_5$  can only be obtained by increasing the input ampere turns  $N_3I$ .

An optimum condition will now be found such that  $N_5I_7$  is a maximum for a given input  $N_3I$ . This means that a maximum number of ampere turns is applied to core 3 for a given number of ampere turns applied to the advance winding of core 2. It defines the minimum possible input energy to transfer a "1" in a given time. It will be assumed that  $N_7^2(\bar{R}o)$  is much greater than  $Rr$  so that the equivalent circuit of Fig. 5(b) reduces to that of 5(c). From 5(c)

$$I_7 = \frac{N_3IN_7\bar{R}o(R_1 + Rr)}{(Rr + R_1 + N_5^2\bar{R}o)^2 + N_7^2\bar{R}o(R_1 + Rr)}. \quad (10)$$

In this expression  $I$ ,  $\bar{R}o$ ,  $N_3$ ,  $R_1$ , and  $Rr$  are constant.  $N_5$  will be held constant, and a value of  $N_7$  found which will make  $I_7$  a maximum, thereby making  $N_5I_7$  a maximum. Setting  $dI_7/dN_7=0$ , and solving

$$\frac{N_7}{N_5} = \frac{1 + (F_{23})^2}{F_{23}} \quad \text{and} \quad N_5I_7 = N_3I/2 \left( 1 + \frac{1}{F_{23}} \right). \quad (11)$$

Examination of (11) shows that  $N_5I_7$  has its maximum possible value for  $F_{23}=1$ . Corresponding to this value of  $F_{23}$

$$\frac{N_7}{N_5} = 2; \quad R_1 + Rr = N_5^2\bar{R}o; \quad 4N_5I_7 = N_3I. \quad (12)$$

Physically, these results mean that in an optimum design, the flux change in cores 2 and 3 proceed at the same rate ( $T_2=T_3$ ), and the ampere turns applied to the advance winding of core 2 equals 4 times the ampere turns applied to the input winding of core 3. To achieve an optimum design two things must be done. The turns ratio must be made 2 to 1, and the sum of the rectifier resistance ( $Rr$ ) and the series resistance ( $R_1$ ) must be

made equal to the equivalent resistance of the input winding of core 3. Before discussing variations from optimum conditions, an example will be worked to make the design procedure clear.

The cores to be used are made up of 2 wraps of  $\frac{1}{8}$  inch wide, 1.1 mil thick orthonik. The core has a mean-path length of 1.2 inches. Switching time  $T_2=T_3=8 \mu\text{sec}$ . The rectifier selected has a forward resistance = 100 ohms. The "0" to "1" ratio =  $\frac{1}{2}$ . From this

$$H_M = 1.5 \text{ oersteds (see Fig. 4 } H_M \text{ vs } T \text{ curve).}$$

$$N_5I_7 \doteq 2IIML = 3.6 \text{ ampere turns.}$$

$$\bar{R}o = 1.85 \times 10^{-2} \text{ ohms per turns squared.}$$

$$R_1 = 300 \text{ ohms (equation (9), } N_5/N_7 = .5, F_{12} = F_{23} = 1).$$

$$N_5^2\bar{R}o = 400 \text{ ohms (equation 12).}$$

Using these values

$$N_5 = 147 \text{ turns}$$

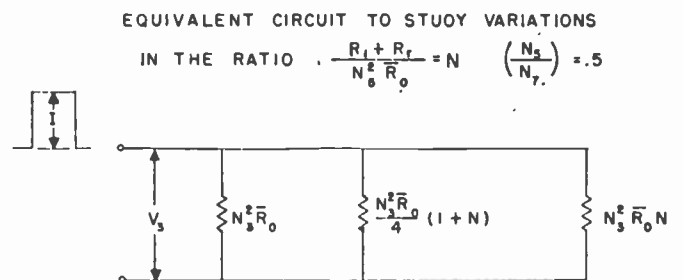
$$N_7 = 294 \text{ turns}$$

$$N_3I = 14.4 \text{ ampere turns}$$

The choice of  $N_3$  depends on the current available from the advance driver tube.

The optimum design condition can be equivalently stated as follows: For a given value of  $N_3I$ , the fastest possible transfer time is realized when  $N_7/N_5=2$ , and  $R_1+Rr=N_5^2\bar{R}o$ . In a practical design, however,  $R_1+Rr$  should be chosen to be smaller than  $N_5^2\bar{R}o$  to allow for the variation of  $\bar{R}o$  from core to core, to allow for the effects of leakage inductance and rectifier capacitance. The variation of the transfer time ( $T_2$ ) as the ratio  $R_1+Rr/N_5^2\bar{R}o=N$  is varied will now be considered.

The circuit of Fig. 5(c) reduces to that of Fig. 6(a). As  $N$  is made smaller core 2 takes an increasingly longer time to switch than core 3. At time  $T_3$ , when core 3 saturates, its input impedance changes from  $N_5^2\bar{R}o$  to zero. Therefore, the equivalent circuit of 6(a) must be



VALID FOR  $0 \leq N \leq T_3$

Fig. 6(a)

replaced by that of 6(b) after time  $T_3$ , and is valid until time  $T_2$ , when core 2 saturates. Switching times  $T_2$  and  $T_3$  will now be found as functions of  $N$ . The total equivalent input resistance as seen at the advance winding terminals ( $N_3$ ) of Fig. 6(a) is

$$(R_{in})_3 = \frac{N_5^2\bar{R}o(1+N)(N)}{N^2 + 6N + 1}. \quad (13)$$

At time  $T_3$ , from the voltage-flux time relations in core 3

$$\frac{(B_R + B_M)A}{10^8} = \frac{2IR_{in}T_3}{N_3(1 + N)}, \quad (14)$$

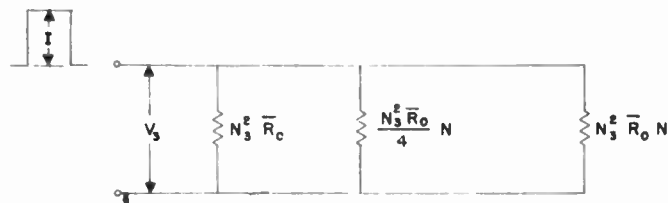
so that

$$T_3 = \frac{(B_R + B_M)A(N^2 + 6N + 1) \times 10^{-8}}{2N_3I\bar{R}_oN}. \quad (15)$$

The flux change in core 2 at time  $T_3$  is

$$F_{23}(B_R + B_M)A = \frac{1 + N}{2}(B_R + B_M)A \quad \text{from (4)}. \quad (16)$$

$T_3$  is a minimum for  $N=1$ , which confirms the fact that the fastest possible transfer time corresponds to  $R_1 + R_7 = N_5^2\bar{R}_o$ , and  $N_7/N_5 = 2$ .



VALID FOR  $T_3 < t_1 \leq T_2$

Fig. 6(b)

After core 3 has switched, core 2 works into the circuit of Fig. 6(b) for which the equivalent input resistance is

$$(R_{in})_2 = \frac{N_3^2\bar{R}_oN^2}{5N + N^2}. \quad (17)$$

To find  $T_2$ , use is made of the fact that the ratio of  $V_3$  before core 3 has switched to  $V_3$  after core 3 has switched is the same as the ratio of  $(R_{in})_3/(R_{in})_2$ ; so that

$$\frac{F_{23}/T_3}{1 - F_{23}} = \frac{(R_{in})_3/(R_{in})_2}{T_2 - T_3} = \frac{(N + 1)(N + 5)}{N^2 + 6N + 1}. \quad (18)$$

Substituting (15) and (16) in (18) and solving for  $T_2$

$$T_2 = T_3 \frac{(2N + 6)}{N^2 + 6N + 1} = \frac{(B_R + B_M)A(2N + 6) \times 10^{-8}}{(2N_3I\bar{R}_o)(N)}. \quad (19)$$

The table below gives  $T_2/T_3$  and

$$T_2 \left( \frac{2N_3I\bar{R}_o \times 10^8}{(B_R + B_M)A} \right) = D$$

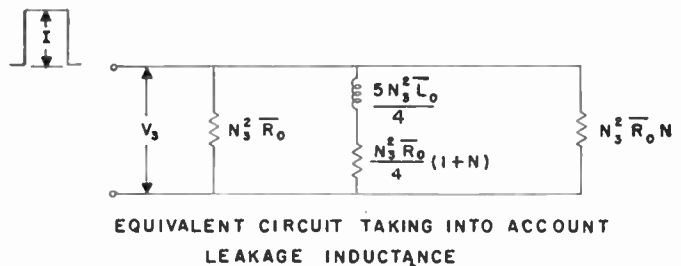
as functions of  $N$

$N$	$D$	$T_2/T_3$
1	8	1
0.8	9.5	1.18
0.6	12	1.45
0.5	14	1.65
0.3	22	2.29

### SECTION C. THE EFFECTS OF LEAKAGE INDUCTANCE ON STABILITY AND MAXIMUM SPEED OF OPERATION OF A MAGNETIC SHIFT REGISTER

Of great importance in the design of a magnetic shift register is the number of cores that can be driven from a given sized driver tube. To reduce the energy dissipated per core, it is desirable to reduce the cross-sectional area of the iron to a minimum. The lower limit on the amount of iron to be used is the maximum allowable leakage inductance in the transfer loop. If there is too much leakage inductance, a "1" cannot be transferred reliably.

Fig. 6(c) shows an equivalent circuit which takes into account the leakage inductance in the output winding of core 2, and the input winding of core 3. All quantities are



EQUIVALENT CIRCUIT TAKING INTO ACCOUNT LEAKAGE INDUCTANCE

Fig. 6(c)

referred to the input winding  $N_3$ .  $\bar{L}_o$  is the leakage inductance per turns squared. It can be shown that

$$\frac{1}{F_{23}} = \frac{2(1 + N) \left\{ 1 - \left( \frac{T}{T_3} \right) (1 - e^{-T_3/T}) \right\}}{(1 + N)^2 + 4N \frac{T}{T_3} (1 - e^{-(T_3/T)})} \quad \text{for } N_7/N_5 = 2, \quad (20)$$

where

$$T = \frac{5\bar{L}_o}{\bar{R}_o} \times \frac{(1 + N)}{(1 + 6N + N^2)}.$$

The condition for maximum allowable leakage inductance consistent with a reliable transfer is found by setting  $F_{23} = 1$ . For all values of  $F_{23}$  greater than 1, core 2 switches before core 3. Fig. 7 is a plot of the maximum allowable  $N$  ( $N_{max}$ ), such that  $F_{23} = 1$ , for various values of  $T/T_3$ . For any value of  $N$  greater than  $N_{max}$ , there will not be a reliable transfer. On the same curve is plotted the ratio as a function of  $T/T_3$

$$\frac{T}{\bar{L}_o/\bar{R}_o}.$$

The way these curves may be used will be illustrated in the following example for which  $N=0.81$  and  $T_3=8$   $\mu$ sec. From Fig. 7 (page 998) for this value of  $N$

$$\frac{T}{T_3} = 0.05, \text{ so that } T = 0.4 \mu\text{sec}.$$

and

$$\frac{\bar{L}_o}{\bar{R}_o} = \frac{T}{1.37}$$

Using the core in the example in Section B,

$$\bar{R}_o = 1.85 \times 10^{-2} \text{ ohms per turns squared,}$$

so that

$$\bar{L}_o = 0.54 \times 10^{-8} \text{ henries per turns squared.}$$

Therefore, the maximum allowable leakage inductance in the output winding of the previous example is 466  $\mu$ h if core 3 is to switch in 8  $\mu$ sec. The expression for  $\bar{L}_o$ , in this example, can be rearranged as follows

$$\bar{L}_o = \frac{0.05\bar{R}_o T_3}{1.37}$$

In this form, it is seen that the maximum allowable leakage inductance is proportional to  $T_3$ , the switching time of core 3. Therefore, the leakage inductance sets a lower limit on the switching time obtainable with a given core.

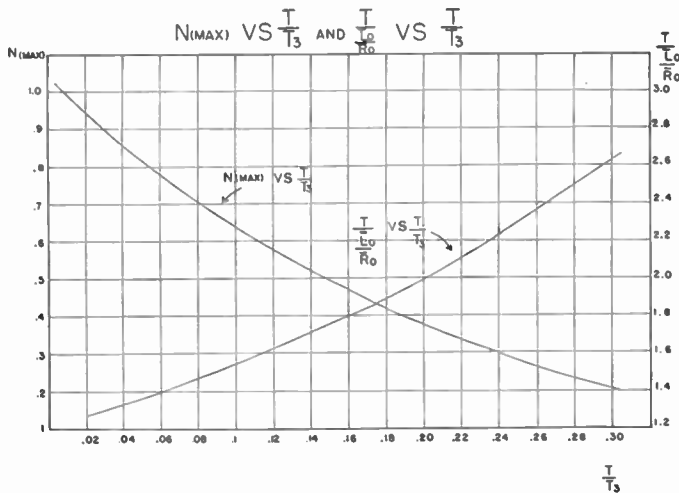


Fig. 7

One of the design criteria previously discussed was the amount of allowable back flow of information. It was stated that the flux change in core 1, when a "1" was being transferred from core 2 to core 3, should not be greater than  $\frac{1}{8}(B_R + B_M)A$ . Let us assume a flux change of  $\frac{1}{8}(B_R + B_M)A$  has taken place in core 1. On the next advance A current pulse, a voltage produced by this back flux appears on the output winding ( $N_7$ ) of core 1 in such a direction as to magnetize core 2 in the positive flux direction. If the flux change in core 2 is greater than in core 1, the magnetic shift register will become unstable because the noise level builds up in succeeding cores in the same manner as between cores 1 and 2. If the noise flux in core 1 is called  $(d\phi)_{1p}$ , and the noise flux change produced in core 2 by  $(d\phi)_{1p}$

is called  $(d\phi)_{2p}$ , the necessary condition for stability in the magnetic shift register is that  $(d\phi)_{2p}/(d\phi)_{1p}$  be less than 1.

The noise voltage appearing at the output terminals of core 1 lasts about one eighth as long as the voltage pulse occurring when a "1" is read out because the flux change is one eighth as great. Examination of Fig. 7 shows that  $N_{\text{max}}$  decreases with  $T_3$ . If  $\bar{L}_o$  is chosen so that it is about  $\frac{2}{3}$  of the maximum allowable leakage inductance per turns squared for the reliable transfer of a "1" in time  $T_3$ , then it will be great enough so that for a noise pulse of time duration  $T_3/8$ ,  $(d\phi)_{2p}/(d\phi)_{1p}$  is less than 1. If  $\bar{L}_o$  is too small, the shift register will become unstable. Therefore, there is an upper limit and a lower limit as well. If the leakage inductance is too large, a "1" cannot be transferred reliably; if it is too small, the shift register becomes unstable. In the example worked out, the maximum value of  $\bar{L}_o$  consistent with the reliable transfer of a "1" was  $\bar{L}_o = .54 \times 10^{-8}$  henries per turns squared. Values of  $\bar{L}_o$  between 0.067 and  $0.54 \times 10^{-8}$  henries per turns squared would be such as keep the shift register stable and allow for a reliable transfer. Since the maximum allowable  $\bar{L}_o$  is proportional to switching time, and the switching time is proportional to total flux change, the larger the noise flux, the less stable the register. For this reason, the stability of the magnetic-shift register is determined by the smallest noise flux such that  $(d\phi)_{2p}/(d\phi)_{1p} = 1$ . Once a noise flux occurs which makes this ratio greater than 1, stability cannot be achieved at some further point in the shift register.

CONCLUSIONS

1. In a magnetic shift register made of identical cores, the minimum possible applied field strength necessary to transfer a "1" from one core to another in a given time  $T$ , is  $4H_M$ .
2. The minimum possible applied field-strength condition is achieved by making the turns ratio of output winding to input winding 2:1, and making the resistance in the transfer loop  $(R_1 + R_r)$  equal to the equivalent resistance of the core as seen from its input winding,  $(N_5^2 \bar{R}_o)$ .
3. The minimum applied field strength condition is not critical with respect to turns ratio, provided the resistance in the transfer loop is properly adjusted. For instance, if a turns ratio of 3 to 1 is selected, and the resistance in the transfer loop is made twice that of the equivalent resistance of the core as viewed from its input winding, the applied field strength need only be increased from  $4H_M$  to  $4.25H_M$ .
4. The applied field strength required to transfer a "1" in a given time  $T$ , varies appreciably with reduction of the resistance in the transfer loop from its optimum value. For instance, a reduction of 50 per cent in this resistance from optimum necessitates an increase in applied field strength from  $4H_M$  to  $6.6H_M$ .

5. The maximum allowable leakage inductance for which reliable transfers can be obtained is directly proportional to the product of the equivalent resistance per turns squared and to the switching time.

6. The leakage inductance is primarily responsible for the prevention of noise build-up in a magnetic-shift register.

7. The allowable value of leakage inductance is bounded. It must be great enough to prevent noise build-up, but small enough to allow reliable transfer of information.

#### ACKNOWLEDGMENTS

The experimental work done was made considerably easier by the excellent pulse control equipment designed by Harold Kenosian and Joseph Chedaker of the Burroughs Adding Machine Company. The author wishes to thank Lyman Orr, Lyle Thompson, Isaac Auerbach, and Felix Kroll of the Burroughs Adding Machine Company for their help, and Martin Littman and Don Dieterle of the Armco Steel Company for their kindness in providing him with magnetic materials and pertinent data.

## Debunching of Electron Beams Constrained by Strong Magnetic Fields\*

M. CHODOROW†, SENIOR MEMBER, IRE, E. L. GINZTON†, FELLOW, I.R.E., AND E. J. NALOS†

**Summary**—To obtain a clearer insight into the design of velocity modulated tubes, a more complete understanding of the bunching process is required. A theory, to be useful in the design of high power tubes, should include the effects of space charge and large signals. Although such a theory has not yet been developed, a small signal theory, due to Feenberg, including the effects of space charge, has been obtained for some useful physical configurations. This paper deals with the experimental confirmation of this theory and the determination of its range of validity. Numerous experiments were devised to check the various aspects of the theory, and results of these are presented. Tests were made on a conventional two-cavity klystron with a cylindrical drift-tube and gridless gaps at the cavities. Transverse motion of the electrons was constrained by a large axial magnetic field. The extrapolation of the theory beyond its obvious range of validity is shown to be accurate even for large values of the bunching parameter such as to include the first peak of the output current.

#### INTRODUCTION

THE FIRST ORDER kinematic theory due to Webster<sup>1</sup> predicts, for a two-cavity klystron,

$$I_2 = 2I_0 J_1(x) \quad (1)$$

where  $I_2$  is the output radio frequency current,  $I_0$  is the direct beam current, and

$$x = \pi N \alpha \quad (2)$$

where  $N$  = cycles of transit time in drift-tube and

$$\alpha = \frac{\text{RF voltage}}{\text{DC voltage}}$$

This expression, however, does not include the effect of the mutual repulsion of electrons due to space charge. In an attempt to include space charge, Webster<sup>2</sup> solved

the equations of motion for the infinite beam, assuming positive ion neutralization, and considering longitudinal debunching only (no transverse motion of electrons allowed). The resulting expression for the fundamental component of the output current is given by

$$I_2 = 2I_0 J_1 \left( x \frac{\sin hl}{hl} \right), \quad (3)$$

provided

$$\left( x \frac{\sin hl}{hl} \right)$$

is less than unity. The debunching wave number  $h$  is defined by the relation

$$\begin{aligned} ha &= \left( \frac{60I_0 c}{V_0 u_0} \right)^{1/2} = 174 \sqrt{\frac{I_0 \text{ (amps)}}{V_0^{3/2} \text{ (volts)}}} \\ &= 174 \sqrt{\text{perveance}} \end{aligned} \quad (4)$$

where  $a$  is the beam radius,  $l$  is the drift-tube length, and  $u_0$  the dc beam velocity. Space charge is seen to manifest itself in a change of the effective bunching parameter. A larger voltage at the input gap is required to maximize the output, but the magnitude of the output current is not affected. The over-all effect on the output radio frequency current is described by the debunching parameter

$$hl = \omega_p T, \quad (5)$$

where  $\omega_p = \sqrt{ep/m\epsilon_0}$  = plasma frequency and  $T$  = dc transit time.

The physical phenomenon that is described by (3) is somewhat as follows. If in a region having uniform density of positive and negative charge (including the case in which the negative charge is moving with uniform velocity), a small region of charge is displaced from its equilibrium position, the restoring forces will cause

\* Decimal classification: R339.3X R138. Original manuscript received by the Institute, December 17, 1952.

† Stanford University, Stanford, California.

<sup>1</sup> D. L. Webster, "The theory of klystron oscillations," *Jour. of Applied Physics*, vol. 10, pp. 864-872; December, 1939.

<sup>2</sup> D. L. Webster, "Cathode-ray bunching," *Jour. of Applied Physics*, vol. 10, pp. 501-508; July, 1939.



this charge to perform an oscillation around this position at the plasma frequency. For the infinite beam, this plasma frequency is a constant depending only on the charge density and, of course, the mass of the particles. The amplitude of the oscillation is determined by the velocity modulation of the electron as it enters the drift tube, since this determines the initial velocity away from its equilibrium position in the beam. The behavior of the electrons is analogous to that of a string of pendulums tied to a belt moving at the beam velocity past a gap which excites oscillations in the pendulum, the initial excitation of each depending on when it passes the gap. Although this description of debunching is satisfactory from the point of view of visualizing the motion of each electron, it turns out that mathematically these oscillations can be described more conveniently in terms of electromagnetic waves propagating through the beam. It can be shown that the fields which cause the above motion of electrons can be expressed as a sum of four waves, each of a different propagation constant  $\gamma_n$ . Since two values of  $\gamma_n$  depend on the charge density in the beam, these waves are known as space charge waves. Their velocities differ only slightly from the beam velocity and they interfere in such a way as to produce the net effect described by (3). The remaining two waves are unaffected by the beam.

A more useful result is that due to Feenberg<sup>3</sup> who has solved the field equations and the force equation subject to the proper boundary conditions for some actual beam configurations. The results are restricted to small signals, nonrelativistic velocities, positive ion neutralization, and non-crossing of electron trajectories. For the finite beam the fields in the drift tube are made up of space charge waves whose propagation constants depend on the transverse boundary conditions as well as the charge density. Moreover, to satisfy the initial conditions at the gaps, infinite sums rather than single terms of such waves must be taken to represent the forced modulation. As an example, for a cylindrical drift tube with no angular variations, the transverse dependence must be of the form  $J_0(T_m r)$ . Allowed values of  $T_m$  are determined by boundary conditions at the walls, a different value of the propagation constant  $\gamma_{nm}$  corresponding to each value of  $T_m$ . In order to satisfy the conditions at the gaps, the known modulation voltage at the input must be expressed in an infinite sum of  $J_0(T_m r)$ , hence the total fields are of the form

$$\sum_{n=1}^4 \sum_{m=1}^{\infty} (A_{nm}) e^{\gamma_{nm} z} J_0(T_m r) \quad (6)$$

The physical gap configuration determines how many terms of this infinite expansion in "m" are important. Strictly speaking, each term of this infinite series corresponds to space charge waves of different plasma

oscillation frequency, which is no longer determined by the charge density alone, but by the finiteness of the drift tube as well. The fields in the drift tube can thus be considered as a superposition of many space charge waves of different plasma frequencies. With a large axial magnetic field two of these infinite sums drop out, and the resulting output current can be written as

$$I_2 = \frac{I_0 x F\left(hl, r, k'a, \frac{b}{a}\right)}{l} \quad (7)$$

where  $F/l$  is a function tabulated by Feenberg (Fig. 1),  $r$  is the radial position,  $k' = \omega/u_0$ ,  $u_0$  is the dc beam velocity,  $a$  is the beam radius, and  $b$  is the drift tube radius. Debunching in the finite beam is thus expressed by the function  $F$ , given by Feenberg and reproduced in Fig. 1 for a typical condition. As before, it is a function of the debunching parameter  $hl$ , but in addition depends on the radial position  $r$  and the normalized beam and drift tube radii  $k'a$  and  $k'b$ .

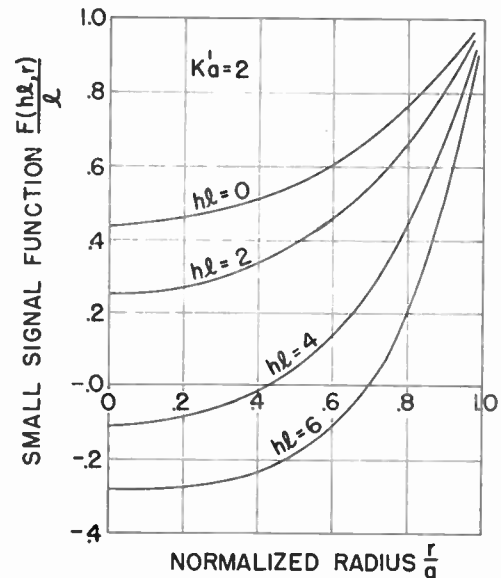


Fig. 1—Feenberg's small signal function for  $k'a = 2$  for gridless gaps, infinite magnetic field, and beam filling cylindrical drift tube.

Feenberg's theory may be arbitrarily extrapolated to include large values of the bunching parameter by considering both the exact solution of the small signal problem and Webster's first order bunching theory. For small values of  $x$ , (1) reduces to

$$I_2 = I_0 x. \quad (8)$$

On the other hand, the small signal solution of (7) implies that the effective bunching parameter now has a value of  $(x(F/l))$ . Using this value of the bunching parameter, as obtained by Feenberg for the space charge problem, the output current for large bunching parameters can be written in terms of the usual Bessel function without regard for the fact that the effective

<sup>3</sup> E. Feenberg, "Notes on velocity modulation," Sperry Gyroscope Company Report No. 5221-1043; 1945.

bunching parameter was calculated on the basis of small signals. Thus

$$I_2 = 2I_0J_1 \left\{ x \frac{F(hl, r, k'a, b/a)}{l} \right\} \quad (9)$$

which for small signals reduces to the proper form. The validity of such an arbitrary extrapolation can only be checked experimentally and is confirmed by the experiments described later in the paper.

#### GENERAL REMARKS

An inspection of (9) and the Feenberg function  $F$  reveals some interesting features of the output current.

(a) Since the small signal function  $F$  depends on radial position, the output current density is no longer constant across the beam. In general, the current density near the center is smaller, since debunching forces are stronger there.

(b) The rf current density decreases for increasing values of  $hl$  but not in a simple way, as in the case of the infinite beam.

(c) For a sufficiently large value of  $hl$ , the output current density becomes zero at some radial position regardless of the value of the bunching parameter (i.e., driving voltage), since the function  $F$  itself becomes zero (Fig. 1). This first occurs at  $r=0$  and moves outward as  $hl$  is increased. The existence and location of this critical radius would lend strong support to the theory.

(d) For still larger values of  $hl$ , the output current density near the center actually becomes negative. This reversal should be experimentally observable. Mathematically, the reason for this reversal of current density can be seen from the nature of the solution required by presence of walls surrounding the beam. As stated previously, to satisfy the initial conditions at the gap, it is necessary to superimpose an infinite set of waves with different propagation constants. The motion of the beam is described by adding an infinite set of plasma oscillations of different amplitudes with slightly different frequencies. Since each plasma wave has a different radial dependence, their sums will interfere differently at various radii; in particular, near the center of the beam these waves interfere in such a way that electrons there will reach their maximum displacement earlier than those at the edge, start moving back toward equilibrium, pass through it, and have displacements from equilibrium of the opposite sign. This results in a current density at the center of opposite sign to that at the edge, and indeed, one can make the obvious statement that electrons right at the edge of the wall must have their plasma oscillations superimposed in such a way that there is no debunching at all. Thus the electrons near the wall never have any oscillatory behavior, since the longitudinal field at the wall must be zero.

Alternately, this may be seen by considering the debunching forces themselves. At the wall these forces are

neutralized by image forces outside the beam, but at the center, these image forces are not as effective, resulting in stronger debunching. For sufficiently high current densities (large values of  $hl$ ), the electron charge density may be such as to cause an anti-bunch to be formed at the center, while at the wall, a bunch may exist.

#### DESCRIPTION OF EXPERIMENTS

(a) *Tube Design.* To investigate the various aspects of (9) described in the previous section, a conventional two-cavity klystron was constructed. A strong axial magnetic field was used to constrain the beam. Eq. (9) shows that it is sufficient to specify the parameters  $hl$ ,  $k'a$ ,  $b/a$ , and the value of  $x$  to completely determine the normalized output current. The tube was designed to include a sufficiently wide range of these parameters to be useful in tube design and at the same time provide adequate information about regions where debunching forces are large. The parameter  $hl$  was varied by varying the tube perveance (changing cathode-anode spacing), the parameter  $k'a$  by changing the dc beam voltage, and the value of  $x$  by changing the input power to the bunching cavity.

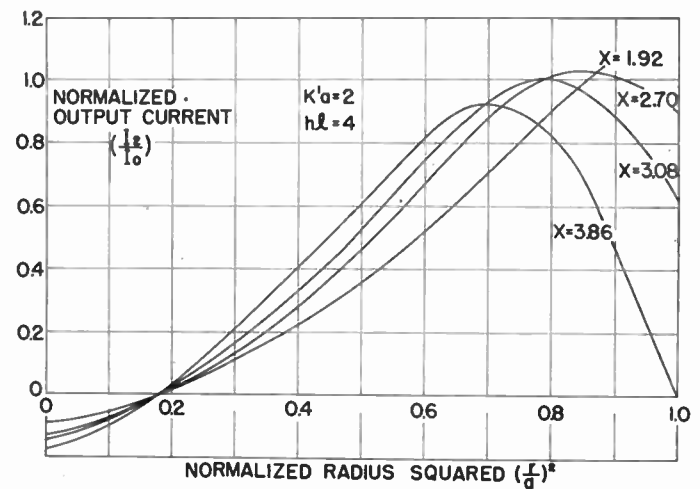


Fig. 2—Typical contributions to the output current from various radial positions for several values of the bunching parameter.

(b) *Interpretation of (9).* Eq. (9) gives two kinds of results: first, the current density as a function of radius, and second the total current which can be obtained by averaging these contributions over the beam cross-section. A typical variation of the normalized output current as a function of radius for  $k'a=2$  and  $hl=4$  is shown in Fig. 2. The total current (Fig. 3) is proportional to the area under this curve for each value of the bunching parameter. Universal curves for  $k'a=2$  and 3 are shown in Figs. 4 and 5. These curves apply to gridless cavities, but can be applied to gridded cavities if the correct function  $F$  is taken from reference 3.

(c) *Experiments.* The object of the following experiments was to check the various aspects of these curves

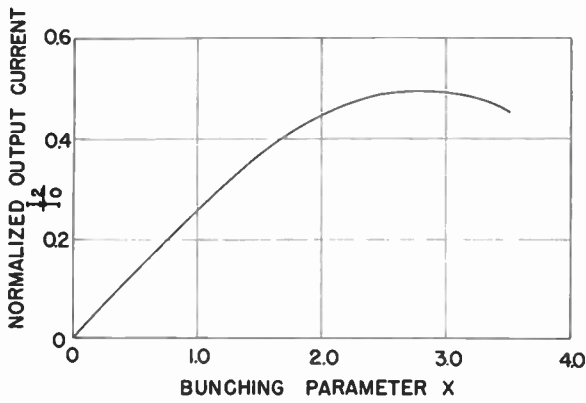


Fig. 3—Output current as a function of bunching parameter.

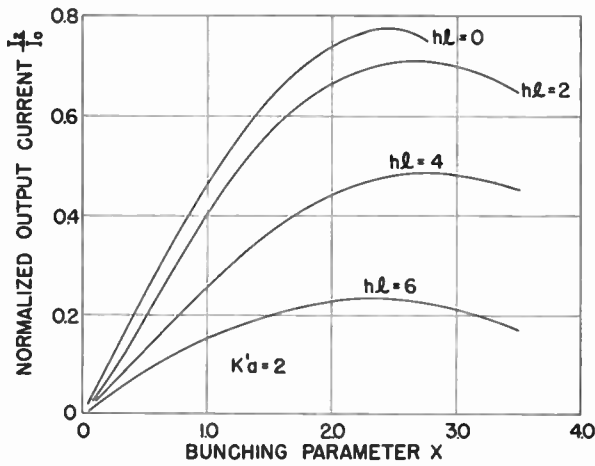


Fig. 4—Design chart for  $k'a=2$ .

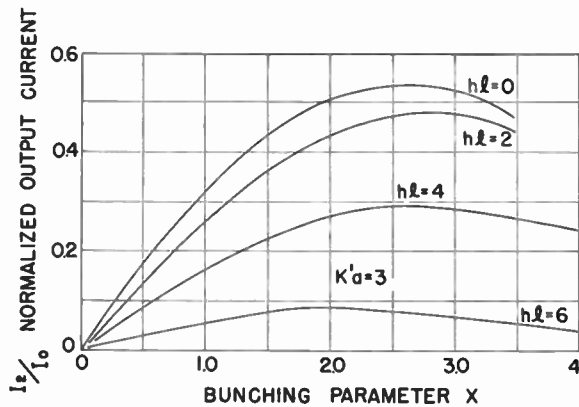


Fig. 5—Design chart for  $k'a=3$ .

and to see over what range of parameters they apply. The total rf current was measured by sweeping the input power to the buncher cavity dynamically and observing the rectified crystal current from the output cavity on an oscilloscope. Fig. 6 shows the circuit used to make these measurements. To obtain absolute values of the radio frequency current and bunching parameter  $x$ , a careful calibration of the microwave equipment was made.

The ratio of shunt impedance  $R$  to  $Q$  of the cavity is a quantity independent of loss and can be measured by perturbation methods.<sup>4</sup> The  $Q$  under operating conditions can be measured by plotting cavity impedance as a function of frequency in a conventional way. The relative variations of rf power at both input and output were obtained using a carefully calibrated square law crystal. Absolute values of power for a given condition were obtained by using a matched bolometer and bridge circuit. Knowing  $R/Q$ ,  $Q$  and the power, the rf voltage across the gap can be calculated. The rf current at the output can be deduced from  $I = V/R$ , provided the output voltage is sufficiently small compared to the beam voltage. This was achieved by loading down the output cavity.

The individual radial contributions to the output current were measured by placing a thin metallic sheet just ahead of the output cavity. A hole, small compared to the beam diameter, was drilled in this sheet. By means of a bellows arrangement, this sheet, together with the hole, was made to traverse the beam so that the hole explored all radial positions along a given diameter. The small fraction of the rf current reaching the output cavity through this hole was observed dynamically as described. Additionally, the exploring hole was used to check the uniformity of the dc beam in the drift tube. The expected reversal of phase of the output current at a critical radius was checked by comparing its phase with a reference signal from the input, using a standing wave detector padded with matched attenuators at

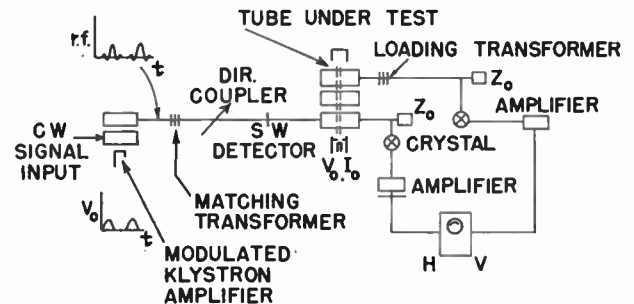


Fig. 6—Experimental setup.

both ends. If a single frequency signal is fed in from one end, no reflections are observed. The same argument is valid for a signal fed in from the other direction. If both signals are fed in simultaneously, a combination of the two waves traveling in opposite directions results in a standing wave. If the phase of one of these is shifted, the position of the node of the standing wave is also shifted; in fact, a phase shift of 180 degrees results in a shift of the node of quarter wavelength. Thus feeding a portion of the input signal of the tube to one end of a

<sup>4</sup> W. W. Hansen and R. F. Post, "On the measurement of cavity impedance," *Jour. of Applied Physics*, vol. 19, no. 11, pp. 1059-1061; November, 1948.

padded standing wave detector, and the signal from the output cavity to the other end of this detector, a shift of the node should be observed as the exploring hole is moved through the critical radius. This 180 degree phase shift was actually observed. Additional amplification was required to raise the output power level sufficiently, but this only introduces a constant phase shift.

### DISCUSSION OF RESULTS

The results of these experiments are shown in Figs. 7 and 8 for the case of optimum bunching. It is sufficient to discuss this case since the measured output current

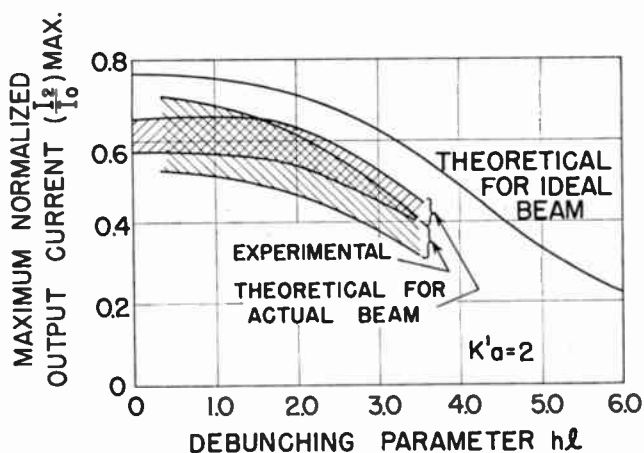


Fig. 7—Comparison of experimental and theoretical results for  $k'a=2$ .

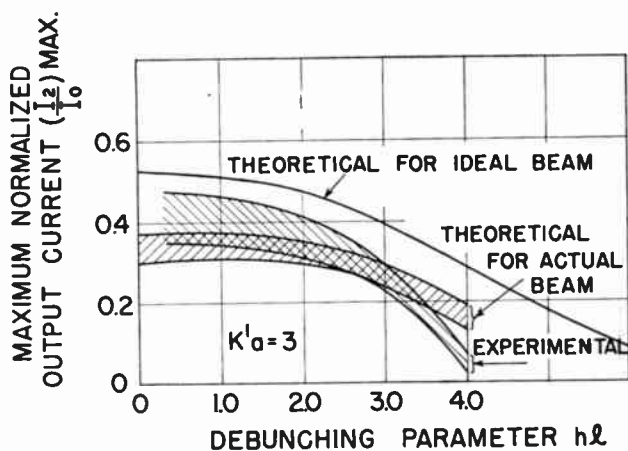


Fig. 8—Comparison of experimental and theoretical results for  $k'a=3$ .

as a function of the bunching parameter closely follows the Bessel function  $J_1(x)$  (Fig. 3). Before making a comparison with predicted results, the theoretical curves must be modified to include the effect of imperfect beam shape. The theoretical curves assume a completely uniform beam filling the drift tube which was not achieved in practice. However, a correction can be made, since the actual beam distribution was known from exploring

hole measurements. The range of modified theoretical values due to this condition is shown in Figs. 7 and 8 together with the experimental values within the accuracy of calibration of the microwave equipment.

From these curves, a comparison between theory and experiment can be made. The over-all results of this comparison are:

(a) Small signal space charge theory due to Feenberg is valid if the debunching parameter  $hl$  is less than 3.5 (i.e., for most practical designs).

(b) The extrapolated theory holds for the same values of  $hl$  but includes all values of the bunching parameter up to 4 (i.e., well beyond the first peak of output current).

(c) For large values of  $hl$ , debunching forces appear larger than given by the extrapolated theory.

(d) For large values of the bunching parameter (above 4), experimental results no longer agree with predictions of extended theory. Additional verification was obtained from cross-sectional studies where the reversal of rf current at a critical radial position was confirmed. The position of the critical radius agreed with predictions for the above ranges of parameters.

### CONCLUSION

Evidence has been presented to show that Feenberg's small signal space charge theory is valid over a sufficiently wide range to be applicable to meet all reasonable tube designs. Moreover the extrapolation of this theory is valid for all values of bunching parameter used in conventional tubes. In all cases, it is found that the output radio frequency current decreases for increasing values of  $hl$ , and the voltage at the input required to maximize the output current increases with  $hl$  for all reasonable tube designs. It is important to note that voltages at both gaps were kept well below the beam voltage. The normalized input voltage was at most  $\alpha = .3$  so that small signal theory can be safely applied to the input. The output voltage was kept small to simplify the evaluation of the rf current only. Since the theoretically predicted current at the output gap was obtained, the velocity and time of arrival of electrons at this gap are probably correctly predicted by the theory. The above knowledge makes it possible to obtain valid results for large signals at the output by merely integrating the equations of motion of the electrons through the gap to get the net transfer of power for any given rf voltage. It would be interesting to confirm this experimentally. It is indeed fortunate that this theory, and its extension, can be trusted under conditions for which it was not intended.

### ACKNOWLEDGMENT

The research reported in this paper was made possible by funds from Sperry Gyroscope Company, Great Neck, N. Y.

# A Simple Graphical Analysis of a Two-Port Waveguide Junction\*

J. E. STORER†, L. S. SHEINGOLD†, ASSOCIATE, IRE, AND S. STEIN‡, STUDENT MEMBER, IRE

**Summary**—A graphical analysis based on the original work of Deschamps is presented for obtaining the scattering matrix of a two-port waveguide junction from standing-wave measurements. The section may have losses, and can be asymmetrical. In addition, a method is outlined whereby the reflection coefficient of a load terminating the junction can be obtained graphically from the measurement of the reflection coefficient as seen through the junction.

## INTRODUCTION

A GRAPHICAL METHOD was recently introduced by Deschamps<sup>1</sup> for obtaining the scattering matrix of a two-port waveguide junction from a set of standing-wave measurements. He also outlined a procedure whereby the reflection coefficient of a load terminating the junction can then be obtained graphically from a measurement of the reflection coefficient of the load as seen through the junction. (Some of the ideas involved have also been noted previously.<sup>2</sup>) The proofs given by Deschamps were largely in terms of projective and non-Euclidean geometry.

Deschamps' method requires less calculation than the direct algebraic computation of the scattering matrix from the measurements, and fewer measurements than using the Weissfloch-tangent technique<sup>3</sup> to obtain the equivalent circuit of the junction. The new method is general, and can be used without modifica-

tion for lossy, asymmetrical junctions. Also, in its application, certain checks are set up for the elimination of errors of measurement.

Since this new method is of importance to engineers unfamiliar with higher geometry, its presentation using more familiar mathematics appears desirable. Certain additional features of the constructions also are discussed. The procedure for the use of the method is outlined first, with proofs and additional remarks given in the appendix.

## I. PROCEDURE FOR OBTAINING THE SCATTERING MATRIX OF A TWO-PORT JUNCTION

Consider a junction between two guiding systems (transmission lines or waveguides) indicated symbolically in Fig. 1 as a two-port network. The two systems need not be identical, e.g., one side could feed into a two-wire line, the other into a coaxial line.



Fig. 1—Equivalent network representation of a two-port waveguide junction.

### A. The Scattering Matrix

If the junction is equivalent to a linear passive network, its character can be described completely by the "scattering matrix"  $S$  of the junction, where

$$S = \begin{vmatrix} S_{11} & S_{12} \\ S_{21} & S_{22} \end{vmatrix}$$

A typical matrix element  $S_{ij}$  has the usual interpretation of being the reflected ("scattered") wave at terminal  $i$  due to a unit-wave incident on the junction at terminal  $j$ .

Owing to reciprocity,  $S_{12} = S_{21}$ , and  $S_{12} = T$ , where  $T$  is the transmission coefficient of the junction. The impedance matrix is related to the scattering matrix by<sup>4</sup>

<sup>4</sup> C. G. Montgomery, R. H. Dicke, and E. M. Purcell, *Principles of Microwave Circuits*, vol. 8, pp. 146-149, Radiation Laboratory Series, McGraw-Hill, New York; 1948.

\* Decimal classification: R118. Original manuscript received by the Institute, October 16, 1952; revised manuscript received February 27, 1953. The research in this paper was made possible through support extended Cruft Laboratory, Harvard University, by the National Research Council and jointly by the Navy Department (Office of Naval Research), the Signal Corps of the U. S. Army, and the U. S. Air Force, under ONR Contract N5ori-76, T. O. 1.

† Cruft Laboratory, Harvard University, Cambridge, Mass.

‡ RCA Fellow in Electronics under the National Research Council, Harvard University.

<sup>1</sup> G. Deschamps, "Application of Non-Euclidean Geometry to the Analysis of Waveguide Junctions," URSI-IRE Spring Meeting, 1952. Also in sections of Interim Reports 1-8 and Final Report on "Near-Zone Electromagnetic Waves," Federal Telecommunications Laboratories, Inc., Contract AF 33-038-13289.

<sup>2</sup> H. Wheeler and D. Dettinger, "Measuring the efficiency of a superheterodyne converter by the input impedance circle diagram," Wheeler Monographs, no. 9; March 1949. H. Wheeler, "The transmission efficiency of linear networks and frequency changers," Wheeler Monographs, no. 10; May 1949.

<sup>3</sup> N. Marcuvitz, "On the representation and measurement of waveguide discontinuities," PROC. I.R.E., vol. 36, pp. 728-735; 1948; also, A. A. Oliner and H. Kurss, "The Precision Measurements of the Equivalent Circuit Parameters of Dissipative Microwave Structures," Paper no. 78, I.R.E. National Convention, New York, N. Y.; 1951.

$$Z = \begin{vmatrix} \sqrt{Z_c^{(1)}} & 0 \\ 0 & \sqrt{Z_c^{(2)}} \end{vmatrix} \| \| I - S \|^{-1} \| I + S \| \begin{vmatrix} \sqrt{Z_c^{(1)}} & 0 \\ 0 & \sqrt{Z_c^{(2)}} \end{vmatrix}$$

where  $Z_c^{(1)}$  and  $Z_c^{(2)}$  are the characteristic impedances of the two lines. Thus a knowledge of  $S$  is equivalent to a knowledge of  $Z$ . The scattering (or impedance) matrix of a two-port junction is usually obtained by terminating one side of the junction in various lengths of short-circuited line and measuring the reflection coefficients as seen from the other side.

In particular, by making such measurements for three different positions of the short circuit, it is possible to compute the scattering matrix of the junction by solving a system of three linear algebraic equations for the three unknown matrix elements. To insure accurate results (i.e., to guard against experimental errors), it is necessary to consider more positions of the short circuit, and essentially recalculate the values of these matrix elements, comparing them with those previously obtained.

Alternatively, by taking measurements for many positions of the short circuit, an equivalent circuit may be obtained by a modification of the Weissfloch-tangent technique<sup>3</sup> which, however, involves considerable labor.

Compared to these two procedures, Deschamps' approach is a simple and much less time-consuming graphical technique for obtaining the  $S$ -matrix elements from construction lines and angles. Measurements are needed for only four positions of the short circuit (6 or 8 may be used for increased accuracy), with checks possible for consistency of the data.

**B. Graphical Evaluation of  $S_{11}$**

Suppose the values of the measured reflection coefficient  $\Gamma' = \gamma' e^{+i\phi'}$  are plotted in the complex plane. (The harmonic time dependence  $e^{+i\omega t}$  has been assumed.) Since by physical considerations  $0 \leq \gamma' \leq 1$ , all possible values lie within the unit circle, and the diagram is conveniently drawn on the usual Smith chart if the reflection-coefficient circles are available. (The resistance and reactance lines of the chart are of no concern whatever in this method.) Moreover, it is well known (see appendix) that when the output of the junction is connected to an arbitrary load, through a length  $l$  of lossless line, the values of reflection coefficient measured at the junction input lie on a circle, Fig. 2, when  $l$  is varied.

Deschamps' method proceeds as follows: The output port of the junction is connected to a short-circuited line of electrical length  $kl$ , and the complex reflection coefficients seen at the input port are measured for four lengths of line; these lengths are taken in pairs,  $kl_1, kl_1 + \pi/2$ ;  $kl_2, kl_2 + \pi/2$ . (A good distribution of the data may be achieved conveniently by placing the short circuit at four positions equally spaced along a half-wavelength of the output line.)

These reflection coefficients are plotted in the complex plane (points  $P_n'$  in Fig. 2). The points  $P_1'(kl = kl_1)$

and  $P_3'(kl = kl_1 + \pi/2)$  are connected by a straight line, as are  $P_2'(kl = kl_2)$  and  $P_4'(kl = kl_2 + \pi/2)$ ; the intersection of these lines is labeled  $S_{11}'$  and termed the "cross-over point." Also a circle  $G'$  is fitted to the  $P_n'$  with center  $C'$  located, for example, as the intersection of the perpendicular bisectors of the chords  $P_1'P_3'$  and  $P_2'P_4'$ .

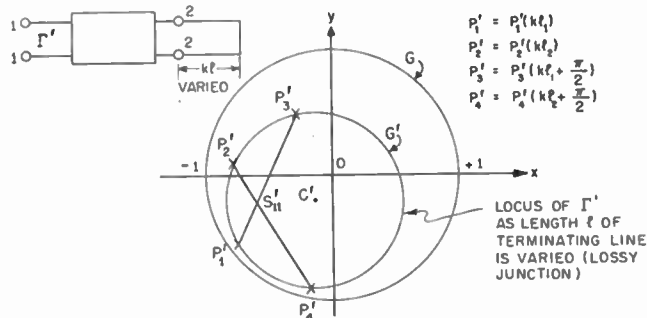


Fig. 2—Plot of measured reflection coefficients.

The line  $S_{11}'C'$  is drawn, and perpendiculars  $S_{11}'A'$  and  $C'B'$  are erected as shown in Fig. 3. The intersection of  $A'B'$  with  $S_{11}'C'$  is labeled  $S_{11}$  and termed the "iconocenter." The complex number corresponding to this point in the complex plane is the coefficient  $S_{11}$  in magnitude and phase. Thus the reflection coefficient when the junction is matched at its output is already determined.

$$|S_{11}| = \overline{OS_{11}} \quad \text{Arg } S_{11} = \angle (OP, OS_{11})$$

$$|S_{12}| = \frac{S_{11}E'}{\sqrt{r}} \quad \text{Arg } S_{12} = \frac{1}{2} \angle (OP, C'P_3'')$$

$$|S_{22}| = \frac{S_{11}C'}{r} \quad \text{Arg } S_{22} = \angle (S_{11}C', C'P_3'')$$

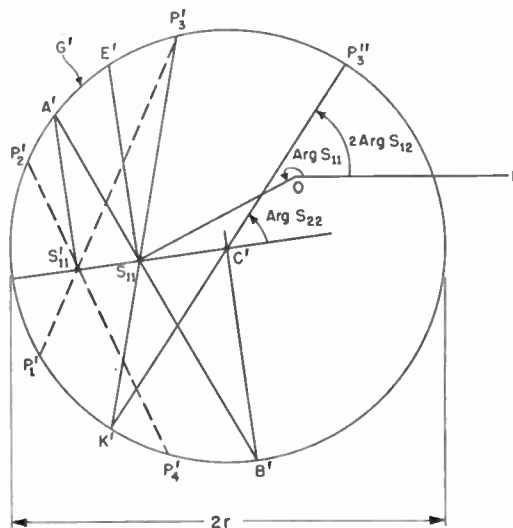


Fig. 3—Construction for elements of the scattering matrix.

**C. Graphical Method—Evaluation of  $S_{12}$  and  $S_{22}$**

For the determination of the other elements of  $S$ , alternative procedures (i.e., the measurement of lengths





Note that this method requires the knowledge of the junction parameter  $S_{22}$ .

Note also that as  $S_{11}'$  approaches close to  $C'$ , the point  $Q'$  tends to fall off the sheet. In this case the following slightly different construction, which actually is useful in all cases, may be employed: Referring to Fig. 5, the lines  $D'T_z'$  and  $C'T_z'$  are drawn. From the point  $U'$  where  $S_{11}'C'$  intersects the circle  $G'$ , a line is drawn paral-

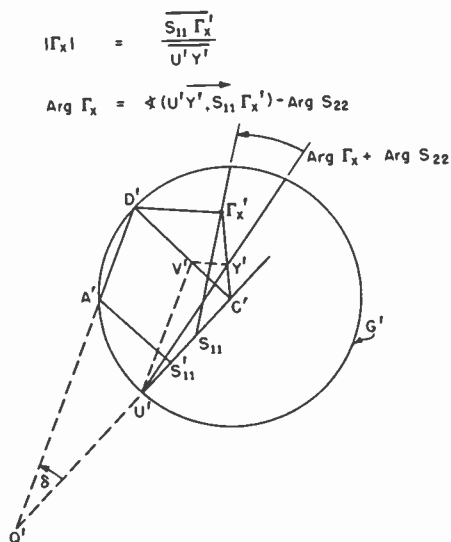


Fig. 5—Alternative construction for  $\Gamma_z$ .

lel to  $A'D'$ , intersecting  $C'D'$  at  $V'$ . Through  $V'$  another line is drawn parallel to  $D'T_z'$ , and intersecting  $C'T_z'$  in  $Y'$ . (E. W. Matthews, Cruft Laboratory, has pointed out that  $V'$  can be found more simply by marking off  $C'V' = S_{11}C'$ . The fact that  $C'V' = S_{11}C'$  can immediately be seen from proof, using Fig. 5, by noting that this is just

$$\frac{\overline{C'V'}}{\overline{C'D'}} = \frac{\overline{C'V'}}{\overline{C'U'}} = \frac{\overline{S_{11}C'}}{r}$$

The elimination of the one parallel-line construction greatly increases both the speed and the accuracy of the procedure.) Then (see the appendix, part F),

$$|\Gamma_z| = \gamma_z = \frac{\overline{S_{11}\Gamma_z'}}{\overline{U'Y'}} \\ \arg \Gamma_z = \phi_z = \angle (U'Y', S_{11}\Gamma_z') - \arg S_{22}$$

### III. APPLICATION TO AN ILLUSTRATIVE EXAMPLE

In most practical situations the power transmitted through, and reflected from, an arbitrary junction is of most interest. In addition, one is frequently faced with the problem of determining the impedance of an arbitrary load terminating a two-port junction located somewhere between the standing-wave detector and the load. In fact, in practically *all* direct measurements of

load impedances there exist discontinuities (connectors, adapters, cables, and so on) between the standing wave detector and the load to be measured. The usual procedure involved in determining the impedance of a load through such a junction has been to determine first the impedance matrix characterizing the junction, and then to calculate the impedance of the load from the measured-input impedance to the combined junction and load. This procedure is tedious and requires the knowledge of *all* the impedance elements representing the four-terminal network of the junction. Using the simple graphical construction described above, the load impedance, usually the only quantity of interest, can be determined relatively quickly.

As illustration, a typical junction will now be analyzed and the elements of its scattering matrix determined graphically. An arbitrary load will then be placed at the output terminals of the junction and its impedance also determined graphically. Again, it is emphasized that the methods described are not unique and quite possibly simplifications may be made as the technique is developed in the future.

The experimental data were obtained from standing-wave measurements on a symmetrical lossy junction, although the symmetry was not necessary for use of the method. The characteristic impedance of the input and output transmission lines were equal. The impedance at the input terminals was measured with the short-circuiting plunger in the output line at positions of  $kl=0, \pi/8, \pi/4, 3\pi/8, \pi/2, 5\pi/8, 3\pi/4, 7\pi/8$ , with  $kl=0$  corresponding to a short circuit at the output reference plane ( $\Gamma = e^{-i\pi}$ ) and  $kl=\pi/2$  an open circuit ( $\Gamma = 1$ ).

Instead of only four data points, eight points were taken in order to provide additional accuracy against experimental errors. The positions of the short-circuiting pistons were spaced equally along a half-wavelength in the output line so as to obtain a good distribution of data.

The experimental values of impedance measured at the input terminals of the junction are plotted on a Smith chart in Fig. 6 (following page) for the indicated positions of the short-circuiting plunger in the output circuit. Since the constructions are to be carried out in the reflection-coefficient plane, it is advisable to use a Smith chart with superimposed reflection-coefficient circles. Obviously, the accuracy of the results depends on the accuracy of the constructions; hence, for precision measurements, an enlarged reflection-coefficient chart should be used. Here, for a desired three-place accuracy, graph paper one meter square was used.

Corresponding pairs of data points for  $kl=(0, \pi/2), (\pi/8, 5\pi/8), (\pi/4, 3\pi/4)$  and  $(3\pi/8, 7\pi/8)$  are joined by straight lines and the nature of intersection observed. Theoretically these chords should intersect in the cross-over point  $S_{11}'$ . Owing to experimental error they may not, and the quality of their intersection is a measure of the consistency of the experimental data. Thus, if the four lines intersect in the manner shown in the enlarged

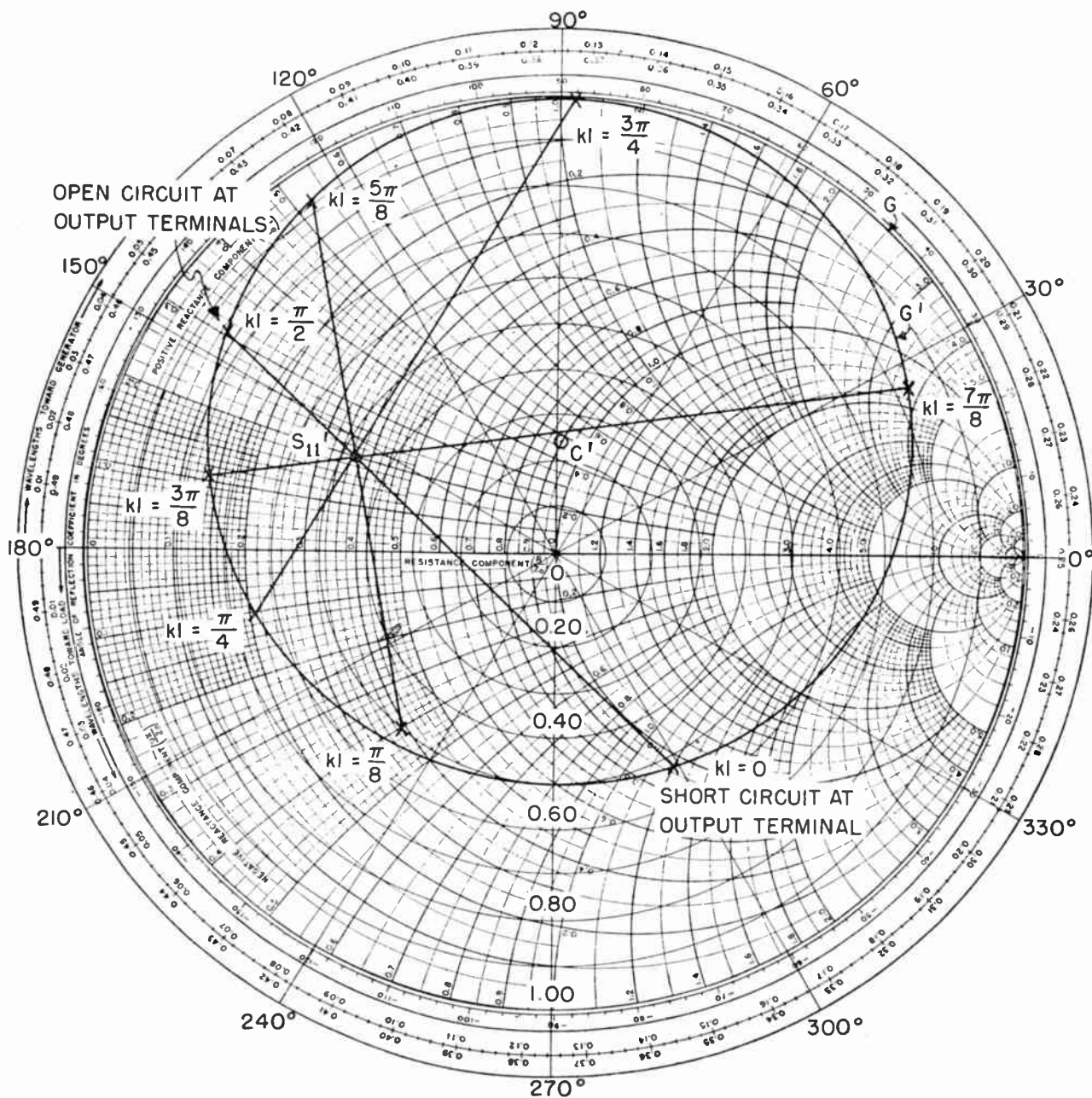


Fig. 6—Experimental data plotted on Smith-reflection coefficient chart and constructions for locating  $S_{11}'$  and  $C'$ .

view of the crossover region in Fig. 7, there is an indication of error in one of the two measurements associated with what appears to be a “bad” chord, i.e., for the shorting circuiting piston at either  $kl = \pi/8$  or  $5\pi/8$ . Since two extra pairs of points have been taken, it appears reasonable to disregard this one line and take  $S_{11}'$  at the center of the tiny triangle formed by the other three lines. This analysis of the data can be performed directly as the readings are taken.

It has been shown that all measured points should lie on a circle of center  $C'$ . If the center of the circle is to be found by the intersection of the perpendicular bisectors of the various chords, a similar situation is encountered as in determining the crossover point. Again,

only the six reliable points are used, and an appropriate center  $C'$  for the circle is chosen at the center of the triangle. Finally, the circle is drawn with an average radius, determined by averaging the distances from  $C'$  to the measured points. It is now apparent that the point corresponding to  $kl = \pi/8$  is the one in error, probably owing to the fact that the standing-wave measurement was partially masked by noise.

Now that  $S_{11}'$  and  $C'$  have been found and the circle  $G'$  drawn, graphical constructions are performed as shown in Figs. 8 and 9 to determine the amplitudes and phases of the scattering matrix elements. Although these amplitude and phase constructions have been carried out here separately for clarity, in practice all can be per-

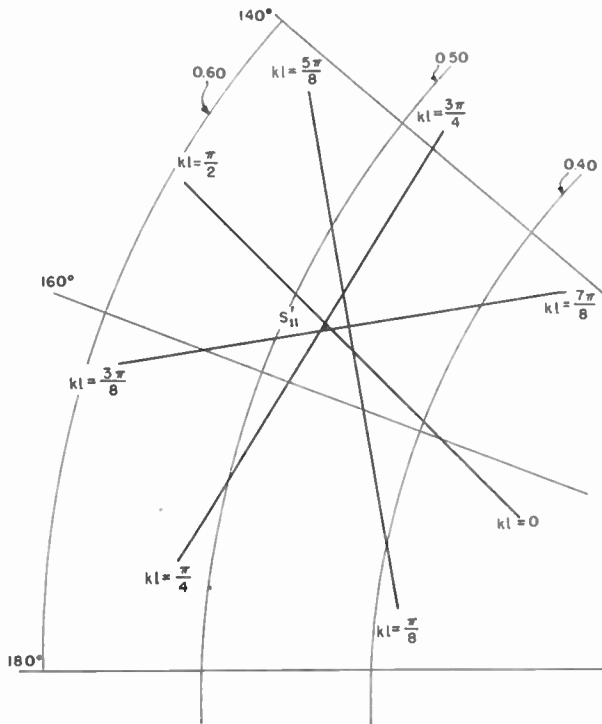


Fig. 7—Enlarged view of cross-over region.

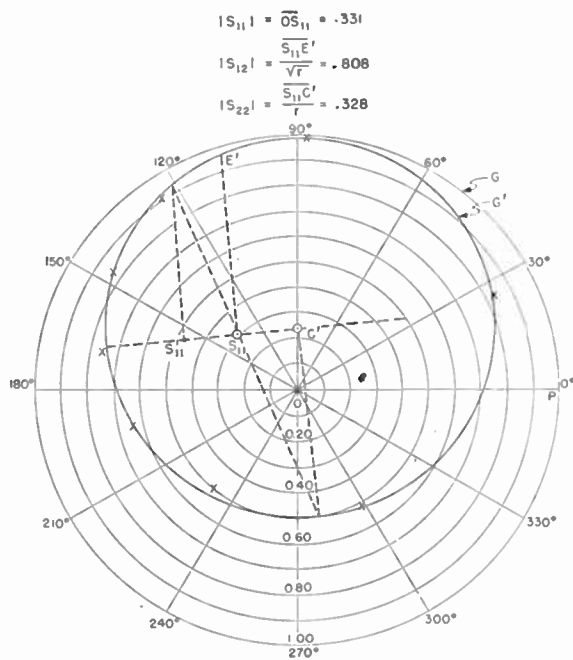


Fig. 8—Graphical determination of amplitudes of scattering matrix elements.

formed on the same sheet, and, with experience, many of the construction lines omitted.

Note that the amplitude results of Fig. 8 suffice to determine the division of power between the reflected wave and that transmitted, when the junction is terminated in a matched load. In this case, to calculate also a matching network at the input requires additionally only

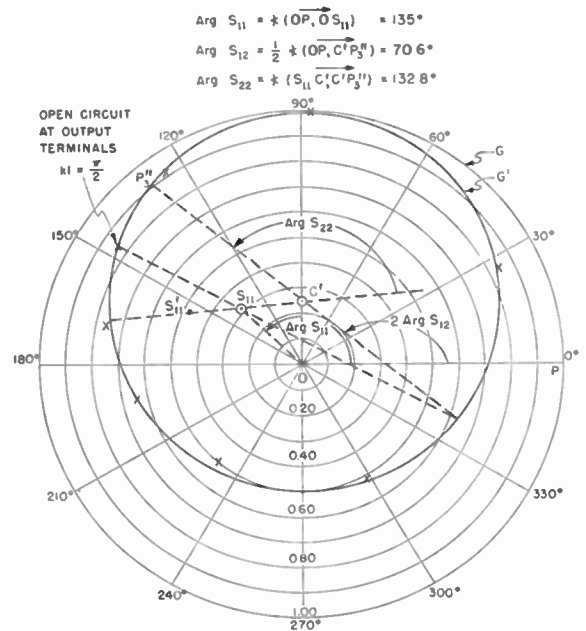


Fig. 9—Graphical determination of phase angles of scattering matrix elements.

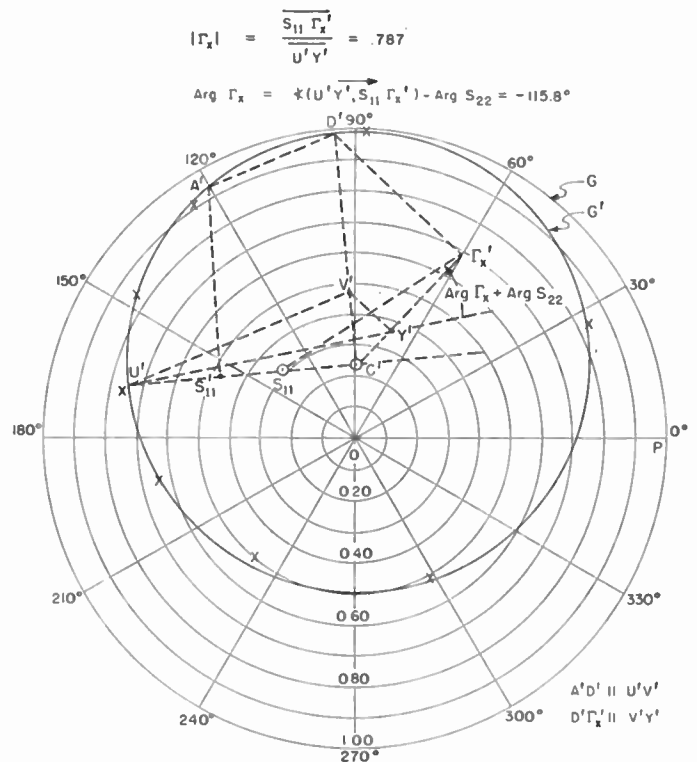


Fig. 10—Graphical method for obtaining reflection coefficient of a load terminating a symmetrical waveguide junction.

$\arg S_{11}$ , which is also available from Fig. 8 alone.

Next, an unknown impedance is used to terminate the junction, instead of the short-circuiting plunger. The reflection coefficient  $\Gamma_x' = 0.70e^{j80^\circ}$  is measured at the input terminals and plotted in Fig. 10. After performing the indicated constructions the reflection coefficient is found to be

$$|\Gamma_x| = \gamma_x = \frac{S_{11}\overline{\Gamma_x'}}{U'\overline{Y'}} = 0.787$$

$$\arg \Gamma_x = \phi_x = \angle (\overline{U'Y'}, S_{11}\overline{\Gamma_x'}) - \angle S_{22} = -115.8^\circ.$$

The normalized load impedance can now be calculated as

$$Z_x = \frac{1 + \Gamma_x}{1 - \Gamma_x} = 0.165 - j0.615.$$

## APPENDIX

### A. The junction as a bilinear transformation

With the junction terminated in a load of reflection coefficient  $\Gamma$ , the reflection coefficient  $\Gamma'$  measured at the input port is easily expressed in terms of  $\Gamma$ , using the definitions of the elements of the scattering matrix, by

$$\Gamma' = S_{11} + \frac{S_{12}^2 \Gamma}{1 - S_{22} \Gamma} = \frac{S_{11} + (S_{12}^2 - S_{11} S_{22}) \Gamma}{1 - S_{22} \Gamma}. \quad (1)$$

This relation between the complex numbers  $\Gamma'$  and  $\Gamma$  is therefore of the form of a bilinear transformation, of which certain general properties are well-known.<sup>6</sup> For example: a) with straight lines considered as limiting cases of circles, the bilinear transformation (1) will map circles in the  $\Gamma$ -plane into other circles in the  $\Gamma'$ -plane, though generally with a different radii and centers; b) the transformation is conformal, i.e., if two curves intersect in  $\Gamma$  at a certain angle, their images will intersect in  $\Gamma'$  at the same angle, and with the same sense.

Now when the output to the junction consists of a load characterized by  $\Gamma_L = \gamma_L e^{i\phi_L}$ , viewed through a section of lossless line of electrical length  $kl$ , the reflection coefficient terminating the junction is

$$\Gamma = \gamma_L e^{i(\phi_L - 2kl)}.$$

The plot of this  $\Gamma$  in the complex plane as  $l$  is varied is a circle  $G$  of radius  $\gamma_L$ , centered at the origin. Hence when this circle is mapped by (1) into the  $\Gamma'$ -plane (i.e., when measurements are made through the junction), the image points will lie on some circle  $G'$  of center  $C'$ ; and, since any diameter of  $G$  cuts  $G$  orthogonally, its image in  $w$  must be an arc passing through  $O'$  (image of the origin  $O$ ) and intersecting  $G'$  orthogonally (Fig. 11). Every diameter is thus such an arc. The particular case of interest at the moment is when the load is a short circuit,  $\Gamma_L = -1$ , and  $G$  therefore the unit circle.

Now from (1) the image of  $\Gamma = 0$  is  $\Gamma' = S_{11}$ . This point, labeled  $O'$ , or more suggestively,  $S_{11}$ , therefore locates the complex number representing the matrix element  $S_{11}$  in both magnitude and phase. How to determine this "iconocenter" from the measured points located around  $G'$  will be discussed later; for the mo-

ment, let it be assumed to be located. Then, in Fig. 11, the diameter  $A_1' C' A_2'$  through  $S_{11}$  is a particular case of an arc through  $O'$ , orthogonal to  $G'$ ; hence its original  $A_1 A_2$  must also have been a diameter of  $G$ . Putting  $\Gamma = \rho e^{i\theta}$  along  $A_1 A_2$  and  $S_{22} = |S_{22}| e^{i \arg S_{22}}$ , the image of  $A_1 A_2$  is seen from (1) to be

$$\Gamma' = S_{11} + \frac{S_{12}^2 \rho e^{i\theta}}{1 - \rho |S_{22}| e^{i(\theta + \arg S_{22})}} \theta = \text{constant}, \rho \text{ varying.}$$

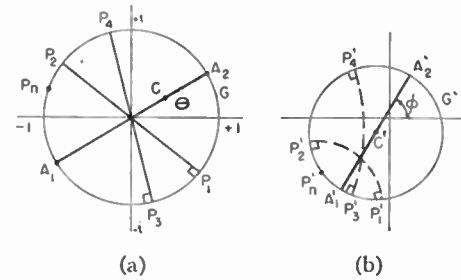


Fig. 11—(a) Original circle in  $\Gamma$ -plane (b) Image circle in  $\Gamma'$ -plane.

This in turn, however, can only be the straight line in  $\Gamma'$ , as  $\rho$  varies, if  $A_1 A_2$  is so oriented that

$$\theta = -\arg S_{22}. \quad (3)$$

Hence points along the particular diameter  $A_1' S_{11} A_2'$  are given parametrically by

$$\Gamma' = S_{11} + \frac{S_{12}^2 \rho e^{i\theta}}{1 - \rho |S_{22}|}. \quad (4)$$

The end points  $A_1$  and  $A_2$  (lying on the unit circle) are characterized by  $\rho = \mp 1$ . Hence the radius  $r$  of  $G'$  can be determined as

$$\begin{aligned} r &= \frac{1}{2} |\Gamma'_{A_2'} - \Gamma'_{A_1'}| \\ &= \frac{1}{2} \left| \frac{S_{12}^2}{1 - |S_{22}|} + \frac{S_{12}^2}{1 + |S_{22}|} \right| = \frac{|S_{12}|^2}{1 - |S_{22}|^2}. \end{aligned} \quad (5)$$

Further, since  $\Gamma'_{O'} = S_{11}$ , the length  $\overline{O'A_1'}$  (or  $\overline{S_{11}A_1'}$ ) is

$$\overline{S_{11}A_1'} = |\Gamma'_{A_1'} - S_{11}| = \frac{|S_{12}|^2}{1 + |S_{22}|}. \quad (6)$$

Finally, noting that

$$\overline{S_{11}C'} = r - \overline{S_{11}A_1'}, \quad (7)$$

it follows that

$$\frac{\overline{S_{11}C'}}{r} = 1 - \frac{\overline{S_{11}A_1'}}{r} = |S_{22}|. \quad (8)$$

Thus, if the point  $S_{11}$  is known, the construction for  $|S_{22}|$  is given by (8).

<sup>6</sup> R. V. Churchill, "Introduction to Complex Variables," McGraw-Hill, New York, N. Y.; 1948.

Further, using (8), (5) may be solved for

$$\begin{aligned} |S_{12}|^2 &= r[1 - |S_{22}|^2] \\ &= \frac{1}{r} [r^2 - r^2 |S_{22}|^2] = \frac{1}{r} [r^2 - \overline{S_{11}C'^2}] \\ &= \frac{1}{r} (\overline{S_{11}E'^2}) \end{aligned}$$

where  $S_{11}E'$  is drawn as in Fig. 3.

The result that

$$|S_{12}| = \frac{\overline{S_{11}E'}}{\sqrt{r}} \tag{9}$$

follows immediately.

*B. Some geometric theorems and constructions*

Before examining the actual determination of  $S_{11}$ , or of the phase angles, it will be necessary to point out certain easily proved<sup>5</sup> geometric theorems and constructions.

*Theorem 1:* Let circles  $G_1$  and  $G_2$  intersect orthogonally at  $P, Q$ ; and  $L$  be an arbitrary point on arc  $PQ$  of circle  $G_2$ , shown in Fig. 12. Draw  $QL$  and  $PL$  extended to  $M$  and  $N$  respectively. Then line  $MN$  is a diameter of  $G_1$ , and is parallel to the tangent  $RS$  drawn at  $L$  to  $G_2$ .

*Construction 1:* Given two circles  $G_1$  and  $G_2$  intersecting orthogonally at  $P, Q$ . A line may then be drawn through center  $C_1$  of  $G_1$ , parallel to the tangent drawn to  $G_2$  at any arbitrary point  $L$  of arc  $PQ$ . For, using Fig. 12, if  $QL$  is drawn extended to  $M$ , the diameter  $MC_1N$  is then the desired line, by theorem 1. (Note  $PLN$  is also a straight line.)

*Construction 2:* Given a diameter  $MN$  of circle  $G_1$ , and an arbitrary point  $L$  within the circle, using Fig. 12, then a circle  $G_2$  may be drawn through  $L$ , such that  $G_1$  and  $G_2$  intersect orthogonally, and that the tangent

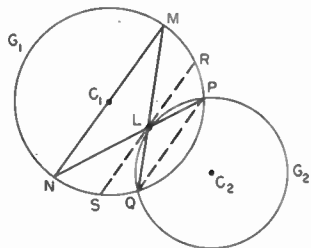


Fig. 12

to  $G_2$  at  $L$  shall be parallel to  $MN$ . For, if  $ML$  is drawn extended to  $Q$ , and  $NL$  extended to  $P$ , the circle through  $P, L, Q$  is then the required  $G_2$ . (Three points uniquely determine a circle.)

*Construction 3:* If, in the above,  $LC_1$  is perpendicular to  $MN$ , a slightly simpler construction is available, since now  $PQ$  is parallel to  $MN$ . Thus one can extend  $ML$  to  $Q$ , and obtain  $P$  by drawing  $PQ$  parallel to  $MN$ .

*Theorem 2:* Using Fig. 13, from an external point  $T$ , let  $TP$  be drawn tangent to a given circle  $G$  of center

$C$  ( $TP$  may also be regarded as the radius from center  $T$ , of a second circle intersecting  $G$  orthogonally at  $P$ ).

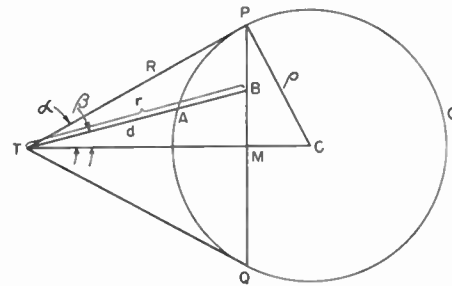


Fig. 13

Draw chord  $PQ \perp TC$ , cutting  $TC$  at  $M$ . Now draw any line from  $T$ , cutting arc  $PQ$  at  $A$  and chord  $PMQ$  at  $B$ . Then with  $TA = d, TB = r, TP = R$ , the relation holds that

$$r = d \frac{2R^2}{R^2 + d^2} \tag{10}$$

This relation between  $r, d, R$  holds in particular when  $A$  and  $B$  lie along the line  $TC$ . But then, given only a required value  $R$  for the length  $TP$  (but without prior knowledge of  $G$ ), it will be possible to construct either  $A$  or  $B$  when the other is given (i.e., with  $R$  given, the relationship is *unique*). For, with reference to the interior of the circle centered at  $T$ , of radius  $TP$ , the resemblance to the situation described in Construction 3 is obvious. This leads to

*Construction 4:* With Fig. 14, given a circle  $G_2$  of center  $T$ , and an interior point  $A$ , by drawing diameter  $MN \perp TA$ , and applying Construction 3, the line  $PQ$  is obtained with the property that arc  $PAQ$  intersects  $G_2$  orthogonally. But then radius  $TP$  is a tangent to the arc, and if  $TA$  (extended) intersects chord  $PQ$  at  $B$ , the relation between  $TA, TB$ , and  $TP$  is just that given in Theorem 4. Similarly, if  $B$  is given,  $A$  may be found by drawing diameter  $MN \perp TB$ , and chord  $PBQ \perp TB$ , and locating  $A$  as the intersection of  $MQ$  with  $TB$ .

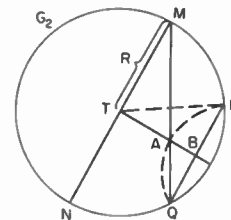


Fig. 14

The fact that in the above construction for locating (for a given circle) a point of character  $B$  from a point of character  $A$ , use has been made of (10) for the case when  $A$  and  $B$  lie on the line of centers between the two circles involved, *should not obscure* the fact that the ultimate result of Construction 4 is solely that  $TA, TB$ , and the radius  $R$  satisfy (10). That is, for any points  $A$  and  $B$  related to a circle by Construction 4, any chord



drawn through  $B$  will determine an arc through  $A$  necessarily orthogonal to the circle. The relationship is unique, and Construction 4 is just its prescription.

C. The crossover property

As mentioned in part A, a short-circuited length of line has a reflection coefficient

$$\Gamma = -\epsilon^{-j2l},$$

and the values of  $\Gamma$  lie on the unit circle  $G$  as  $l$  is varied. Therefore, pairs of values of  $kl$  differing by  $\pi/2$  represent points at opposite ends of diameters of  $G$ . Subsequently, when these values are transformed by the bilinear transformation (1), all diameters of  $G$  map into arcs passing through  $O'$  and intersecting  $G'$  orthogonally, as in Fig. 11. But then, by Construction 4, a point  $O$  can be found which lies on the chord of any such arc, and is hence a common point of intersection of all the chords. This is what has been termed the crossover point, and the general property may be stated as follows: Under any conformal transformation which maps circles into circles, the chords drawn in the image circle between the images of points originally at opposite ends of a diameter, all have a point in common; which point, further, is uniquely related to the image of the original center. (Note: This could have been shown more directly by noting that the diameter endpoints have the center as a center of negative inversion, and such a center must then also exist under the transformation; or, following Deschamps, by comparing stereographic and orthographic projections of a sphere onto its equatorial plane.)

The crossover property is the justification for the work in Section I, where first the crossover point, labeled there  $S_{11}'$ , was located (knowing *a priori* of its existence) and then, by the method of Construction 4, the iconocenter  $S_{11}$  was located from  $S_{11}'$ .

D. "Reversion" of the image circle

Consider two points  $P_1'$  and  $P_2'$  on the image circle  $G'$ , where  $P_1'$  and  $P_2'$  are images in the  $\Gamma'$ -plane of the points  $P_1$  and  $P_2$  in  $\Gamma$  of Fig. 15. If  $O'$  is the iconocenter, there are known to be arcs  $P_1'O'Q_1'$  and  $P_2'O'Q_2'$  orthogonal to  $G'$ . By Construction 1, applied as shown in Fig. 15 the diameters  $N_1C'P_1''$  and  $N_2C'P_2''$  are obtained, which, respectively, are parallel to the tangents of  $O'$  to these arcs. Therefore,  $\angle P_1''C'P_2''$  included between these lines at  $C'$  is equal to the angle at which the arcs intersect at  $O'$ . But these arcs are themselves the images of the original diameters through  $P_1$  and  $P_2$ , and by the angle-preserving properties of the bilinear transformation, intersect at the same angle as these original diameters. Therefore,  $\angle P_1''C'P_2'' = \angle P_1OP_2$ , so that the points  $P_1''$  and  $P_2''$  are located on the circumference of  $G'$  in the same relative positions as were the original points  $P_1$  and  $P_2$  on  $G$ . This process, of going from any  $P_n'$  to a  $P_n''$  by use of Construction 1 and the particular point  $O'$  (the iconocenter) may be termed "reversion." If reversion is applied to each point of the measured (image) circle  $G'$ , the resulting points (those double-primed in Fig. 15) will obviously then all be distributed

around the circumference of  $G'$  in the same relative positions as were the corresponding original points (i.e., the points of  $G$  on which the bilinear transformation acted). Thus, the "reverted circle," the set of double-primed points may be thought of as a scaled-down, and rotated, version of the original circle  $G$ . Note that nothing has been said in this description about applying geometrical transformations to points of interior of  $G'$ .

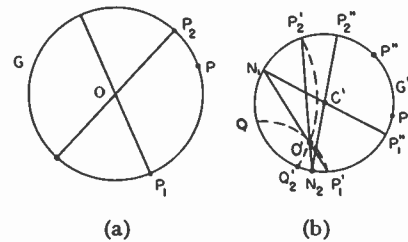


Fig. 15—(a) Original circle (b) image.

E. The elements of the scattering matrix

The phases of the  $S$ -matrix elements now may be calculated by using the reversion process. Referring to Fig. 11, it has been shown that the angle  $\theta$  at which  $A_1A_2$  is oriented in the original circle is equal to  $-\arg S_{22}$ . Hence, the latter may be determined by finding  $\theta$ . Now,  $\theta = \angle(OP, OA_2)$ , where  $P$  is the point on the real axis in  $\Gamma$  at  $\Gamma = +1$  (corresponding to an open circuit at the junction output). But  $A_2$  maps into  $A_2'$  and  $P$  into a point  $P'$ . Suppose for the moment that the point  $P'$  has been one of the measured points. Then let reversion be

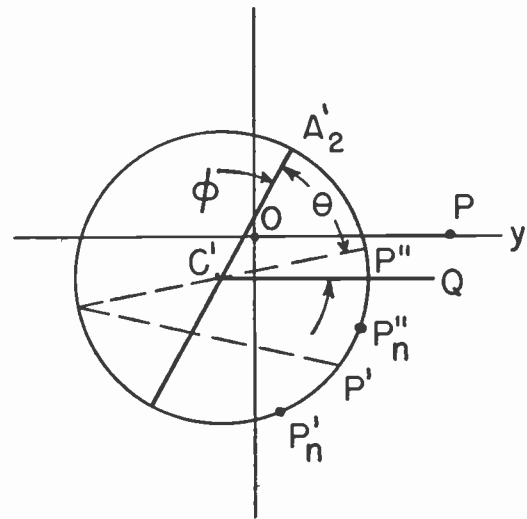


Fig. 16

applied to the points  $A_2'$  and  $P'$ . By its nature  $A_2'$  is unaffected, but  $P'$  goes into  $P''$ , as in Fig. 16, so that by the property of the reversion it follows that

$$\angle(C'P'', C'A_2') = \angle(OP, OA_2) = \theta.$$

or

$$\begin{aligned} \arg S_{22} &= -\theta = \angle(C'A_2', C'P'') \\ &= \angle(S_{11}C', C'P''). \end{aligned}$$

The last step follows by inspection.

Next, it follows from (4) that the orientation of  $A_1'A_2'$  with respect to the horizontal axis in  $\Gamma'$  is given by the angle  $\phi$  in Fig. 16, where  $\phi = 2 \arg S_{12} + \theta$ . Or  $\arg S_{12} = \frac{1}{2}(\phi - \theta)$ , so that if on this diagram  $Q$  is a point on the horizontal line through  $C'$ ,  $\arg S_{12} = \frac{1}{2}[\angle(C'Q, CP'')]$ . If the real axis of this complex plane also has been labeled  $OP$ , so that  $OP$  and  $C'Q$  are parallel, then

$$\arg S_{12} = \frac{1}{2} \angle(OP, C'P'')$$

These results are given in Section I for the case when  $P'$  is one of the measured points (short circuit placed  $\lambda/4$  past the junction).

If  $P'$  is unavailable and, instead, an arbitrary one of the measured points,  $P_n'$  is reverted into  $P_n''$  and the angles measured, the difference is just that of the angle  $\alpha$  included between  $C'P''$  and  $C'P_n''$ . But this angle is that between the originals of these points in the  $\Gamma$ -plane. With  $P_n$  corresponding to the use of a length  $l$  of lossless line and  $P$  to a length  $l_0$ , it follows that

$$\alpha = \angle(C'P_n'', C'P'') = \arg(\epsilon^{-j2kl}) - \arg(\epsilon^{-j2kl_0}),$$

or

$$\alpha = 2(kl - kl_0).$$

This is the quantity which must be added to the measured angles in each case in order to get the correct values for  $\arg S_{22}$  and  $\arg S_{12}$ .

F. Measurements of an impedance through the junction

The procedure originally proposed by Deschamps makes extensive use of the reversion constructions. A simpler and quicker method has been outlined in Section II, and only this method will be discussed.

The proof proceeds from (1), applied to the case of a junction terminated in an unknown load  $\Gamma_x$ ;  $\Gamma_x'$  is measured, giving the value

$$\Gamma_x' = S_{11} + \frac{S_{12}^2 \Gamma_x}{1 - S_{22} \Gamma_x} \tag{11}$$

This equation may be solved for  $\Gamma_x$ , yielding

$$\Gamma_x = \frac{1}{S_{22}} \left[ \frac{\Gamma_x' - S_{11}}{\Gamma_x' - \left( S_{11} - \frac{S_{12}^2}{S_{22}} \right)} \right] \tag{12}$$

Suppose now that  $\Gamma_x'$  is plotted in the complex  $\Gamma'$ -plane, and also as point  $Q'$  the complex number  $[S_{11} - (S_{12}^2/S_{22})]$ , as shown in Fig. 17. Then, with

$$\begin{aligned} \Gamma_x &= \gamma_x e^{j\phi_x} \\ |\Gamma_x| &= \gamma_x = \frac{1}{|S_{22}|} \frac{|\Gamma_x' - S_{11}|}{|\Gamma_x' - Q'|} \\ &= \frac{\overline{S_{11}\Gamma_x'}}{|S_{22}| \cdot Q'\Gamma_x'} \end{aligned}$$

and

$$\begin{aligned} \arg \Gamma_x = \phi_x &= \arg(\Gamma_x' - S_{11}) - \arg(\Gamma_x' - Q') - \arg S_{22} \\ &= \angle(Q'\Gamma_x', S_{11}\Gamma_x') - \arg S_{22}. \end{aligned}$$

It remains to be shown that  $Q'$  is indeed the point obtained by the construction of Fig. 4. This is easily seen by noting that the point  $\Gamma = \infty$  maps by (1) into just this value of  $\Gamma' = S_{11} - (S_{12}^2/S_{22})$ . But  $\Gamma = 0$  and  $\Gamma = \infty$  are inverse<sup>6</sup> with respect to the unit circle  $G$  in the  $\Gamma$ -plane and it is another property of bilinear transformations that their images (the points  $S_{11}$  and  $Q'$ ) must be inverse with respect to the image circle  $G'$ . That is,  $Q'$  can be located as the point on the radius through  $S_{11}$ , for which  $(\overline{Q'C'}) (S_{11}C') = r^2$ , where  $r$  is the radius of  $G'$ . That the construction of Fig. 4 gives this result is readily shown from geometry.<sup>5</sup>

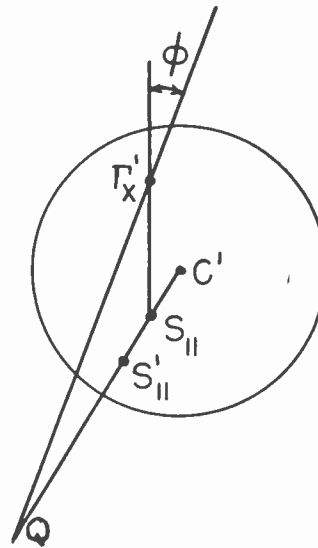


Fig. 17

As previously noted this method fails if  $Q'$  lies off the paper being used, i.e. if  $S_{11}C'$  becomes too small.

However by proceeding from Fig. 4 to the construction in Fig. 5, a scaled-down version of the picture is obtained. Further, using the formula

$$|S_{22}| = \frac{\overline{S_{11}C'}}{r}$$

it may be noted from Figs. 4 and 5 that the scaling factor is just

$$\frac{\overline{C'U'}}{Q'C'} = \frac{\overline{C'D'}}{Q'C'} = \tan \delta = \frac{\overline{S_{11}C'}}{r} = |S_{22}|$$

and hence that

$$\frac{\overline{U'Y'}}{Q'\Gamma_x'} = |S_{22}|,$$

or

$$\overline{U'Y'} = \overline{Q'\Gamma_x'} \cdot |S_{22}|; \tag{13}$$

and by the parallelism of  $U'Y'$  and  $Q'\Gamma_x'$ ,

$$\angle(U'Y', S_{11}\Gamma_x') = \angle(Q'\Gamma_x', S_{11}\Gamma_x'). \tag{14}$$

The results claimed in Section II then follow immediately from (13), and (14).

# The Gyrator as a 3-Terminal Element\*

JACOB SHEKEL†, ASSOCIATE, IRE

**Summary**—A 3-terminal circuit element, that has properties similar to those of a gyrator, is described. A method is derived to realize such an element with any unilateral transducer such as a vacuum-tube or a transistor. The effect of loading a gyrator by admittors in parallel or in series with its terminals is investigated. It is also shown that suitable loading of a gyrator may transform it into another gyrator of different gyrating admittance.

## INTRODUCTION

THE GYRATOR, a 2-terminal-pair network element that violates the theorem of reciprocity, has been postulated and analyzed by Tellegen.<sup>1</sup> Its properties are described by the "gyrating admittance"  $G$ , in

$$\left. \begin{aligned} I_1 &= GV_2 \\ I_2 &= -GV_1 \end{aligned} \right\} \quad (1)$$

Given such an element, Tellegen proceeds to formulate a general method for synthesizing networks that may violate the reciprocity law.<sup>2</sup>

The physical realization of a gyrator seems to call for a medium that exhibits gyromagnetic properties. Such a medium has been used to construct a gyrator working in microwave frequencies.<sup>3</sup>

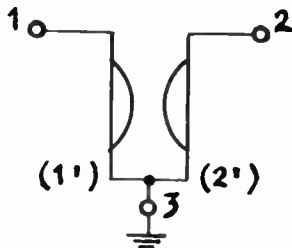


Fig. 1—Gyrator as a 3-terminal element.

If we short-circuit terminals 1' and 2' of the gyrator shown in Fig. 1, a 3-terminal element is obtained, whose admittance matrix, according to (1), is

$$\left\| \begin{array}{cc} 0 & G \\ -G & 0 \end{array} \right\| \quad (2)$$

The 3-terminal element may be used with node 1 or 2 grounded. The indefinite-admittance matrix,<sup>4</sup> that is

\* Decimal classification: R143. Original manuscript received from the Institute, August 28, 1952; revised manuscript received, March 2, 1953.

† Scientific Department, Ministry of Defense of Israel; Haifa, Israel.

<sup>1</sup> B. D. H. Tellegen, "The gyrator, a new electric network element," *Phillips Res. Rep.*, 3, pp. 81-101; 1948.

<sup>2</sup> B. D. H. Tellegen, "The synthesis of passive, resistanceless four-poles that may violate the reciprocity relation," *Phillips Res. Rep.*, 3, pp. 321-337; 1948.

<sup>3</sup> C. L. Hogan, "The ferromagnetic Faraday effect at microwave frequencies and its applications—the microwave gyrator," *Bell Sys. Tech. Jour.*, vol. 31, p. 1; January, 1952.

<sup>4</sup> J. Shekel, "Matrix representation of transistor circuits," *PROC. I.R.E.*, vol. 40, p. 1493; November, 1952.

obtained from (2) by completing each row and column to zero, is

$$\left\| \begin{array}{ccc} 0 & G & -G \\ -G & 0 & G \\ G & -G & 0 \end{array} \right\| \quad (3)$$

When any terminal is grounded, the corresponding row and column are crossed out. It is obvious that, no matter which terminal is grounded, the resultant  $2 \times 2$  matrix is always the same as (2) (with a possible reversal of sign). The 3-terminal gyrator exhibits the same properties in all grounding positions.

In view of this circular symmetry, the symbol of Fig. 2 is proposed to represent a 3-terminal gyrator. When the gyrator is incorporated in a network, elements  $Y_{pq} = \pm G$  appear in the admittance matrix ( $p$  and  $q$  are two out of the three numbers  $i, j, k$ );  $Y_{pq} = +G$  if  $pq$  is in the order indicated by the arrow, and  $-G$  if  $pq$  is in the reverse order. This may also be described by a 3-index admittance symbol, indicating the order of rotation. Fig. 2 shows a gyrator of gyration admittance

$$Y_{ijk} = G, \quad (4)$$

meaning that, for instance,  $Y_{ki} = G$  and  $Y_{ji} = -G$ .

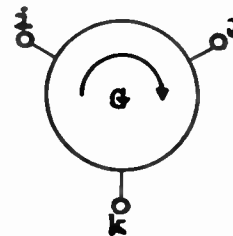


Fig. 2—Proposed symbol for 3-terminal gyrator.

## PARALLEL-LOADED GYRATOR

Consider any linear 3-element network, active or passive, described by a  $2 \times 2$  admittance matrix

$$\left\| \begin{array}{cc} Y_{11} & Y_{12} \\ Y_{21} & Y_{22} \end{array} \right\|, \quad (5)$$

with  $Y_{12} \neq Y_{21}$ . The matrix may be split into symmetric and skew-symmetric components

$$\left\| \begin{array}{cc} Y_{11} & \frac{1}{2}(Y_{12} + Y_{21}) \\ \frac{1}{2}(Y_{12} + Y_{21}) & Y_{22} \end{array} \right\| + \left\| \begin{array}{cc} 0 & \frac{1}{2}(Y_{12} - Y_{21}) \\ \frac{1}{2}(Y_{21} - Y_{12}) & 0 \end{array} \right\|. \quad (6)$$

The skew-symmetric part is a gyrator of gyration admittance

$$G = \frac{1}{2}(Y_{12} - Y_{21}), \tag{7}$$

and the symmetric part is a network composed of a triangle of admittors

$$\begin{aligned} A &= Y_{22} + \frac{1}{2}(Y_{12} + Y_{21}) \\ B &= Y_{11} + \frac{1}{2}(Y_{12} + Y_{21}) \\ C &= -\frac{1}{2}(Y_{12} + Y_{21}) \end{aligned} \tag{8}$$

the whole network being a parallel combination of both, as Fig. 3 shows. (In this discussion and throughout the rest of the paper,  $A, B, C, P$  and  $Q$  will represent admittances, in order not to encumber the equations with indexed  $Y$ 's.)

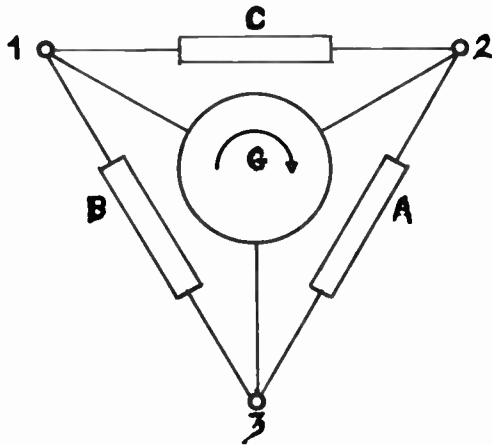


Fig. 3—The general 3-terminal network as a parallel-loaded gyrator.

It is now easy to perceive how an ideal, unloaded gyrator may be realized. It is only necessary to connect an admittance  $-A$  in parallel with  $A$ , and in the same manner to "strip off"  $B$  and  $C$ . As negative resistors or other negative circuit elements are already acceptable circuit elements,<sup>5</sup> the realization of an ideal 3-terminal gyrator does not necessitate the postulation of any new components.

We may start with a triode operating in class A. Let  $G_m$  and  $G_p$  be its mutual conductance and plate conductance, respectively, and let the grid, anode and cathode be numbered in the order mentioned. The admittance matrix for grounded-cathode operation, split into symmetric and skew-symmetric components, is

$$\begin{vmatrix} 0 & 0 \\ G_m & G_p \end{vmatrix} = \begin{vmatrix} 0 & \frac{1}{2}G_m \\ \frac{1}{2}G_m & G_p \end{vmatrix} + \begin{vmatrix} 0 & -\frac{1}{2}G_m \\ \frac{1}{2}G_m & 0 \end{vmatrix}, \tag{9}$$

showing that the triode may be regarded as a loaded gyrator, of gyration admittance

$$Y_{321} = \frac{1}{2}G_m. \tag{10}$$

The external loading necessary to "strip" the gyrator is

shown in Fig. 4. It corresponds to a network whose admittance matrix is the negative of the symmetric matrix in (9).

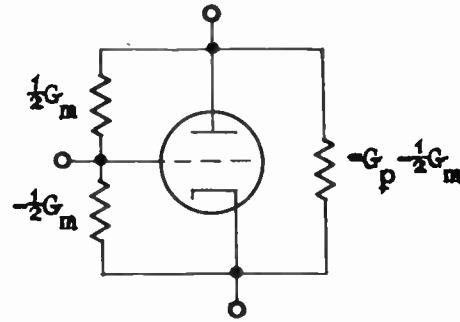


Fig. 4.—Realization of an ideal gyrator.

SERIES-LOADED GYRATOR

We will now investigate the properties of circuits that are composed of a gyrator, with admittors connected in series with some of its terminals.

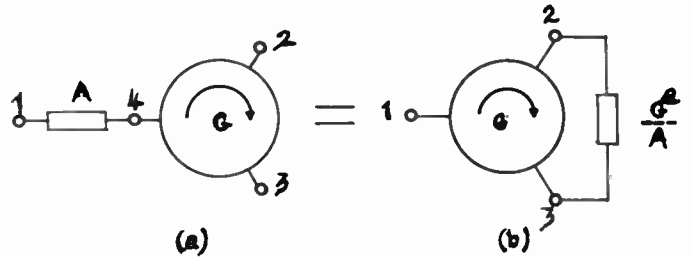


Fig. 5—Gyrator series-loaded with one admittor.

Fig. 5(a) shows a gyrator with one admittor  $A$ . The (indefinite) admittance matrix for this network is

$$\begin{vmatrix} A & 0 & 0 & \dots & -A \\ 0 & 0 & G & \dots & -G \\ 0 & -G & 0 & \dots & G \\ \dots & \dots & \dots & \dots & \dots \\ -A & G & -G & \dots & A \end{vmatrix}. \tag{11}$$

The matrix is written in a partitioned form, for we now want to eliminate the fourth terminal, and treat it as a 3-terminal network, with terminals 1, 2 and 3 only. The elimination<sup>6</sup> results in a  $3 \times 3$  admittance matrix

$$\begin{vmatrix} A & 0 & 0 \\ 0 & 0 & G \\ 0 & -G & 0 \end{vmatrix} = \begin{vmatrix} -A \\ -G \\ G \end{vmatrix} \times \begin{vmatrix} -A & G & -G \end{vmatrix} = \begin{vmatrix} 0 & G & -G \\ -G & \frac{G^2}{A} & G - \frac{G^2}{A} \\ G & -G - \frac{G^2}{A} & \frac{G^2}{A} \end{vmatrix}. \tag{12}$$

<sup>5</sup> H. W. Bode, "Network Analysis and Feedback Amplifier Design," pp. 185-188; Van Nostrand Publishing Co., New York, N. Y., 1945.

<sup>6</sup> G. Kron, "Tensor Analysis of Networks," Chap. X, "Reduction formulas," equations 10.2 and 10.7, pp. 243-244, Wiley and Sons Publishers, New York, N. Y.; 1939.

This is the same gyrator, parallel-loaded by an admittor  $G^2/A$  between terminals 2 and 3 as Fig. 5(b) shows. (This series-parallel transformation is also a property of the two-terminal-pair gyrator.)<sup>1</sup>

Consider now a gyrator with two admittors,  $A$  and  $B$ , in series with two of its terminals as shown in Fig. 6(a).

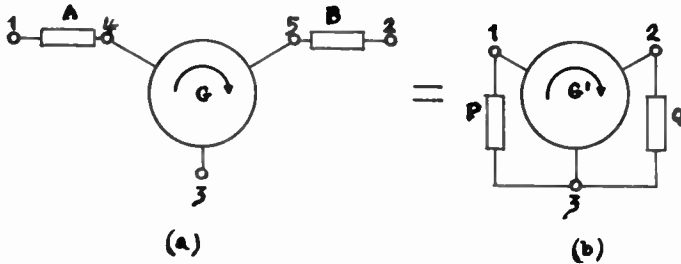


Fig. 6—Gyrator series-loaded with two admittors.

We will eliminate nodes 4 and 5, and thus find the equivalent network between nodes 1, 2 and 3. The complete indefinite admittance is

$$\begin{vmatrix} A & 0 & 0 & \dots & -A & 0 \\ 0 & B & 0 & \dots & 0 & -B \\ 0 & 0 & 0 & \dots & G & -G \\ \dots & \dots & \dots & \dots & \dots & \dots \\ -A & 0 & -G & \dots & A & G \\ 0 & -B & G & \dots & -G & B \end{vmatrix} \quad (13)$$

Elimination of nodes 4 and 5 results in the admittance matrix

$$\begin{aligned} & \begin{vmatrix} A & 0 & 0 \\ 0 & B & 0 \\ 0 & 0 & 0 \end{vmatrix} - \begin{vmatrix} -A & 0 \\ 0 & -B \\ G & -G \end{vmatrix} \times \begin{vmatrix} A & G \\ -G & B \end{vmatrix}^{-1} \times \begin{vmatrix} -A & 0 & -G \\ 0 & -B & G \end{vmatrix} \\ &= \begin{vmatrix} A & 0 & 0 \\ 0 & B & 0 \\ 0 & 0 & 0 \end{vmatrix} - \frac{1}{AB+G^2} \begin{vmatrix} -A & 0 \\ 0 & -B \\ G & -G \end{vmatrix} \times \begin{vmatrix} B & -G \\ G & A \end{vmatrix} \times \begin{vmatrix} -A & 0 & -G \\ 0 & -B & G \end{vmatrix} \\ &= \begin{vmatrix} A & 0 & 0 \\ 0 & B & 0 \\ 0 & 0 & 0 \end{vmatrix} - \frac{1}{AB+G^2} \times \begin{vmatrix} A^2B & -ABG & ABG+AG^2 \\ ABG & AB^2 & -ABG+BG^2 \\ -ABG+AG^2 & ABG+BG^2 & -AG^2-BG^2 \end{vmatrix} \\ &= \frac{G}{AB+G^2} \times \begin{vmatrix} AG & AB & -AB-AG \\ -AB & BG & AB-BG \\ AB-AG & -AB-BG & AG+BG \end{vmatrix} \quad (14) \end{aligned}$$

Writing, for short,

$$\frac{ABG}{AB+G^2} = G'; \quad \frac{AG^2}{AB+G^2} = P; \quad \frac{BG^2}{AB+G^2} = Q \quad (15)$$

(14) reduces to

$$\begin{vmatrix} P & G' & -G'-P \\ -G' & Q & G'-Q \\ -P+G' & -Q-G' & P+Q \end{vmatrix}, \quad (16)$$

which is a gyrator  $G'$  parallel-loaded by  $P$  and  $Q$  as seen in Fig. 6(b).

The result may be applied to realize a gyrator of any gyrating admittance out of any given gyrator. If, in Fig. 6(a), an admittor  $-P$  is connected between 1 and 3, and  $-Q$  between 2 and 3, the result is an ideal, unloaded gyrator of admittance  $G'$ . (Given  $G$  and  $G'$ ,  $A$  and  $B$  are not determined uniquely, as only the product  $AB$  appears in the expression for  $G'$ .)

Series-loading all three terminals will give a similar result: a gyrator of different gyrating admittance, parallel-loaded by three admittors. The complete derivation of this result is not presented here, as it gives no new effects.

CONCLUSION

It was shown that a three-terminal element may be conceived, that has properties similar to those of the 2-terminal-pair gyrator. This element may be considered as the nucleus of any 3-terminal network that violates the reciprocity relation. Suitable loading of any such network, (e.g. vacuum-tube or transistor), by positive or negative bilateral admittors, may result in stripping the gyrator to its ideal, unloaded form.

Given a gyrator of any gyrating admittance, it is possible to realize gyrators of other admittance values by suitable series and parallel loading.

The necessary components for realizing a 3-terminal gyrator of any gyrating admittance are: a 3-terminal element or network that violates the reciprocity relation, the usual passive and bilateral network elements, and negative resistances.

# A Method for Improving the Read-Around-Ratio in Cathode-Ray Storage Tubes\*

JOSEF KATES†, ASSOCIATE, IRE

**Summary**—Cathode-ray storage tubes are subject to interference which is caused by secondary electron flow between storage locations. A method of reducing this interference by modulating the cathode-ray tube differently during “action” and “regeneration” periods is described. This modulation builds up during “regeneration” periods a negative charge barrier around each spot. The negative charge barrier in turn reduces the flow of secondary electrons from one spot to adjacent spots during “action” periods. This results in decreased secondary electron flow from one storage location to another during “action” periods at the expense of increased secondary electron flow between storage locations during “regeneration” periods. Thus advantage is taken of the fact that practical computer stores can tolerate during “regeneration” periods redistribution currents between adjacent storage locations of the order of 100 times those flowing during “action” periods.

## I. INTRODUCTION

SINCE THE WORK of Williams and Kilburn<sup>1</sup> was published the ordinary cathode-ray tube has been widely adopted as a high-speed store for digital electronic computers. However, a serious defect of the cathode-ray tube store has become apparent, especially in parallel machines. When the area adjacent to a given storage location is consulted too frequently, the content of this storage location is obliterated. The maximum number of times spots adjacent to a given spot  $S$  may be consulted between regenerations of  $S$  without changing the information stored at  $S$  may be defined as the Read-Around-Ratio (R.A.R.) of  $S$ . In many machines the lowest R.A.R. has been found to be of the order of 20, while for foolproof performance a

$$\text{R.A.R.} \geq \frac{\text{Number of spots in array}}{\text{Regenerations per action}}$$

is required. A R.A.R. between 100 and 1,000 is dictated by the above requirement for the optimum utilization of cathode-ray storage tubes in practical machines.

A method for increasing the R.A.R. is outlined below.

## II. POTENTIALS OF THE FACE OF A CATHODE-RAY STORAGE TUBE

In a cathode-ray storage tube electrostatic charges are stored in a discrete array (raster) of spots, termed storage locations, shown in Fig. 1. By charging a storage location either directly with the primary electron beam, or indirectly with a secondary electron beam emanating from an area closely adjacent to the storage location

proper, the storage location may be charged relatively positively or negatively. Three areas of the inside surface of the cathode-ray tube screen are of interest.

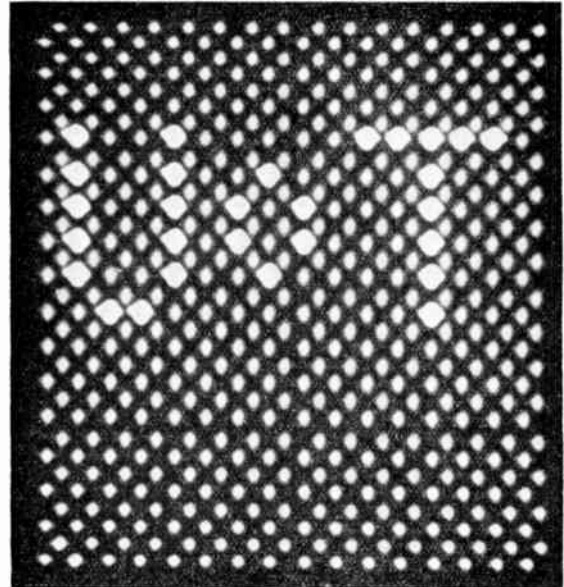


Fig. 1—Array of storage locations.

These are

- a) The storage locations proper.
- b) The areas adjacent to the storage locations which are bombarded by the primary beam in order to furnish secondary electrons to the storage locations proper whenever the storage location is to be charged negatively. These areas will be termed secondary cathodes.
- c) The remainder of the tube screen which serves neither for storage locations nor as secondary cathodes. This comprises usually the greater part of the screen area and will be termed the separation-area.

The potential diagram<sup>2-4</sup> of a cross-section of a cathode-ray storage-tube screen in the absence of beam current is indicated in Fig. 2. The space between lines  $a_1$  and  $b_1$  is a section of the storage location  $S_1$ . The space between  $b_1$  and  $c_1$  is a section of the secondary cathode of  $S_1$ . The space between  $c_1$  and  $a_2$  is a section of the

\* Decimal classification: R138.31. Original manuscript received by the Institute February 25, 1952; revised manuscript received February 24, 1953.

† Research Engineer, Computation Centre, University of Toronto, Toronto, Ontario, Canada.

<sup>1</sup> F. C. Williams and T. Kilburn, “A storage system for use with binary digital computing machines,” *Proc. I.E.E.*, (London), part II, vol. 96; April 1949.

<sup>2</sup> L. Brillouin, “Theory of the Williams’ Tube.” Report on the 11th Annual Conference on Physical Electronics held March 29–31, 1951, at M.I.T.

<sup>3</sup> W. B. Nottingham, “Bombardment of Insulating Surfaces by Electron Beams.” Report on the 11th Annual Conference on Physical Electronics, March 29–31, 1951, at M.I.T.

<sup>4</sup> J. Kates, “Space Charge Effects in Cathode-Ray Storage Tubes.” Ph.D. Thesis, University of Toronto; 1951.

separation area between  $S_1$  and  $S_2$ . The potential is referred to that of the electrode collecting the secondary electrons, usually the last anode of the tube. It will be noted that the separation area is at a negative potential with respect to the secondary electron collector. The storage locations and secondary cathodes are positive with respect to the separation area.

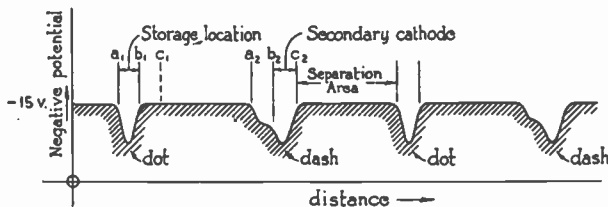


Fig. 2—Potential of a cross-section of the screen.

When the cathode-ray beam bombards a spot on the tube face, secondary electrons will leave this spot. The potential of the spot is governed by the potential drop in the secondary beam flowing to the secondary electron collector and, in a given tube, depends chiefly on the primary beam intensity. Some of the secondaries from the spot will flow to the separation area and to adjacent storage locations. The separation area will charge to a potential with respect to that of the storage locations and secondary cathodes, such that the integrated secondary electron current flowing to any spot of the separation area is equal to the integrated electron current leaking off the same spot. Since the secondary electrons leave the storage locations and secondary cathodes with a range of initial energies, the separation area has to charge negatively with respect to the area bombarded by the primary beam in order to limit the stray secondary electron current flowing to the separation area.

The full line of Fig. 3 is a potential diagram of a cross-section of a cathode-ray storage tube face while the primary beam bombards one spot. Primary and secondary electron paths have also been indicated. Vertical potential scale refers solely to the heavy potential lines. A vertical distance scale would refer to electron paths.

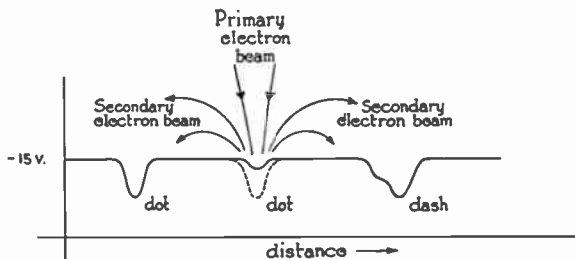


Fig. 3—Screen potential during bombardment.

The negative potential of the storage location and its immediate surroundings is in part due to the space charge in the electron beams traveling to and from the storage location. Hence, when the primary beam is removed, the potential of the storage location and its immediate surroundings will become more positive as indicated by the dotted line of Fig. 3.

### III. "ACTION" and "REGENERATION" PERIODS

The operation of a cathode-ray tube store is divided, not necessarily equally, into "action" and "regeneration" periods.<sup>1</sup> During action periods, the store furnishes some particular portion of its contents to other machine organs or places new contents into some particular place in the store.

Regeneration periods are interspersed with action periods to prevent the loss of information held in the store due to secondary electron redistribution, electrical leakage, stray ionization currents and so on. During successive regeneration periods, successive storage locations are scanned and their contents are restored.

Interference between storage locations is caused by the flow of secondary electrons from one storage location to another. This is aggravated by the fact, that during action periods the electron beam may bombard the immediate vicinity of a given storage location  $S$  a considerable number of times, between the times at which the given storage location  $S$  is regenerated.

Interference could be greatly decreased if the secondary electron flow between adjacent storage locations could be decreased or prevented during action periods, even at expense of increased secondary electron flow between storage locations during regeneration periods. This result is achieved by method here proposed.

### IV. THEORY OF THE METHOD

The separation area surrounding a given storage location and its corresponding secondary cathode, will charge slightly negatively with respect to the most negative potential of the storage location and (or) the secondary cathode. The potential distribution will be such that the small-charge leakage from the separation area will just be replaced by secondary electrons from the area bombarded by primary electrons.

The principle of the method here proposed is to adjust conditions differently during action and regeneration periods, so that secondary electrons cannot flow to and over the separation area from a storage location or secondary cathode during action periods. This can be achieved by adding a so-called "guard" period which will usually be merged with the regeneration period. During the guard period the storage location and/or the secondary cathode or some portion of the separation area is driven to a more negative value than during any other period by

- Intensifying the primary beam (i.e. increasing the beam current, adjusting the beam focus, or a combination of these methods). This increases the potential drop between the electrode or electrodes collecting or governing the secondary beam and the spot bombarded by the primary beam.
- Pulsing negatively the electrodes or electrode collecting secondary electrons or governing flow.
- Pulsing positively the pick-up electrode; or
- A combination of some or all of a), b), and c).



The guard period will usually, but not necessarily, be merged with the regeneration period. During the guard period the storage location or the secondary cathodes or some portion of the separation area may be bombarded by the primary beam. The areas bombarded by the primary beam must be chosen so that the separation area is charged to an extent which diminishes or prevents secondary electron current flow between adjacent storage locations during action periods. Merging the guard period with the regeneration period achieves this automatically.

This method ensures that during the guard periods the separation area or a portion thereof is charged so negatively as to greatly diminish or prevent the flow of secondaries from one storage location or its secondary cathode to another storage location during action periods. The negative charge leaking off the separation area is replaced chiefly or only during the guard periods. This is indicated in Fig. 4 where the potential of a spot is shown during guard (full line) and action (dotted line) periods.

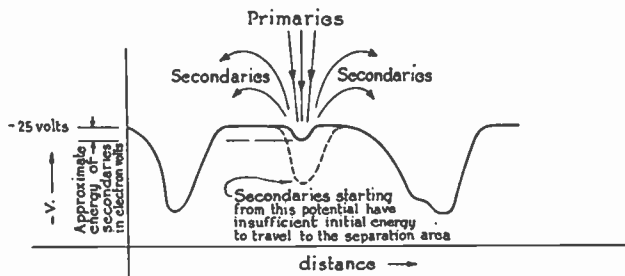


Fig. 4—Potential distribution during "guard" (full line) and "action" (dotted line) periods.

V. EXAMPLES OF THE METHOD

This section will illustrate a number of ways in which the method may be applied.

Fig. 5 shows the grid and deflection pulses of a cathode-ray storage tube during action, regeneration, and guard periods for both dots and dashes. If this system were to be applied to a defocus-focus system, the focus waveform would take the form of the deflection waveform shown in Fig. 5.

Another way of applying the method is shown in Fig. 6 where the potential of the post accelerator (third anode) is made negative during the guard period.

This may be combined with the beam modulation of Fig. 5. During the guard period the pick-up plate may be pulsed positively as shown in Fig. 7. This will have substantially the same result as the method of Fig. 6.

A way of effecting a similar result is to work with a defocused beam at all times except during the guard period at which time the beam is sharply focused. This is indicated in Fig. 8.

A combination of these methods may be used also. In every case the potential of a number of spots is depressed either directly (Figs. 5, 6, and 8) or indirectly,

as Fig. 7 shows, while these spots are bombarded by the primary electron beam. The secondary electrons emanating from these spots charge the separation area so negatively that subsequently only the fastest secondaries from action spots can overcome the potential barrier so created.

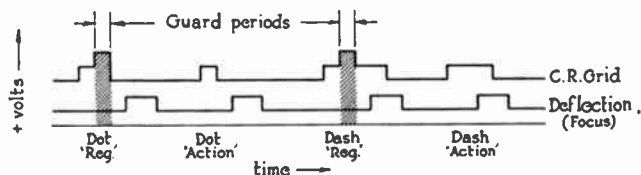


Fig. 5—Intensification of the beam during the guard period.

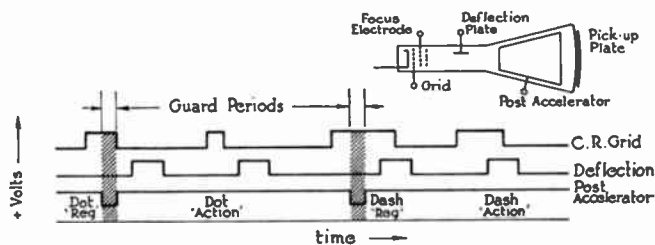


Fig. 6—Pulsing the post accelerator electrode during the guard period.

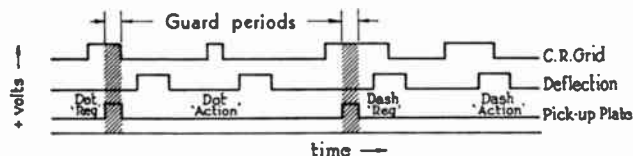


Fig. 7—Pulsing the pick-up plate during the guard period.

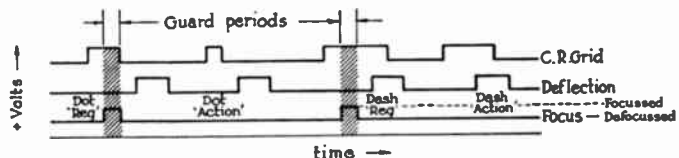


Fig. 8—Focusing the beam during the guard period.

The method shown in Fig. 5 has been adopted for the electronic computer model (UTECH) at the University of Toronto. This method appears to be most suitable because it results in the least amount of excessive signal at the input of the pick-up amplifier.

VI. EXPERIMENTAL RESULTS

The method described above was tested on 2BP 1, 3 BP 1, 3 JP 1, and 3 JP 11 tubes. Modulation of the cathode-ray tube beam similar to the method illustrated in Fig. 5 was employed throughout these experiments. Fig. 9 is a photograph of the computer on which these experiments were carried out.

The cathode-ray tubes were connected as shown in Fig. 10. Note that the restoring circuit fixes the most negative potential of the bright-up pulse. Fig. 11 shows a photograph of typical bright-up pulses. Action and regeneration periods alternated.



Initially all spots in the raster are cleared to "zeros." Due to secondary electron redistribution from the action spots those spots having a R.A.R. less than  $2^n$  will change into "ones." Once a spot becomes a "one" it will remain a "one." The number of spots having a R.A.R. less than  $2^n$  are counted in 30-second intervals. This number is plotted for various heights of the step  $E$

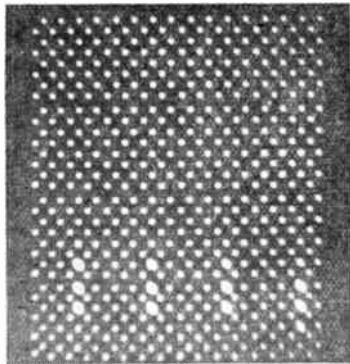


Fig. 12—Cathode-ray tube display during R.A.R. test.

and for different values of the R.A.R. ( $2^n$ ) in Figs. 13, 14 and 15, for three typical tubes. Results were similar for a total of 15 tubes tested. Results also were similar for the same tube when different operating conditions were employed, such as larger than optimum beam focus, smaller or larger raster size, different accelerating voltages and so forth. The actual R.A.R. would, of course, be sensitive to these variations in operating parameters, but the variation in R.A.R. with the step took the same form as illustrated in Figs. 13, 14, 15 and 16.

A programmed R.A.R. test was also employed on a few tubes. In this test, four spots adjacent to a given spot  $S$ , ( $S$  being initially a "zero") are each bombarded for  $n$  successive action periods.  $S$  is then tested. If  $S$  is still a "zero"  $n$  is increased by unity and the above process repeats. This is continued until  $S$  changes into a "one" or until  $n$  reaches the value 128 which corresponds to a R.A.R. of 4 times 128, i.e. 512. The value of

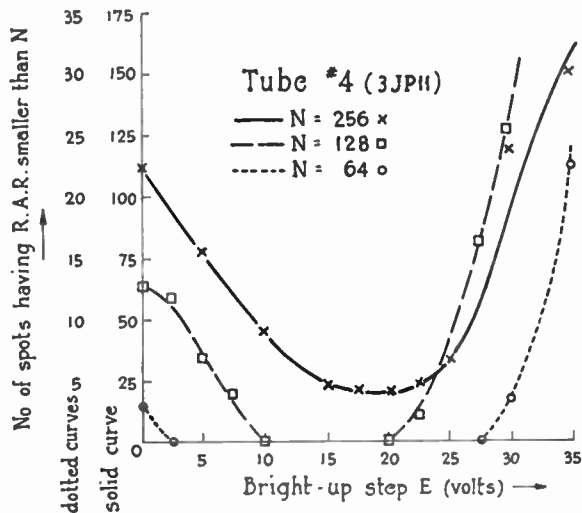


Fig. 13—Number of spots having R.A.R. less than  $N$  plotted against height of bright-up step  $E$ .

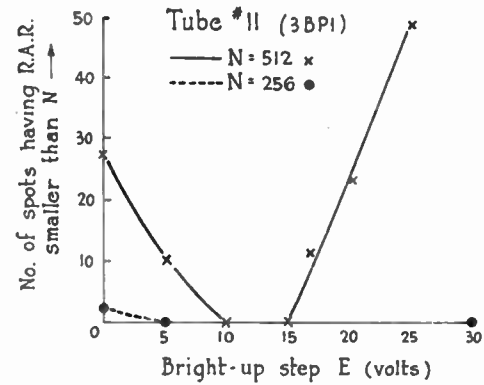


Fig. 14—Number of spots having R.A.R. less than  $N$  plotted against height of bright-up step  $E$ .

$n$  is then printed out by the computer and a different spot  $S$  is selected. Fig. 16 shows typical values of the R.A.R. so obtained plotted against the height of the bright-up step  $E$ .

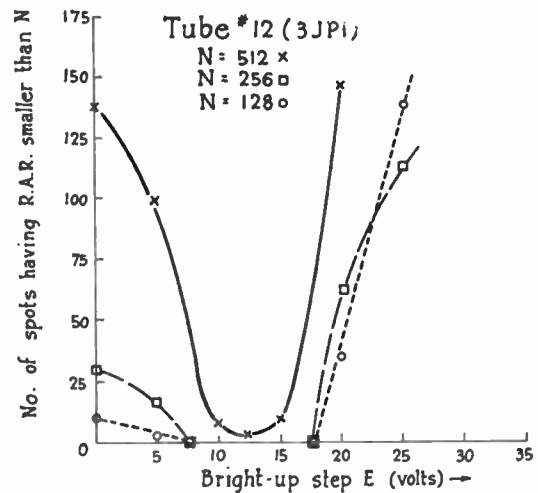


Fig. 15—Number of spots having R.A.R. less than  $N$  plotted against height of bright-up step  $E$ .

Figs. 13 to 16 show that the R.A.R. reaches a definite maximum and then decreases again as the bright-up step is increased. This would be expected from the following considerations.

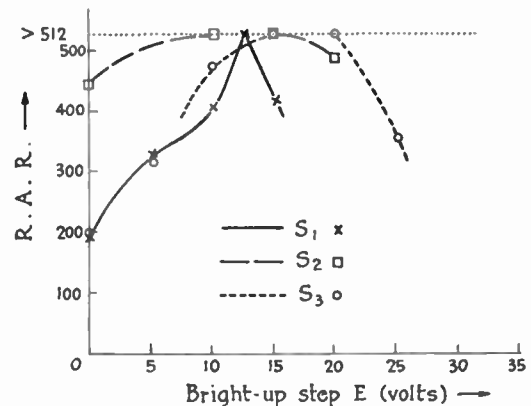


Fig. 16—Typical variation of R.A.R. with bright-up step for 3 spots,  $S_1$ ,  $S_2$ , and  $S_3$ .

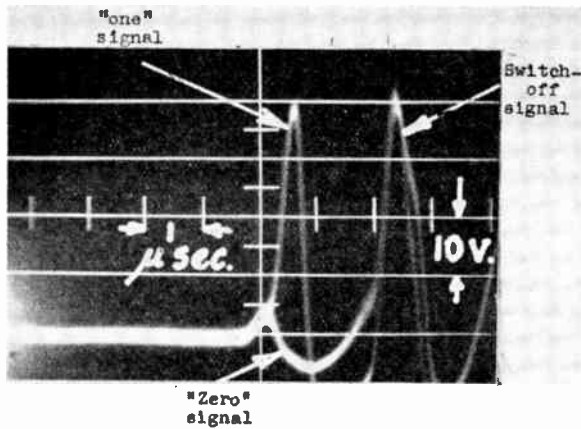


Fig. 17—Typical "one" and "zero" signals in the absence of interference.

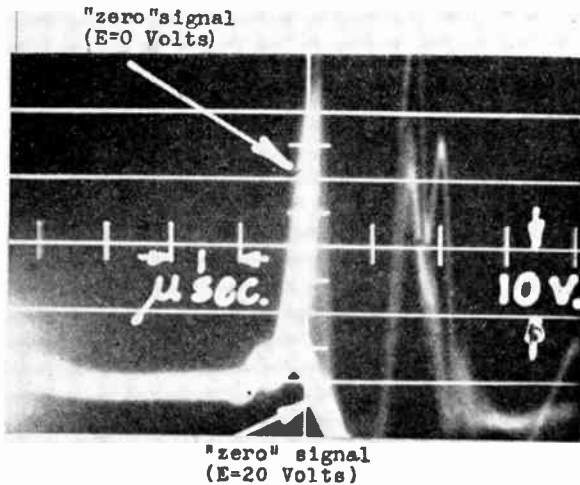


Fig. 18—Output signals from spot  $S$  adjacent to action-spot  $S_1$  in the absence and presence of 20-volt bright-up step during guard period.

During each action bombardment of a spot adjacent to a given spot  $S$ , an average redistributed charge  $\rho_A$  will flow to  $S$ . During each regeneration bombardment of a spot adjacent to a given spot  $S$ , an average redistributed charge  $\rho_R$  will flow to  $S$ . Experiment shows that the effect of the eight spots immediately adjacent to  $S$  only needs to be considered. The total redistributed charge  $\rho$  which flows to  $S$  between two successive regenerations of  $S$  is given by

$$\rho = A\rho_A + 8\rho_R, \quad (1)$$

where  $A$  is the number of action bombardments of spots adjacent to  $S$  between two regenerations of  $S$ . The R.A.R. of  $S$  will vary inversely as  $\rho$ . Due to the extra bright-up step  $E$  during regenerations,  $\rho_R$  will be an increasing function of  $E$  and  $\rho_A$  will be a decreasing function of  $E$ . When  $E$  is zero  $\rho_A$  and  $\rho_R$  will be substantially equal. Since the maximum possible  $A$  is usually much greater than 8, the decrease in the first term in (1) will dominate the expression as  $E$  is increased from zero.  $\rho_A$  is bounded as  $E$  is increased since it cannot decrease below zero.  $\rho_R$  will increase with increasing  $E$  in an unbounded fashion.

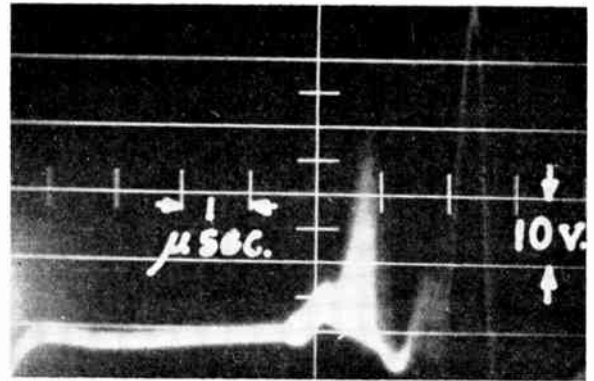


Fig. 19—Output signal from  $S$  due to 10-volt bright-up step during guard periods.

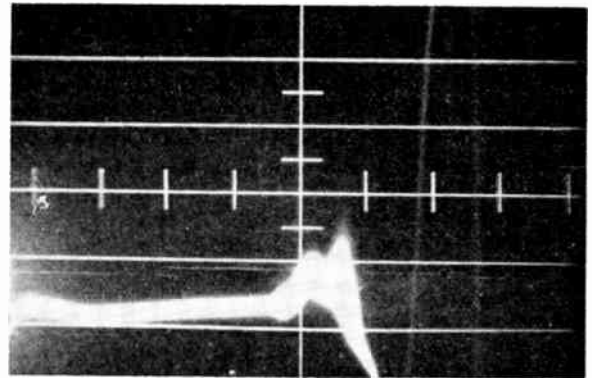


Fig. 20—Output signal from  $S$  due to 25-volt bright-up step during guard periods.

For example assume that  $\rho_A$  and  $\rho_R$  are exponentially dependent on  $E$  as given by

$$\rho_A = Ke^{-bE}; \quad \rho_R = Ke^{bE}, \quad (2)$$

then

$$\rho(E) = AKe^{-bE} + 8Ke^{bE},$$

which is a concave upward curve having an initial value of

$$(A + 8)K,$$

and having a minimum value  $\rho(E)_{\min} \equiv 2K\sqrt{A8}$  for a step  $E$  given by

$$E = \frac{1}{2b} \ln \frac{A}{8}.$$

Little is known at present about the exact functional dependence of  $\rho$  on  $E$ . The optimum value of  $E$  must, therefore, be obtained by direct experiment. Experiment shows that the maximum R.A.R. as a function of  $E$  is broad enough so that a single adjustment for bright-up step height should suffice for a complete cathode-ray tube storage system.

Fig. 17 is a photograph of "zero" and "one" output signals in the absence of interfering secondary electron currents. Figs. 18, 19 and 20 are photographs of the signals from a spot  $S$  adjacent to a spot  $S_1$ . During every action period  $S_1$  was bombarded. This resulted in

the maximum flow of interfering secondary electron currents to  $S$ .

To prevent the "zero" stored at  $S$  from changing into a "one" the strobe pulse, shown in Fig. 10, was disconnected while the photographs of Figs. 18, 19, and 20 were taken. In Fig. 18 the output signals from  $S$  for no bright-up step and for a 20-volt bright-up step are superimposed. The output signal in the absence of a step would clearly cause the spot to change into a "one" if the regeneration loop were actuated by the strobe pulse. The lower signal shows how the step has reduced the interference and is almost as good as the "zero" signal of Fig. 17. Note that the step itself results in a negative output signal during the rise of the step and a positive signal during the fall of the step. The latter signal merges with the positive signal on beam switch off. As a result the switch-off signals increase with increasing steps. Fig. 19 shows the output signal from  $S$  for a 10-volt step, and Fig. 20 shows the output signal for a 25-volt step.

The blurring of the output signals from  $S$  is caused by changes in the positive interference signal during the time (1 min.) of the exposure. These changes are quite large and repetitive. They are believed to be due to the discontinuous nature of charge leakage on the insulator. It is believed that a wall of negative charge builds up between  $S$  and  $S_1$ . When the wall charges to a certain negative potential there is a sudden breakdown and some of the charges flow to adjacent portions of the screen resulting in a levelling of the screen potential in the neighbourhood of  $S$ . Just before this breakdown, the interfering currents to  $S$  will be at a minimum, and just after the breakdown, these currents will be at a maximum. The actual nature of the variations in the output signals from  $S$  strongly suggests such an explanation.

The variations are erratic yet repetitive. The positive interference signal always increases suddenly to a maximum and then decreases in a slower jumpy fashion to a minimum. The duration of the cycle itself varies quite greatly. This appears to rule out interference variations due to steady pulsations, such as raster repetition frequencies, power supply ripple and so on. Signals from

other spots which receive a negligible flow of interfering currents were perfectly steady throughout the experiment.

The changes of the maximum interfering signal from an amplitude of 50 volts for no bright-up step, shown in Fig. 18, through an amplitude of about 30 volts for a 10-volt step, shown in Fig. 19, and an amplitude of about 6 volts for a 20-volt step, appearing in Fig. 18, to an amplitude of about 15 volts for a 25-volt step, shown in Fig. 20, are quite evident. The discrimination bias is 20 volts so that  $S$  would change into a "one" for steps up to 10 volts and would be able to store "zeros" for steps from 15 to 25 volts, in the presence of the interference from  $S_1$ .

## VII. CONCLUSIONS

The method here proposed adds essentially a new function to the beam of cathode-ray storage tubes. This function is to create between storage locations a potential barrier which greatly reduces or prevents the flow of secondaries from action spots to adjacent storage locations. The potential barrier may be thought of as taking the place of the barrier grid in barrier-grid storage tubes. Thus the advantages of a barrier grid may be at least partially realized in a cathode-ray storage tube without actually incorporating such a grid in the tube.

This method may be combined with other methods<sup>5</sup> for improving the R.A.R. The benefits of the several methods should then be additive. Experimental work has shown that the method here described gives good results.

## VIII. ACKNOWLEDGMENT

The writer's work was carried out under a grant of the Canadian Defence Research Board and the National Research Council of Canada. The writer also wishes to acknowledge with gratitude the technical assistance of L. Casciato and numerous discussions with colleagues at the University of Toronto and other projects.

<sup>5</sup> R. Schumann, "Improvement of Williams' Memory Reliability," Paper presented at the Meeting of the A.C.M. at the University of Toronto; September 1952.



# Stagger-Tuned Loop Antennas for Wide-Band Low-Frequency Reception\*

DAVID K. CHENG† SENIOR MEMBER, IRE AND RALPH A. GALBRAITH†, SENIOR MEMBER, IRE

**Summary**—This paper describes a system of stagger-tuned high- $Q$  loop antennas designed for 100 kc Loran pulse reception. The individual loop antenna outputs are first added in a summing amplifier followed by a grounded-grid amplifier and a cathode-follower stage before being fed to the receiver. Based upon preliminary theoretical analysis, an experimental antenna array is developed, which confirms its capability of achieving a wide bandwidth with relatively small dimensions. A squaring scheme of obtaining omnidirectional reception property is suggested; and a modified electrolytic tank method, which is adaptable to the present system in synthesizing a given response characteristic, is also described.

## INTRODUCTION

IN LOW-FREQUENCY LORAN TRANSMISSION, where the carrier frequency is in the neighborhood of 100 kc, efficiency and bandwidth considerations demand an antenna system of large dimensions if a vertical antenna is used. At 100 kc the wavelength is 3,000 meters; portable units cannot be provided with antennas of adequate length. If short antennas were used, the effective  $Q$  would be extremely high, and external damping must be provided in order to obtain the desired bandwidth for pulse reception. External damping reduces circuit efficiency. In the present system, high- $Q$  loop antennas of small dimensions are used. The individual loop antennas are stagger-tuned to different frequencies within the required bandwidth. Their outputs are added in a summing amplifier, which is followed by a grounded-grid amplifier to improve stability and a cathode-follower stage to match the input impedance of the receiver unit. It proves to be a feasible and desirable substitute for long vertical antennas.

## THE INPUT SUMMING AMPLIFIER

The input summing amplifier is used to add the signals received by the stagger-tuned loop antennas. The primary requirements on the part of the summing amplifier are: (1), small interaction among the different input channels, (2), low noise, (3), wide band, and (4), linear operation.

The arrangement chosen was a parallel-plate summing amplifier circuit. There were as many tube sections as the number of input channels. The plates of all tube sections were tied together and the output was

taken from across a common plate tuned circuit properly loaded to give the required bandwidth. When identical tubes are used, the output voltage can readily be shown to be

$$e_0 = - \frac{g_m}{Y_L + nY_p} \sum_{i=1}^n e_{gi} \quad (1)$$

where  $e_{gi}$  are input voltages at the grids;  $n$ , the total number of input channels;  $Y_L$ , the admittance of the common load circuit; and  $g_m$  and  $Y_p$ , the transconductance and the plate conductance respectively of the tubes. The weighting factors are the same for all channels and will decrease as the number of input channels increases. It is to be pointed out that the input voltages  $e_{gi}$  may be a quite complicated function of frequency and loop parameters. Type 6J6 miniature dual-triode tubes were chosen because of their high  $g_m$  (5,000 micromhos). Special care should be exercised in selecting the tubes and the associated circuit components to achieve uniformity for the different input channels.

If high-transconductance triodes like 6J6 are used, the noise-equivalent resistance is only several hundred ohms. This multi-tube parallel-plate arrangement has considerable improvement in the over-all noise figure of the receiving system as compared to a summing amplifier with resistive feedback and large isolating resistances in the grid circuit. It also possesses the advantages of high input impedance and almost zero coupling among input channels.

## THE CASCODE AMPLIFIER AND CATHODE FOLLOWER STAGES

If the summing amplifier is connected directly to a sensitive receiver, the receiving system bursts into oscillation very easily when the gain of the receiver is set moderately high. In order to maintain the high gain of the receiver and achieve stability at the same time, a grounded-grid amplifier stage is placed between the summing amplifier and the input to the receiver. This arrangement of grounded-cathode (summing amplifier) and grounded-grid stages has been referred to as a cascode amplifier.<sup>1</sup> It combines the advantages of the high voltage amplification and stability of a pentode and the low noise factor of a triode. The input resistance of the grounded-grid stage is very low and approaches the reciprocal of the transconductance of the tube if its load resistance is small in comparison with the plate re-

\* Decimal classification: R125.3×R512.2. Original manuscript received by the Institute, August 27, 1952; revised manuscript received February 11, 1953. Presented, National I.R.E. Convention, New York, N. Y., March 29, 1951. The work covered by this paper was done under Contract No. AF 28(099)-111 sponsored by Watson Laboratories, AMC, USAF.

† L. C. Smith College of Engineering, Syracuse University, Syracuse, New York.

<sup>1</sup> H. Wallman, A. B. MacNee, and C. P. Gadsden, "A low-noise amplifier." *PROC. I.R.E.*, vol. 36, p. 700; June 1948.

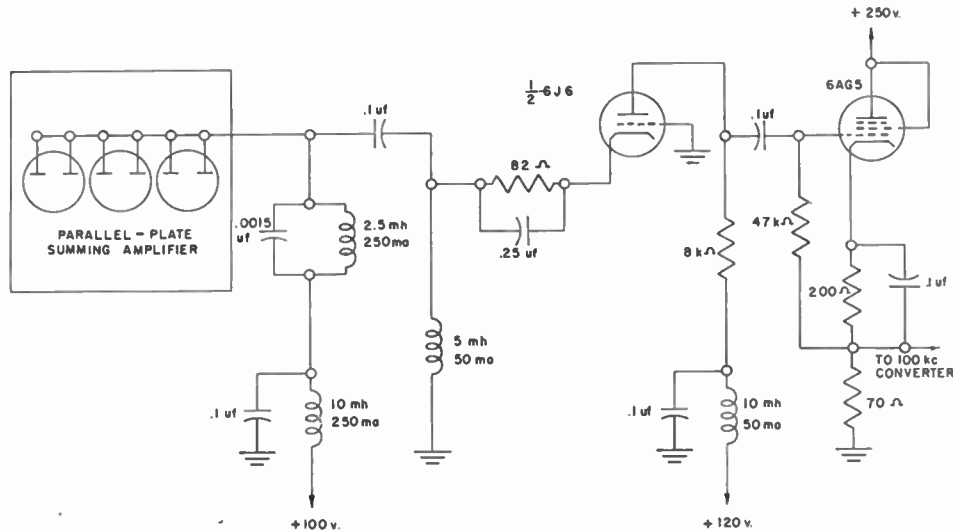


Fig. 1—Cascode amplifier and cathode follower stages.

sistance. This low resistance accounts for the low amplification of the summing amplifier stage and hence the greater stability. This arrangement also has a broad response with respect to frequency. With the circuit shown in Fig. 1, the 3-db band extends from about 40 to 200 kc, and the voltage gain over the range of 70 to 140 kc is substantially constant.

Lowering the load resistance in the grounded-grid stage would result in a lower input resistance and thus further improve stability and widen bandwidth, but it was found that this would accentuate the difference in the amplification of the different channels in the summing amplifier due to non-uniformity of tubes and other circuit elements. It would also reduce the over-all voltage amplification.

The input to the 100 kc converter leading to the Loran receiver has a series L-C tuned circuit for all four channels. The cascode amplifier arrangement of the grounded-cathode and grounded-grid stages as described above, however, has a high output impedance. In order to achieve a better impedance match, a cathode-follower stage is designed which serves as an impedance-transforming device. This circuit is included in Fig. 1.

ANALYTICAL DETERMINATION OF SUMMING AMPLIFIER OUTPUT WITH STAGGERED INPUTS

Before one can proceed to design a stagger-tuned loop antenna system, it is necessary to know the dependence of its resultant response upon such factors as the number of loops and their relative orientation, the spacing of the resonant frequencies, and the Q, the area, and the number of turns of each individual loop. One method of analyzing the resultant response would be to use the modified electrolytic tank method described in the Appendix. This method provides a convenient way of synthesizing the desired amplitude and phase responses on a cut-and-try basis. However, because of the lack of time for constructing and experimenting with an electrolytic tank, this method was not tried. Instead, an

analytical method was developed which is described below and which may be used with relative ease to find the response characteristics of the stagger-tuned system.

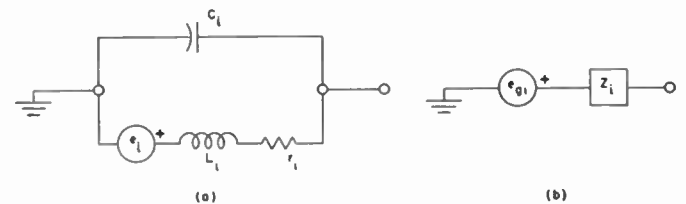


Fig. 2—Equivalent representations of tuned loop antenna circuit.

If each tuned loop antenna is schematically represented by the circuit in Fig. 2(a) and Fig. 2(b) as its series equivalent, then

$$e_{oi} = \frac{e_i}{\left(1 - \frac{\omega^2}{\omega_i^2}\right) + j \frac{1}{Q_i} \frac{\omega}{\omega_i}}, \tag{2}$$

$$Z_i = r_i \left[ \frac{1 + jQ_i \frac{\omega}{\omega_i}}{\left(1 - \frac{\omega^2}{\omega_i^2}\right) + j \frac{1}{Q_i} \frac{\omega}{\omega_i}} \right], \tag{3}$$

where  $\omega = 2\pi f$ ,  $f$  = frequency in cps,  $\omega_i^2 = 1/L_i C_i$ , and  $Q_i = \omega_i L_i / r_i = Q$  of  $i$ th loop antenna at its resonant frequency. Substituting (2) and (1) and rearranging terms, one gets

$$e_0 = \frac{g_m}{Y_L + nY_p} \sum_{i=1}^n \frac{\omega_i^2 e_i}{2\beta_i^2} \left[ \frac{1}{\left(\frac{\omega}{\beta_i} - 1\right) - j \frac{\alpha_i}{\beta_i}} - \frac{1}{\left(\frac{\omega}{\beta_i} + 1\right) - j \frac{\alpha_i}{\beta_i}} \right], \tag{4}$$

with

$$\alpha_i = \frac{r_i}{2L_i} = \frac{\omega_i}{2Q_i}, \quad \beta_i = \omega_i \sqrt{1 - \frac{1}{4Q_i^2}},$$



and  $\alpha_i^2 + \beta_i^2 = \omega_i^2$ . Under the easily realizable condition  $(1/4Q_i^2) \ll 1$ , further simplification results because  $\beta_i \doteq \omega_i$ . Thus,

$$e_0 = \frac{g_m}{2(Y_L + nY_p)} \sum_{i=1}^n e_i \left[ \frac{1}{\left(\frac{\omega}{\omega_i} - 1\right) - j \frac{1}{2Q_i}} - \frac{1}{\left(\frac{\omega}{\omega_i} + 1\right) - j \frac{1}{2Q_i}} \right]. \quad (5)$$

In the application under consideration, interest is centered on frequencies in the range of 90 to 110 kc. The ratio  $\omega/\omega_i$  then has values very nearly equal to 1. Since  $1/2Q_i$  is usually very small compared with 2, the first terms in the square bracket, under the summation sign will in general be much larger than the corresponding second terms, each of the latter having a magnitude of  $1/2$  to a good approximation. If one substitutes  $\Delta\omega_i$  for  $\omega - \omega_i$ , the typical first term can be written as

$$\frac{e_i}{\frac{\Delta\omega_i}{\omega_i} - j \frac{1}{2Q_i}} = (2Q_i e_i \sin \theta_i) \epsilon^{j\theta_i}, \quad (6)$$

with

$$\theta_i = \tan^{-1} \left( \frac{1}{2Q_i} \cdot \frac{\omega_i}{\Delta\omega_i} \right). \quad (7)$$

For loops of equal area, a change in the incoming angular frequency  $\omega$  changes the angle  $\theta_i$ ; the relative values of the induced voltage  $e_i$  remain unchanged. The amplitude and phase response of the system can be computed with relative ease.

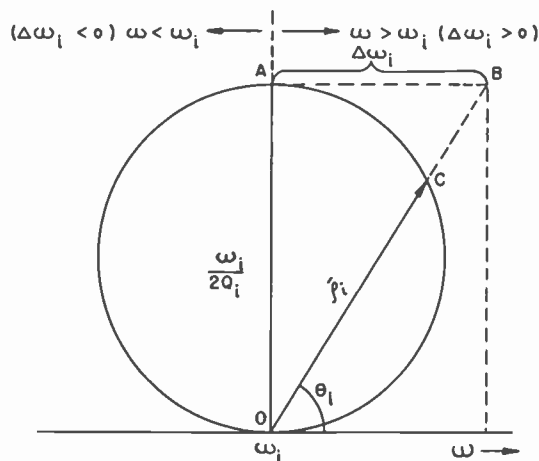


Fig. 3—Graphical method of determining the contribution of a loop.

Since one can treat (6) as a vector, a graphical method may also be conveniently employed. It is easy to show that if a circle of diameter  $\omega_i/2Q_i = r_i/2L_i = \alpha_i$  is drawn on the frequency axis at  $\omega_i$  for a given loop as shown in Fig. 3, then for any given angular frequency  $\omega$ , which determines the length of  $\overline{AB} = \Delta\omega_i$ , the vector  $\overline{OC}$  represented by  $\overline{OC}$  determines the relative contribution of this particular loop at the given frequency. It is noted that  $\alpha_i$  is equal to one half of the 3-db bandwidth of the

$i$ th loop. The typical first term as expressed in (6) is  $4(Q_i^2/\omega_i)e_i\bar{\rho}_i$ . For the special case of identical loops, circles of equal diameter  $r/2L$  may be drawn at the resonant angular frequencies  $\omega_i$  of the individual loops, and the resultant response determined by adding the vectors  $\bar{\rho}_i$  accordingly.<sup>2</sup>

#### THE LOOP ANTENNAS

The effective height of a loop antenna for vertically polarized incoming wave is

$$h_e = \frac{2\pi NA}{\lambda}, \quad (8)$$

where  $h_e$  = effective height,  $N$  = total number of turns,  $A$  = area of the loop, and  $\lambda$  = wavelength of the incoming signal. Equation (8) holds true for loop antennas of any shape provided that the plane of the loop is in the direction of the incoming signal and that the thickness of loop sides is very small compared with loop dimensions. The effect of tuning and orientation on the resultant output is to be accounted for by a staggering or detuning factor, and a directional factor respectively.

Formulas are usually available for calculating the inductance and the resistance of a loop of given configuration and given number of turns when the size of the wire is known. But seldom is account taken of the effect of distributed capacitances. The effective inductance of a closely wound coil at 100 kc. may indeed be quite different from the so-called low-frequency inductance given by the formulas neglecting distributed capacitances.

Single-plane spiral-wound coils were used as the loops because of their inherent advantages of physical compactness, low distributed capacity and high- $Q$  properties. The final design of the loops has the following physical data: Outside dimensions 20" × 20", Inside dimensions: 6" × 6", Total number of turns: 70, Size of wire: AWG No. 26, enamel covered. The measured effective inductance of the loop has an average value of 1.9 millihenrys and its  $Q_e$  is about 60 at 100 kc.

#### EXPERIMENTAL INVESTIGATION

Twelve identical loops were used in the experimental set-up. They were initially tuned to frequencies from 90 to 110 kc at 2 kc intervals, the twelfth loop being equipped with a variable air condenser which may be set at any desirable frequency within this range so as to smooth out the resultant amplitude response. There are an infinite number of ways to arrange the loop antennas. It must be settled at some compromise between the mutual coupling effect, the space occupied, and the reception characteristics. Data presented herein were obtained with all twelve loops in parallel. They were arranged such that no two loops would have mutual effects more than those arising from a space separation of 3 feet and a frequency separation of 4 kc.

<sup>2</sup> For details and simplifying recurrence formulas, which have been developed for this purpose, the reader is referred to "Stagger-Tuned Loop Antennas for Wide-Band Low-Frequency Reception," Watson Laboratories Contract No. AF 28(099)-111, Final Report, Syracuse University, September 1950.

For taking the amplitude and phase characteristics of the antenna system as a function of frequency, a special wide-band trf receiver, consisting of two stages of single-tuned rf amplifier, two stages of resistance-capacitance coupled amplifier and a tuned power amplifier stage, was constructed. The over-all 3-db bandwidth of the receiver was over 20 kc and the amplification at the center of the band was over  $4 \times 10^6$ . There are two output positions on this receiver. At one position, the output from the power amplifier appears directly at the output terminals, which may be used to feed an indicator directly for cycle-matching purposes; at the other position, a detector stage is switched into the circuit but the by-pass condenser is purposely made small so that the number of rf cycles can still be counted on the rectified pulse envelope. The receiver was used in conjunction with the indicator section of a DAS-4 Loran set when the actual wave shape of the receiver pulses was photographed.

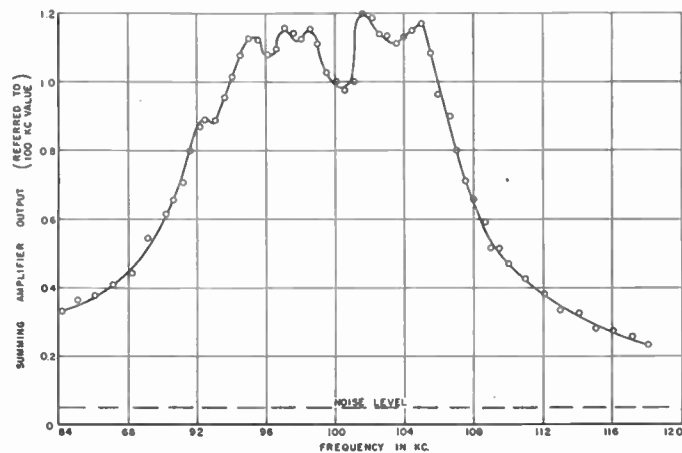


Fig. 4—Amplitude response of a 12-element stagger-tuned loop antenna system.

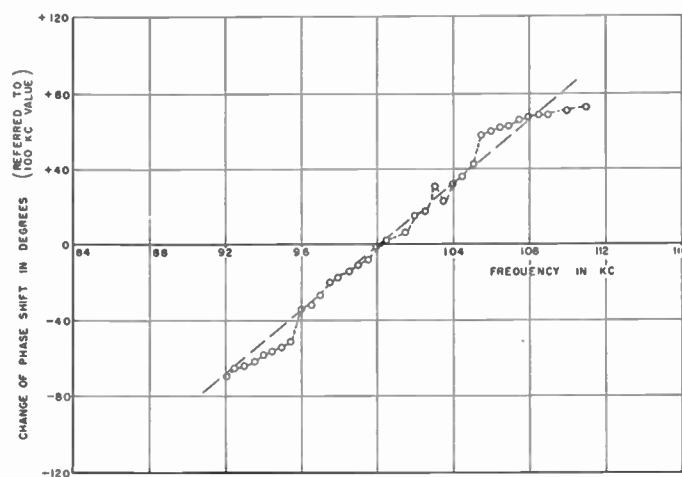


Fig. 5—Phase response of a 12-element stagger-tuned loop antenna system.

Figs. 4 and 5 show respectively the amplitude and phase response characteristics of the 12-element stagger-tuned loop antenna system. It is seen that the 3-db bandwidth of this system is about 16.5 kc and that the amplitude response outside of this frequency band drops quite rapidly, thus reducing noise pick-up outside of the

band where no significant signal frequency components are present. The phase characteristic shows the existence of a linear relationship between the phase shift and the frequency within the "pass-band." This linear phase characteristic is essential for pulse reproduction. There are minor peaks and dips in the amplitude response, but they do not prove to be important. The number of peaks does not correspond to the number of loop antennas because some of the peaks partly merge and the presence of mutual-coupling effects has a tendency to make this more so. Through meticulous retuning, the response curves can doubtlessly be made more smooth.

The shapes of the Loran pulses as received through the trf receiver and DAS-4 indicator combination using stagger-tuned loop antennas under different conditions were recorded photographically. Fig. 6(a) gives

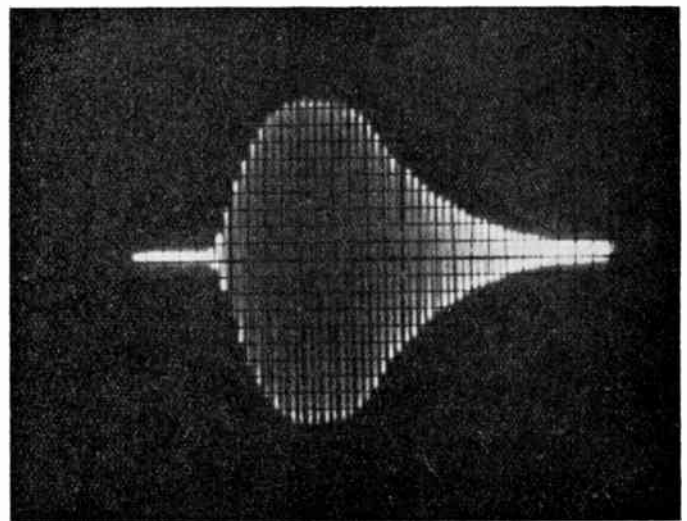


Fig. 6(a)—Pulse shape at the transmitter.

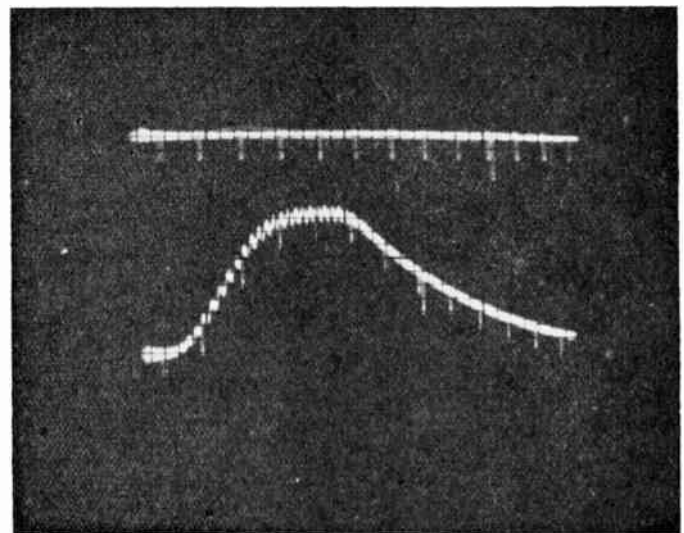


Fig. 6(b)—Envelope of received pulse with twelve stagger-tuned loops.

the shape of the pulse at the transmitter which was located 40 miles away from the receiving site, and Fig. 6(b) shows the envelope of the received pulse when all twelve loops were used and properly tuned. Each rf cycle corresponds to a duration of 10 microseconds

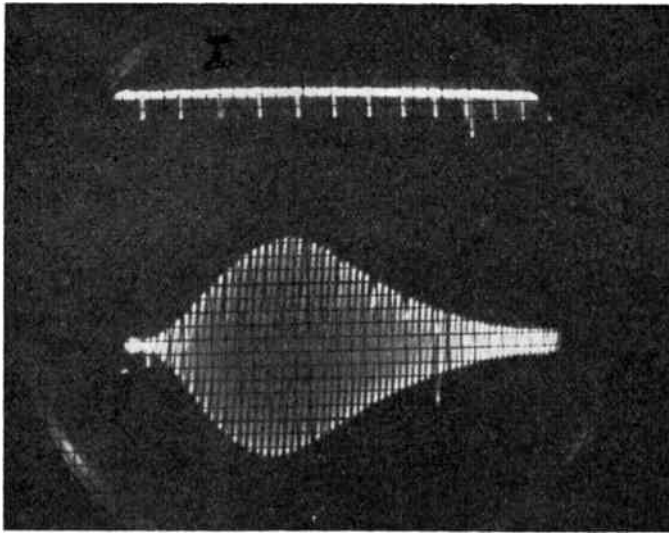


Fig. 7(a)—Received pulse with two lf and two hf loops disconnected.

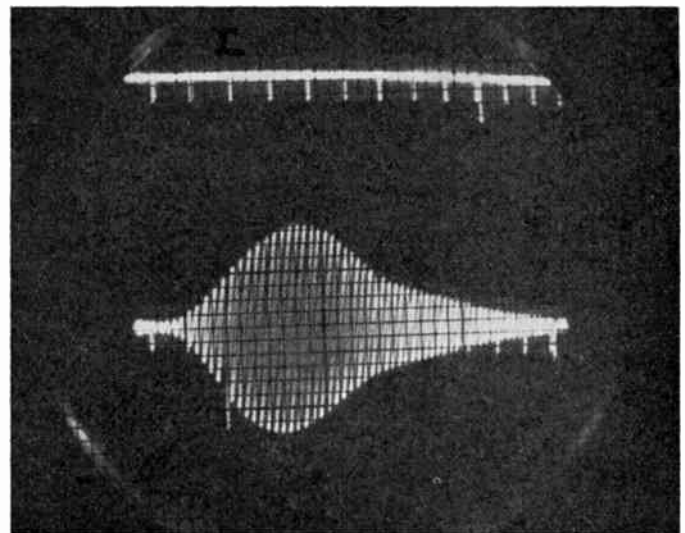


Fig. 8(a)—Received pulse with three lf loops disconnected.

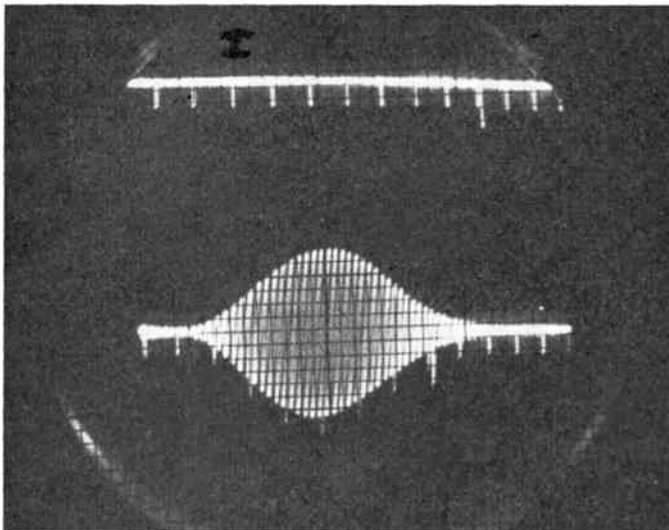


Fig. 7(b)—Received pulse with three lf and three hf loops disconnected.

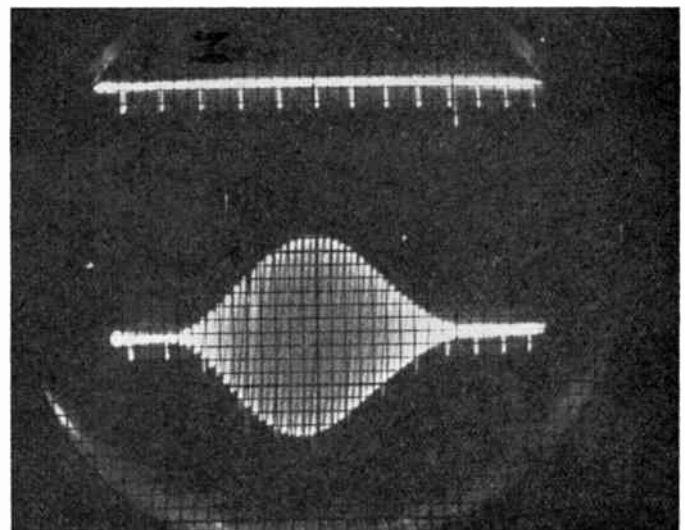


Fig. 8(b)—Received pulse with three hf loops disconnected.

at 100 kc. By comparing these two figures, it is seen that the received pulse represents a quite good reproduction of the pulse at the transmitter. The rise time is somewhat lengthened, but there is no serious deterioration of the pulse shape.

Fig. 7(a) shows the shape of the received pulse when two loops from both the low-frequency and the high-frequency ends of the assigned band were disconnected from the summing amplifier, leaving the tuning and the position of the other eight loops unchanged. It is seen that the rise time is further lengthened and that, the flat portion of the pulse is no longer visible, although the amplitude of the pulse is not much reduced. Both of these effects are accentuated in Fig. 7(b) when three loops are taken out from both ends of the assigned band. Here, the reduction in the amplitude of the pulse is more obvious. The removal of end loops reduces both the amplitude and the effective bandwidth of the resultant amplitude response curve.

The shapes of the received pulses with three low-frequency loops disconnected, and with three high-frequency loops disconnected are shown respectively in Figs. 8(a) and 8(b). The removal of the lf loops resulted in a prolonged delay time. It is evident that Fig. 6(b), with all twelve loops in the circuit and properly tuned, represents by far the best response.

#### SCHEME OF ACHIEVING OMNIDIRECTIVITY

For a wide-band antenna system to be omnidirectional to pulse signals, it should be able to give the same response to signals of frequencies spread over the entire band from all directions. If the response characteristic varies appreciably with signal direction, the system will not be suitable for applications like Loran, wherein pulses from master and slave stations are to be accurately compared.

Arranging a large number of loops radially or in the form of a rectangular polygon does not present a solu-

tion. Fig. 9 depicts the squaring scheme of obtaining omnidirectional reception property from a loop antenna system.

As indicated in the figure, the stagger-tuned loops are arranged in two identical groups placed at right angles to each other and the outputs of both groups are passed through a squaring circuit and then added in a summing amplifier. Ignoring the change in magnitude while undergoing squaring and summing operations, which can easily be compensated for, the resultant output is the square of the original signal; the directional angle  $\theta$  does not influence the response. Although nonlinear operation is involved in the process, it is not objectionable because one is interested primarily in the comparison of pulse signals coming from different directions and not in the faithful reproduction of any signal carrying intelligence. Fig. 9 is only schematic, and the loops should not be placed too closely together in practice.

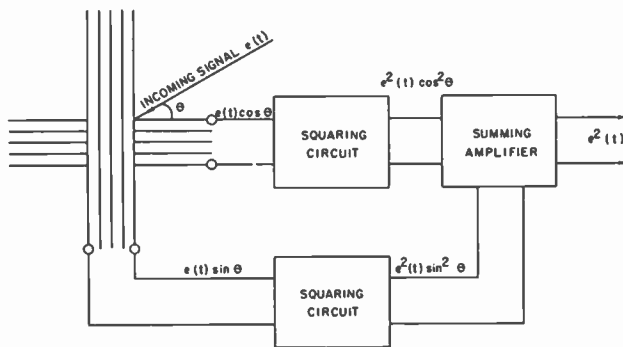


Fig. 9—The squaring scheme for achieving omnidirectivity.

### CONCLUSIONS

The present 12-element stagger-tuned loop antenna system has a 3-db bandwidth of 16.5 kc and a phase shift which varies very nearly linearly with frequency over the desired range. The effective height of the antenna system alone was found to be about 3 meters, and the gain of the parallel-plate summing amplifier with 12 input channels is in the neighborhood of 4. These properties together with the experimental evidence of Loran pulse reception enable one to conclude that a system of high- $Q$  loop antennas of small dimensions properly tuned to different frequencies within the required frequency band is a feasible and desirable substitute of long vertical antennas for wide-band low-frequency reception. The squaring scheme provides the means of achieving omnidirectivity.

Generally, an effective height of 3 meters is not required. With the existence of sensitive receivers, an effective height of one half meter may be sufficient. In that case, the loops can be made with smaller dimensions and fewer turns. The effective  $Q$  of the individual loops would then be lower and it would be easier to tune the system to give a uniform amplitude response. However, analyses<sup>3</sup> show that the noise figure of a tuned

<sup>3</sup> H. G. Pascalar, Master's thesis, L. C. Smith College of Engineering, Syracuse University; October 1950.

loop antenna is very nearly in direct proportion to the loss resistance of the loop and is inversely proportional to its radiation resistance. The use of loops of lower  $Q$  would then result in lower circuit efficiency and less improvement in the noise figure and the absolute sensitivity<sup>4</sup> of the system.

It is possible that loops of fewer turns and smaller dimensions can be made in such a way that the effective  $Q$  is not lowered. The feasibility of employing iron-cored loops should also be well worth investigating.

### ACKNOWLEDGMENT

The authors wish to acknowledge their indebtedness to Messrs. R. N. Lothes and H. G. Pascalar for their valuable contributions in this work, and to Captain O. D. Goldberg of Rome Air Development Center, Rome, New York, for profitable discussions on this project.

### APPENDIX

#### *Modified Electrolytic Tank Method of Analyzing the Response of a Stagger-Tuned Loop Antenna System*

A rational function of a complex variable  $s = \sigma + j\omega$  can be written in the following form:

$$F(s) = K \frac{\prod_{j=1}^{n_z} (s - s_{zj})}{\prod_{k=1}^{n_p} (s - s_{pk})}, \quad (\text{A-1})$$

where  $K$  is a constant, and where the continued product in the numerator indicates that the function has  $n_z$  zeros, and that in the denominator shows that it has  $n_p$  poles. If the logarithm of (A-1) is taken, it will be seen that the logarithm of the magnitude and the phase of  $F(s)$  are analogous to the expression for the electrostatic potential distribution around  $n_z$  equal negative line charges placed at positions corresponding to the zeros and  $n_p$  similar positive line charges at the locations of the poles. Consequently, with a suitable choice of constants, equipotential curves around these line charges correspond to curves of constant absolute magnitude of  $F(s)$ , and an orthogonal set of curves corresponds to lines of constant phase of  $F(s)$ .

In homogeneous and isotropic medium where the Ohm's law is obeyed, the results of electrostatic theory may be applied directly to the state of dynamic equilibrium represented by a steady current flow. Hansen and Lundstrom<sup>5</sup> have utilized this principle to determine experimentally the magnitude and phase of impedance and gain functions by means of an electrolytic tank. It should be stressed, however, that the usefulness of the electrolytic tank method depends primarily upon the de-

<sup>4</sup> D. O. North, "The absolute sensitivity of radio receivers," *RCA Review*, vol. 16, p. 337; January 1942.

<sup>5</sup> W. W. Hansen and O. C. Lundstrom, "Experimental determination of impedance functions by the use of an electrolytic tank," *Proc. I.R.E.*, vol. 33, pp. 528-534; August 1945.

termination of the positions in the complex plane of the zeros and poles of the function concerned. This method will, therefore, be ineffective if the zeros and/or poles of the functions under consideration are difficult to locate.

From (1) and (2) in the text and replacing  $j\omega$  by  $s$ , one can easily show that

$$F(s) = e_0(s) = -\frac{g_m}{Y_L + nY_p} \sum_{i=1}^n \frac{\omega_i^2 e_i}{(s - s_i)(s - s_i^*)}, \quad (\text{A-2})$$

where the conjugate poles are

$$s_i = -\frac{r_i}{2L_i} + j\sqrt{\frac{1}{L_i C_i} - \frac{r_i^2}{4L_i^2}} = -\alpha_i + j\beta_i, \quad (\text{A-3})$$

$$s_i^* = -\frac{r_i}{2L_i} - j\sqrt{\frac{1}{L_i C_i} - \frac{r_i^2}{4L_i^2}} = -\alpha_i - j\beta_i. \quad (\text{A-4})$$

For a single loop antenna ( $n=1$ ) there will be two poles at  $s_1$  and  $s_1^*$  in the complex plane and two zeros at infinity. For two loops ( $n=2$ ), two additional poles at  $s_2$  and  $s_2^*$  and two additional zeros  $\bar{s}_a$  and  $\bar{s}_a^*$  result, where the zeros  $\bar{s}_a$  and  $\bar{s}_a^*$  have to be determined from the following quadratic equation:

$$\omega_1^2(s - s_2)(s - s_2^*) + \omega_2^2(s - s_1)(s - s_1^*) = 0.$$

With  $n$  loops, an algebraic equation of  $2(n-1)$ th degree has to be solved in order to determine the new zeros. This may prove to be very difficult and render the electrolytic tank method impractical. The modified method<sup>6</sup> to be described below solves this difficulty.

Expressing (A-2) in partial fraction form:

$$F(s) = -\frac{g_m}{Y_L + nY_p} \sum_{i=1}^n \frac{\omega_i^2 e_i}{j2\beta_i} \left[ \frac{1}{s + \alpha_i - j\beta_i} - \frac{1}{s + \alpha_i + j\beta_i} \right]. \quad (\text{A-5})$$

But  $s = \sigma + j\omega$ , hence

$$F(s) = \frac{g_m}{Y_L + nY_p} \sum_{i=1}^n \frac{\omega_i^2 e_i}{2\beta_i} \times \left[ \frac{(\omega - \beta_i) + j(\sigma + \alpha_i)}{(\sigma + \alpha_i)^2 + (\omega - \beta_i)^2} - \frac{(\omega + \beta_i) + j(\sigma + \alpha_i)}{(\sigma + \alpha_i)^2 + (\omega + \beta_i)^2} \right]. \quad (\text{A-6})$$

Now consider the case of a *negative* line charge of strength  $D_k$  per unit length located at each pole in the *second quadrant* and an equal *positive* line charge at each pole in the *third quadrant*. The potential due to these line charges at any point  $s = \sigma + j\omega$  in the complex plane will be

$$V = \frac{1}{B} \sum_{k=1}^n D_k [ \ln \sqrt{(\sigma + \alpha)^2 + (\omega - \beta_k)^2} - \ln \sqrt{(\sigma + \alpha)^2 + (\omega + \beta_k)^2} ], \quad (\text{A-7})$$

where  $B$  is a constant whose value depends on the permittivity of the medium and the units employed. From (A-7), one easily obtains,

$$\frac{\partial V}{\partial \sigma} = \frac{1}{B} \sum_{k=1}^n D_k \times \left[ \frac{\sigma + \alpha}{(\sigma + \alpha)^2 + (\omega - \beta_k)^2} - \frac{\sigma + \alpha}{(\sigma + \alpha)^2 + (\omega + \beta_k)^2} \right] \quad (\text{A-8})$$

$$\frac{\partial V}{\partial \omega} = \frac{1}{B} \sum_{k=1}^n D_k \times \left[ \frac{\omega - \beta_k}{(\sigma + \alpha)^2 + (\omega - \beta_k)^2} - \frac{\omega + \beta_k}{(\sigma + \alpha)^2 + (\omega + \beta_k)^2} \right], \quad (\text{A-9})$$

and

$$\frac{\partial V}{\partial \omega} + j \frac{\partial V}{\partial \sigma} = \frac{1}{B} \sum_{k=1}^n D_k \times \left[ \frac{(\omega - \beta_k) + j(\sigma + \alpha)}{(\sigma + \alpha)^2 + (\omega - \beta_k)^2} - \frac{(\omega + \beta_k) + j(\sigma + \alpha)}{(\sigma + \alpha)^2 + (\omega + \beta_k)^2} \right]. \quad (\text{A-10})$$

Comparing (A-6) and (A-10), it is readily seen that if as many pairs of electrodes as there are pairs of conjugate poles (which equals the number of loop antennas) are put in the electrolytic tank, negative in the second quadrant and positive in the third quadrant, the potential gradient in the  $\omega$  and  $\sigma$  directions along the real frequency axis will be proportional respectively to the real and imaginary parts of the response function  $F(s)$  at real frequencies. One condition must here be satisfied, that is:

$$\left( \frac{\omega_i^2 e_i}{\beta_i D_i} \right) = \text{Constant} \quad (\text{A-11})$$

$i = \text{any number from 1 to } n, \text{ or}$

$$D_i = \frac{\omega_i^2 e_i}{\omega_1^2 e_1} \cdot \frac{\beta_1}{\beta_i} D_1. \quad (\text{A-12})$$

When dissipation is low ( $\alpha_i \ll \beta_i, \omega_i \doteq \beta_i$ ) and if the loops are identical and with the same orientation ( $e_i = e_1$ ),

<sup>6</sup> Dr. W. R. LePage, Professor of Electrical Engineering, Syracuse University.

one can write

$$D_i \doteq \frac{\omega_i}{\omega_1} D_1. \quad (\text{A-13})$$

In practice, (A-13) means that the current flowing to or from an electrode should be approximately proportional to its distance from the origin in the complex plane.

This modified method has the advantage that only the positions of the poles need be known. There is no need of solving algebraic equations of high order because the location of zeros does not have to be determined. The effect on the resultant response function by the addition of an extra loop-antenna input channel can be determined experimentally by introducing another pair of electrodes without additional difficulty.

## Amplitude Stability in Oscillating Systems\*

NORMAN R. SCOTT, SENIOR MEMBER, IRE†

**Summary**—As a supplement to the Kryloff and Bogoliuboff method of determining amplitude of oscillation in quasilinear systems, a method based upon energy balance is presented. From the energy balance condition, a criterion for stability of oscillation is deduced for the case of one degree of freedom. The treatment is then generalized to systems of  $n$  degrees of freedom, and the  $n$  stability criteria are derived in terms of rates of change, with respect to amplitude, of the power supplied and dissipated in the  $n$  oscillations.

MUCH INSIGHT INTO the problem of amplitude stability in oscillating systems can be gained by a consideration of the general oscillatory circuit of Fig. 1.

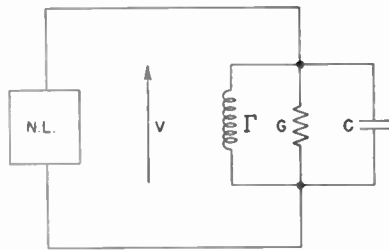


Fig. 1—Equivalent circuit.

In this circuit N. L. represents a nonlinear element which performs the dual functions of: (1) supplying the energy to overcome losses in  $G$ , the tank circuit shunt conductance, and (2) limiting the amplitude of oscillation to some finite value. The amount of nonlinearity need not be large. In fact, the analysis presented here applies only to systems in which the nonlinearity is small. However, virtually all sine wave oscillators belong to this class.

The volt-amp. characteristic of the nonlinear element may be represented by:

$$i = \alpha v + \beta v^2 + \gamma v^3 + \epsilon v^4 + \rho v^5, \quad (1)$$

and  $G_n$ , the nonlinear conductance is

$$G_n = \frac{di}{dv} = \alpha + 2\beta v + 3\gamma v^2 + 4\epsilon v^3 + 5\rho v^4. \quad (2)$$

\* Decimal classification: R140. Original manuscript received by the Institute, May 11, 1952; revised manuscript received January 1, 1953.

† Department of Electrical Engineering, University of Michigan, Ann Arbor, Michigan.

The differential equation for the circuit is:

$$C\ddot{v} + (G + G_n)\dot{v} + \Gamma v = 0 \quad (3)$$

If the nonlinearity is small, this equation may be written as:

$$C\ddot{v} + \Gamma v + \mu f(v, \dot{v}) = 0 \quad (4)$$

where  $\mu$  is a small parameter. The method of Kryloff and Bogoliuboff<sup>1</sup> may be applied to give as the solution:

$$v = a e^{-(G+G_n)t/2C} \cos \omega t \quad (5)$$

where:

$$G_n = \frac{1}{\pi a} \int_0^{2\pi} f(a \cos \theta) \cos \theta d\theta. \quad (6)$$

This equivalent linearized conductance is one which gives rise to the same fundamental component of current as the actual nonlinear conductance when a voltage of  $v = a \cos \omega t$  is impressed.

For a nonlinear element such as that of (1), we obtain:

$$G_n = \frac{1}{\pi a} \int_0^{2\pi} [\alpha a \cos \theta + \beta a^2 \cos^2 \theta + \gamma a^3 \cos^3 \theta] \cos \theta d\theta \quad (7)$$

$$= \alpha + \frac{3}{4}\gamma a^2, \quad (8)$$

where we have used only 3 terms of the polynomial for simplicity. At equilibrium:

$$G + G_n = 0$$

$$a^2 = -\frac{4}{3\gamma}(\alpha + G). \quad (9)$$

An alternate method of solving for the equilibrium amplitude of oscillation consists of recognizing that the steady-state amplitude is that value at which the average energy supplied by the nonlinear element is equal to the average energy dissipated in the linear passive part of the system.

$$-\lim_{T \rightarrow \infty} \left[ \frac{1}{T} \int_0^T i v dt \right] = \frac{a^2 G}{2}. \quad (10)$$

<sup>1</sup> N. Minorsky, "Introduction to Nonlinear Mechanics," Chap. 10. J. W. Edwards, Ann Arbor, Michigan; 1947.

If the nonlinearity is sufficiently well represented by a third-degree polynomial, then this leads to:

$$a^2 = -\frac{4}{3\gamma}(\alpha + G) \quad (11)$$

which is the same value we found in (9). This result has also been derived by Van der Pol.<sup>2</sup>

Graphical representations of power supplied by the nonlinear element and dissipated by the linear element may be used to determine stable and unstable levels of amplitude.  $P_D$ , the power dissipated, is a parabolic function of amplitude, and  $P_S$ , the power supplied, may be any shape curve, depending on the nonlinearity. Fig. 2 shows some possible curves.

Each point of intersection of a  $P_D$  curve with a  $P_S$  curve is a potential stationary value for the amplitude of oscillation. However, each such point must be inspected for stability. We may imagine the amplitude to be perturbed from its stationary value and determine the effect this perturbation has on the exponential factor in (5) which determines the growth or decay of the oscillation. If the sign of the exponent is such as to return the amplitude to its value prior to the perturbation, then the equilibrium is a stable one. However, if the sign of the exponent is such as to increase the change in the amplitude in the direction of the perturbation, then the equilibrium is unstable. This is equivalent to stating that only those points of intersection are stable for which

$$\frac{\partial P_D}{\partial a} > \frac{\partial P_S}{\partial a} \quad (12)$$

We must also recognize that there may exist semi-stable points of equilibrium, which are stable or unstable for either an upward or a downward perturbation of the amplitude, but not for both.

We may now identify as stable points in Fig. 2 the intersection in 2(a), points 1 and 3 in 2(c), point 2 in 2(d), point 2 in 2(e), and 3 in 2(f). Unstable points are the intersection in 2(b), point 2 in 2(c), point 1 and 2(d), point 3 in 2(e), and 2 in 2(f). Semistable points are the points of tangency in 2(e) and 2(f). Thus point 1 of 2(e) is stable for a downward perturbation of the amplitude and unstable for an upward perturbation, while the converse is true of point 1 in 2(f).

Since it is not possible in a physical system for the energy supplied or dissipated to be a multiple valued function of the amplitude, it is evident that stable and unstable points of equilibrium must alternate. However, it is also necessary to include semistable points in this generalization. In the language of nonlinear mechanics, stable and unstable limit cycles must alternate, and a limit cycle stable from the inside but unstable from the

outside must enclose an unstable limit cycle and be enclosed by a stable limit cycle, while the converse is true for a limit cycle unstable from the inside but stable from the outside.

The possibility of simultaneous oscillations occurring at two or more different frequencies in the same circuit is well-known and has frequently been described and investigated.<sup>3-5</sup> The problem of determining the stability of such multiple oscillations may be attacked by methods similar to those we have employed here for circuits of one degree of freedom. Thus, for two degrees of freedom power supplied and power dissipated become functions of  $a_1$  and  $a_2$ , the two amplitudes of oscillation.

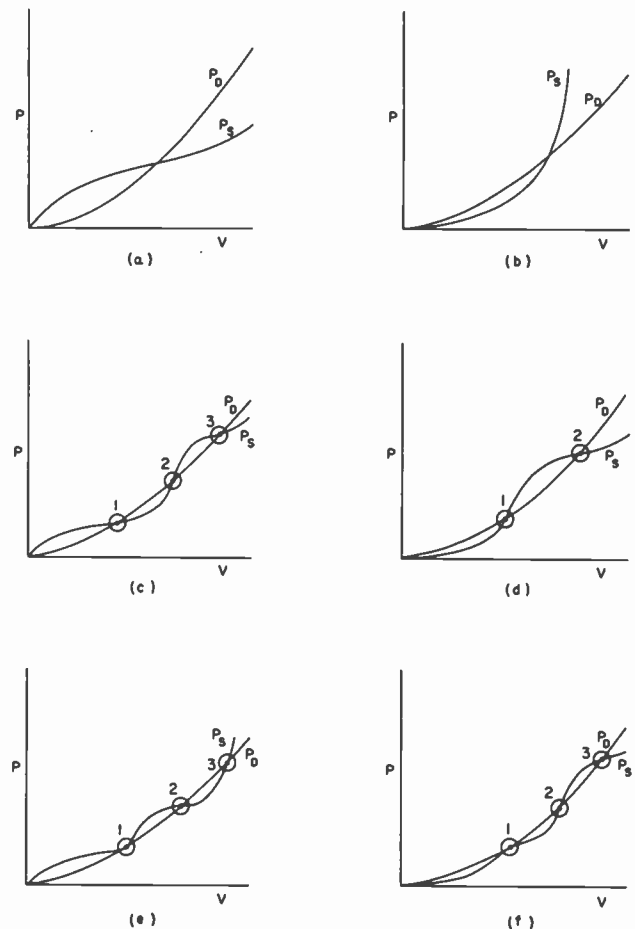


Fig. 2—Curves of power supplied and power dissipated vs. amplitude of voltage.

Although for one degree of freedom a simple criterion regarding the relative slopes of  $P_S$  and  $P_D$  at a point of equilibrium was sufficient to determine the stability, one intuitively expects the situation to be more complex for two degrees of freedom. Thus along a line of intersection of  $P_S$  and  $P_D$  there is an infinite number of points characterized by the same relative slopes of  $P_S$  and  $P_D$ .

<sup>3</sup> L. V. Skinner, "Criteria for Stability in Circuits Containing Non-linear Resistance," Ph.D. Thesis, University of Illinois; June, 1948.

<sup>4</sup> W. H. Huggins, "Multifrequency bunching in reflex klystrons," Proc. I.R.E., vol. 36, pp. 624-630; May, 1948.

<sup>5</sup> J. S. Schaffner, "Almost Sinusoidal Oscillations in Nonlinear Systems," University of Illinois Engineering Experiment Station, Bulletin Series No. 395; May, 1951.

<sup>2</sup> B. Van der Pol, "The nonlinear theory of electric oscillations," Proc. I.R.E., vol. 22, pp. 1051-1086; September, 1934.



Some additional criterion is needed to determine which, if any, of these points is stable. To do this we employ the method of perturbations, taking the initial perturbations to be small enough so that the calculation of their growth or decay may be handled as a linear problem. We shall derive the criteria for  $n$  degrees of freedom and then apply these results to the cases of two and three degrees of freedom. We define:

- $P_{Sj}$  = power supplied to the  $j$ th oscillation
- $P_{Dj}$  = power dissipated in the  $j$ th oscillation
- $a_j$  = amplitude of the  $j$ th oscillation

If all  $a_j$  undergo small perturbations, all  $P_{Sj}$  will also be perturbed. Evidently:

$$\frac{dP_{Sj}}{dt} = \sum_{i=1}^n \frac{\partial P_{Sj}}{\partial a_i} \frac{da_i}{dt} = \sum_{i=1}^n \frac{\partial P_{Sj}}{\partial (a_i^2)} \frac{d(a_i^2)}{dt} \quad (13)$$

If the system is stable, all  $P_{Sj}$  and  $a_j$  will return to their initial values, and we will have

$$\frac{dP_{Sj}}{dt} \rightarrow 0,$$

which will occur when all

$$\frac{d(a_i^2)}{dt} \rightarrow 0.$$

It may be shown that:

$$\frac{d(a_i^2)}{dt} = - \frac{2a_i^2 \delta_{0i}}{G_i} (G_i + G_{ei}), \quad (14)$$

where  $\delta_{0i}$  is the logarithmic decrement of the linear circuit at the frequency  $\Omega_i$  of the  $i$ th oscillation,  $G_i$  is the conductance of the linear circuit at  $\Omega_i$ , and  $G_{ei}$  is the equivalent linearized conductance of the nonlinear circuit at  $\Omega_i$ .

Now let all amplitudes of oscillation undergo small perturbations:

$$a_i'^2 = a_{is}^2 + \Delta_i, \quad (15)$$

where  $a_{is}$  is the steady-state amplitude at the point where we are investigating stability,  $a_i'$  is the perturbed amplitude, and  $\Delta_i$  is the difference of their squares. Then:

$$\begin{aligned} \frac{d(a_i'^2)}{dt} &= \frac{d(a_{is}^2)}{dt} + \frac{d\Delta_i}{dt} \\ &= - \frac{2(a_{is}^2 + \Delta_i)\delta_{0i}}{G_i} [G_i + f_i(a_{1s}^2 + \Delta_1, a_{2s}^2 + \Delta_2, \dots, a_{ns}^2 + \Delta_n)], \end{aligned} \quad (16)$$

where  $f_i(a_{1s}^2 + \Delta_1, a_{2s}^2 + \Delta_2, \dots, a_{ns}^2 + \Delta_n)$  is the equivalent linearized conductance at frequency  $\Omega_i$  and amplitudes  $a_1 \dots a_n$ . Of course, the term  $d(a_{is}^2)/dt$  is zero, since  $a_{is}$  is the steady-state amplitude. However, it will be convenient to carry the term along in our equations.

We have now:

$$\begin{aligned} \frac{d\Delta_i}{dt} &= \frac{d(a_i'^2)}{dt} - \frac{d(a_{is}^2)}{dt} \\ &= - \frac{2a_{is}^2 \delta_{0i}}{G_i} [f_i(a_{1s}^2 + \Delta_1, \dots, a_{ns}^2 + \Delta_n) - f_i(a_{1s}^2, \dots, a_{ns}^2)] \\ &\quad - \frac{2\Delta_i \delta_{0i}}{G_i} [G_i + f_i(a_{1s}^2 + \Delta_1, \dots, a_{ns}^2 + \Delta_n)]. \end{aligned} \quad (17)$$

Now a Taylor's Series expansion of  $f_i$  can be made and substituted into this equation. However, since we are postulating small perturbations of the system, we may omit second and higher order terms. We thus obtain:

$$\begin{aligned} \frac{d\Delta_i}{dt} &= - \left[ \frac{2a_{is}^2 \delta_{0i}}{G_i} \sum_{k=1}^n \frac{\partial f_i}{\partial (a_k^2)} \Delta_k \right] \\ &\quad - \frac{2\Delta_i \delta_{0i}}{G_i} [G_i + f_i(a_{1s}^2, \dots, a_{ns}^2)], \end{aligned} \quad (18)$$

which is a system of  $n$  first order differential equations each containing  $n$  unknowns. Equation (18) may be rewritten as:

$$\dot{\Delta}_i = \sum_{j=1}^n a_{ij} \Delta_j \quad (19)$$

where

$$a_{ii} = - \frac{2\delta_{0i}}{G_i} \left[ a_{is}^2 \frac{\partial f_i}{\partial (a_i^2)} + G_i + f_i(a_{1s}^2, \dots, a_{ns}^2) \right] \quad (20)$$

$$a_{ij} = - \frac{2a_{is}^2 \delta_{0i}}{G_i} \frac{\partial f_i}{\partial (a_j^2)}. \quad (21)$$

The characteristic equation for this system is:

$$\begin{vmatrix} (a_{11} - \rho) & a_{12} & \dots & a_{1n} \\ a_{21} & (a_{22} - \rho) & \dots & \\ \vdots & & \ddots & \\ a_{n1} & & \dots & (a_{nn} - \rho) \end{vmatrix} = 0. \quad (22)$$

The roots of this equation are the exponents in the solutions for the  $\Delta_i$ , and evidently must have no positive parts if the perturbations are to die out, i.e., if the amplitudes of oscillation are to be stable. This condition is insured by Routh's criterion, which, in the case of three degrees of freedom, requires that:

- (a)  $a_{11} + a_{22} + a_{33} < 0,$
- (b)  $-(a_{11} + a_{22} + a_{33}) \cdot (a_{11}a_{22} + a_{11}a_{33} + a_{22}a_{33} - a_{12}a_{21} - a_{13}a_{31} - a_{23}a_{32}) - (a_{11}a_{22}a_{33} - a_{11}a_{23}a_{32} - a_{12}a_{21}a_{33} + a_{12}a_{31}a_{33} + a_{13}a_{21}a_{32} - a_{13}a_{31}a_{22}) > 0,$
- (c)  $a_{11}a_{22}a_{33} - a_{11}a_{32}a_{23} - a_{12}a_{21}a_{33} + a_{12}a_{31}a_{23} + a_{13}a_{21}a_{32} - a_{13}a_{31}a_{22} > 0.$

For two degrees of freedom the criteria become:

$$\begin{aligned} \text{(a)} \quad & a_{11} + a_{22} < 0, \\ \text{(b)} \quad & -(a_{11} + a_{22}) \cdot (a_{11}a_{22} - a_{12}a_{21}) > 0, \end{aligned} \quad (24)$$

which may be obtained from (23) by eliminating all terms having 3's in the subscripts.

The power supplied at each frequency can be expressed in terms of the amplitude of that oscillation and the equivalent linearized conductance. Thus:

$$P_{S_i} = -\frac{a_{1i}^2}{2} G_{s_i} = -\frac{a_{1i}^2}{2} f_i(a_{1i}^2, a_{2i}^2, \dots, a_{ni}^2). \quad (25)$$

Also

$$P_{D_i} = +\frac{a_{1i}^2}{2} G_i. \quad (26)$$

Now let

$$P_i = P_{D_i} - P_{S_i}.$$

In terms of these quantities the criteria (24) now become:

$$\begin{aligned} \text{(a)} \quad & \frac{\delta_{01}}{G_1} \frac{\partial P_1}{\partial(a_1^2)} + \frac{\delta_{02}}{G_2} \frac{\partial P_2}{\partial(a_2^2)} > 0, \\ \text{(b)} \quad & \frac{\partial P_1}{\partial(a_1^2)} \frac{\partial P_2}{\partial(a_2^2)} - \frac{\partial P_{S1}}{\partial(a_2^2)} \frac{\partial P_{S2}}{\partial(a_1^2)} > 0. \end{aligned} \quad (27)$$

The three criteria for the case of three degrees of freedom can be readily written down in similar manner, but to save space, only criterion (a) is given:

$$\frac{\delta_{01}}{G_1} \frac{\partial P_1}{\partial(a_1^2)} + \frac{\delta_{02}}{G_2} \frac{\partial P_2}{\partial(a_2^2)} + \frac{\delta_{03}}{G_3} \frac{\partial P_3}{\partial(a_3^2)} > 0. \quad (28)$$

This is of the same form as (27)(a), but contains more terms. By dividing out the factor  $(a_{11} + a_{22} + a_{33})$ , (23)(b) is seen to be dimensionally a sum of double products of derivatives of power. It is thus of the same form as (27)(b), but also includes more terms. Criterion (23)(c) may be recognized as a new form of criterion, however, which is made up of terms which are triple products of derivatives of power. If we now recall the stability criterion for one degree of freedom, namely,  $(\partial P_D / \partial a) > (\partial P_S / \partial a)$  or equivalently,  $(\partial P_D / \partial a^2) > (\partial P_S / \partial a^2)$ , the trend of the stability criteria becomes evident. As the degrees of freedom are increased, so also are the stability criteria, the same number being required as there are degrees of freedom. Successive criteria which are added as required by additional degrees of freedom become successively more complex, while those criteria already established retain their basic form, but add more terms.

The first criterion is a relation between rates of change of power supplied and power dissipated. The other criteria apparently represent higher order energy balance

and interchange relations among the various oscillations. The number of criteria appearing in a given case is equal to the number of degrees of freedom of the oscillatory circuit, provided the system is not in internal resonance, a condition in which the oscillations are synchronized and their frequencies are in ratios of small integers. In systems in which internal resonance occurs, additional criteria arise to represent the requirements for stability of synchronization. This has been studied by Fontana for two degrees of freedom with internal resonance.<sup>6</sup>

In conclusion it should be noted that the analysis presented here is of particular application to the stability of systems subjected to small perturbations. However, if the perturbation is large, the question of whether it will increase or will return to zero is unaffected unless the perturbation is so large as to carry the system beyond an adjacent limit cycle. In this case the perturbation cannot return to zero, and the response of the system is radically changed. Thus, in Fig. 2(c), a small perturbation of the amplitude about point 1 will always decay to zero. If the perturbation is large enough to carry the amplitude beyond point 2, however, the amplitude will continue to increase to the value corresponding to point 3. The limiting size of perturbation to which any amplitude may be subjected without crossing an adjacent limit cycle is, of course, known as soon as the equilibrium amplitudes have been calculated. If, however, the perturbation is large, but not large enough to cross an adjacent limit cycle, the system will behave qualitatively the same as it would for small perturbations. For this reason, the question of whether an equilibrium point is stable or unstable is best handled by assuming small perturbations and obtaining a system of linear differential equations. For the more general case in which perturbations may be large and precise, information is desired as to their manner of growth or decay, and the resulting differential equations describing them must be nonlinear. However, the nonlinearity involved is of the same type as that in the original problem of determining amplitudes of equilibrium, and the solution of this problem may be expected to be no more difficult than that of the amplitude problem. An interesting aspect of this problem which is currently being studied by several investigators is the determination of the optimum type of nonlinearity to be included in a system to obtain a particular desired behavior of the perturbed system.

#### ACKNOWLEDGMENT

The author wishes to acknowledge the encouragement and helpful guidance of Dr. Lloyd T. DeVore in the accomplishment of the work reported here.

<sup>6</sup> R. E. Fontana, "Internal resonance in circuits containing nonlinear resistance," *Proc. I.R.E.*, vol. 39, pp. 945-951; August, 1951.

# The Constants in the Equation for Atmospheric Refractive Index at Radio Frequencies\*

ERNEST K. SMITH, JR.†, MEMBER, IRE, AND STANLEY WEINTRAUB‡

**Summary**—Recent improvements in microwave techniques have resulted in precise measurements which indicate that the conventional constants  $K_1 = 79^\circ\text{K}/\text{mb}$  and  $K_2' = 4,800^\circ\text{K}$  in the expression for the refractivity of air,  $N = (n-1)10^6 = [K_1/T](p + K_2' e/T)$  should be revised. Various laboratories appear to have arrived at this conclusion independently. In much of radio propagation work the absolute value of the refractive index of the atmosphere is of small moment. However, in some work it is important and it seems highly desirable to decide upon a particular set of constants.

Through consideration of the various recent experiments this paper arrives at a relation

$$N = \frac{77.6}{T} \left( p + 4,810 \frac{e}{T} \right)$$

where

$p$  = total pressure in millibars

$e$  = partial pressure of water vapor in millibars

$T$  = absolute temperature =  $^\circ\text{C} + 273$

This expression is considered to be good to 0.5 per cent in  $N$  for frequencies up to 30,000 mc and normally encountered ranges of temperatures, pressure and humidity.

RECENT IMPROVEMENTS in microwave techniques have resulted in measurements at the National Bureau of Standards,<sup>1</sup> the National Physical Laboratory<sup>2</sup> and elsewhere<sup>3-5</sup> which have indicated that the conventional constants in the expression for the refractive index of air at radio frequencies should be revised. Various laboratories appear to have arrived at this conclusion independently with the result that there are several different sets of constants in current use.<sup>6-9</sup> The sources of these recent changes, such as have been run to earth, have been found to be based on individual rather than collective results. Almost all of the proposed constants seem to represent a substantial improvement over the former values. The authors propose a set of constants derived from what is felt to be the most reliable of the recent microwave and optical measurements of the refractive index of dry air and from a recent survey of water vapor Debye constants. It is hoped these new constants will provide a common meeting ground for the laboratories desiring change rather than inject just another set of values into the field.

\* Decimal classification: R216.3. Original manuscript received by the Institute, October 10, 1952.

† Central Radio Propagation Laboratory, Boulder, Colorado.

‡ G. Birnbaum, S. J. Kryder and H. Lyons, "Microwave measurements of the dielectric properties of gases," *Jour. Appl. Phys.*, vol. 22, p. 95; 1951.

<sup>1</sup> L. Essen and K. D. Froome, "The refractive indices and dielectric constants of air and its principal constituents at 24,000 Mc/s," *Proc. Phys. Soc. (London)*, B, vol. 64, p. 862; 1951.

<sup>2</sup> C. M. Crain, *Phys. Rev.*, vol. 74, p. 691; 1948.

<sup>3</sup> W. F. Gabriel, *Proc. I.R.E.*, vol. 40, p. 940; August, 1952.

<sup>4</sup> W. E. Phillips, *Proc. I.R.E.*, vol. 38, p. 786; 1950. See also comments by C. M. Crain, *Proc. I.R.E.*, vol. 40, p. 164; February, 1952.

<sup>5</sup> C. I. Aslakson and C. O. Fickeissen, *Trans. Amer. Geoph. Un.*, vol. 31, p. 819; 1950.

<sup>6</sup> Research Interim Engineering Report No. 13, p. 23, Cornell University E. E.; October 23, 1951.

<sup>7</sup> L. Essen and K. D. Froome, *Nature*, vol. 167, p. 512; 1951.

<sup>8</sup> L. J. Anderson, NEL Report No. 279, page 3; 1952.

For an accuracy of 0.5% in  $N$ , the scaled-up refractivity of moist air [ $N = (n-1)10^6$ , where  $n$  is the refractive index] some simplifying assumptions may be made if the use of the relation is to be restricted to certain limits of the variables. The limits in this case restrict its use to temperature ranges of  $-50$  to  $+40^\circ\text{C}$ , total pressures of 200 to 1,100 mb, water vapor partial pressures of 0 to 30 mb and a frequency range of 0 to 30,000 mc. The constituents of dry air and even water vapor may be assumed to obey the ideal gas law.<sup>10</sup> The refractive index of water vapor, a polar molecule with an electric dipole, may be represented by a two-term Debye relation.<sup>11</sup> The permeability of air at radio frequencies due to oxygen may be taken<sup>1</sup> as  $1 + 0.4 \times 10^{-6}$ . Dispersion may be neglected. The Lorentz polarization term may be ignored.<sup>12</sup> Absolute zero for temperature may be taken as  $-273^\circ\text{C}$  rather than  $-273.16^\circ\text{C}$ .

There has been no proof of variation in the composition of the dry gases of the free atmosphere either with latitude or with height up to the ionosphere.<sup>13</sup> The water vapor content, of course, varies widely. As contributions to the total refractive index obey an additive rule, a three-term expression may be formulated<sup>11</sup> in which the first term expresses the sum of the distortions of electronic charges of the dry gas molecules under the influence of an applied electromagnetic field, the second term this distortion for water vapor, and the third term the effect of the orientation of the electric dipoles of water vapor under the influence of a field. Thus, using  $N$  for the scaled-up refractivity [ $N = (n-1)10^6$ ]

$$N = K_1 \frac{p_d}{T} + K_2 \frac{e}{T} + K_3 \frac{e}{T^2} \quad (1)$$

where:

$n$  = the refractive index at radio frequencies

$p_d$  = partial pressure of the dry gases

$e$  = partial pressure of water vapor

$T$  = absolute temperature

In radio work one is interested in propagation through the free atmosphere, therefore the composition of air should be taken to include an average amount of carbon dioxide. However, laboratory measurements usually are made on  $\text{CO}_2$ -free air due to variable concentrations of  $\text{CO}_2$  in the laboratory. Hence the values of  $\epsilon - 1$  orig-

<sup>10</sup> H. Barrell and J. E. Sears, "On the refraction and dispersion of air for the visible spectrum," *Philos. Trans. A.*, vol. 238, p. 2; 1940.

<sup>11</sup> "Propagation of Short Radio Waves," Edited by D. E. Kerr, Radiation Laboratory Series, McGraw-Hill Book Co., Inc., N. Y., vol. 13, p. 189, 1951.

<sup>12</sup> *Ibid.*, p. 643.

<sup>13</sup> "Ionospheric radio propagation," National Bureau of Standards, Circ. 462, p. 35; June 1948.

inally published for CO<sub>2</sub>-free air have been adjusted for 0.03% CO<sub>2</sub> content by raising them 0.02%. These values are also given on a real rather than an ideal gas basis. Three determinations shown in Table I are considered. The first shown, that of Barrell,<sup>14</sup> is an average of the constant term ( $n$  for  $\lambda = \infty$ ) of the optical Cauchy dispersion equations for standard air used in three of the principal metrology laboratories of the world. Theoretical considerations indicate that the dielectric constant for dry air will be the same for optical and radio frequencies. Barrell's value is converted to dielectric constant from the relation  $n = \sqrt{\mu\epsilon}$  with  $\mu$ , the permeability taken as unity at optical frequencies. The second value, that of Birnbaum, Kryder and Lyons<sup>1</sup> was originally published on an ideal basis but has here been converted to the value pertinent to real gases. Last determination, (Essen and Froome<sup>2</sup>) has been adjusted to include CO<sub>2</sub>. Uncertainties listed are standard errors.

TABLE I  
DRY AIR REFRACTIVE INDEX AND DIELECTRIC CONSTANT  
AT 0°C AND 1 ATMOSPHERE

	Freq. of Measurement	Measured $N$	$(\epsilon-1)10^6$	Year
1. Barrell <sup>14</sup>	Optical	287.7 <sub>6</sub> ± 0.0 <sub>65</sub>	575.6 ± 0.1 <sub>3</sub>	1951
2. Birnbaum, Kryder and Lyons <sup>1</sup>	9,000 mc		575.8 ± 0.3 <sub>6</sub>	1951
3. Essen and Froome <sup>2</sup>	24,000 mc	288.2 <sub>1</sub> ± 0.1	576.1 ± 0.2	1951
	Mean Value of $(\epsilon-1)10^6$		575.7 <sub>6</sub> ± 0.1 <sub>6</sub>	
	Mean Value of $N$ †	288.0 <sub>4</sub> ± 0.0 <sub>6</sub>		

† Derived from  $n = \sqrt{\mu\epsilon}$  where  $\mu-1 = 0.4 \times 10^{-6}$  is taken for radio frequencies to account for the permeability.

The statistical mean value of dielectric constant is then converted to refractive index. The constant  $K_1$  is evaluated from

$$N = K_1 \frac{p_d}{T} \quad (2)$$

which stems from (1) when  $e = 0$ . Setting  $N = 288.04$ ,  $p = 1,013.25$  mb,  $T = 273^\circ\text{C}$  and solving for  $K_1$ :

$$K_1 = 77.60_7 \pm 0.01_3 \frac{^\circ\text{K}}{\text{mb}} \quad (3)$$

A recent survey of determinations of the dielectric constant of water vapor in the microwave region by Birnbaum and Chatterjee<sup>15</sup> is used to evaluate the water vapor constants  $K_2$  and  $K_3$  in (1). Assuming ideal gas behavior, which is permissible here as only low partial pressures are of interest, the constants may be evaluated from the Debye constants  $A$  and  $B$  (molar polarization  $P = A + B/T$ ) determined by Birnbaum and Chatterjee. This results in:

<sup>14</sup> H. Barrell, "The dispersion of air between 2500A and 6500A," *Jour. Opt. Soc. Amer.*, vol. 41, p. 295; 1951.

<sup>15</sup> G. Birnbaum and S. K. Chatterjee, "The dielectric constant of water vapor in the microwave region," *Jour. Appl. Phys.*, vol. 23, p. 220; February, 1952.

$$K_2 = 71.6 \pm 8.5 \frac{^\circ\text{K}}{\text{mb}} \quad (4)$$

$$K_3 = (3.74_7 \pm 0.03_1)10^6 \frac{^\circ\text{K}^2}{\text{mb}} \quad (5)$$

where the uncertainties are again standard errors. Substituting the values of (3), (4) and (5) in (1) and reducing the values to three figures where significant

$$N = 77.6 \frac{p_d}{T} + 72 \frac{e}{T} + 3.75 \times 10^6 \frac{e}{T^2} \quad (6)$$

Utilizing the total pressure  $p = p_d + e$  one may write

$$N = 77.6 \frac{p}{T} - 6 \frac{e}{T} + 3.75 \times 10^6 \frac{e}{T^2} \quad (7)$$

TABLE II  
TABLE OF CONSTANTS USED BY DIFFERENT AUTHORS

$$N = (n-1)10^6 = K_1 \frac{p}{T} + K_2 \frac{e}{T} + K_3 \frac{e}{T^2}$$

	Year	$K_1$	$K_2$	$K_3 \times 10^{-6}$
1. Schelleng, Burrows & Ferrell <sup>16</sup>	1933	79	675	1.35
2. Englund, Crawford & Mumford <sup>17</sup>	1935	79.1	68.3	3.81
3. Waynick <sup>18</sup>	1940	79	68.5	3.72
4. Smith-Rose & Strickland <sup>19</sup>	1943	79	68	3.77
5. Burrows & Attwood-NDRC <sup>20</sup>	1946	79	68	3.8
6. Met. Factors in Propagation <sup>21</sup>	1946	79	68	3.8
7. Kerr, <i>Rad. Labs.</i> , vol. 13 <sup>11</sup>	1951	79	(79)	3.8
8. Essen & Froome <sup>2</sup>	1951	77.64	64.68	3.718
9. Smith & Weintraub	1952	77.6	72	3.75

For use in the limited temperature range  $-50^\circ\text{C}$  to  $+40^\circ\text{C}$ , negligible error is incurred through lumping the second and third terms in (7). This may be accomplished by dividing these terms by  $e/T$  and solving for the composite constant,  $K_4$ , in the relation:

$$\frac{3.75 \times 10^6}{T} - 6 = \frac{K_4}{T} \quad (8)$$

which, for  $T = 273^\circ\text{K}$ , results in:

$$K_4 = 3.73 \times 10^6 \quad (9)$$

The two-term formula for moist air is now

$$N = 77.6 \frac{p}{T} + 3.73 \times 10^6 \frac{e}{T^2} \quad (10)$$

<sup>16</sup> J. C. Schelleng, C. R. Burrows, and E. B. Ferrell, "Ultra-short-wave propagation," *Proc. I.R.E.*, vol. 21, p. 427; 1933.

<sup>17</sup> C. R. Englund, A. B. Crawford, and W. W. Mumford, "Further results of a study of ultra-short-wave transmission phenomena," *Bell Sys. Tech. Jour.*, vol. 14, p. 369; 1935.

<sup>18</sup> A. H. Waynick, "Experiments on the propagation of ultra-short radio waves," *Proc. I.R.E.*, vol. 28, p. 468; 1940.

<sup>19</sup> R. L. Smith-Rose and A. C. Strickland, "A study of propagation over the ultra-short-wave radio link between Guernsey and England on wavelengths of 5 and 8 meters," *J.I.E.E.*, vol. 90, III, p. 12; 1943.

<sup>20</sup> "Radio Wave Propagation," Consolidated Summary Technical Report on the Committee on Propagation, NDRC. Edited by C. R. Burrows and S. S. Attwood, p. 219 (Academic Press Inc., New York, N. Y. 1949.)

<sup>21</sup> "Meteorological Factors in Radio Wave Propagation," *The Physical Society*, London: 1946. Foreword.

which may be written

$$N = \frac{77.6}{T} \left( p + 4.81 \times 10^3 \frac{e}{T} \right). \quad (11)$$

These last two relations are the ones proposed for general radio meteorological use.

Listed in Table II are some of the values of  $K_1$ ,  $K_2$  and  $K_3$  that have been used by authors through the years. In examples 1 through 7 the constant  $K_1$  was drawn from the Smithsonian Physical Tables (1933).

The water vapor constants  $K_2$  and  $K_3$  in examples 2 through 7 represent an average of the determinations of several different workers in each case. Essen and Froome in example 8 relied on their own excellent experimental work to evaluate  $K_1$  and  $K_3$ . Their value of  $K_1$  is seen from Table I to be in excellent agreement with the values of Barrell and of Birnbaum, Kryder and Lyons.

However, their value for  $K_3$  is low because of the fact that their measured value of the dielectric constant of water vapor is about 1% lower than those determined by other recent workers in the field. It is true that their measurements were performed in a region adjacent to the 1.35 cm water vapor absorption band, but this effect has been shown to be too small to account for the discrepancy. As Essen and Froome did not have refractive index determinations over the wide temperature range necessary to evaluate  $K_2$  and  $K_3$  independently, they utilized an optical value of refractive index ( $K_3=0$ ) to determine  $K_2$ . Consequently, their value for  $K_2$  is about 10% low at radio frequencies; however, the effect of this on the equation is negligible.

The authors wish to thank Mr. George Birnbaum, Dr. Arthur Maryott, Mr. Jack W. Herbstreit and Mr. Kenneth A. Norton for their advice and assistance in this work.

## Reduction of Forced Error in Closed-Loop Systems\*

LEONARD H. KING†

**Summary**—This paper illustrates a method for reducing the forced-dynamic error in servomechanisms by design based on error coefficients. After a brief review of the dependence of the forced dynamic error upon error coefficients, the relationship between error coefficients and the parameters of a servomechanism is derived. This relationship is then used to show how closed-loop systems can be modified to obtain favorable error coefficients that reduce the forced-dynamic error. The method has been tested by simulation, and photographs of simulator response show how the effect of additional integrations can be achieved by error-coefficient adjustment.

### I. INTRODUCTION

IN A PERFECT POSITIONAL SERVOMECHANISM, the output position would always be aligned with the input command position regardless of noise, disturbing torques, or variations in the input position. As it is impossible to build a perfect positional servomechanism, good design practice consists largely of trying to reduce the following components of error:

1. Noise error, due to the transmission of input and internal noise to the output.
2. Position error, caused by disturbing torques.
3. Transient error, due to initial conditions or input discontinuities. By definition, this error disappears in one response time after which the output remains within five per cent of the correct output for a step change in the input.<sup>1</sup>
4. Forced dynamic error, which exists after one response time and is due to variations in the input command position.

\* Decimal classification: 621.675.104. Original manuscript received by the Institute, December 24, 1952.

† Instrumentation Laboratory, Massachusetts Institute of Technology, Cambridge, Mass.

<sup>1</sup> C. S. Draper, W. McKay, and S. Lees, "Instrument Engineering," vol. 1, McGraw-Hill Book Co., Inc., New York, N. Y.; 1952.

This paper illustrates a method for reducing the forced dynamic component of error by design based on error coefficients.<sup>2-5</sup> After a brief review of the dependence of the forced dynamic error upon error coefficients, the relationship between error coefficients and the parameters of a servomechanism is derived. This relationship is then used to show how closed-loop systems can be modified to obtain favorable error coefficients that reduce the forced dynamic error. The method has been tested by simulation, and photographs of simulator response show how the effect of additional integrations can be achieved by error coefficient adjustment. Specifically, it is shown (1) how a loop with no integrations can be made to have zero positional and velocity error and (2) how a loop with one integration can be made to have zero velocity and acceleration error.

### II. RELATIONSHIP BETWEEN FORCED-DYNAMIC ERROR AND ERROR COEFFICIENTS

If the input to a servo system varies continuously with time, then there will be a forced dynamic error  $E(t)$  between the desired input  $q_{in}(t)$  and the actual system output  $q_{out}(t)$ . For finite derivatives of the input function, the forced dynamic error can generally be ex-

<sup>2</sup> H. M. James, N. B. Nichols, and R. S. Phillips, "Theory of Servomechanisms," vol. 25, Rad. Lab. Series, McGraw-Hill Book Co., Inc., New York, N. Y.; 1947.

<sup>3</sup> G. H. Floyd, Jr., and R. H. Eisengrein, "Design of Fire-Control Systems," Servomechanisms Laboratory, M.I.T., Cambridge, Mass. (Confidential), July, 1950.

<sup>4</sup> J. L. Bower, "A note on the error coefficients of a servomechanism," *Jour. Appl. Phys.*, vol. 21; July, 1950.

<sup>5</sup> H. Chestnut and R. W. Mayer, "Servomechanisms and Regulating System Design," vol. 1, John Wiley & Sons, Inc., New York, N. Y.; 1951.

panded in a series as

$$E(t) = a_0 q_{in}(t) + a_1 \frac{d}{dt} q_{in}(t) + a_2 \frac{d^2}{dt^2} q_{in}(t) + \dots + a_n \frac{d^n}{dt^n} q_{in}(t) + \dots \quad (1)$$

where

- $E(t)$  is the forced dynamic error.
- $q_{in}(t)$  is the input function.
- $a_0$  = zero-order (positional) error coefficient.
- $a_1$  = first-derivative (velocity) error coefficient.
- $a_2$  = second-derivative (acceleration) error coefficient.
- $a_n$  =  $n^{\text{th}}$ -derivative error coefficient.

For example, if  $q_{in}(t)$  can be represented as  $1 + 0.1t + 0.01t^2$ , the error as a function of time, after initial conditions have disappeared, can be evaluated completely as

$$E(t) = a_0(1 + 0.1t + 0.01t^2) + a_1(0.1 + 0.02t) + a_2(0.02).$$

It can be seen that the error coefficients lead directly to the evaluation of the resulting error for all values of time rather than only for time equal to infinity, as with error constants, which have been treated elsewhere in the literature.<sup>6-8</sup>

### III. EVALUATION OF ERROR COEFFICIENTS

A perfect servo is defined as one having all error coefficients equal to zero. In practice, it is desired to make as many of the lower-order error coefficients zero as possible. This is equivalent to making the more familiar error constants  $K_p, K_v, K_a$ , etc., infinite.

The error coefficients can be calculated by considering the Laplace transform of the error between the input and the output of the system.

Let

$$E(s) = q_{out}(s) - q_{in}(s), \quad (2)$$

where  $E(s)$  is the Laplace transform of the error  $E(t)$  between the output and input quantities  $q_{out}(t)$  and  $q_{in}(t)$ . Dividing both sides of (2) by  $q_{in}(s)$  yields

$$\frac{E(s)}{q_{in}(s)} = \left[ \frac{q_{out}(s)}{q_{in}(s)} - 1 \right], \quad (3)$$

where  $q_{out}(s)/q_{in}(s)$  is the closed-loop transfer function if zero initial conditions are assumed. Equation (3) can be expanded in a Maclaurin series for small values of  $s$  as

$$\frac{E}{q_{in}}(s) = a_0 + a_1s + a_2s^2 + \dots + a_ns^n + \dots \quad (4)$$

From the similarity between (1) and (4), it can be seen that the  $a$ 's are the so-called error coefficients.

<sup>6</sup> H. M. James, et al., *loc cit.*  
<sup>7</sup> H. Chestnut and R. W. Mayer, *loc cit.*  
<sup>8</sup> G. S. Brown and D. P. Campbell, "Principles of Servomechanisms," John Wiley & Sons, Inc., New York, N. Y.; 1948.

It is possible to evaluate successive error coefficients from the following relationships derived from (4)

$$a_0 = \lim_{s \rightarrow 0} \left[ \frac{E(s)}{q_{in}(s)} \right], \quad (5a)$$

$$a_1 = \lim_{s \rightarrow 0} \frac{1}{s} \left[ \frac{E(s)}{q_{in}(s)} - a_0 \right], \quad (5b)$$

$$a_n = \lim_{s \rightarrow 0} \frac{1}{s^n} \left[ \frac{E(s)}{q_{in}(s)} - \sum_{k=0}^{n-1} a_k s^k \right]. \quad (5c)$$

Instead of calculating error coefficients from the Maclaurin expansion of  $[(q_{out}/q_{in})(s) - 1]$ , it is easier and more instructive to calculate the values from  $(q_{out}/q_{in})(s)$ , which is the familiar closed-loop transfer function. From (3) and (4), it can be seen that

$$\frac{q_{out}}{q_{in}}(s) = 1 + a_0 + a_1s + a_2s^2 + \dots + a_ns^n + \dots \quad (6)$$

Equation (6) is used to calculate the error coefficients. Let

$$a_0' = 1 + a_0 \quad (7)$$

and

$$\frac{q_{out}}{q_{in}}(s) = \frac{n_0 + n_1s + n_2s^2 + \dots + n_ns^n}{1 + d_1s + d_2s^2 + \dots + d_ms^m} \quad (8)$$

Then, from (6), (7) and (8);

$$a_0' = \lim_{s \rightarrow 0} \left[ \frac{q_{out}}{q_{in}}(s) \right] = n_0, \quad (9)$$

$$a_1 = \lim_{s \rightarrow 0} \frac{1}{s} \left[ \frac{q_{out}}{q_{in}}(s) - a_0' \right] = n_1 - a_0'd_1, \quad (10)$$

$$a_2 = \lim_{s \rightarrow 0} \frac{1}{s^2} \left[ \frac{q_{out}}{q_{in}}(s) - a_0' - a_1s \right] = n_2 - a_0'd_2 - a_1d_1, \quad (11)$$

$$a_n = \lim_{s \rightarrow 0} \frac{1}{s^n} \left[ \frac{q_{out}}{q_{in}}(s) - a_0' - \sum_{k=1}^{n-1} a_k s^k \right] = n_n - a_0'd_n - \sum_{y=1}^{n-1} a_y d_{n-y}. \quad (12)$$

Equation (12) provides a simple method of computing higher-order error coefficients in terms of lower-order error coefficients. Moreover, (8) and (12) give an insight into how  $(q_{out}/q_{in})(s)$  should be modified to provide the desired error coefficients. For example, with all the lower-order error coefficients up to  $a_n$  equal to zero, the coefficient  $a_n$  is made zero by making  $n_n$  equal  $d_n$ .

### IV. METHODS OF OBTAINING ZERO ERROR COEFFICIENTS

To correlate the desired error coefficients with the parameters of  $(q_{out}/q_{in})(s)$ , two block diagrams are next examined in detail in order to see how error coefficients of order  $n$  and  $n+1$  can be made equal to zero in single loops containing integrations of order  $n$ . Photographs of test results are shown.

**A. Loop with No Integrations**

First, it is shown how the the system of Fig. 1, which contains no integrations, can be modified to obtain zero positional and zero velocity error coefficients. With  $K_2$  gain compensation inserted into the feedback loop of Fig. 1.  $(q_{out}/q_{in})(s)$  can be written as follows

$$\frac{q_{out}}{q_{in}}(s) = \frac{s^2 \left( \frac{K_1 T_1 T_3}{1 + K K_2} \right) + s \left( \frac{K T_1 + K T_3}{1 + K K_2} \right) + \frac{K}{1 + K K_2}}{s^2 \left( \frac{T_2 T_4 + K K_2 T_1 T_3}{1 + K K_2} \right) + s \left( \frac{T_2 + T_4 + K K_2 T_1 + K K_2 T_3}{1 + K K_2} \right) + 1} \quad (13)$$

Equations (7) and (9) show that for  $a_0$  to be equal to zero,  $(1 + K K_2)$  must equal  $K$ . Therefore  $K_2$  must equal  $(1 - (1/K))$ , and with this value the system of Fig. 1 now can be classified as a positional servomechanism since it has zero positional error. The same system configuration with unity feedback, however, does not meet with the zero positional error requirement of a servo.

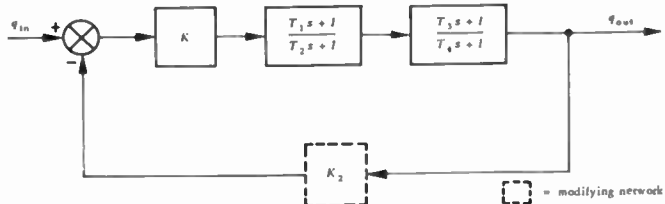


Fig. 1—General closed-loop system containing no integration.

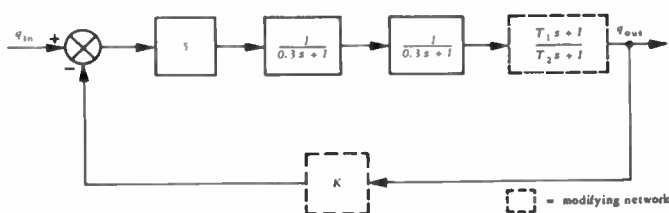


Fig. 2—Sample loop containing no integrations.

To determine  $a_1$ , (10) is now used

$$a_1 = \frac{K T_1 + K T_3}{1 + K K_2} - \frac{T_2 + T_4 + K K_2 T_1 + K K_2 T_3}{1 + K K_2} \quad (14)$$

But

$$K K_2 = K - 1, \quad (15)$$

therefore

$$a_1 = \frac{K(T_1 + T_3) - T_2 - T_4 - (K - 1)(T_1 + T_3)}{K} \quad (16)$$

$$= \frac{T_1 + T_3 - T_2 - T_4}{K} \quad (17)$$

By adding a network to the forward loop so that the sum of the time constants in the numerator equals the sum of the time constants in the denominator, the servo will now have a zero velocity error coefficient.

In order to illustrate the effectiveness of the proposed method of compensation, the block diagram of Fig. 2 was examined on the General-Purpose Simulator at the Instrumentation Laboratory, Massachusetts Institute of Technology, and photographs were taken of the transient response as seen on an oscilloscope. The pic-

tures of Fig. 3 show that the forced-dynamic error of this specific system has been reduced by using eight-tenths feedback instead of unity feedback. Furthermore, the gain of the feedback loop  $K$  is not critical in the system. As long as  $K$  is between six-tenths and unity, the forced-dynamic error of the system would be less than that present with unity feedback.

It can also be seen from the pictures of Fig. 3 that the forced dynamic error for a ramp input has been reduced to zero by insertion of a passive network in

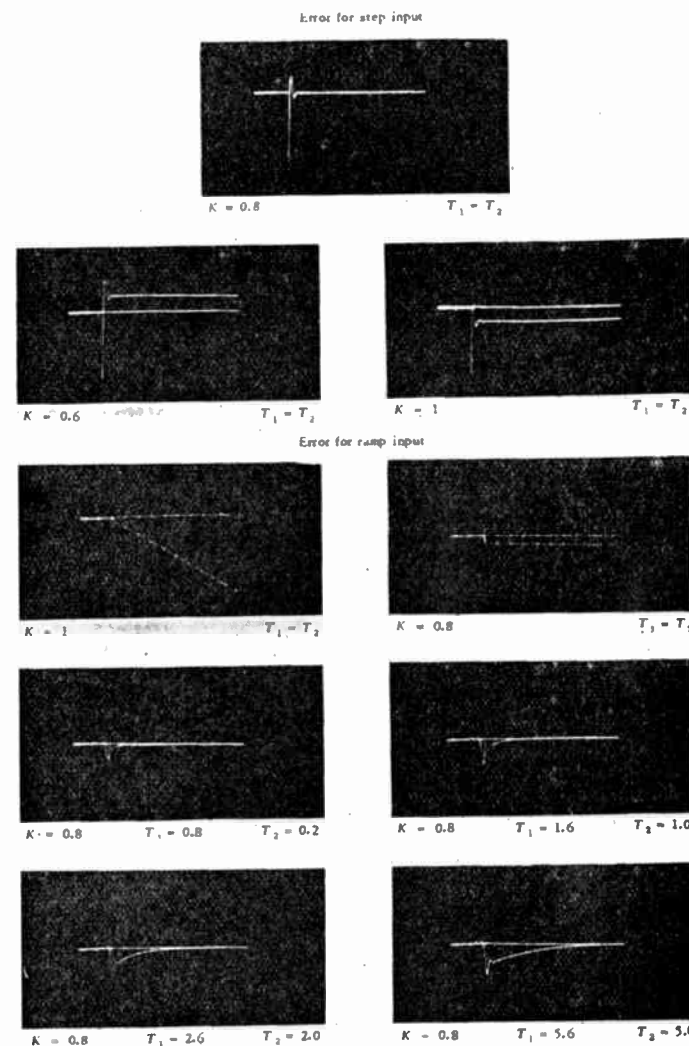


Fig. 3—Simulator results obtained for system of Fig. 2.



the forward path. As there is a wide choice in the parameters of the actual network used, the transient error responses are shown for several different networks.

### B. Single Loop with One Integration

It will now be shown how the system of Fig. 4, which contains a single integration, can be modified to obtain zero velocity and acceleration coefficients.

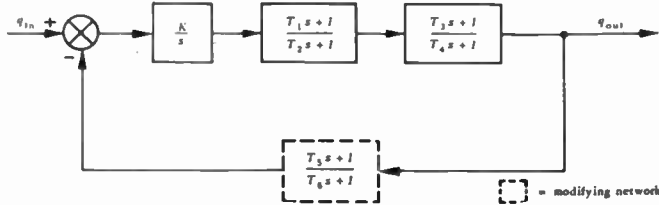


Fig. 4—General closed-loop system containing one integration.

As a first modification, the network  $(T_6s+1)/(T_6s+1)$  is placed in the feedback path. Then

$$\frac{q_{out}}{q_{in}}(s) = \frac{\frac{T_1s+1}{T_2s+1} \times \frac{T_3s+1}{T_4s+1} \times \frac{K}{s}}{1 + \frac{T_1s+1}{T_2s+1} \times \frac{T_3s+1}{T_4s+1} \times \frac{T_6s+1}{T_6s+1} \times \frac{K}{s}}, \quad (18)$$

$$\frac{q_{out}}{q_{in}}(s) = \frac{n_0 + n_1s + n_2s^2 + n_3s^3}{1 + d_1s + d_2s^2 + d_3s^3 + d_4s^4}, \quad (19)$$

where

$$\begin{aligned} n_0 &= 1 \\ n_1 &= T_1 + T_3 + T_6 \\ n_2 &= T_1T_3 + T_1T_6 + T_3T_6 \\ d_1 &= T_1 + T_3 + T_6 + \frac{1}{K} \\ d_2 &= T_1T_3 + T_3T_6 + T_1T_6 + \frac{1}{K}(T_2 + T_4 + T_6). \end{aligned} \quad (20)$$

From these equations, used in conjunction with (12), it is seen that

$$a_0 = 0,$$

and

$$\begin{aligned} a_1 &= T_1 + T_3 + T_6 - \left( T_1 + T_3 + T_6 + \frac{1}{K} \right) \\ &= T_6 - \left( T_6 + \frac{1}{K} \right) \end{aligned} \quad (21)$$

Therefore,  $a_1$  is dependent only upon the parameters of the feedback path and the gain of the forward path. Specifically, in order for  $a_1$  to be equal to zero,  $T_6$  must equal  $T_6 + (1/K)$ . With  $T_6$  equal to zero and  $a_1$  made equal to zero by the proper choice of  $T_6$ ,  $a_2$  is now given by

$$\begin{aligned} a_2 &= T_1T_3 + T_1T_6 + T_3T_6 - T_1T_3 \\ &\quad - \frac{1}{K}(T_2 + T_4 + T_6). \end{aligned} \quad (22)$$

Because  $T_6 = 1/K$ , then

$$a_2 = \frac{T_1}{K} + \frac{T_3}{K} - \frac{T_2}{K} - \frac{T_4}{K} - \frac{1}{K^2}. \quad (23)$$

With  $a_1$  equal to zero,  $a_2$  can, therefore, be made equal to zero by ensuring that in the forward part of the loop the sum of the first-order time constants in the numerator is equal to the sum of the first-order time constants in the denominator plus  $1/K$ .

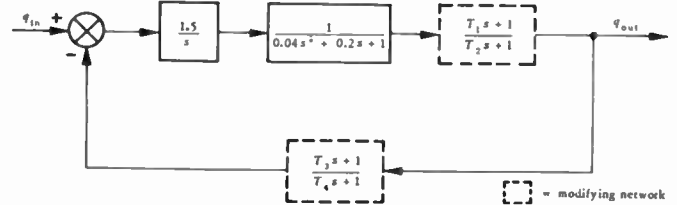


Fig. 5—Sample loop containing one integration.

To illustrate further the results obtainable by the use of error coefficients, the block diagram of Fig. 5 was also examined on the General Purpose Simulator. The results, summarized in Fig. 6, show that it is possible to obtain zero velocity and zero acceleration error coefficients without appreciably changing the stability or response time of the system.

### C. Generalized Technique

The effect of a servo in the feedback loop, such as in Fig. 7, is considered next. For a constant angular velocity input  $q_{in}$ , the following steady-state equations can be written

$$q_1 = q_{in} - \frac{\dot{q}_{in}}{K} \quad (24)$$

$$q_1 = q_{out} - \frac{\dot{q}_{out}}{K_A} \quad (25)$$

$$\dot{q}_{in} = \dot{q}_{out}. \quad (26)$$

For  $q_{out}$  to be equal to  $q_{in}$ ,  $K_A$  must therefore equal  $K$ . However, from the viewpoint of the over-all loop, the servo in the feedback path is equal to the passive network  $1/[1+(1/K)s]$ , which is identical with the modifying network that was calculated for the servo in Fig. 4. Consequently, the modifying passive network acts as though it were a servo having the proper velocity constant. In fact, any passive network which has a transfer function equal to the closed-loop transfer function of a servo having the correct velocity constant can be used in the feedback path of Fig. 4 to obtain a zero velocity error coefficient. In general, this analog method can be used for selecting the network necessary to make  $a_n$  equal to zero in a loop containing  $n$  integrations where  $n$  is 1 or larger.

### D. Alternate Compensation Techniques

Previously in this paper, emphasis has been placed on using a network in the feedback path in order to make the  $a_n$  error coefficient equal to zero in an  $n$  integration loop. In many cases, it may be impossible or inconven-

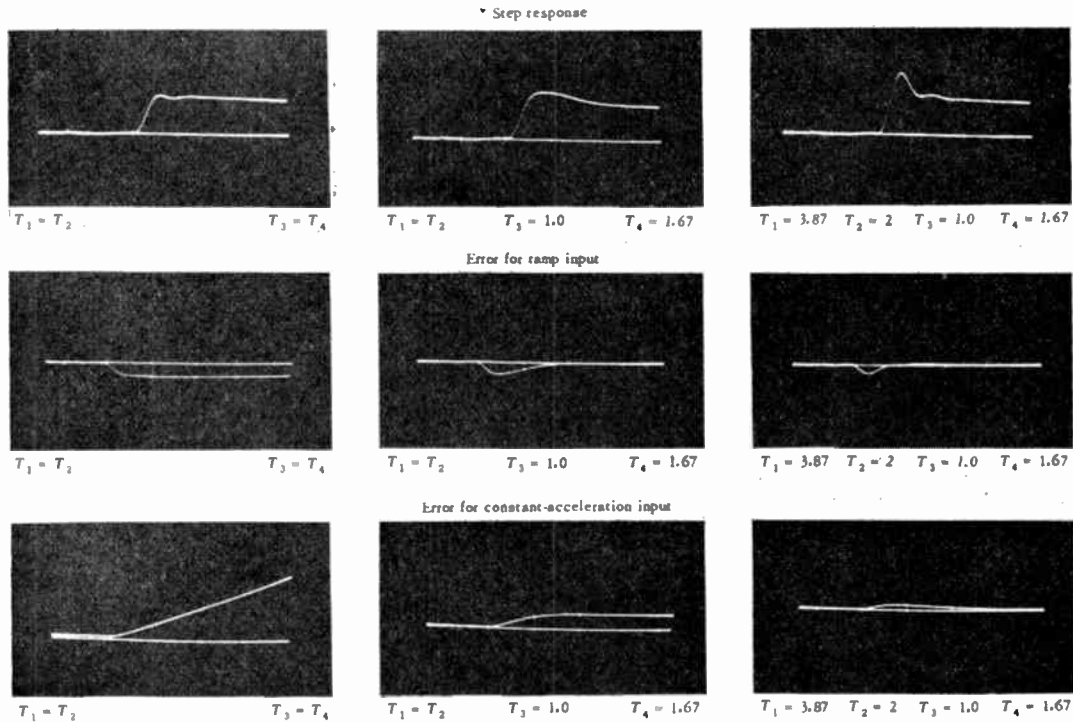


Fig. 6—Simulator results obtained for system of Fig. 5.

ient to put a network in the feedback path, due to the nature of the system components. However, even with a unity feedback path, it may still be possible to have the desired error coefficient. Fig. 8 shows two possible ways in which this may be done. In multiloop systems more ways are possible and the equivalent method of compensation will depend, to a large extent, upon the ingenuity of the designer.

*E. Use of Additional Integrations*

In a single-loop system with unity feedback, higher-order error coefficients can be made equal to zero by the insertion of additional integrations in the forward path. Thus, the compensation techniques developed in this paper are mathematically equivalent to the use of extra integrations in the forward path of a unity feedback system. For example, the system of Fig. 5, which contains only one integration and two passive compensating networks, is mathematically equivalent to a system with unity feedback and three integrations in the forward path. In general, each additional passive compensation network in a single-loop system can be replaced by an active integrator. However, in multiloop systems, it may be possible to have one network take the place of several integrators.

V. EFFECT OF ZERO ERROR COEFFICIENT MODIFICATIONS UPON SYSTEM RESPONSE

*A. Stability and Bandwidth*

It has been shown in the preceding section that the passive network used in the feedback loop is equivalent to a servo. If the bandwidth of the equivalent servo is sufficiently larger than the bandwidth of the original

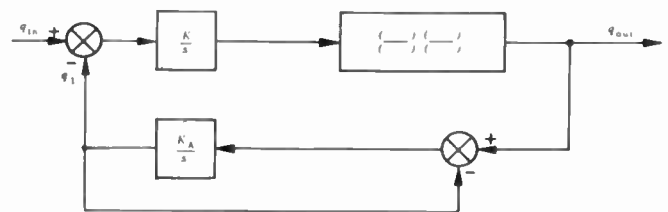


Fig. 7—Example of system containing a servo in the feedback path

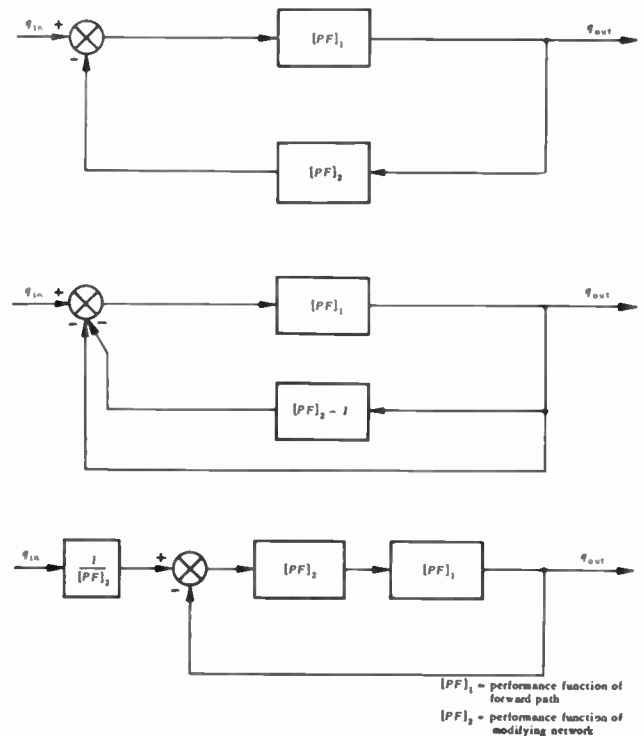


Fig. 8—Equivalent methods of compensation.

loop, then the over-all loop will see unity feedback inside its bandwidth. Since unity feedback does not change the phase lag at the resonant frequency, the passive network will not appreciably affect the stability or bandwidth of the over-all loop. Therefore, it is generally possible to design the passive network used in the feedback path so that it does not adversely affect the stability or bandwidth of the over-all loop. Moreover, if the original loop has marginal stability as a result of trying to achieve a large error constant, then both the stability and error constants of the loop can be increased by reducing the forward loop gain and using a network in the feedback loop.

The modifying network used in the forward loop has the function of making the  $a_{n+1}$  error coefficient equal to zero in an  $n$  integration loop. In a zero integration loop, this network should be such that the sum of the numerator time constants is equal to the sum of the denominator time constants. Since only the over-all sum is important, the networks shown below can be considered equivalent in the steady state.

$$\frac{5s + 1}{7s + 1} \quad \text{or} \quad \frac{1s + 1}{3s + 1} \quad \text{or} \quad \frac{3s + 1}{6s + 1} \times \frac{2s + 1}{1s + 1}.$$

Consequently, there is a wide latitude in the choice of the modifying network, and it may be possible to pick the forward loop network so that it does not affect the stability or bandwidth. Likewise, in higher-order systems there is a wide latitude in the choice of the modifying network.

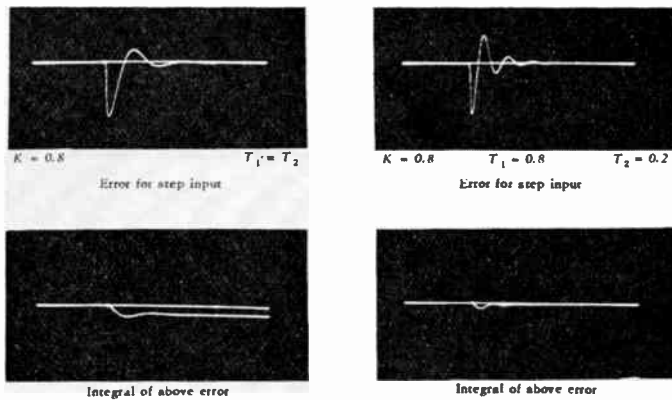


Fig. 9—Effect of modifications on transient response of system of Fig. 2.

### B. Reshaping of Transient Response

It is known that the set of linear differential operators with constant coefficients is commutative.<sup>9</sup> Consequently, since a ramp function is the integral of a step function, the error response to a ramp input of a linear system with constant coefficients can be found by in-

tegrating the error response of the system for a step input. Similarly, the error response for a constant acceleration input is the double integral of the error response for a step input. Making higher-order error coefficients equal to zero, therefore, means that the error response to a step input is modified so that higher integrals of this response become equal to zero. This is illustrated in the pictures of Fig. 9.

## VI. CONCLUSION

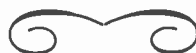
A method has been presented for reducing the forced dynamic error in a closed-loop system. In general, there is a wide latitude in the specific parameters of the networks used to accomplish this effect, and it is possible to design a network that does not appreciably change the stability or response time of the system.

Furthermore, even though it is a matching method of compensation that assumes the system parameters do not change, significant reduction of forced dynamic error can often be obtained without the network parameters having to be set precisely. For example, if a network  $1/(T_7s+1)$  is used instead of the theoretically correct network  $1/(T_6s+1)$  in the feedback path of Fig. 4, then the forced dynamic error for a ramp input will be less than would be present with unity feedback as long as  $0 < T_7 < 2T_6$ . The choice of the network can be facilitated by the following general rule:

In a single loop containing  $n$  integrations, the error coefficient  $a_n$  is independent of the dynamic lags of the forward path. It does, however, depend upon the gain of the forward path and the parameters of the feedback path. Specifically, in a loop containing no integrations, a zero positional error coefficient can be obtained by using a feedback path gain of one minus the reciprocal of the gain of the forward path. In a loop containing one integration, a zero velocity error coefficient can be obtained by using the feedback network  $(T_6s+1)/(T_6s+1)$ , where  $T_6$  equals  $T_6$  plus the reciprocal of the gain of the forward path.

Although this paper is restricted to the consideration of positional servomechanisms, the techniques developed here are applicable to a larger class of systems. If it is desired that the output  $q_{out}$  be some function of the input  $f(q_{in})$ , then the system error may be defined as  $q_{out} - f(q_{in})$ . With this definition of error, a new set of error coefficients may be formulated in terms of the system parameters. The system parameters may then be modified intelligently to reduce the forced dynamic error. Finally, since the compensation used is contingent upon modifying the feedback loop, it has been shown conclusively that servo performance can be improved by using other than unity feedback.

<sup>9</sup> F. B. Hildebrand, "Advanced Calculus for Engineers," Prentice-Hall, Inc., New York, N. Y.; 1949.



# Theory of AFC Synchronization\*

WOLF J. GRUEN†, MEMBER, IRE

**Summary**—The general solution for the important design parameters of an automatic frequency and phase-control system is presented. These parameters include the transient response, frequency response and noise bandwidth of the system, as well as the hold-in range and pull-in range of synchronization.

## I. INTRODUCTION

**A**UTOMATIC FREQUENCY and phase-control systems have been used for a number of years for the horizontal-sweep synchronization in television receivers, and more recently have found application for the synchronization of the color subcarrier in the proposed NTSC color-television system. A block diagram of a general AFC system is shown in Fig. 1.

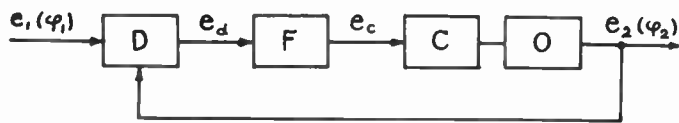


Fig. 1—Block diagram of A.F.C. loop.

The phase of the transmitted synchronizing signal  $e_1$  is compared to the phase of a local oscillator signal  $e_2$  in a phase discriminator  $D$ . The resulting discriminator output voltage is proportional to the phase difference of the two signals, and is fed through a control network  $F$  to a frequency-control stage  $C$ . This stage controls the frequency and phase of a local oscillator  $O$  in accordance with the synchronizing information, thereby keeping the two signals in perfect synchronism. Although in practice the transmitted reference signal is often pulsed and the oscillator comparison voltage non-sinusoidal, the analysis is carried out for sinusoidal signal voltages. The theory, however, can be extended for a particular problem by writing the applied voltages in terms of a Fourier series instead of the simple sine function. An AFC system is essentially a servomechanism, and the notation that will be used is the one followed by many workers in this field. An attempt will be made to present the response characteristics in dimensionless form in order to obtain a universal plot of the response curves.

## II. DERIVATION OF THE BASIC EQUATION

If it is assumed that the discriminator is a balanced phase detector composed of peak-detecting diodes, the discriminator-output voltage can be derived from the vector diagram in Fig. 2. For sinusoidal variation with time, the synchronizing signal  $e_1$  and the reference signal

$e_2$  can be written

$$e_1 = E_1 \cos \phi_1 \tag{1}$$

and

$$e_2 = E_2 \sin \phi_2. \tag{2}$$

$\phi_1$  and  $\phi_2$  are functions of time and, for reasons of simplicity in the later development, it is arbitrarily assumed that  $\phi_1$  and  $\phi_2$  are in quadrature when the system is perfectly synchronized, that is when  $\phi_1 = \phi_2$ .

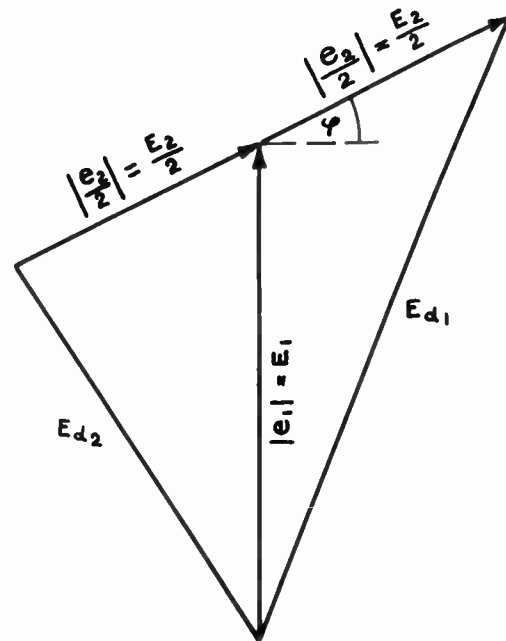


Fig. 2—Discriminator vector diagram.

While one of the discriminator diodes is fed with the sum of  $e_1$  and  $e_2/2$ , the other is fed with the difference of these two vectors as shown in Fig. 2. The resulting rectified voltages  $E_{d1}$  and  $E_{d2}$  can be established by simple trigonometric relations. Defining a difference phase

$$\phi \equiv \phi_1 - \phi_2, \tag{3}$$

one obtains

$$E_{d1}^2 = E_1^2 + \frac{E_2^2}{4} + E_1 E_2 \sin \phi \tag{4}$$

and

$$E_{d2}^2 = E_1^2 + \frac{E_2^2}{4} - E_1 E_2 \sin \phi. \tag{5}$$

The discriminator output voltage  $e_d$  is equal to the dif-

\* Decimal classification: R583.5. Original manuscript received by the Institute, August 21, 1952; revised manuscript received February 25, 1953.

† General Electric Co., Syracuse, N. Y.

ference of the two rectified voltages, so that

$$e_d = E_{d1} - E_{d2} = \frac{2E_1E_2}{E_{d1} + E_{d2}} \sin \phi. \quad (6)$$

If the amplitude  $E_1$  of the synchronizing signal is larger than the amplitude  $E_2$  of the reference signal, one obtains

$$E_{d1} + E_{d2} \cong 2E_1. \quad (7)$$

The discriminator output voltage then becomes

$$e_d = E_2 \sin \phi \quad (8)$$

and is independent of the amplitude  $E_1$  of the synchronizing signal. As  $\phi_1$  and  $\phi_2$  are time-varying parameters, it should be kept in mind that the discriminator time constant ought to be shorter than the reciprocal of the highest difference frequency  $d\phi/dt$ , which is of importance for the operation of the system.

Denoting the transfer function of the control network  $F$  as  $F(p)$ , the oscillator control voltage becomes

$$e_c = F(p)E_2 \sin \phi. \quad (9)$$

Assuming furthermore that the oscillator has a linear-control characteristic of a slope  $S$ , and that the free-running oscillator frequency is  $\omega_0$ , the actual oscillator frequency in operational notation becomes

$$p\phi_2 = \omega_0 + Se_c. \quad (10)$$

Substituting (3) and (9) into (10) then gives

$$p\phi + SE_2F(p) \sin \phi = p\phi_1 - \omega_0. \quad (11)$$

The product  $SE_2$  repeats itself throughout this paper and shall be defined as the gain constant

$$K \equiv SE_2. \quad (12)$$

$K$  represents the maximum frequency shift at the output of the system per radian phase shift at the input. It has the dimension of radians/second.

Equation (11) can be simplified further by measuring the phase angles in a coordinate system which moves at the free-running speed  $\omega_0$  of the local oscillator. One obtains

$$\boxed{p\phi + F(p)K \sin \phi = p\phi_1}. \quad (13)$$

This equation represents the general differential equation of the AFC feedback loop.  $p\phi$  is the instantaneous-difference frequency between the synchronizing signal and the controlled-oscillator signal and  $p\phi_1$  is the instantaneous-difference frequency between the synchronizing signal and the free-running oscillator signal.

Equation (13) shows that all AFC systems with identical gain constants  $K$  and unity d.c. gain through the control network have the same steady-state solution, provided that the difference frequency  $p\phi_1$  is constant. If this difference frequency is defined as

$$\Delta\omega \equiv p\phi_1 = \omega_1 - \omega_0, \quad (14)$$

the steady-state solution is

$$\sin \phi = \frac{\Delta\omega}{K}. \quad (15)$$

This means the system has a steady-state phase error which is proportional to the initial detuning  $\Delta\omega$  and inversely proportional to the gain constant  $K$ . Since the maximum value of  $\sin \phi$  in (15) is  $\pm 1$ , the system will hold synchronism over a frequency range

$$|\Delta\omega_{\text{Hold-in}}| \leq K. \quad (16)$$

Equations (15) and (16) thus define the static performance limit of the system.

### III. LINEAR ANALYSIS

An AFC system, once it is synchronized, behaves like a low-pass filter. To study its performance it is permissible, for practical signal-to-noise ratios, to substitute the angle for the sine function in (13). Then, with the definition of (3), one obtains

$$p\phi_2 + KF(p)\phi_2 = KF(p)\phi_1. \quad (17)$$

This equation relates the output phase  $\phi_2$  of the synchronized system to the input phase  $\phi_1$ . It permits an evaluation of the behavior of the system to small disturbances of the input phase, if the transfer function  $F(p)$  of the control network is specified.

a.  $F(p) = 1$

This is the simplest possible AFC system, and represents a direct connection between the discriminator output and the oscillator control stage. Equation (17) then becomes

$$p\phi_2 + K\phi_2 = K\phi_1. \quad (18)$$

If the initial detuning is zero, the transient response of the system to a sudden step of input phase  $|\phi_1|$  is

$$\frac{\phi_2}{|\phi_1|}(t) = 1 - e^{-Kt}. \quad (19)$$

Likewise, the frequency response of the system to a sine-wave modulation of the input phase is

$$\frac{\phi_2}{\phi_1}(j\omega) = \frac{1}{1 + j\frac{\omega}{K}}. \quad (20)$$

The simple AFC system thus behaves like an RC-filter and has a cut-off frequency of

$$\omega_c = K \text{ [radians/sec]}. \quad (21)$$

George<sup>1</sup> has shown that the m.s. phase error of the system under the influence of random interference is proportional to the noise bandwidth, which is defined as

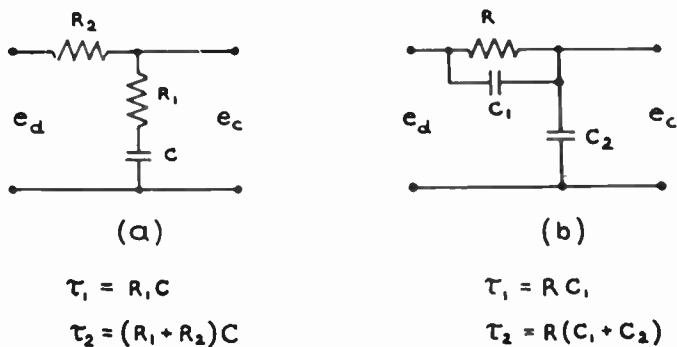
<sup>1</sup> T. S. George, "Synchronizing systems for dot interlaced color TV," Proc. I.R.E., February, 1951.

$$B = \int_{-\infty}^{+\infty} \left| \frac{\phi_2}{\phi_1}(j\omega) \right|^2 d\omega. \quad (22)$$

The integration has to be carried out from  $-\infty$  to  $+\infty$  since the noise components on both sides of the carrier are demodulated. Inserting (20) into (22) then yields

$$B = \pi K \text{ [radians/sec]}. \quad (23)$$

It was shown in (15) that for small steady-state phase errors due to average frequency drift, the gain constant  $K$  has to be made as large as possible, while now for good noise immunity, i.e., narrow bandwidth, the gain constant has to be made as small as possible. A proper compromise of gain then must be found to insure adequate performance of the system for all requirements. This difficulty, however, can be overcome by the use of a more elaborate control network.



$$\frac{e_c}{e_d}(p) = \frac{1 + \tau_1 p}{1 + \tau_2 p}$$

Fig. 3—Proportional plus integral control networks.

$$b. F(p) = \frac{1 + \tau_1 p}{1 + \tau_2 p}$$

Networks of this type are called proportional-plus integral-control networks<sup>2</sup> and typical network configurations are shown in Fig. 3. Inserting the above transfer function into (17) yields

$$p^2 \phi_2 + \left( \frac{1}{\tau_2} + K \frac{\tau_1}{\tau_2} \right) p \phi_2 + \frac{K}{\tau_2} \phi_2 = K \frac{\tau_1}{\tau_2} p \phi_1 + \frac{K}{\tau_2} \phi_1. \quad (24)$$

$\phi_1$  and  $\phi_2$  are again relative phase angles, measured in a coordinate system which moves at the free-running speed of the local oscillator. To integrate (24), it is convenient to introduce the following parameters

$$\omega_n^2 \equiv \frac{K}{\tau_2} \quad (25)$$

and

$$2\zeta \omega_n \equiv \frac{1}{\tau_2} + K \frac{\tau_1}{\tau_2}. \quad (26)$$

$\omega_n$  is the resonance frequency of the system in the absence of any damping, and  $\zeta$  is the ratio of actual-to-critical damping. In terms of the new parameters the time constants of the control network are

$$\tau_1 = \frac{2\zeta}{\omega_n} - \frac{1}{K} \quad (27)$$

and

$$\tau_2 = \frac{K}{\omega_n^2}. \quad (28)$$

With these definitions (24) becomes

$$p^2 \phi_2 + 2\zeta \omega_n p \phi_2 + \omega_n^2 \phi_2 = \left( 2\zeta \omega_n - \frac{\omega_n^2}{K} \right) p \phi_1 + \omega_n^2 \phi_1. \quad (29)$$

The transient response of the system to a sudden step of input phase  $|\phi_1|$  is found by integration of (29) and the initial condition for the oscillator frequency is obtained from (10). The transient response then is

$$\frac{\phi_2}{|\phi_1|}(t) = 1 - e^{-\zeta \omega_n t} \left[ \cos \sqrt{1 - \zeta^2} \omega_n t - \frac{\zeta - \frac{\omega_n}{K}}{\sqrt{1 - \zeta^2}} \sin \sqrt{1 - \zeta^2} \omega_n t \right]. \quad (30)$$

For  $\zeta < 1$  the system is underdamped (oscillatory), for  $\zeta = 1$  critically damped and for  $\zeta > 1$  overdamped (non-oscillatory). In order to avoid sluggishness of the system, a rule of thumb may be followed making  $4 < \zeta < 1^2$ . The transient response of (30) can be plotted in dimensionless form if certain specifications are made for the ratio  $\omega_n/K$ . As the time constant  $\tau_1$  of the control network must be positive or can at most be equal to zero, the maximum value for  $\omega_n/K$  is found from (27), yielding

$$\frac{\omega_n}{K} \Big|_{\max} = 2\zeta. \quad (31)$$

In this case the control network is reduced to a single time constant network ( $\tau_1 = 0$ ). On the other hand, if for a fixed value of  $\omega_n$  the gain of the system is increased towards infinity, the minimum value for  $\omega_n/K$  becomes

$$\frac{\omega_n}{K} \Big|_{\min} = 0. \quad (32)$$

Fig. 4 shows the transient response of the system for these two limits and for a damping ratio of  $\zeta = 0.5$ .

<sup>2</sup> G. S. Brown and D. P. Campbell, "Principles of Servomechanisms," John Wiley & Sons Publishing Co., New York, N. Y., 1948.

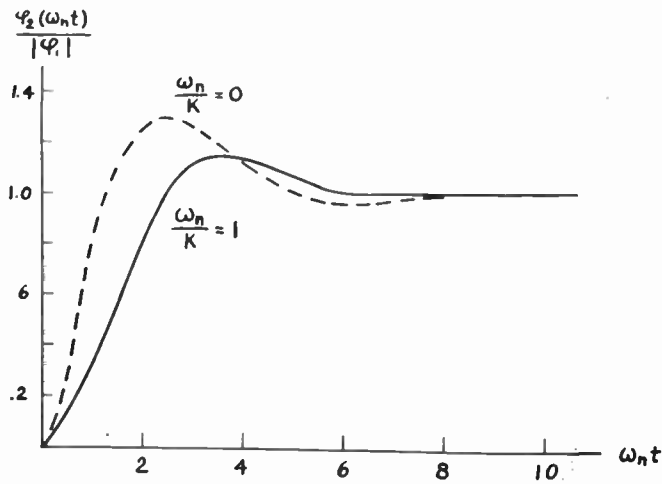


Fig. 4—Transient response for  $\zeta=0.5$ .

The frequency response of the system is readily found from (24) and one obtains

$$\frac{\phi_2}{\phi_1}(j\omega) = \frac{1 + j2\zeta \frac{\omega}{\omega_n} \left(1 - \frac{\omega_n}{2\zeta K}\right)}{1 + j2\zeta \frac{\omega}{\omega_n} - \left(\frac{\omega}{\omega_n}\right)^2} \quad (33)$$

Its magnitude is plotted in Fig. 5 for the two limit values of  $\omega_n/K$  and for a damping ratio  $\zeta=0.5$ . The curves show that the cut-off frequency of the system, for  $\zeta=0.5$ , is approximately

$$\omega_c \cong \omega_n \text{ [radians/sec.]} \quad (34)$$

If  $\phi_1$  and  $\phi_2$  in (33) are assumed to be the input and output voltage of a four-terminal low-pass filter, the frequency response leads to the equivalent circuit of Fig. 6.

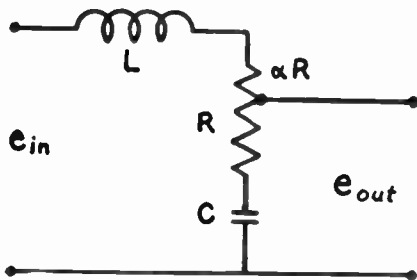


Fig. 6—Equivalent low-pass filter.

The noise bandwidth of the system is established by inserting (33) into (22) and one obtains

$$B = \omega_n \int_{-\infty}^{+\infty} \frac{1 + 4\zeta^2 \left(\frac{\omega}{\omega_n}\right)^2 \left[1 - \frac{\omega_n}{2\zeta K}\right]^2}{1 - (2 - 4\zeta^2) \left(\frac{\omega}{\omega_n}\right)^2 - \left(\frac{\omega}{\omega_n}\right)^4} d\left(\frac{\omega}{\omega_n}\right) \quad (35)$$

The integration, which can be carried out by partial fractions with the help of tables, yields

$$B = \frac{4\zeta^2 - 4\zeta \frac{\omega_n}{K} + \left(\frac{\omega_n}{K}\right)^2 + 1}{2\zeta} \pi \omega_n \quad (36)$$

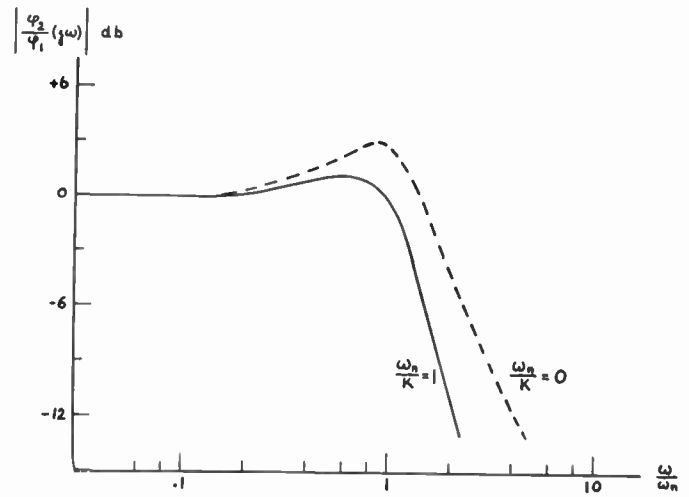


Fig. 5—Frequency response for  $\zeta=0.5$ .

For small values of  $\omega_n/K$ , it is readily established that this expression has a minimum when  $\zeta=0.5$ . Hence, the noise bandwidths for the limit values of  $\omega_n/K$  and  $\zeta=0.5$  become

$$B|_{(\omega_n/K) \rightarrow 1} = \pi \omega_n = \pi K \text{ [radians/sec]} \quad (37)$$

and

$$B|_{(\omega_n/K) \rightarrow 0} = 2\pi \omega_n \text{ [radians/sec.]} \quad (38)$$

The above derivations, as well as the response curves of Figs. 4 and 5, show that the bandwidth and the gain constant of the system can be adjusted independently if a double time-constant control network is employed.

*c. Example*

The theory is best illustrated by means of an example. Suppose an AFC system is to be designed, having a steady state phase error of not more than  $3^\circ$  and a noise bandwidth of 1,000 cps. The local oscillator drift shall be assumed with 1,500 cps.

The required gain constant is obtained from (15), yielding

$$K = \frac{\Delta\omega}{\sin \phi} = \frac{2\pi \cdot 1,500}{\sin 3^\circ} = 180,000 \text{ radians/sec.}$$

Since  $K$  is large in comparison to the required bandwidth, the resonance frequency of the system is established from (38).

$$\omega_n = \frac{B}{2\pi} = \frac{2\pi \cdot 1,000}{2\pi} = 1,000 \text{ radians/sec.}$$

The two time constants of the control network, assuming a damping ratio of 0.5, are determined from (27) and (28) respectively

$$\tau_1 = \frac{2\zeta}{\omega_n} - \frac{1}{K} = \frac{1}{1,000} - \frac{1}{180,000} \cong 10^{-3} \text{ sec,}$$

and

$$\tau_2 = \frac{K}{\omega_n^2} = \frac{180,000}{1,000^2} = 0.18 \text{ sec.}$$



These values  $K$ ,  $\tau_1$ , and  $\tau_2$  completely define the AFC system. A proper choice of gain distribution and control-network impedance still has to be made to fit a particular design. For example, if the peak amplitude of the sinusoidal oscillator reference voltage is  $E_2 = 6$  volts, the sensitivity of the oscillator control stage must be  $S = 30,000$  radians/sec/volt to provide the necessary gain constant of 180,000 radians/sec. Furthermore, if the capacitor  $C$  for the control network of Fig. 3(a) is assumed to be 0.22  $\mu f$ , the resistors  $R_1$  and  $R_2$  become 4.7 k $\Omega$  and 820 k $\Omega$  respectively, to yield the desired time constants.

#### IV. NON-LINEAR ANALYSIS

While it was permissible to assume small phase angles for the study of the synchronized system, thereby linearizing the differential (13), this simplification cannot be made for the evaluation of the pull-in performance of the system. The pull-in range of synchronization is defined as the range of difference frequencies,  $p\phi_1$ , between the input signal and the free-running oscillator signal, over which the system can reach synchronism. Since the difference phase  $\phi$  can vary over many radians during pull-in, it is necessary to integrate the nonlinear equation to establish the limit of synchronization.

Assuming that the frequency of the input signal is constant as defined by (14), (13) can be written

$$p\phi + F(p)K \sin \phi = \Delta\omega. \quad (39)$$

Mathematically then, the pull-in range of synchronization is the maximum value of  $\Delta\omega$  for which, irrespective of the initial condition of the system, the phase difference  $\phi$  reaches a steady state value. To solve (39), the transfer function of the control network again must be defined.

##### a. $F(p) = 1$

The pull-in performance for this case has been treated in detail by Labin.<sup>3</sup> With  $F(p) = 1$  (39) can be integrated by separation of the variables and it is readily found that the system synchronizes for all values of  $|\Delta\omega| < K$ . The condition for pull-in then is

$$|\Delta\omega|_{\text{Pull-in}} < K. \quad (40)$$

Large pull-in range and narrow-noise bandwidth thus are incompatible requirements for this system.

$$b. F(p) = \frac{1 + \tau_1 p}{1 + \tau_2 p}$$

Inserting this transfer function into (39) and carrying out the differentiation yields

$$\frac{d^2\phi}{dt^2} + \left[ \frac{1}{\tau_2} + K \frac{\tau_1}{\tau_2} \cos \phi \right] \frac{d\phi}{dt} + \frac{K}{\tau_2} \sin \phi = \frac{\Delta\omega}{\tau_2}. \quad (41)$$

<sup>3</sup> Edouard Labin, "Theorie de la synchronization par controle de phase," *Philips Res. Rep.*, (in French); August, 1941.

This equation can be simplified by inserting the coefficients defined in (25) and (26), and by dividing the resulting equation by  $\omega_n^2$ . This leads to the dimensionless equation.

$$\frac{d^2\phi}{\omega_n^2 dt^2} + \left[ \frac{\omega_n}{K} + \left( 2\zeta - \frac{\omega_n}{K} \right) \cos \phi \right] \frac{d\phi}{\omega_n dt} + \sin \phi = \frac{\Delta\omega}{K}. \quad (42)$$

A further simplification is possible by defining a dimensionless difference frequency

$$y \equiv \frac{d\phi}{\omega_n dt} \quad (43)$$

and one obtains a first order differential equation from which the dimensionless time  $\omega_n t$  has been eliminated. It follows

$$\frac{dy}{d\phi} = \frac{\frac{\Delta\omega}{K} - \sin \phi}{y} - \frac{\omega_n}{K} - \left( 2\zeta - \frac{\omega_n}{K} \right) \cos \phi. \quad (44)$$

There is presently no analytical method available to solve this equation. However, the equation completely defines the slope of the solution curve  $y(\phi)$  at all points of a  $\phi - y$  plane, except for the points of stable and unstable equilibrium,  $y = 0$ ;  $\Delta\omega/K = \sin \phi$ . The limit of synchronization can thus be found graphically by starting the system with an infinitesimal velocity  $\Delta y$  at a point of unstable equilibrium,  $y = 0$ ;  $\phi = \pi - \sin^{-1} \Delta\omega/K$ , and finding the value of  $\Delta\omega/K$  for which the solution curve just reaches the next point of unstable equilibrium located at  $y = 0$ ;  $\phi = 3\pi - \sin^{-1} \Delta\omega/K$ . The method is discussed by Stoker<sup>4</sup> and has been used by Tellier and Preston<sup>5</sup> to find the pull-in range for a single time constant AFC system.

To establish the limit curve of synchronization for given values of  $\zeta$  and  $\omega_n/K$ , a number of solution curves have to be plotted with  $\Delta\omega/K$  as parameter. The limit of pull-in range in terms of  $\Delta\omega/K$  then can be interpolated to any desired degree of accuracy. The result, obtained in this manner, is shown in the dimensionless graph of Fig. 7, where  $\Delta\omega/K$  is plotted as a function of  $\omega_n/K$  for a damping ratio  $\zeta = 0.5$ . Since this curve represents the stability limit of synchronization for the system, the time required to reach synchronism is infinite when starting from any point on the limit curve. The same applies to any point on the  $\Delta\omega/K$ -axis, with exception of the point  $\Delta\omega/K = 0$ , since this axis describes a system having either infinite gain or zero bandwidth, and neither case has any real practical significance. The practical pull-in range of synchronization, therefore, lies inside the solid boundary. The individual points

<sup>4</sup> J. J. Stoker, "Non-linear vibrations," *Interscience*; New York, 1950.

<sup>5</sup> G. W. Preston and J. C. Tellier, "The Lock-in Performance of an A.F.C. Circuit," *Proc. I.R.E.*; February, 1953.

entered in Fig. 7 represent the measured pull-in curve of a particular system for which the damping ratio was maintained at  $\zeta=0.5$ . For small values of  $\omega_n/K$  this

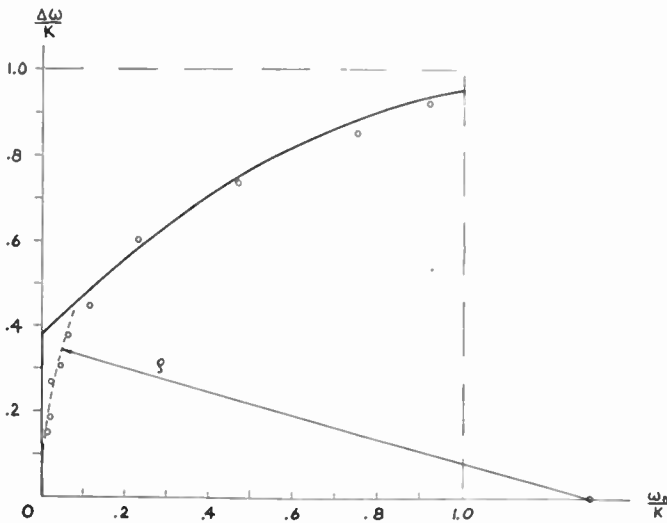


Fig. 7—Pull-in range of synchronization for  $\zeta=0.5$ .

pull-in curve can be approximated by its circle of curvature which, as indicated by the dotted line, is tangent to the  $\Delta\omega/K$ -axis and whose center lies on the  $\omega_n/K$ -axis. The pull-in range thus can be expressed analytically by the equation of the circle of curvature. If its radius is denoted by  $\zeta$ , the circle is given by

$$\left(\frac{\omega_n}{K} - \zeta\right)^2 + \left(\frac{\Delta\omega}{K}\right)^2 = \zeta^2. \quad (45)$$

Hence, for  $(\omega_n/K) \rightarrow 0$ , the pull-in range of synchronization is approximately

$$|\Delta\omega_{\text{Pull-in}}|_{(\omega_n/K) \rightarrow 0} < \sqrt{2\zeta\omega_n K - \omega_n^2} \cong \sqrt{2\zeta\omega_n K}. \quad (46)$$

$\zeta$  can be interpreted as a constant of proportionality which depends on the particular design of the system, and which increases as the system gets closer to the theoretical limit of synchronization.

Equation (46) shows that the pull-in range for small values of  $\omega_n/K$  is proportional to the square root of the product of the cut-off frequency  $\omega_n$  and the gain constant  $K$ . Since the bandwidth of a double time constant AFC system can be adjusted independently of the gain constant, the pull-in range of such a system can exceed the noise bandwidth by any desired amount.

## V. CONCLUSIONS

The performance of an AFC system can be described by three parameters. These are the gain constant  $K$ , the damping ratio  $\zeta$  and the resonance or cut-off frequency  $\omega_n$ . These parameters are specified by the requirements of a particular application and define the over-all design of the system. It has been shown that among the systems with zero, single and double time constant control networks, only the latter fulfills the requirement for achieving good noise immunity, small steady-state phase error and large pull-in range.

# A New Solution for the Current and Voltage Distributions on Cylindrical, Elliptical, Conical or Other Axisymmetrical Antennas\*

O. ZINKE†

## ABSTRACT<sup>1</sup>

TO FIND THE CURRENT DISTRIBUTION we only need four results derived from a treatment of the problem by means of Maxwell's equations:

1. The voltage (the scalar potential) varies nearly sinusoidally along a cylindrical antenna

$$V = V_{\max} \left[ \cos 2\pi \frac{L + l_v - z}{\lambda} + j \frac{R_{\text{rad}}}{Z} \sin 2\pi \frac{L + l_v - z}{\lambda} \right]. \quad (1)$$

\* Decimal classification: R120. Original manuscript received by the Institute, April 16, 1952.

† Zentrallaboratorium, Siemens and Halske Aktiengesellschaft, Munich, Germany.

<sup>1</sup> For complete paper order Document 3923 from American Documentation Institute Auxiliary Publications Project, Photo-duplication Service, Library of Congress, Washington, D. C. \$2.00 for microfilm, or \$3.75 for photoprints readable without optical aid.

$L$  = length of the half of the antenna.

$l_v$  = equivalent length of the end plate  $\approx r_0\sqrt{2}$ .

$z$  = variable, reckoned from the plan of symmetry along the surface of the antenna

$\lambda$  = wavelength.

$R_{\text{rad}}$  = radiation resistance =  $f(L/\lambda)$ .

$Z$  = characteristic impedance = 120 (log<sub>e</sub> 2L/D - const.) ohms.

2. The field strength  $E_n$  normal to the antenna surface is derived from  $E_n = -\partial\phi/\partial n$  as in the electrostatic case

$$E_n = -\frac{d\phi_{\text{stat}}}{dn} \left[ \cos 2\pi \frac{L + l_v - z}{\lambda} + j \frac{R_{\text{rad}}}{Z} \sin 2\pi \frac{L + l_v - z}{\lambda} \right]. \quad (2)$$

Herein  $d\phi_{stat}/dn$  is found either by field plotting or experimentally in the electrolytic trough or by calculation (method of Southwell).

3. The charge  $q$  per unit length of the antenna surface is obtained as product of the known field strength  $E_n$  and the antenna radius  $r_0$

$$q = E_n \epsilon_0 \epsilon_{rel} 2\pi r_0. \quad (3)$$

4. By the continuity law of the current  $dI_z/dz = j\omega q = j\omega E_n \epsilon_0 \epsilon_{rel} 2\pi r_0$  we thus know the slope of the current at any point  $z$ . The current  $I_z$  itself is now after integration

$$I_z = \frac{j}{60\Omega} \int_{z=L+l_v}^z r_0 \frac{d\phi_{stat}}{dn} \left[ \cos 2\pi \frac{L+l_v-z}{\lambda} + j \frac{R_{rad}}{Z} \sin 2\pi \frac{L+l_v-z}{\lambda} \right] d\left(\frac{2\pi z}{\lambda}\right). \quad (4)$$

From (4) it is obvious that the irregularities of the function  $r_0(d\phi_{stat}/dn)$  govern the distortion of the current curve. For homogeneous lines  $r_0$  and  $d\phi_{stat}/dn$  are constant; for elliptical antennas the product  $r_0(d\phi_{stat}/dn)$  is constant (except the ends). In accordance with (4) the current distribution will thus remain sinusoidal.

For cylindrical antennas, however,  $d\phi_{stat}/dn$  varies rapidly with  $z$  along the surface. The influence of the "distortion function"  $r_0(d\phi_{stat}/dn)$  is particularly remarkable in the case of voltage resonance as seen in Fig. 1 where

- (a) shows the field strength  $E_{stat} = -(d\phi_{stat}/dn)$ ,
- (b) the two voltage components  $V_1$  and  $V_2$  according to (1).
- (c) gives the two charges  $q_1$  and  $q_2$  corresponding to (3).

The charge  $q_1$  is strongly distorted near the feed point. The integration of the charge distribution curves  $q_1$  and  $q_2$  yields at once the currents  $i_1$  and  $i_2$ , as shown in (d) of Fig. 1. The main current  $i_1$  presents a maximum at the zero point of  $V_1$  and  $q_1$ . The length from the antenna end to this maximum is nearly  $\lambda/4$ . It is only now that antenna shortening begins. The current  $i_1$  becomes zero when the negative area of  $q_1$  equals the

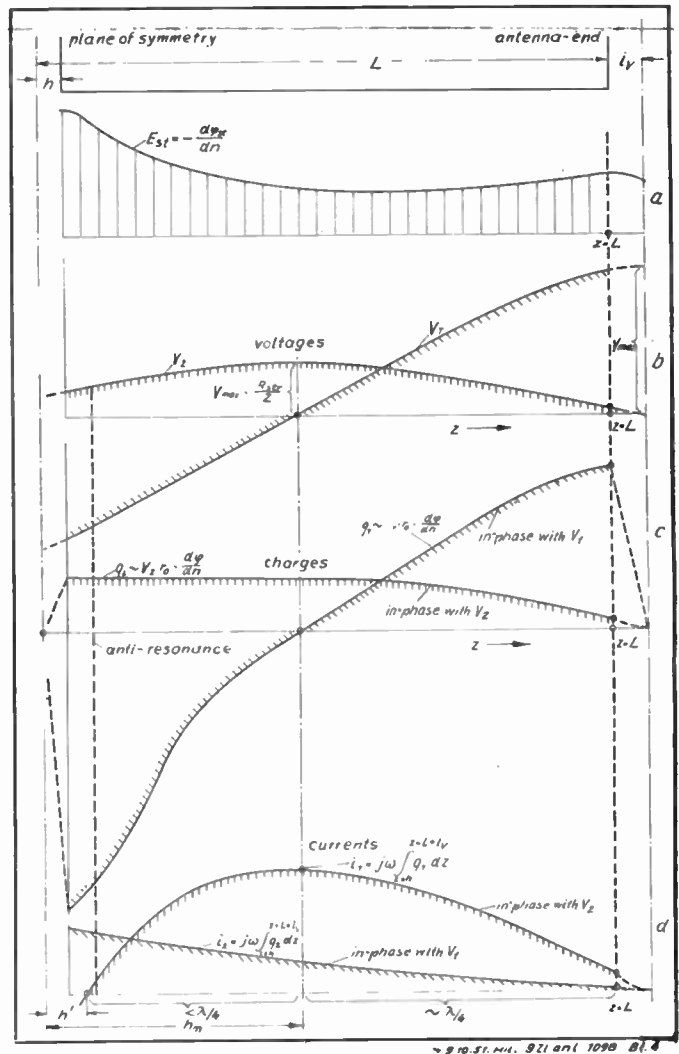


Fig. 1—Voltage charge and current dependent on  $z$  for an antenna at voltage resonance ( $L < \lambda/2$ ).

positive area. Such is the case at  $z=h'$ . Now  $h_m - h'$  is considerably smaller than  $\lambda/4$ .

The shortening of the cylindrical antenna at anti-resonance is thus determined by the strong-charge accumulation near the feeding gap. The reason of the non-sinusoidal current distribution is not radiation but lack of uniformity in the static surface charge. Radiation merely produces a second component in phase quadrature to the reactive component, according to (4).



# Wide-Band Phase-Delay Circuit\*

HARRY SOHON†, SENIOR MEMBER, IRE

**Summary**—A wide-band phase-delay circuit can be constructed provided phase delay is made to depend on both differences in length and differences in cutoff frequencies of the waveguides of the circuit.

## INTRODUCTION

IN UHF EQUIPMENT where signals of the same frequency are fed through two or more parallel channels it is sometimes desirable to cause a phase shift to be developed between signals in two of the channels. This might be to produce an arbitrary phase difference or to compensate for a phase shift introduced in some other part of the equipment.

Suppose that two lengths of waveguide are supplied with signals of the same frequency and phase at the input end. The relative phase at the output end will be determined by the lengths of the guides and by the respective guide wavelengths.

If the waveguides are identical except for length, a phase difference will be produced proportional to the difference in lengths. If the operating frequency is changed by accident, or by modulation, the phase shift will be changed. If, on the other hand, the waveguides are of the same length, the phase difference can be produced by making them have different guide wavelengths. In this case a change in operating frequency also will change the phase difference, but the change will now be in the opposite direction.

## WIDE-BAND PHASE-DELAY CIRCUIT

It was suggested that by combining these two methods of obtaining phase delay the variation of the phase difference with frequency might be reduced, thereby producing a wide-band phase-delay circuit.

Let  $\phi$  be the phase difference obtained in two guides of lengths  $L_1$  and  $L_2$ .

- Let
- $f$  = the operating frequency.
  - $f_1$  = the cutoff frequency for guide 1.
  - $f_2$  = the cutoff frequency for guide 2.
  - $\lambda, \lambda_1,$  and  $\lambda_2$  the wavelengths in free space corresponding to  $f, f_1$  and  $f_2$ .
  - $\lambda_{\theta 1}$  = the guide wavelength obtained in guide 1.
  - $f_0, \lambda_0$  = the design frequency and corresponding wavelength in free space.

\* Decimal classification: R310. Original manuscript received by the Institute, October 10, 1950; revised manuscript received February 26, 1953. The work described here was done by the Engineering Products Dept., RCA Victor Division, Radio Corporation of America, an associated contractor of the Applied Physics Laboratory, The Johns Hopkins University, operating under contract NOrd-9826. N. I. Korman was responsible for the development engineering.

† Associate Professor, Moore School of Electrical Engineering, University of Pennsylvania, Philadelphia, Pa.

Since the guide wavelength for guide 1 is

$$\lambda_{\theta 1} = \frac{\lambda}{\sqrt{1 - \frac{\lambda^2}{\lambda_1^2}}} = \frac{c}{\sqrt{f^2 - f_1^2}}, \quad (1)$$

the total phase delay produced in guide 1 is, in radians

$$\text{phase delay} = \frac{2\pi L_1}{\lambda_{\theta 1}} = \frac{2\pi L_1}{c} \sqrt{f^2 - f_1^2}. \quad (2)$$

A similar expression holds for guide 2; consequently the total phase difference obtained in the two guides is

$$\phi = \frac{2\pi L_2}{c} \sqrt{f^2 - f_2^2} - \frac{2\pi L_1}{c} \sqrt{f^2 - f_1^2}. \quad (3)$$

With four parameters,  $L_1, L_2, f_1, f_2$ , to be determined, one would expect to be able to impose four conditions on the design. The primary objective is to produce a requisite phase shift  $\phi_0$  and to maintain the phase shift as constant as possible in spite of frequency variations. The objective can be better understood by referring to Taylor's series for the phase shift

$$\phi = \phi_0 + (f - f_0) \left( \frac{d\phi}{df} \right)_0 + \frac{(f - f_0)^2}{2!} \left( \frac{d^2\phi}{df^2} \right)_0 + \dots \quad (4)$$

To produce a very wide-band device it would be well to have as many derivatives equal zero as possible. Therefore one might try to choose the four parameters such that  $\phi_0$  has the required value and the first three derivatives are equal to zero. However, it is pointed out below that only the first derivative can be made zero.

Since the second and third derivatives cannot be made zero, two other specifications are required to produce a unique design. A design procedure is given below which gives a coupler having a minimum length for a required range of operating frequencies. Hence the four specifications used are

1. Specific phase difference,  $\phi_0$
2. Wide-Band operation; first derivative equals zero.
3. Specified frequency range.
4. Minimum length of complete coupler.

Substituting  $f = f_0$  in (3) the expression for  $\phi_0$  is obtained

$$\phi_0 = \frac{2\pi}{c} [L_2 \sqrt{f_0^2 - f_2^2} - L_1 \sqrt{f_0^2 - f_1^2}]. \quad (5)$$

Introducing two new symbols

$$m_1 = \sqrt{1 - \frac{f_1^2}{f_0^2}}, \quad m_2 = \sqrt{1 - \frac{f_2^2}{f_0^2}}, \quad (6)$$

(5) becomes

$$\phi_0 = \frac{2\pi f_0}{c} [L_2 m_2 - L_1 m_1]. \quad (7)$$

The derivatives are obtained by repeated differentiation of (3) with respect of  $f$ . At  $f=f_0$  the first three derivatives are written in terms of  $m_1$  and  $m_2$ .

$$\left(\frac{d\phi}{df}\right)_0 = \frac{2\pi}{c} \left[ \frac{L_2}{m_2} - \frac{L_1}{m_1} \right] \quad (8)$$

$$\left(\frac{d^2\phi}{df^2}\right)_0 = \frac{2\pi}{cf_0} \left[ \frac{L_1}{m_1^3} - \frac{L_2}{m_2^3} \right] \quad (9)$$

$$\left(\frac{d^3\phi}{df^3}\right)_0 = \frac{6\pi}{cf_0^2} \left[ \frac{L_1}{m_1^3} - \frac{L_2}{m_2^3} + \frac{L_2}{m_2^5} - \frac{L_1}{m_1^5} \right]. \quad (10)$$

The first derivative can be made zero by making

$$\frac{L_2}{m_2} = \frac{L_1}{m_1}. \quad (11)$$

In this case

$$\left(\frac{d^2\phi}{df^2}\right)_0 = \frac{2\pi}{cf_0} \frac{L_2}{m_2} \left[ \frac{1}{m_1^2} - \frac{1}{m_2^2} \right] \quad (12)$$

$$\left(\frac{d^3\phi}{df^3}\right)_0 = \frac{6\pi L_2}{cf_0 m_2} \left[ \frac{1}{m_1^2} - \frac{1}{m_2^2} \right] \left[ 1 - \frac{1}{m_1^2} - \frac{1}{m_2^2} \right]. \quad (13)$$

Clearly these cannot be made zero unless  $m_1$  equals  $m_2$ . If use is made of (7) and (11) these derivatives can be written in terms of the phase difference desired

$$\left(\frac{d^2\phi}{df^2}\right)_0 = \frac{\phi_0}{m_1^2 m_2^2 f_0^2} \quad (14)$$

$$\left(\frac{d^3\phi}{df^3}\right)_0 = \frac{3\phi_0}{m_1^2 m_2^2 f_0^3} \left( 1 - \frac{1}{m_1^2} - \frac{1}{m_2^2} \right). \quad (15)$$

By substituting (14) and (15) into (4) and rearranging slightly, the result obtained is two terms in Taylor's series for the fractional variation of phase difference with frequency

$$\frac{\phi - \phi_0}{\phi_0} = \left( \frac{f - f_0}{f_0} \right)^2 \frac{1}{2m_1^2 m_2^2} + \left( \frac{f - f_0}{f_0} \right)^3 \frac{1 - \frac{1}{m_1^2} - \frac{1}{m_2^2}}{2m_1^2 m_2^2}. \quad (16)$$

It is convenient to rewrite (7)

$$\phi_0 = \frac{2\pi}{\lambda_0} \frac{L_2}{m_2} (m_2^2 - m_1^2). \quad (17)$$

Taking  $L_2/m_2 = L_1/m_1$  as constant, the maximum effect is obtained by making  $m_2$  as large and  $m_1$  as small as possible. Hence for a given  $\phi_0$  this same choice will make the length of the coupler a minimum.

Now if  $m_1$  is small and  $m_2$  is large, according to (6)  $f_1$  is large and  $f_2$  is small. In order to estimate the possible

range of values of  $f_1$  and  $f_2$  consider a standard waveguide 0.75×0.375 inches. This has a cutoff frequency 7.87 kmc and the recommended range of operation is 10 to 15 kmc. Since

$$10 \leq f \leq 15 \\ 1.27 = \frac{10}{7.87} \leq \frac{f}{f_1} \leq \frac{15}{7.87} = 1.91, \quad (18)$$

where  $f_1$  is the cutoff frequency of the guide. Similarly

$$1.27 \leq \frac{f}{f_2} \leq 1.91, \quad (19)$$

where  $f_2$  is the cutoff frequency of guide 2.

Assume for definiteness  $L_2 > L_1$  then  $m_2 > m_1$  and

$$\frac{f}{f_2} > \frac{f}{f_1};$$

therefore

$$1.27 \leq \frac{f}{f_1} < \frac{f}{f_2} \leq 1.91. \quad (20)$$

If the range of operation is given by  $f_0 \pm F$ , then

$$1.27 \leq \frac{f_0 - F}{f_1} < \frac{f_0 + F}{f_2} \leq 1.91, \quad (21)$$

and to obtain maximum separation between  $f_1$  and  $f_2$  and hence between  $m_1$  and  $m_2$  use the equalities in (21).

$$f_1 = \frac{f_0 - F}{1.27} \quad (22)$$

$$f_2 = \frac{f_0 + F}{1.91}. \quad (23)$$

Equations (22) and (23) along with (5) and (11) give four relations to determine uniquely the four parameters  $L_1$ ,  $L_2$ ,  $f_1$ , and  $f_2$ .

#### NUMERICAL EXAMPLE

Suppose that a coupler is desired that produces a 90° phase shift, to operate between 4 and 5 kmc. Then  $f_0 = 4.5$  kmc and  $F = 0.5$  kmc, and (22) and (23) give

$$f_1 = \frac{4}{1.27} = 3.15 \text{ kmc} \quad (24)$$

$$f_2 = \frac{5}{1.91} = 2.62 \text{ kmc}. \quad (25)$$

The values given in (24) and (25) are extreme values. For example  $f_1$  can be made less than 3.15 and/or  $f_2$  can be made greater than 2.62 if desired. If there is a standard waveguide available having a cutoff frequency between 2.62 and 3.15 it can be used in place of one of the waveguides called for. However, if these extreme values are used, the over-all length of the coupler will be a minimum. If it is decided to use these extreme values then waveguides having cutoff frequencies 2.62

and 3.15 kmc should be constructed. Their cross sections will be  $2.25 \times 1.125$  and  $1.875 \times 0.937$  inches inside.

To determine the deviation expected compute  $m_1$  and  $m_2$  and substitute into (16).

$$m_1^2 = 1 - \frac{f_1^2}{f_0^2} = 0.509, \quad (26)$$

$$m_2^2 = 1 - \frac{f_2^2}{f_0^2} = 0.660, \quad (27)$$

Use

$$\frac{f - f_0}{f_0} = \pm 0.111, \quad (28)$$

Hence

$$\begin{aligned} \frac{\phi - \phi_0}{\phi_0} &= \frac{0.111^2}{2(0.509)(0.660)} \\ &\pm \frac{0.111^3 \left( 1 - \frac{1}{0.509} - \frac{1}{0.660} \right)}{2(0.509)(0.660)} \\ &= 0.0184 \mp 0.00507. \end{aligned} \quad (29)$$

This variation is about 2 per cent compared to a variation of 20 per cent as would be experienced if the phase difference were obtained by difference in guide length alone. In the expression above one sign corresponds to one side of the frequency band, the other sign to the opposite side of the band. Hence the design can be improved by choosing the design frequency,  $f_0$ , to one side of the central frequency. In this way the variation in phase can be made the same at both sides of the operating range. This requirement will not be investigated here.

Solving (16) for  $L_2$ ,

$$L_2 = \frac{\phi_0 \lambda_0}{2\pi} \frac{m_2}{m_2^2 - m_1^2} = 20.1 \frac{\phi_0}{2\pi}. \quad (30)$$

For a phase difference of one-quarter cycle

$$L_2 = \frac{20.1}{4} = 5.02 \text{ in.} \quad (31)$$

and

$$L_1 = L_2 \frac{m_1}{m_2} = 4.39 \text{ in.}$$

If it would be more convenient to have greater lengths the design can be changed to bring  $f_1$  and  $f_2$  nearer equality. In this illustration where the working range is 4 to 5 kmc the guides adopted have normal working ranges of 3.33 to 5 and 4 to 6 kmc. One of these could be replaced by a guide having a normal working range of, say, 3.67 to 5.5 kmc. Not only will this change increase the over-all length but it will also reduce the deviation computed in (29).

### CONCLUSION

If the required range of operation is less than two-to-three this type coupler can be used. Determine the cutoff frequencies of the guides to satisfy (22) and (23). If a standard waveguide has a cutoff frequency between the cutoff frequencies computed, then the standard guide can be used and its cutoff frequency should replace one of those determined in (22) and (23) in the computations that follow. If no standard waveguide can be used, it will be necessary to have two custom-made guides instead of one. After it has been determined whether a standard guide can be used the length of the coupler is computed as in (17) or (30). If the computed length is unsatisfactory it can be increased by choosing the cutoff frequencies closer together. Generally the length computed, as in the example above, is a minimum. However, if the arbitrary selection of a standard waveguide has brought the two cutoff frequencies closer together than the values obtained by (22) and (23), the length will be greater than the minimum. In such a case it will be possible to reduce the length by discarding the standard waveguide and using two custom-made guides with a greater difference between their cutoff frequencies.

In constructing these couplers, the difference in length has been obtained by bending the guides to arcs of circles. The same theory and method of construction has also been used to obtain a "zero phase shift" angle by designing for  $\phi_0$  equal to  $2\pi$  radians.



# Coding by Feedback Methods\*

B. D. SMITH†, ASSOCIATE, IRE

**Summary**—This paper describes the basic feedback coder; that is, a device which converts an analog quantity such as a voltage into a digital quantity such as a binary number by the feedback method. The basic feedback coder consists of a decoding device or network together with an error amplifier and control circuits. The decoding network and its operation as a feedback element to produce a coding system are described in terms of a number system having any base,  $b$ . The particular case of a binary coder (base 2) is considered in detail. In addition, feedback coding systems employing a binary coded decimal number system are discussed. The advantages and disadvantages of the feedback method as compared to other coding methods are discussed. A method of nonlinear coding (or signal compression) directly in the coding process is presented.

## INTRODUCTION

THERE are many fields in which the transmission and processing of information can best be done by digital methods rather than analog methods. Pulse code modulation systems, digital computers, and digital data transmitters are examples of systems which process information in numerical form. There are many applications in which analog-to-digital conversion devices or coders are required so that the digital equipment can accept input information in analog form, such as a voltage or current. The purpose of this paper is to describe the basic feedback method of converting an electrical signal, in the form of a voltage or current, into digital form, such as a binary number.

A number of coding methods have been described in the literature. The counting method<sup>1,2</sup> and the coding tube method<sup>3</sup> have been employed in the past. The feedback method<sup>4,5</sup> has not received as much attention, although it offers some advantages over the counting and coding tube methods.

## DECODING NETWORKS

The term "feedback" as applied to coding methods means that some form of a decoder (a device to convert from digital to analog form) is used as an integral part of the coder together with an error amplifier and control circuits. An accurate coder can be made by employing an accurate decoder as a feedback element.

The principle of operation of a decoder is based directly upon the definition of a number. Any number is represented by a series of digits,  $a_1, a_2, a_3$ , and so on, each of which can have one of a number of integral values beginning with zero. The number of digit values is the base,  $b$ , of the number system; for example, in the binary system (base 2) the digits can be either 0 or 1, and in the decimal system (base 10) they can be any integer from 0 to 9. A number is usually written with the least significant digit,  $a_1$ , last, and has a numerical value,  $n$ , defined by (1).

$$n = \sum_{k=1}^K a_k b^{k-1}. \tag{1}$$

For example,

$$10101 \text{ (base 2)} = 1 \times 2^4 + 0 \times 2^3 + 1 \times 2^2 + 0 \times 2^1 + 1 \times 2^0 = 21 \text{ (base 10)}.$$

If the digits of a number are represented by voltage or current sources, then it is possible to construct networks such as are shown in Figs. 1 and 2 in which the output voltage or current is related to the voltage sources in the same manner as (1). These networks act as decoders since they convert the digital information determined by the states of the sources,  $e_1$  to  $e_K$ , into an analog quantity which is the output voltage or current. Fig. 1 shows

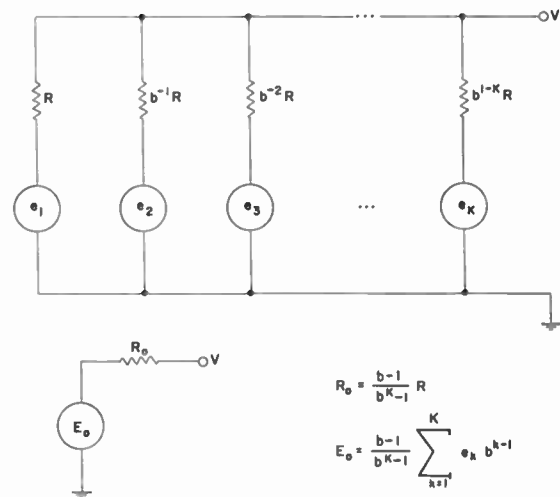


Fig. 1—Shunt resistor decoding network and equivalent circuit.

a shunt resistor network and its equivalent circuit. The equivalent circuit is obtained by applying the superposition theorem. The open-circuit voltage, the short-circuit current, and the voltage or current into any constant load resistance are all proportional to the number

\* Decimal classification: 621.375.2. Original manuscript received by the Institute, August 29, 1952; revised manuscript received February 3, 1953.

† Melpar, Inc., 452 Swann Ave., Alexandria, Va.

<sup>1</sup> A. H. Reeves, United States Patent Number 2,272,070 (International Standard Electric Corp.); February 3, 1942.

<sup>2</sup> H. S. Black, and J. O. Edson, "PCM equipment," *Elec. Eng.*, vol. 66, p. 1122; November, 1947.

<sup>3</sup> L. A. Meacham, and E. Peterson, "An experimental multichannel pulse code modulation system of toll quality," *Bell Sys. Tech. Jour.*, vol. 27, p. 1; January, 1948.

<sup>4</sup> W. M. Goodall, "Telephony by pulse code modulation," *Bell Sys. Tech. Jour.*, vol. 26, p. 395; July, 1947.

<sup>5</sup> B. D. Smith, "Pulse-Code Modulation Method," M.S. Thesis, M.I.T., Cambridge, Mass.; June, 1948.



represented by the voltage sources. Fig. 2 shows a ladder network having the same properties. The advantage of this network is that the impedances seen by the sources are more equal. The sources, if they are to represent the digits of a number, will have a finite number of stable states corresponding to the number base. The

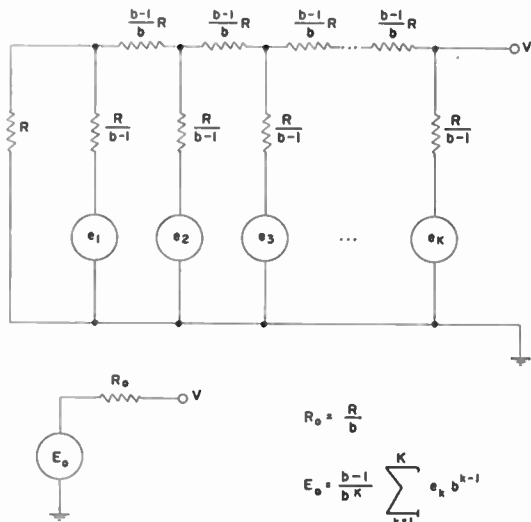


Fig. 2—Ladder resistor decoding network and equivalent circuit.

base 2 requires the simplest type of source since only two stable states are required. The sources in this case may be replaced by bistable devices such as flip-flops, switches, relays, and so forth. The use of a higher number base requires multistable devices such as stepping relays or combinations of bistable devices. Fig. 3 shows a binary decoding network in which the sources are re-

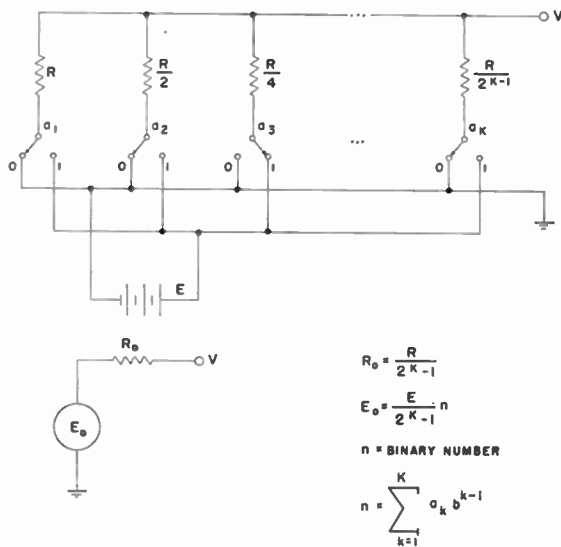


Fig. 3—Binary decoding network and equivalent circuit.

placed by relay or switch contacts and a single common "battery"  $E$ . The equivalent circuit is also shown in Fig. 3. The output voltage is proportional to the binary number represented by the contacts  $a_1$  to  $a_K$ . If the bistable devices have internal impedance, it should be taken into account by reducing network resistors appropriately.

FEEDBACK CODER OPERATION

The basic feedback coder is shown in Fig. 4. The equivalent circuit of the decoding network, consisting of a voltage source proportional to the number,  $n$ , and an equivalent series resistance, is shown instead of the complete decoding network. The digits of the decoding network are controlled by the control circuits in response to the output of an error amplifier. The voltage to be coded,  $V_i$ , is connected through an input resistor,  $R_i$ , to the input of the error amplifier. The output of the decoding network is also fed to the input of the error amplifier as in a conventional feedback system. The basic coding process is to change the digits of the decoding network so as to minimize the error signal at the input to the error amplifier. The purpose of the amplifier is to indicate whether the error signal is above or below a certain potential, which for convenience will be considered zero or ground potential so that the output of the amplifier indicates the polarity of the error signal. If the error signal is above ground by any amount, the output

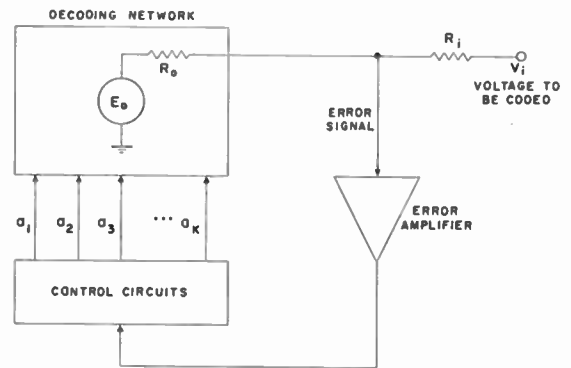


Fig. 4—Basic feedback coder.

of the amplifier will be a positive voltage; if the error signal is below ground by any amount, the output of the amplifier will be a negative voltage. When the error signal is minimized, the number represented by the digits  $a_1$  to  $a_K$  will be the correct representation of  $V_i$  with the appropriate sign, scale factor, and zero intercept determined by the polarity, resistor values, and dc level of the decoding network.

There are two basic methods of controlling the digits in response to the error signal. One method consists of counting in unit steps only. For example, the number,  $n$ , represented by the digits can be made, 0, 1, 2, 3, and so on, until the error signal changes sign, at which time counting is stopped and the value of each digit read out.

The other method, which requires fewer operations, is to determine each digit in sequence, beginning with the most significant digit. For example, all digits may be initially reset to zero except the first (most significant) digit which is set to  $b-1$ , where  $b$  is the number base. If the error signal is negative, the first digit is not changed. If the error signal is positive, the first digit is changed to  $b-2$ ,  $b-3$ , and so forth, until the error signal goes negative, at which point the first digit is not

changed further. The second digit is then changed to  $b-1$ . If the error signal stays negative, the second digit is not changed. If the error signal goes positive, the second digit is changed to  $b-2$ ,  $b-3$ , and so on, until the error signal goes negative, at which point the second digit is not changed further. This same process is continued until the least significant digit is measured. Another variation of this method is its complement, that is, the digits are initially reset to  $b-1$  except the first which is set to 0. The first digit is changed to 1, 2, 3, and so on, until the error signal goes positive. This process is continued in the same manner to measure all of the digits. A third variation is to initially reset all digits to zero (including the first), and change the first digit to 1, 2, 3, and so forth, until the error signal goes positive. The first digit is then set back one unit, and the second digit is measured in the same manner. In any case a maximum of  $K(b-1)$  operations are required as compared to  $b^K$  operations with the "counting" method.

As mentioned previously, the digits of a number having a base greater than 2 can be represented by combinations of bistable devices. An example is the binary-coded decimal system in which a decimal digit is represented by four binary digits. In this case a single decimal digit in the decoding network would be replaced by four bistable sources and four weighting resistors. The coding process may be conducted as given above, or it may be conducted as if the coder were actually a binary coder, that is, the value of each binary digit representing a decimal digit may be determined in sequence. Any general coded  $b$ -base system may be employed in this manner provided each element of the particular code has a fixed weighting factor. For example, a coded decimal system employing a four-element code to represent a decimal number in which the weights of the elements are 5, 4, 2, 1, respectively, can be used. In this case the coding process would begin with all digits reset to 0 except the first which is set to 5. If the error signal is negative, the 5 is retained. If the error signal is positive, the element representing 5 is reset to zero. In the next step a 4 is added, and the error signal indicates whether or not the element representing 4 should be retained or reset to zero. This process is continued for the remaining elements of the first decimal digit so that one decimal digit is measured in four steps. The same process is continued for the remaining decimal digits. It should be noted that a four-element code for a decimal digit results in six unused combinations since 16 combinations of four elements are possible. The coder will not generate any of these unused combinations provided the input voltage is within the range for which the coder was designed.

BINARY FEEDBACK CODER

The description of the coding process above is for the general case of any number base,  $b$ . For a binary coder the coding system is the simplest. Fig. 5 shows one type of binary feedback coder in block diagram form. In this figure the digits are represented by flip-flops, and the

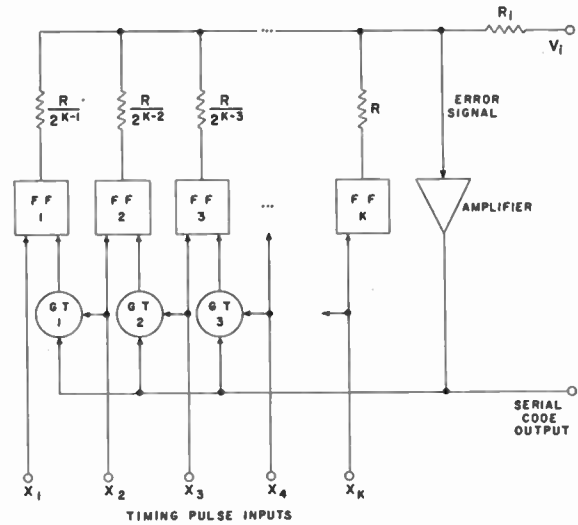


Fig. 5—Binary feedback coder.

control circuits consist of one gate circuit for each digit except the last. For convenience, the order of numbering the flip-flops and the like is reversed, so that subscript 1 corresponds to the *most* significant digit since this digit is determined first. A source of timing pulses,  $X_1$  through  $X_K$ , is required. These pulses are phased in time

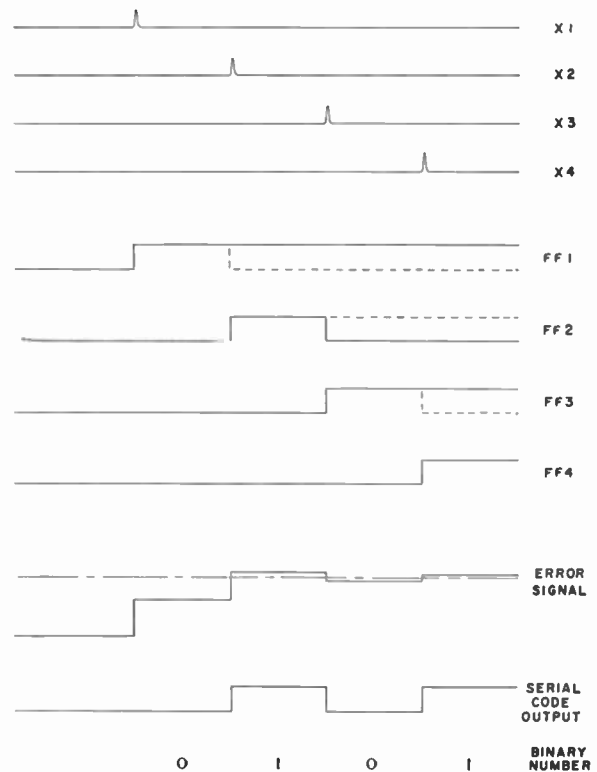


Fig. 6—Waveforms of binary coder shown in Fig. 5.

so that  $X_1$  occurs first,  $X_2$  second,  $X_3$  third, and so on, as shown in Fig. 6. Initially, all flip-flops are set to zero by pulse  $X_1$  except  $FF1$  which is set to 1. If the error signal is negative, then  $FF1$  is not changed further. If the error signal is positive, then  $FF1$  is reset to 0 by means of  $GT1$  when pulse  $X_2$  occurs.  $FF2$  is set to 1 by the same pulse  $X_2$ , and if the error signal is then nega-

tive,  $FF2$  is not changed further. If the error signal is positive, then  $FF2$  is reset to 0 by means of  $GT2$  when pulse  $X_3$  occurs.  $FF3$  is set to 1 by pulse  $X_3$ , and so on. The same process is repeated through all of the digits. Fig. 6 shows typical waveforms of the timing pulses, the flip-flop outputs, the error signal, and the serial code output (error amplifier output) for a particular value of the input voltage,  $V_i$ . The dotted lines show other possible waveforms produced by the flip-flops for other values of  $V_i$ . The error signal waveform shows that the error signal changes at each step in the coding process so as to approach zero. There need be no lost time between individual coding processes, that is, the first digit of one code can follow immediately after the last digit of the preceding code.

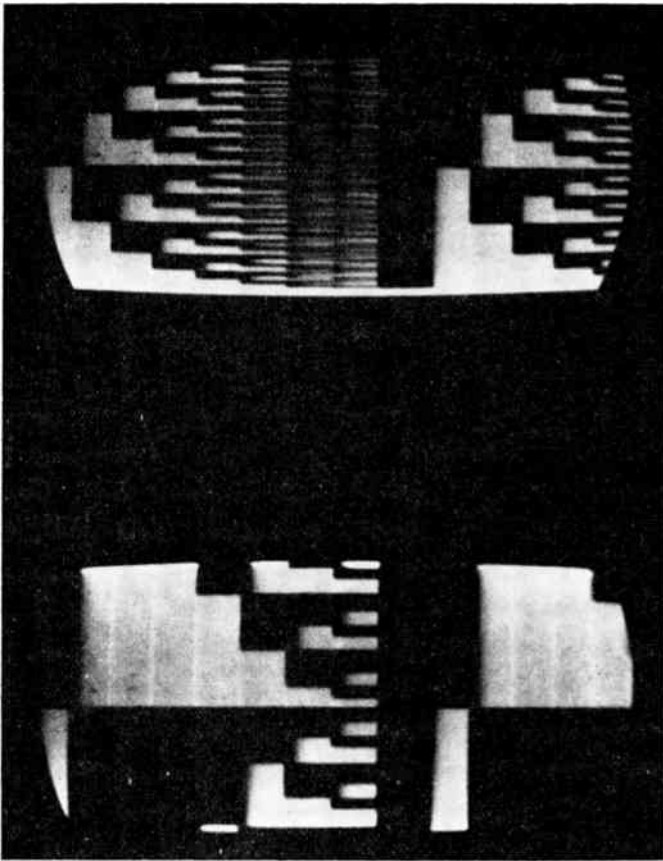


Fig. 7—Modulation pattern of an eight-digit coder.

Fig. 7 shows two views of the modulation pattern of an 8-digit binary feedback coder. This pattern is obtained by applying a slowly varying voltage simultaneously to the coder and to the  $Y$ -axis of an oscilloscope. The oscilloscope beam is swept horizontally in synchronization with the coder repetition rate so that a raster similar to a television raster is produced. When the  $Z$ -axis (intensity) is modulated by the output pulse code, the characteristic patterns shown in Fig. 7 are obtained. The upper view shows the complete pattern obtained with the slowly varying signal covering the full range of the coder (256 levels). The lower view shows the

same pattern with the signal fed to the coder attenuated so as to cover only 20 levels. This results in an "expanded" view showing the details of the last digit which are unresolved in the upper view. Both patterns cover (horizontally) one complete code group and five digits of the following code group. The time scale is  $4.1 \mu\text{sec}$  per digit. There is an unused time interval following each code to provide sufficient sampling time since this particular coder is used in a multiplex system. The "expanded" view of the modulation pattern shows that the eighth digit is reasonably uniform and free of noise. This type of modulation pattern is useful in aligning the coder and detecting errors in the operation of the coder.

#### SERIAL CODE OUTPUT

It should be noted that the digital information obtained from the coding process is obtained from the output of the error amplifier. In a binary coder, for example, the error amplifier output is a serial binary pulse code, as shown in Fig. 6, which is suitable for transmission to a remote point or for use in a digital computer. The serial code output is a binary number proportional to the input voltage,  $V_i$ . The state of the flip-flops at the end of the coding period is actually the complement of this number for the particular circuit and polarities assumed in Figs. 5 and 6. There is no need to read out or otherwise sense the condition of the flip-flops unless all digits must be transmitted in parallel or in some unusual manner. The most significant digit always occurs first in time in the serial output of a feedback coder.

In the general  $b$ -base coder the error amplifier output is also a serial pulse code of a particular type depending upon how the coding is conducted. If the coding process is conducted by counting in unit steps, then the serial output is a pulse whose duration is variable in unit steps; that is, a 0 is represented by a pulse of zero duration; a 1 by a pulse of 1 unit duration, a 2 by a pulse of 2 units duration, and so on. It is of passing interest to note that if a binary coder is considered a special case ( $b=2$ ) of the general  $b$ -base coder, then the binary code output might be considered as a series of pulses of 0 or 1 unit *duration* and not a series of pulses of 0 or 1 unit *amplitude*. If a coded  $b$ -base number system is employed and the coding process is conducted as if the coder were straight binary, then the error amplifier output is a serial code in which each  $b$ -base digit is represented by a serial pulse code. For example, in a two-digit decimal coder using a code in which each decimal digit is composed of four elements, the serial output would be an eight pulse code. The first four pulses would be the coded decimal representation of the first decimal digit, and the last four elements the representation of the last or least significant decimal digit. A feedback coder operates so that the digits and also the elements of each digit are produced in the order of their significance, that is, the most significant element of the most significant digit first, and so forth. The so-called "excess-3" decimal code (that is,  $0=0011$ ,  $1=0100$ ,

2 = 0101, and so on) can be generated directly provided each decimal register in the coder is reset to 0011 instead of 0000 and set to 1000 when the first element of that particular decimal digit is to be found. Otherwise the control circuits are the same as a binary coder.

COMPARISON WITH OTHER CODING METHODS

The relative merits of the feedback coding method in comparison with the counting and coding tube methods depend, of course, upon the particular application; but certain general advantages and disadvantages can be given. With respect to the counting method of binary coding, these points of comparison are important:

1. With the counting method it is necessary to operate two coders alternately or provide a temporary storage register if no lost time can be tolerated in a serial output coder. This is due to the fact that a single counter cannot be read out at the same time it is counting. With a feedback coder the first digit of one code group can follow immediately after the last digit of the preceding code group with no lost time.

2. Serial output is obtained very simply in a feedback coder. With respect to parallel output, the two methods are approximately equal in complexity.

3. With respect to speed, the feedback coder can be made considerably faster because of the fewer operations required.

4. With respect to accuracy and reliability, the two methods are approximately equal. Since the bistable elements in a feedback coder are either set or reset instead of being triggered as in a flip-flop counter chain, better reliability can be attained. However, there are sources of errors in a feedback coder (such as inaccuracies in the decoding network resistors) which do not occur with the counting method.

In a comparison of the feedback method with the coding tube method, the following points are important:

1. The coding tube method requires separate circuits for quantization since large coding errors can occur if the coding tube input changes even a small amount during the coding process. With the feedback coder no such circuits are required; if the signal changes during the coding process, the generated code always corresponds to some value of the input signal in between the values at the beginning and end of the coding period.

2. With the feedback method it is not necessary to use special nonbinary codes, such as the Grey or reflected binary code, to eliminate errors such as are produced when the input signal is on the dividing lines between levels in a coding tube. This source of error is eliminated by the internal positive feedback or "flip-flop" action designed into the error amplifier of a feedback coder.

3. With respect to speed, the coding tube method is definitely superior. A coding tube system has been developed which is suitable for coding wide-band signals such as television, indicating a coding speed which is approximately 50 times that of the feedback coder whose modulation pattern is shown in Fig. 7.

4. In accuracy, the two methods are comparable.

5. The coding tube method makes it possible to transmit a binary code with the least significant digit first, which permits the use of simpler decoding devices, such as the Shannon-Rack decoder.

The choice of one or the other of these coding methods depends upon all of the factors involved, such as speed, accuracy, size, weight, ruggedness, and the requirements of the over-all system in which it is to be employed.

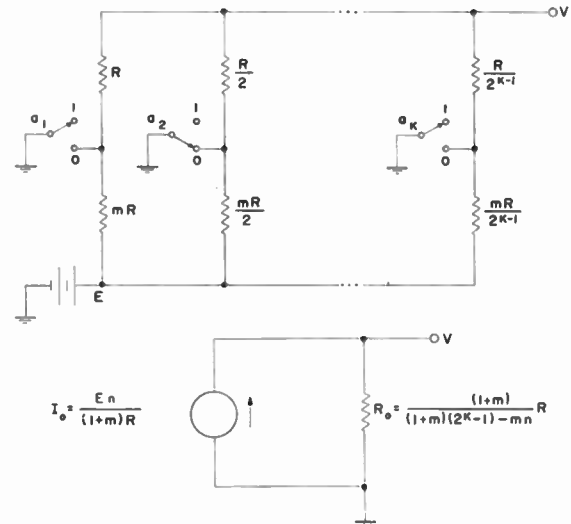


Fig. 8—Nonlinear decoding network and equivalent circuit.

NONLINEAR CODING METHODS

The feedback coding method offers the possibility of nonlinear coding or signal compression in the coding process. Fig. 8 shows a binary decoding network which is nonlinear in that the impedance seen at point *V* is a function of the settings of the switches. The equivalent

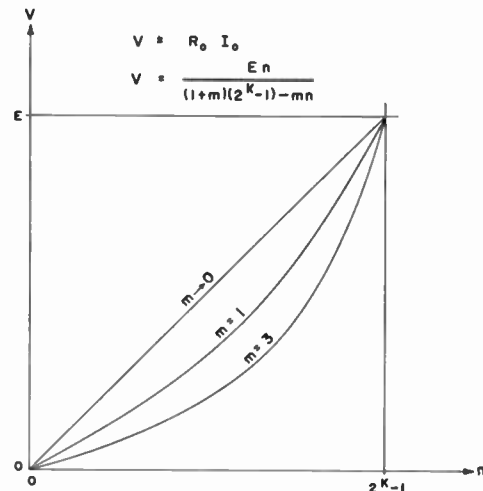


Fig. 9—Characteristic curves of the decoding network shown in Fig. 8.

circuit in terms of a current source and equivalent resistance is also shown in Fig. 8. The short-circuit current is linear with *n*, but the open-circuit voltage is proportional to *n* divided by a constant minus *n*. That is, as the switches are changed from one number to the next, the open-circuit voltage will lie on one of the curves

(section of hyperbolas) shown in Fig. 9, depending upon the value of the constant  $m$ . A decoder of this type produces a voltage which is an expanded (positive curvature) function of the binary number,  $n$ . By using this type decoder in the feedback loop of a feedback coder,  $n$  will be a compressed (negative curvature) function of the input voltage to the coder. A cathode follower can be used to preserve the open-circuit condition for the network. The over-all transfer function from the voltage input to a coder, to the output voltage of a decoder in a complete system will be linear. The effect of the compression-expansion process is that signals, such as speech, which require a wide dynamic range can be transmitted with less average quantization distortion. Symmetrical compression and expansion curves can be obtained by modifying the coding and decoding processes for plus-minus operation.

In comparison with other compression systems, such as are obtained by the use of varistors or other nonlinear impedances, this method has the advantage of possibly better over-all system linearity without the need for closely matching pairs of varistors. The compression curves are mathematically defined and can be changed readily if desired. Simple networks producing smooth nonlinear curves other than sections of hyperbolas

should be possible but have not been found. The nonlinear codes represent an additional step toward the ideal coding system prescribed by information theory which takes into account all *a priori* information on the inputs, outputs, and noise in a communication system.

#### CONCLUSIONS

The problem of analog-to-digital conversion can be solved by a number of coding systems, one of which is the feedback system described in this paper. A feedback coder can be made as accurate as coders using other methods, and in many applications offers some advantages. The feedback coder can be designed to operate with any number base and with the coded-decimal systems used in computers, but is simplest when employed as a binary coder to generate a serial pulse code. The feedback coder can be employed to generate a number which is a nonlinear function of the input signal, suitable for use where signal compression is desired.

#### ACKNOWLEDGMENT

The author wishes to express his appreciation for the advice and encouragement of Dr. W. G. Tuller, and for the help of B. H. Dennison and A. H. Ballard, all of the Melpar engineering staff.

#### Discussion on

## “Synthesis of Narrow-Band Direct-Coupled Filters”\*

H. J. RIBLET

J. Reed:<sup>1</sup> Dr. Riblet's recent paper is based on the simple but erroneous theory that one is dealing with constant shunt susceptances. His formula (7) can readily be shown to be identical with that of Mumford's.<sup>2</sup> Since the contribution<sup>3</sup> of the frequency consciousness of inductive irises to the  $Q$  of filter stages like those Dr. Riblet considers is of the order of 10 per cent, it would seem that this contribution is definitely not a second-order effect.

H. J. Riblet: I am indebted to John Reed for drawing my attention to the applicability of the results of his paper entitled, “Low  $Q$  Microwave Filters” to the design of narrow-band filters. In my examination of the literature, I was misled by the title of his paper. The numerical equivalence between my expression for the  $Q$  of a cavity, equation (7), and the formulas used by

Mumford was shown in graphs submitted with the first version of the paper and then omitted finally in the interest of brevity. Mr. Reed is correct in his observation that equation (7) and Mumford's  $Q \doteq \sqrt{B^4 + 4B^2} \tan^{-1}(2/B)/4$  are identical. Those who wonder why my exact expression (7) and the approximate expression used by Mumford are identical will find the answer in a slight difference in the definition of  $Q$ .

Whether or not the 10-per cent error, referred to by Reed, in the  $Q$ 's of the end cavities of “maximally flat” filters is significant in the design of narrow-band filters is open to question in view of the approximate nature of the entire procedure and the considerable experimental success which previous workers have had using the assumption of constant susceptance. Nevertheless, the inclusion of this frequency dependence does appear to be sound; and since it involves no additional design effort, it certainly merits serious consideration.

For this purpose, the method of my paper is immediately applicable. In proceeding from equation (2) to the first-order admittance transformation of the anti-resonant element analogous to equation (4), one only

\* H. J. Riblet, “Synthesis of narrow-band direct-coupled filters,” *Proc. I.R.E.*, vol. 40, pp. 1219-1223; October, 1952.

<sup>1</sup> Raytheon Manufacturing Co., Newton, Mass.

<sup>2</sup> W. W. Mumford, “Maximally flat filters in waveguide,” *Bell Sys. Tech. Jour.*, vol. XXVII, p. 699, Fig. 11; October, 1948.

<sup>3</sup> J. Reed, “Low  $Q$  microwave filters,” *Proc. I.R.E.*, vol. 38, p. 794, Formula 8 and Table I; July, 1950.

has to include the variation of  $\phi$  with respect to  $\Omega$ . For inductances,  $B = -A\lambda g$ , and it is readily found that  $d\phi/d\Omega = \sin \phi_0 \cos \phi_0$ , where  $\phi_0 + (2\pi l/\lambda g_0) = \psi_0 = 0$  at antiresonance. For capacitances,  $B = A/\lambda g$  and  $(d\phi/d\Omega) = -\sin \phi_0 \cos \phi_0$  at antiresonance. Then we find that

$$Y_i = \frac{j(1 + \cos \phi_0 - k_1\Omega) + k_2\Omega Y_0}{k_2\Omega + j(1 - \cos \phi_0 + k_1\Omega)} \quad (4')$$

where

$$k_1 = \pm \sin^2 \phi_0 \cdot \cos \phi_0$$

$$k_2 = \phi_0 \mp \sin \phi_0 \cdot \cos \phi_0,$$

and the upper signs are used with inductances and the lower signs with capacitances. A pair of such antiresonant elements separated by a half-guide wavelength has the first-order admittance transformation,

$$Y_i = \frac{j \frac{(1 + \cos \phi_0)(\pi(1 + \cos \phi_0) - 2k_2)\Omega}{(1 + \cos \phi_0)(1 - \cos \phi_0) + 2k_1 \cos \phi_0 \Omega} + Y_0}{1 + j \frac{(1 - \cos \phi_0)(\pi(1 - \cos \phi_0) - 2k_2)\Omega}{(1 + \cos \phi_0)(1 - \cos \phi_0) + 2k_1 \cos \phi_0 \Omega} Y_0} \quad (5')$$

For frequencies in the pass band of the filter  $Y_0 \approx 1$ , and we may expand by the binomial theorem and obtain

$$Q = \frac{\cos \phi_0(\pi - k_2)}{\sin^2 \phi_0} \quad (7')$$

For the inductive case this is identically equivalent to Mr. Reed's equation (8).

The extension to the design of direct-coupled filters proceeds as in my paper. Analogous to (9) we find

$$Y_i = j \frac{(1 - \cos \phi_0 + k_1\Omega) + (k_2 - \pi)\Omega Y_0}{(k_2 - \pi)\Omega + j(1 + \cos \phi_0 - k_1\Omega)Y_0} \quad (9')$$

and for (10)

$$Y_i = j \frac{[(1 - \cos \phi_0')(1 - \cos \phi_0'') + A\Omega] + B\Omega Y_0}{C\Omega + j[(1 + \cos \phi_0')(1 + \cos \phi_0'') - D\Omega]Y_0} \quad (10')$$

where

$$A = k_1''(1 - \cos \phi_0') + k_1'(1 - \cos \phi_0'')$$

$$B = k_2' + k_2'' + (\pi/2 - k_2'') \cos \phi_0' - (\pi/2 - k_2') \cos \phi_0''$$

$$- \frac{3\pi}{2} - \pi/2 \cos \phi_0' \cos \phi_0''$$

$$C = k_2' + k_2'' - (\pi/2 - k_2'') \cos \phi_0' + (\pi/2 - k_2') \cos \phi_0''$$

$$- \frac{3\pi}{2} - \frac{\pi}{2} \cos \phi_0' \cos \phi_0''$$

$$D = k_1'(1 + \cos \phi_0'') + k_1''(1 + \cos \phi_0')$$

As before, equivalence at resonance is established by equation (11). Moreover, an approximate first-order equivalence can be obtained by a suitable transformation of the  $\Omega$  scale, for any given numerical case.

# Correspondence

## A Note on Sommerfeld's 1909 Paper\*

Sommerfeld presented, in his 1909 paper,<sup>1</sup> the development of approximate expressions for the field strength due to a vertical oscillating doublet located at the surface of a plane earth with arbitrary electrical properties. Sommerfeld's formulas, however, have been found to be in error. Though Niessen discussed the mathematical error appearing in Sommerfeld's derivation in a 1937 article<sup>2</sup> (in German), the contents of this paper are not very widely known. Thus, articles still appear rather frequently in the literature giving erroneous explanations as to why Sommerfeld's results are in error, two of the more notable of these being the papers by Kahan and Eckart<sup>3</sup> and Epstein.<sup>4</sup>

The purpose of this note is to point out that, as explained by Niessen, the error is due to an incorrect choice of a square root that appears in Sommerfeld's variable,  $\alpha$ . The angle of  $\alpha^2$  falls in the first quadrant, and Sommerfeld made the natural but er-

roneous choice of placing  $\alpha$  in the first quadrant. A closer analysis reveals that the proper angle to be associated with  $\alpha$  is in the third quadrant.

The critical portion of Sommerfeld's derivation involves the approximating of an integral where the path of integration is along the positive real axis. This integral is converted into one whose path is around a branch cut and a pole. The contributions to the integral associated with the portion of the path around the branch cut and around the pole will be denoted by  $Q$  and  $P$ , respectively. Sommerfeld arrived at the same results by two methods, the first involving evaluating  $Q$  and  $P$  independently by integrating around the branch cut and pole separately, and the second involving determination of the value of  $(Q+P)$  by employing a single path inclosing both the branch cut and the pole. Sommerfeld's formulas have been found to be in error by an amount equal to  $P$ .

Some of the shortcomings of the explanations given in references 3 and 4 as to why Sommerfeld's results are incorrect are given briefly below. Epstein notes that  $P$  satisfies the wave equation and, indeed, all the conditions of a solution, except that it is singular at  $r=0$  for all  $z$  and not just at  $z=0$ , as required by the problem. Thus Sommerfeld's initial integral satisfies the same conditions when the path of integration is along the

positive real axis and when the path is transformed to pass around the other side of the pole, except for the type of singularity at  $r=0$ . Epstein interprets this as showing that Sommerfeld's uniqueness proof is not valid and that the transformed path must indeed be the correct one, since this changes Sommerfeld's results by  $P$ , the amount they are in error. Actually Sommerfeld embodies the type of singularity at  $r=0$  into his uniqueness proof which is perfectly valid. A quick and easy check of Sommerfeld's integral with the path along the positive real axis reveals that it is singular at  $r=0$  for  $z=0$  only and thus is the correct path to be taken in this problem rather than the path suggested by Epstein.

Kahan and Eckart point out that a saddle point is located between the pole and the branch cut. If the value of the residue of the pole is thought of as being calculated by the saddle point method, the major contribution comes from that portion of the path in the neighborhood of the saddle point. They reason, on the basis of the path of integration encircling the branch cut and pole separately, that there will be a contribution to  $Q$  when the integration path passes the saddle point (but in the opposite direction) that will just cancel  $P$  and that Sommerfeld must have overlooked the existence of the saddle point and so does not properly take it into account. However, when considering

\* Received by the Institute, March 30, 1953. Prepared at Cornell University under U. S. Air Force Contract AF 33(038)-1091. Now with Electrical Engineering Research Laboratory, The University of Texas, Austin, Texas.

<sup>1</sup> Sommerfeld, *Ann. Physik*, 28, p. 665; 1909.  
<sup>2</sup> Niessen, *Ann. Physik*, 29, p. 585; 1937.  
<sup>3</sup> Kahan and Eckart, *Proc. I.R.E.*, 38, p. 807; 1950.  
<sup>4</sup> Epstein, *Proc. Nat. Acad. Sci.*, 33, p. 195; 1947.

this path of integration Sommerfeld obtained an asymptotic series and replaced it by a function having the same asymptotic expansion. He carefully pointed out that, simply due to the character of asymptotic expansions, his results could be in error by an amount of the order of magnitude of  $P$ , the consideration of the saddle point thus being of no importance. Sommerfeld actually considers the single path inclosing both the branch cut and pole when developing the convergent series expansion, which rigorously verifies his final results. Thus Kahan and Eckart's comments are not relevant.

BOB M. FANNIN

Electrical Engineering Research Laboratory  
The University of Texas  
Austin, Texas

### Collector-Base Impedance of a Junction Transistor\*

Recently, J. M. Early<sup>1</sup> described an extension of Shockley's theory for the current voltage relationships of a junction transistor which explained certain experimental results. For example, Early's analysis included an explanation for observed values of collector resistance.

It is possible to extend Early's analysis to include the effect of the frequency of the ac variations. As a result of this further extension, an experimentally observed frequency variation of the open-circuit collector-base admittance of fused-impurity  $p-n-p$  junction transistors has been explained.<sup>2</sup> The nature of this frequency variation may be described moderately well by an (approximate) expression of the form<sup>3</sup>

$$1/z_{22}^{(b)} = j\omega C_c + g_c + j\omega C_d [\tanh(j\omega\tau_D)]^{1/2} / (j\omega\tau_D)^{1/2}, \quad (1)$$

where it is assumed that the internal base impedance is small in comparison with the

right-hand member of (1). In this equation,  $z_{22}^{(b)}$  is the open-circuit collector-base impedance;  $C_c$  is the barrier capacitance of the collector-base diode;  $g_c$  is the low-frequency collector conductance, a theoretical value for which was calculated by Early;  $C_d$  is a diffusion capacitance due to charge stored in the base-layer of the transistor by the dc emitter current; and  $\tau_D$  is a constant that may be determined from the alpha-cutoff frequency<sup>4</sup>  $\omega_c/2\pi$  of the transistor from the relation  $\tau_D = 2.43/\omega_c$ . The diffusion capacitance  $C_d$  may be determined from the difference between the value of the low-frequency collector-base capacitance corresponding to a given emitter current and that for zero emitter current.

Alternatively, the nature of the frequency variation of  $z_{22}^{(b)}$ , as well as that of the current-amplification factor  $\alpha$  may be described approximately by a new equivalent circuit employing an RC transmission line, as shown in Fig. 1. In this circuit,  $z_e$ ,  $z_b$  are complex emitter and base impedances,  $\mu$  is a complex form of the voltage-feedback factor introduced by Early,  $\alpha_0$ ,  $g_c$  and  $C_c$  are as defined above, and  $r_d$  and  $c_d$  are the per-unit-length constants of the line of length  $w$ , i.e.,  $r_d = R_d/w$ ,  $c_d = C_d/w$ , with  $C_d$  as defined above, and with  $R_d = \tau_D/C_d$ .

At low frequencies, the open-circuit collector-base admittance reduces to that of a parallel combination of the conductance  $g_c$ , the collector capacitance  $C_c$ , and the additional diffusion capacitance  $C_d$ . As the frequency is increased, the open-circuit collector-base conductance increases with increasing frequency, ultimately as  $\omega^{1/2}$ , whereas the capacitance decreases with increasing frequency as  $\omega^{-1/2}$  from its low-frequency value of  $(C_c + C_d)$  to an ultimate value of  $C_c$ .

R. L. PRITCHARD

Communications Research Section  
General Electric Co.  
Schenectady, N. Y.

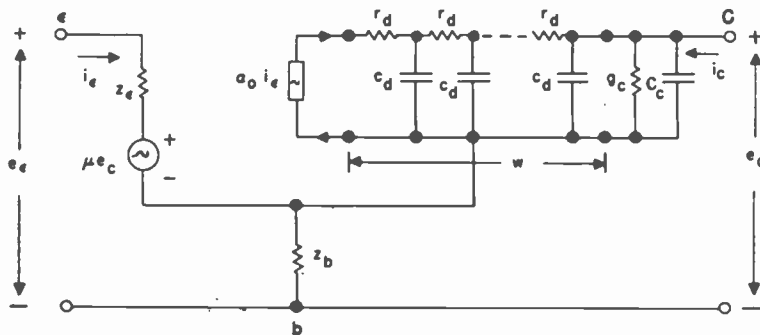


Fig. 1—Equivalent circuit including RC transmission line for junction transistor.

\* Received by the Institute, December 22, 1952.

<sup>1</sup> J. M. Early, "Effects of space-charge layer widening in junction transistors," *Proc. I.R.E.*, vol. 40, pp. 1401-1406; November, 1952.

<sup>2</sup> Details of the extension and the experimental results will be described by the writer in a forthcoming paper.

<sup>3</sup> This expression follows from the theoretical result if it is assumed that the low-frequency value  $\alpha_0$  of the current-amplification factor is close to unity.

<sup>4</sup> Alpha-cutoff frequency  $\omega_c/2\pi$  is defined as the frequency for which the amplitude of the current-amplification factor  $\alpha$  is 3 db below its low-frequency value  $\alpha_0$ . According to Shockley's theory (W. Shockley, *et al.*, " $p-n$  junction transistors," *Phys. Rev.*, vol. 83, no. 1, p. 161; July 1, 1951), the frequency variation of  $\alpha$  under certain conditions may be described by the expression  $\alpha_0/\cosh(j\omega\tau_D)^{1/2}$ . Hence, when  $\omega\tau_D = 2.43$ ,  $|\alpha| = 0.707 \alpha_0$ . For further details, see R. L. Pritchard, "Frequency variations of current-amplification factor for junction transistors," *Proc. I.R.E.*, vol. 40, appendix, pp. 1480-1481; November, 1952.

### Remarks on the Neutrino Communication System\*

There have recently appeared in these pages two communications dealing with the possible role played by the neutrino in telepathic communication. Hammond<sup>1</sup> first suggested that the neutrino may be the agency for such communication, and based his suggestion primarily upon the fact that the interaction of neutrinos with matter is extremely small; so small that barriers would not interfere with telepathic transmission. Following this suggestion, Tyson<sup>2</sup> noted that the potassium isotope of mass 40, which is radioactive, is found in human organisms and would be expected to emit neutrinos during its decay process. This writer pointed out further that the amount of  $K^{40}$  in the human brain would result in the emission of some 400 neutrinos per second.

Apart from any considerations of the evidence for or against telepathic communication, it should be evident that the neutrino can play no part in such a phenomenon. In the first place, the argument set forth by Hammond regarding the great penetrating power of the neutrino applies as well to the interaction of this particle with the brain. The detection of a neutrino signal implies the transfer of energy to the receiver, while the fact is that the neutrino has not yet been observed directly simply because its interaction with matter is so very weak. Experiments to date have succeeded only in establishing upper limits to the cross-sections, the limits being imposed by the sensitivity of the detection equipment. These measurements have shown that the scattering cross-section<sup>3</sup> is certainly less than  $10^{-34}$  cm<sup>2</sup>/electron, while the cross-section for the expected process of inverse  $\beta$ -decay is estimated<sup>4</sup> to be of the order of  $10^{-44}$  cm<sup>2</sup>. Unless there is some process, entirely outside our present knowledge, through which a neutrino can transfer energy to a free electron with good probability, the weak interaction argues most strongly against its participation in thought transmission.

In addition, one must consider the question of noise in the communication channel. All radioactive sources which decay via a beta process emit neutrinos with energies ranging from zero to several Mev in some cases. For example, the  $C^{14}$  present in the body emits some  $2 \cdot 10^8$  neutrinos/sec, and the radium in a typical luminous dial watch produces about  $10^6$  neutrinos/sec. While the neutrino emission from such sources, and from the natural radioactivity in the earth, is considerably greater than that from the  $K^{40}$  in the brain, even these sources are negligible in comparison with the emission from the sun. This is so great that the neutrino intensity at the earth is estimated<sup>5</sup> to be  $10^{11}$  neutrinos/sec-cm<sup>2</sup>. Nor would this be the only major neutrino flux on the earth. In the vicinity of a high power reactor one

\* Received by the Institute, April 8, 1953.

<sup>1</sup> A. L. Hammond, "Note on Telepathic Communication," *Proc. I.R.E.*, vol. 40, p. 605; May, 1952.

<sup>2</sup> G. N. Tyson, "On the possibilities of a neutrino communication system," *Proc. I.R.E.*, vol. 41, p. 294; February, 1953.

<sup>3</sup> J. H. Barrett, *Phys. Rev.*, vol. 79, p. 907; 1950.

<sup>4</sup> H. A. Bethe, "Elementary Nuclear Theory," John Wiley and Sons, Inc., New York; 1947.

<sup>5</sup> E. Fermi, "Nuclear Physics," *Rev. Ed.*, U. of Chicago Press, Chicago; 1950.



could expect a flux of the order of  $10^{12}$  neutrinos/sec-cm<sup>2</sup>, and even at a distance of 10 miles from the explosion of a nominal atomic bomb, the flux at the end of the first minute would be some  $10^9$  neutrinos/sec-cm<sup>2</sup>. The transmission of a neutrino signal in the presence of such a high noise level is inconceivable.

M. H. SHAMOS  
Physics Department  
Washington Square College  
New York University

**Response Characteristics\***

"The Response Characteristics of Resistance-Reactance Ladder Networks," treated by R. R. Kenyon in the May issue of the PROCEEDINGS OF THE I.R.E., can be obtained with much greater facility by means of the methods presented in my paper on the same type of network.<sup>1</sup>

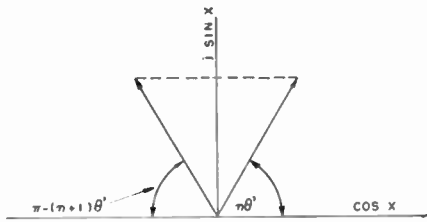


Fig. 1.—Positioning of  $e^{jn\theta'}$  to satisfy  $\sin(n+1)\theta' = \sin n\theta'$ .

It has been shown there (Eq. j) that for the  $n$ -section network of Fig. 1:

$$\frac{E_0}{E_{i,n}} = \frac{\sinh \theta}{\sinh(n+1)\theta - \sinh n\theta} \quad (j)$$

$$\cosh \theta = 1 + \frac{\rho T}{2}$$

is equivalent to Kenyon's or Tschudi's<sup>2</sup>

$$\frac{E_0}{E_{i,n}} = \frac{1}{\sum_{m=0}^n a_{m,n}(\rho T)^m}$$

$$a_{m,n} = \binom{n+m}{2m},$$

where the variables  $\rho$  and  $s$  are interchangeable.

The partial-fraction expansion of the voltage transfer ratio (j)

$$\frac{E_0}{E_{i,n}} = \frac{1}{\sum_{m=0}^n a_{m,n}(\rho T)^m} = \frac{1}{\prod_{m=1}^n (\rho T - b_{m,n})}$$

$$= \sum_{m=1}^n \frac{B_{m,n}}{\rho T - b_{m,n}}$$

is required in connection with transient problems. In order to obtain it, the roots

$b_{m,n}$ ,<sup>3</sup> of  $\sum_{m=0}^n a_{m,n}(\rho T)^m = 0$  must be found. Rather than solve this  $n$ 'th order equation, consider the equivalent equation

$$\sinh(n+1)\theta = \sinh n\theta.$$

It is satisfied by purely imaginary values of  $\theta(\theta = j\theta')$ , such that

$$\pi - (n+1)\theta' = n\theta',$$

as is apparent from Fig. 1. Consequently, the complete solution is

$$\theta' = (2m-1) \frac{\pi}{2n+1} = \alpha_m,$$

$$m = 1, 2, 3, \dots, n.$$

Since  $\rho T = 2(\cosh \theta - 1)$ , the  $n$  roots  $\rho T = b_{m,n}$  are given by

$$b_{m,n} = 2(\cos \alpha_m - 1).$$

While Kenyon's method requires the solution of an  $n$ 'th order equation,  $n$  being the number of network sections, the present method reduces the process to looking up the values in a table of cosines. The simplification is very substantial when several sections are involved.

Furthermore, even the coefficients of the partial fractions can be compared with greater economy by means of this method. Since the roots are all linear and distinct, the coefficients  $B_{m,n}$  are given by

$$B_{m,n} = \frac{\sinh \theta}{\frac{1}{T} \cdot \frac{d}{d\rho} [\sinh(n+1)\theta - \sinh n\theta]_{\theta=j\alpha_m}}$$

$$= \frac{1 - \cos 2\alpha_m}{(2n+1) \cos n\alpha_m}.$$

If the input  $e_{i(t)}$  is of the unit impulse form (Dirac function), so that the Laplace transform  $E_{i(\rho)} = 1$ , then the output voltage as a function of time is given directly and without intermediate calculations by

$$e_{0(t)} = \frac{e^{-2t/T}}{(2n+1)T} \sum_{m=1}^n \frac{1 - \cos 2\alpha_m}{\cos n\alpha_m} e^{2 \cos \alpha_m \cdot t/T}$$

$$\alpha_m = (2m-1) \frac{\pi}{2n+1}, \quad m = 1, 2, 3, \dots, n.$$

Supposing the input voltage  $e_{i(t)}$  to be a unit step function (Heaviside function), the partial fraction  $1/\rho$  is added and the coefficients of the other partial fractions become

$$T \frac{B_{m,n}}{b_{m,n}} = - \frac{1 + \cos \alpha_m}{(2n+1) \cos n\alpha_m} \cdot T.$$

Consequently, the output voltage as a function of time is given explicitly by

$$e_{0(t)} = 1 - \frac{e^{-2t/T}}{2n+1} \sum_{m=1}^n \frac{1 + \cos \alpha_m}{\cos n\alpha_m} e^{2 \cos \alpha_m \cdot t/T}$$

$$\alpha_m = (2m-1) \frac{\pi}{2n+1}, \quad m = 1, 2, 3, \dots, n.$$

LEO STORCH  
Advanced Electronics Techniques Dept.  
Hughes Aircraft Co.  
Culver City, Calif.

**A Note on the Impedance Transformation Properties of the Folded Dipole\***

The impedance transformation properties of the half wave folded dipole (Fig. 1) have been investigated by R. Guertler<sup>1</sup> under the following restrictions: (a) The cross-section dimensions of the elements and the distance between them is small in comparison with  $\lambda/2$ . (b) The elements are of circular (or nearly circular) cross section. (c)  $[a_2/a_1 > 1; s/a_2 \geq 2.5$  (Fig. 1)]. It is the purpose of this note to point out a way of removing restrictions (b)(c).

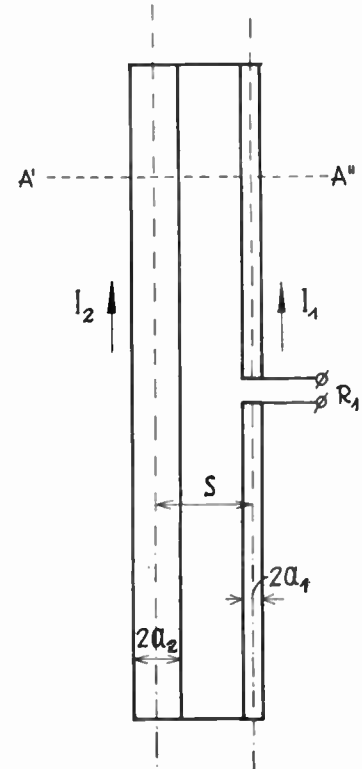


Fig. 1—The folded dipole.

As shown in reference 1 the impedance transformation of the folded dipole is given by:

$$\frac{R_1}{R_0} = (1+n)^2, \quad (1)$$

where  $R_1$  is the input impedance of the folded dipole,  $R_0$  the input impedance of the simple dipole, and  $n$  stands for the current ratio:

$$n = \frac{I_2}{I_1}. \quad (2)$$

From the equation of continuity (Div  $j = -i\omega\rho$ )

$$\frac{j_2}{j_1} = \frac{\rho_2}{\rho_1}, \quad (3)$$

or:

$$\frac{I_2}{I_1} = \frac{q_2}{q_1}. \quad (4)$$

\* Original manuscript received by the Institute April 27, 1953.

<sup>1</sup> R. Guertler, "Impedance transformation in folded dipoles," Proc. I.R.E., Vol. 38, p. 1042; September, 1950.

\* Received by the Institute, May 23, 1951.  
<sup>1</sup> Leo Storch, "The Multisection RC Filter Network Problems," Proc. I.R.E., pp. 1456-1458; November, 1951.  
<sup>2</sup> R. R. Kenyon, "Response characteristics of resistance-reactance ladder networks," Proc. I.R.E., vol. 39, pp. 557-559; May, 1951.  
<sup>3</sup> E. W. Tschudi, "Admittance and Transfer Function for a  $n$ -Mesh RC Filter Network," Proc. I.R.E., vol. 38, pp. 309-310; March, 1950.

<sup>3</sup> This  $b_{m,n}$  and the one used in footnote reference 1 have entirely different meanings.

The impedance transformation is thus defined by the ratio of charges in the elements. The ratio of charges  $q_1$  and  $q_2$  can be found with the aid of the condition that the scalar potential on the conductor boundary remains constant at any cross section of the dipole (A'A''—Fig. 1).

Assuming a sinusoidal charge distribution along the Z direction (Fig. 2).

$$q(x'y'z') = f(x'y') \cos \frac{2\pi z'}{\lambda}, \quad (5)$$

where  $q$  represents the charge distribution and  $x'y'z'$ —a point of the surface of the conductors. The scalar potential is given by:

$$\phi = \frac{1}{4\pi\epsilon_0} \iiint \frac{1}{r} [q] dx'dy'dz', \quad (6)$$

the integration should be carried out over the whole surface of the conductors;  $[q]$  is the retarded charge, and  $r = \sqrt{(x-x')^2 + (y-y')^2 + (z-z')^2}$ . By a proper choice of the time origin, the retarded charge can be written as:

$$[q] = f(x'y') \cos \frac{2\pi z'}{\lambda} \cos \frac{2\pi r_1}{\lambda}, \quad (7)$$

substituting (7) into (6) and considering the plane  $z=0$ :

$$\phi_{z=0} = \frac{1}{4\pi\epsilon_0} \iint f(x'y') \left\{ \int_0^{\lambda/2} \frac{\cos \frac{2\pi r_1}{\lambda} \cos \frac{2\pi z'}{\lambda}}{\gamma_1} dz' \right\} dx'dy' \quad (8)$$

where:

$$r_1 = \sqrt{(x-x')^2 + (y-y')^2 + z'^2}.$$

The integral in parenthesis has been solved by Guertler,<sup>2</sup> who has shown that when  $\sqrt{(x-x')^2 + (y-y')^2} \ll \lambda/2$  the following approximation holds:

$$\int_0^{\lambda/2} \frac{\cos \frac{2\pi z'}{\lambda} \cos \frac{2\pi r_1}{\lambda}}{r_1} dz' = \ln \frac{A}{[(x-x')^2 + (y-y')^2]^{1/2}}, \quad (9)$$

where  $A$  is a constant; substituting (9) into (8) we have:

$$\phi_{z=0} = \frac{1}{4\pi\epsilon_0} \iint f(x'y') \cdot \ln \frac{A}{[(x-x')^2 + (y-y')^2]^{1/2}} dx'dy' \quad (10)$$

but this is the well known equation of the two dimensional electrostatic field.<sup>2</sup>

From (10) together with the boundary condition that  $\phi$  should be constant on the surface of the elements at any cross section, we may conclude: When the cross section dimensions of the folded dipole are small (in comparison with  $\lambda/2$ ) the ratio of charges in the elements is approximately equal to the electrostatic charge ratio of infinitely long conductors having the same cross section as the folded dipole, all the conductors being on the same potential.

Considering the elements as quasi-line charges<sup>3</sup> immediately leads to the solution given in reference 1. The charge ratio for arbitrary cross sections can be found conveniently with the aid of the electrolytic tank.

MOSHE ZAKHAIM  
Ministry of Defence  
Scientific Department  
Dept. of Electronics  
Israel

<sup>2</sup> J. A. Stratton, "Electromagnetic Theory," McGraw-Hill Book Co., p. 219; 1941.

<sup>3</sup> E. Weber, "Electromagnetic Fields," John Wiley and Sons, vol. 1, p. 106; 1950.

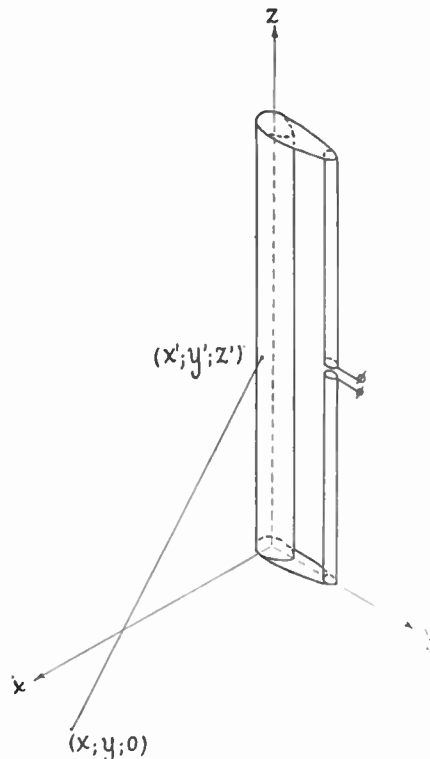


Fig. 2—Folded dipole with arbitrary geometry of cross section.

# Contributors to Proceedings of the I.R.E.

Monte I. Burgett, Jr. (S'42-A'43-SM'51) was born in Midland, Ark. on March 8, 1921. He attended Hendrix College and Georgia School of Technology where in 1943 he received the BS in EE degree, Co-operative Plan. He received his MS in EE degree from the University of Pennsylvania in 1951.



M. BURGETT, JR.

In 1943 Mr. Burgett joined Philco Corporation and has been with that company ever since. During the war years, he worked on airborne radar and bombing equipment, and afterward on auto radio and television tuner development. Since 1950 he has been working on color systems and receivers in the Research Department where he serves as a project engineer.

Mr. Burgett joined the faculty of Drexel Institute of Technology Evening College in 1948, and organized the electronics option of Electrical Engineering. From 1950 to 1952, he served as Assistant Head of the Drexel Electrical Engineering Department.

For a photograph and biography of DAVID K. CHENG, see page 998 of the August, 1952 issue of the PROCEEDINGS OF THE I.R.E.



For a photograph and biography of MARVIN CHODOROW, see page 163 of the January, 1953 issue of the PROCEEDINGS OF THE I.R.E.



G. C. Dacey was born on January 23, 1921, in Chicago, Illinois. He received the B.S. degree in electrical engineering from



G. C. DACEY

University of Illinois in 1942. Upon graduation he joined the staff of the Westinghouse Research Laboratories where he worked on the development of "Resnatrons" and high-power magnetrons.

At the end of the war he enrolled at the California Institute of Technology and completed his studies for the Ph.D. de-

gree in 1950. He remained at the Institute for a year as the A. O. Smith Post-Doctoral Fellow studying radio tracer methods in the investigation of metals.

In 1951, Dr. Dacey joined the staff of the Bell Telephone Laboratories as a member of the transistor physics group.

Dr. Dacey is a member of A.P.S., Eta Kappa Nu, Tau Beta Pi, Sigma Tau, Phi Kappa Phi, and Sigma Xi.



Frederic H. Dickson (S'38-A'43) was born in Bristol, Colorado, on January 10, 1916. He received the B.S. in electrical engineering from Oregon State College in 1939, where he was a graduate assistant in electrical engineering until 1940. Prior to entry in military service in 1942, he was an instructor in the Air Corps Technical Schools. Mr. Dickson served as an assistant radio officer, Allied Forces Headquarters and as Assistant Signal Of-



F. H. DICKSON

ficer, 15th Army Group in the European theatre and returned from overseas as Executive Officer and later Commanding Officer of the Signal Corps Radio Propagation Unit. Upon release from military service in 1946, he joined the Office of the Chief Signal Officer and has been active in application engineering and operational research in the field of radio-wave propagation. He is presently Chief of the Radio Propagation Section.

Mr. Dickson is a member of the USA National Committee, URSI, Chairman of US Commission IV, URSI and is a registered professional engineer in the District of Columbia.

❖

For a photograph and biography of JOHN J. EGLI, see page 163 of the January, 1953 issue of the PROCEEDINGS OF THE I.R.E.

❖

Ralph A. Galbraith was born on August 1, 1911 in Ash Grove, Mo. He received the B.S. degree in 1933 from the University of Missouri and the Ph.D. in Electrical Engineering from Yale University in 1937.



R. A. GALBRAITH

Dr. Galbraith has held the posts of research engineer for the Detroit Edison Company in 1937, and research editor, the following year. From 1938 until 1939, he was an instructor in electrical engineering at the University of Missouri, and from 1939 until 1944, an assistant professor to associate professor of electrical engineering at the University of Texas. During the summer of 1941 he was research engineer at Century Electric Company. He was a staff member at M.I.T. Radar School from 1944 until 1946, and professor of electrical engineering at Georgia Institute of Technology in 1946. For the next five years Dr. Galbraith was chairman in the department of electrical engineering at Syracuse University.

From that time until now he has been dean of the college of engineering at Syracuse University.

❖

Edward L. Ginzton (S'39-A'40-SM'46-F'51) was born in Russia on December 27, 1915, and came to the United States in 1929.



E. L. GINZTON

He received the B.S. degree in electrical engineering from the University of California in 1936, and the M.S. degree from the same institution in 1937. For graduate study at Stanford University, he received the E.E. degree in 1938, and the Ph.D. degree in 1940.

From 1937 until 1939 Dr. Ginzton acted as assistant in teaching and research at Stanford University, and in 1940 he became a research associate in the physics department.

From 1940 until 1946 Dr. Ginzton was employed in the research laboratories of the Sperry Gyroscope Company. From 1946 to 1948, he has been an assistant professor of applied physics at Stanford University, and an Assistant Director of the Microwave Laboratory. In 1948 he became an associate professor, and in 1951, professor of applied physics and electrical engineering.

Dr. Ginzton has been the Director of the Microwave Laboratory since 1949. He has also been a member of the Executive Committee of the Board of Directors of Varian Associates from 1948 to date. He is a member of Sigma Xi, Tau Beta Pi, and Eta Kappa Nu.

❖

Wolf J. Gruen (M'47) was born in Berlin, Germany, on September 21, 1914. He received the Dipl. Ing. E.T.H. degree in electrical engineering from the Swiss Federal Ins. of Technology in Zurich, in 1940, and the M.E.E. degree from Syracuse University in 1952.



W. J. GRUEN

From 1944 to 1946 Mr. Gruen was in charge of the Laboratory of the Long Lines Department of the Ericsson Telephone Company in Mexico City, Mexico. In 1946 he immigrated to this country and joined the Advanced FM Development Group of the Hazeltine Electronics Corporation in New York.

Since August 1947, Mr. Gruen has been associated with the Receiver Department of the General Electric Company. He is currently a Section Engineer in charge of a development section, engaged in monochrome and color-television circuit development.

Mr. Gruen is a member of Panel 15, NTSC, and has been active on several subcommittees of the NTSC. He currently serves on the Membership Committee of the Syracuse Section of the I.R.E. He is a member of the Scientific Research Society of America, RESA.

❖

For a photograph and biography of J. W. HERBSTREIT, see page 606 of the May, 1952 issue of the PROCEEDINGS OF THE I.R.E.

❖

William R. Hewlett (S'35-A'38-SM'47-F'48) was born in 1913 at Ann Arbor, Mich. He received the A.B. degree from Stanford University in 1934, and the M.S. degree from the Massachusetts Institute of Technology in 1936. In 1939 he received the E.E. degree from Stanford University, after spending the period from 1936 to 1938 engaged in electro-medical research in Palo Alto, Calif.



W. R. HEWLETT

In 1939, Mr. Hewlett joined David Packard in starting

the Hewlett-Packard Company in Palo Alto. During the war he was on active duty with the Army, first assigned to the office of the Chief Signal Officer, and then to the New Developments Division of the War Department's Special Staff in Washington, D.C. Since 1946, he has been associated with the Hewlett-Packard Company.

Mr. Hewlett is a member of Sigma Xi and the American Institute of Electrical Engineers. He received the I.R.E. Fellow award "for his initiative in the development of special radio measuring techniques."

❖

Roland B. Holt was born on July 21, 1920, in San Antonio, Texas. He received his A.B. degree from the University of Texas in 1940; his M.A. degree from the University of Texas in 1942; and his Ph.D. degree from Harvard University in 1947.



ROLAND HOLT

During the period 1942-1950, Dr. Holt held the positions of research associate, National Research Council Predoctoral Fellow, Instructor and Assistant Professor of Physics at Harvard University.

In 1950 Dr. Holt became Director of the Cyclotron Laboratory at Harvard University, a position he held until 1952. During the fall of 1951 he became President of Scientific Specialties Corporation, the position he currently holds as well as President of Transistor Products, Inc.

Ph.D. thesis work involved a study of the role of hydrogen peroxide in the thermal reaction between hydrogen and oxygen.

During World War II at the Radio Research Laboratory of Harvard University, Dr. Holt did work in the field of radio countermeasures.

Dr. Holt is a member of Phi Beta Kappa, Sigma Xi, I.R.E. (senior member), and the A.P.S.

❖

Richard A. Johnson was born in Worcester, Massachusetts on June 30, 1926. For two years during the war he was in Navy Radar program after which he received the A.B. degree in physics from Dartmouth in 1948. He continued his studies at Harvard University, receiving the M.S. Degree in 1950 and the Ph.D. Degree in Engineering Science and Applied Physics in 1952. At Harvard he did research in gas discharge physics and the theory of random processes. At present, Dr. Johnson is affiliated with Transistor Products, Inc., He is a member of A.P.S., Phi Beta Kappa and Sigma Xi.



R. A. JOHNSON

He is a member of A.P.S., Phi Beta Kappa and Sigma Xi.

Josef Kates (S'45-A'52) was born on May 5, 1921, in Vienna, Austria. He received the B.A. degree in the mathematics and physics honor course in 1948, the M.A. degree in applied mathematics in 1949, and the Ph.D. degree in physics in 1951, all at the University of Toronto.



JOSEF KATES

From 1944 to 1948, Dr. Kates worked on problems related to vacuum tubes with Rogers Electronic Tubes, Ltd., Toronto. Since 1948 he has been engaged in the development and design of digital computers with the Computation Centre of the University of Toronto.

Dr. Kates is a member of the Association of Professional Engineers of Ontario, the Canadian Association of Physicists, and the Canadian Mathematical Congress.

Leonard H. King (S'46-A'49) was born in New York City on July 27, 1925. After serving in the Army from October 1943 to May 1946, he entered the Massachusetts Institute of Technology and received a B.S. degree in electrical engineering in June 1950. Mr. King became a research assistant in the M.I.T. Instrumentation Laboratory and received the M.S. degree in electrical engineering in



LEONARD H. KING

June 1951. Since then, he has worked as a research engineer in the airborne fire control section of the M.I.T. Instrumentation Laboratory and presently is in charge of the control aspects of a prototype fire control system.

Mr. King is an associate member of Sigma Xi.

Geoffrey Knight, Jr. was born on July 15, 1922, in Washington D. C. He received his A.B. degree, magna cum laude, from Amherst College in 1943 and his Ph.D. in theoretical physics from M.I.T. in 1949.



GEOFFREY KNIGHT

From 1949 to 1951 Dr. Knight worked in the fields of transistor technology and transistor applications for International Business Machines Corporation. In 1951 he joined Scientific Specialties Corporation, eventually transferring to its affiliate, Transistor Products, Inc. Here he has been chiefly concerned with the design of equipment for measuring transistor characteristics and with transistor circuit applications.

He is a member of the A.P.S., Phi Beta Kappa, and Sigma Xi.

Ervin Joseph Nalos was born in Prague, Czechoslovakia, September 10, 1924. He graduated from King Edward High School, Vancouver, Canada, in 1941. In 1946 he received the degree of Bachelor of Applied Science in electrical engineering, and in 1947, the degree of Master of Applied Science from the University of British Columbia. He continued graduate study as a research and teaching assistant at the Microwave Laboratory at Stanford University under a Sperry Gyroscope Company fellowship, obtaining his Ph.D. in 1951.



E. J. NALOS

Since then Dr. Nalos has been a Research Associate at the Microwave Laboratory, where he is active in high power microwave tube research and the student laboratory instruction program. He is a member of Sigma Xi.

Raymond J. Nordlund (M'46-SM'50) was born in New Effington, South Dakota, on April 20, 1911. He received the B.S. in EE Degree from South Dakota State College in 1933, and completed basic requirements for the M.S. Degree in Radiation at Ohio State University in 1948.



R. J. NORDLUND

From March, 1934, until June, 1941, Mr. Nordlund was engaged in various phases of highway design and engineering for the South Dakota State Highway Commission. In June, 1941, he joined the staff of the Signal Corps Aircraft Radio Laboratory, Wright Field, Ohio, undertaking research in "night effect" in radio-compass airborne navigation.

During 1942 Mr. Nordlund was engaged in component development for the first radar-navigation systems to be used by the U. S. Air Force, SCR-521, SCR-517, and AN/APQ-5. From March, 1943, to January, 1946, he served as project engineer for development of a fire-control radar system and a high-resolution radar bombing system in Radar Laboratory, Wright Field. From January, 1946, to October, 1948, he served as Chief, Ground Position Indicating Systems Unit and as Asst. Chief, Bombing Branch, Aircraft Radiation Laboratory. He was Chief, Strategic Bombing Branch, Armament Laboratory from October, 1948, to April, 1951. At the present time his post is that of Bombing Consultant, Armament Laboratory, Wright Air Development Center, Dayton, Ohio.

Mr. Nordlund is a member of Sigma Tau, and has served on a sub-panel of the Re-

search and Development Board for several years. He holds the rank of Major, USAFR.



IAN M. ROSS

has been since that time a member of the transistor physics group.

For a photograph and biography of EUGENE A. SANDS, see page 1254 of the October, 1952 issue of the PROCEEDINGS OF THE I.R.E.

Norman R. Scott (SM'46) was born in Brooklyn, N. Y., on May 15, 1918. He received B.S. and M.S. degrees in 1941 from Massachusetts Institute of Technology, where he was enrolled in the cooperative course in Electrical Engineering. He worked at the General Electric Co. during his undergraduate training and for a short time after graduation. In 1941 he entered the U. S. Army, serving for five years. He concluded his service with the rank of Major and the position of Chief of Special Projects Laboratory. He joined the faculty of the Dept. of Electrical Engineering at the University of Illinois in 1946 and received his Ph.D. there in 1950. He is now Asst. Professor of Electrical Engineering at the University of Michigan.



NORMAN R. SCOTT

Dr. Scott is a member of Sigma Xi, Eta Kappa Nu, and Phi Kappa Phi.

Leonard S. Sheingold (S'46-A'50) was born in Boston, Mass., on January 14, 1921. He served in the United States Army from 1942 to 1945.



L. S. SHEINGOLD

he was a graduate student in the Dept.

of Engineering Science and Applied Physics at Harvard University.

Mr. Sheingold obtained the A.M. degree from Harvard in 1950 and the Ph.D. degree in Applied Physics in 1953.

During the summers of 1950 and 1951, Dr. Sheingold was employed as a Microwave Engineer for Sylvania Electrical Products Inc., and served as a consultant during 1952. At present Dr. Sheingold is employed as an engineering specialist with the Engineering Lab. of Sylvania Electric Products Inc., Boston, Mass.

Dr. Sheingold is a member of Sigma Xi, Sigma Pi Sigma, and is a member of the papers committee of the Boston Section of the I.R.E.



For a photograph and biography of JACOB SHEKEL, see page 1611 of the November, 1952, issue of the PROCEEDINGS OF THE I.R.E.



Blanchard D. Smith, Jr. (S'45-A'50) was born in New Orleans, La. on August 22, 1925. He received the B.S. degree in electrical engineering from the Georgia Institute of Technology in 1945 and the M.S. degree in electrical engineering from the Massachusetts Institute of Technology in 1948.



B. D. SMITH, JR.

Mr. Smith was a commissioned officer in the U. S. Navy as a radar instructor. He was a research assistant at the Research Laboratory of Electronics, M.I.T., working on telemetering systems and pulse-code modulation.

Since 1948 Mr. Smith has been employed by Melpar, Inc. At present he is a consulting project engineer on electronic research and development projects.

Mr. Smith is a member of Phi Kappa Phi, Tau Beta Pi, Eta Kappa Nu, Sigma Xi.



Ernest K. Smith, Jr. (A'46-M'48) was born in Peiping, China, on May 31, 1922. He came to the United States in 1940 and entered Swarthmore College, where he received the B.A. in Physics in 1944. After graduation, he went into the Army and spent the following two years with the Signal Corps Radio Propagation Unit, Baltimore, Maryland.



ERNEST K. SMITH,

Mr. Smith joined the Engineering Department of the Mutual Broadcasting System in 1946 and later be-

came Chief of the Plans and Allocations Division. In 1949, he entered the School of Electrical Engineering at Cornell University and received the M.S. degree in 1951.

Mr. Smith was employed by the Central Radio Propagation Laboratory of the National Bureau of Standards in Boulder, Colorado from June 1951 to September 1952. He is now a candidate for the Ph.D. degree at Cornell University.



Harry Sohon (A'28-VA'39-SM'50) was born on November 24, 1904, in New York City. He received the E.E. degree from Cornell University in 1926. After graduation he worked for the General Electric Company for two years.



HARRY SOHON

Mr. Sohon returned to Cornell on a McMullin Fellowship and received the M.E.E. degree in 1930. Joining the staff at Cornell as Instructor, he earned the Ph.D. degree in 1932. He continued teaching at Cornell until 1942 when he was appointed Asst. Professor of Electrical Engineering at the University of Connecticut where he remained a year before accepting a similar appointment at the Moore School, University of Pennsylvania, from 1943 to 1945.

Following a year as advanced development engineer in the aviation engineering section of RCA-Victor, Mr. Sohon returned to the Moore School in 1946. In 1951 he was appointed Associate Professor of Electrical Engineering and also Associate Supervisor of Research at the Moore School.

Mr. Sohon is licensed as a professional engineer in the State of Pennsylvania and is a member of Eta Kappa Nu, Phi Kappa Phi, Sigma Xi, the Engineers Club of Philadelphia, the American Society for Engineering Education, the American Association of University Professors, and the American Institute of Electrical Engineers.



Seymour Stein (S'53) was born in Brooklyn, New York, on April 4, 1928. He received the B.E.E. degree from City College, New York, in 1949, and the M.S. degree in Applied Science from Harvard University in 1950. He is now studying at Harvard toward a Ph.D. in Applied Science.



S. STEIN

Mr. Stein was a Teaching Fellow at Harvard during 1950-51, and is now an RCA Fellow in Electronics, under the National Research Council (1951-1953).

Mr. Stein is a member of Eta Kappa Nu, Tau Beta Pi, and Sigma Xi.



James E. Storer was born in Buffalo, N. Y., on October 26, 1927. He received the A.B. degree in physics in June, 1947, from Cornell University,



JAMES E. STORER

followed by the M.S. and Ph.D. degrees in 1948 and 1951, respectively, both from the Dept. of Engineering Sciences and Applied Physics at Harvard University. While at Harvard, he held an Atomic Energy Commission Fellowship. He is a member of the Sigma Xi Society.

Dr. Storer was Research Fellow at the Electronics Research Lab., 1951-53, and Lecturer in the Div. of Applied Science, Harvard, 1952-53. Currently he is Asst. Professor in the Div. of Applied Science, doing research in the fields of Electromagnetic Theory and Random Processes.



Stanley Weintraub was born in New York, N. Y., on April 4, 1922. He entered the City College of New York in 1939,



S. WEINTRAUB

leaving in 1942 to join the Signal Corps Radar Laboratory, enlisting in the Signal Corps the same year. He served as an airborne radar technician in the India-Burma theater from 1943 to 1946. Mr. Weintraub returned to CCNY, receiving the B.S. degree in Physics in 1947.

From 1947 until 1949 he was in the Mechanical Instruments Section of the National Bureau of Standards, Boulder, Colo. Since 1949 he has been with the Central Radio Propagation Laboratory of the Bureau where he is now a member of the radiometeorological group of the Tropospheric Propagation Research Section.



For a photograph and biography of G. S. WICKIZER, see page 1731 of the December, 1952 issue of the PROCEEDINGS OF THE I.R.E.



For a photograph and biography of LOTFI A. ZADEH, see page 1128 of the September, 1952, issue of the PROCEEDINGS OF THE I.R.E.

# Institute News and Radio Notes

## FOREIGN MEMBERS MAY PAY DUES WITH UNESCO COUPONS

The attention of foreign members is called to the availability of UNESCO Coupons for paying IRE membership dues. This coupon is issued by the United Nations Educational, Scientific and Cultural Organization to facilitate payments of this nature between UNESCO member countries.

UNESCO Coupons may be purchased with local currency from the national Distributing Body of each participating country or from UNESCO regional offices. The addresses of Distributing Bodies and UNESCO offices are given below.

### Distributing Bodies

**Austria**—Aussenhandelsstelle für Buch und Graphik, Grunangergasse 4, Vienna 1; **British Colonial and Trust Territories**—Unesco Book Coupons, c/o Book Tokens Ltd., 28 Little Russell Street, London, W.C.1; **Burma**—The Secretary, National Commission Secretariat, Government of Burma, 545-547 Merchant Street, Rangoon; **Cambodia**—Ministere de l'Education Nationale et de la Jeunesse, Phnom Penh; **Ceylon**—The Secretary, National Commission for Unesco, Ministry of Education, Colombo; **Czechoslovakia**—Orbis Company, 37 Narodni, Prague 1; **Egypt**—Administration of General Culture, Ministry of Educa-

tion, Cairo; **France**—Direction des Bibliothèques de France, 55 rue Saint Dominique, Paris-7<sup>e</sup>.

**French Colonial Territories**—Direction des Bibliothèques de France, 55 rue Saint-Dominique, Paris-7<sup>e</sup>; **Germany**—(Bundesrepublik) Notgemeinschaft der deutschen Wissenschaft, Buechelstrasse 55, Bad Godesberg bei Bonn; **Hungary**—Kultura, P.O.B. 149, Budapest 62; **India**—Ministry of Education, New Delhi 3; **Indonesia**—Ministry of Education and Culture, Djalan Tjilatjap 4, Djakarta; **Israel**—Dr. G. J. Ehrlich, Import Licensing Office, Ministry of Education and Culture, Hakirya; **Italy**—Commissione Nazionale dell'Unesco, Villa Massimo, Via di Villa Massimo, Rome; **Japan**—Society for the Promotion of Science, c/o Science Council of Japan, Ueno Park, Tokyo, Japan; **Pakistan**—The Minister of Education and Industries (Education Division), Government of Pakistan, Karachi.

**Persia**—Persian National Commission for Unesco, Avenue du Nusee, Teheran; **Syria**—The Secretary, Syrian National Commission, Ministry of Education, Damascus; **Thailand**—The Thailand National Commission for Unesco, Ministry of Education, Bangkok; **Union of South Africa**—The Secretary, Department of Education, Arts and Science, New Standard Bank Buildings, Pretoria; **U.S.A.**—Unesco Office, UN Building, Room 2201, New York 17, N. Y.; **United Kingdom**—Unesco Book Coupons, c/o Book Tokens Ltd., 28 Little Russell Street, London, W.C.1; **Yugoslavia**—Secrétaire de la Commission Nationale de la République populaire federative de Yougoslavie pour l'Unesco Moskovska 51, Belgrade.

### UNESCO Offices

(Covering Afghanistan, Burma, Ceylon, China, Egypt, Hashemite, Jordan, India, Indochina, Indonesia, Iraq, Israel, Japan, Korea, Lebanon, Persia, Philippines, Pakistan, Saudi Arabia, Syria, Thailand, Turkey.)

**East Asia**—Unesco Science Co-operation Office, United Nations Building, 106 Whangpoo Road, Shanghai, China and Unesco Science Co-operation Office, United Nations Building, Padre Faura, Manila, Philippines; **Middle East**—Unesco Science Co-operation Office, 8 Sh. el Salamlik, Garden City, Cairo, Egypt and Unesco Science Co-operation Office, Istanbul Teknik Universitesi, Gumussuyu, Istanbul, Turkey; **South Asia**—Unesco Science Co-operation Office, University Buildings, Delhi, India; **South-East Asia**—Unesco Science Co-operation Office, Merdeka Seletan 11 Pav., Djakarta, Indonesia.

### IRE SECTIONS FORMED IN LONG ISLAND AND ELMIRA

At its May 5 meeting the IRE Board of Directors approved the establishment of the Long Island Section (formerly a Subsection of New York Section) in Region 2 and the Elmira-Corning Section in Region 4.

These raise IRE Sections to 67.

### IRE AUTHORS FIRST CALL

Prospective authors for the National Convention please submit: name, address, title of paper, 100-word abstract and informational up to 500 words (both in triplicate), to B. R. Lester, IRE, 1 East 79 St., New York, N. Y. by November.

### W. R. G. BAKER

#### RECIPIENT OF TWO AWARDS

Dr. W. R. G. Baker (A'19-F'28), General Electric Company vice president and past president of the IRE, was recently presented the Medal of Freedom by the Honorable Earl D. Johnson, Under Secretary of the Army, during ceremonies in the Pentagon, and the Medal of Honor by the Radio-Television Manufacturers Association at their annual convention in Chicago.



Dr. Baker was awarded the Medal of Freedom for accelerating the application of electronics to the solution of Army research and development problems. He led a mission of leading scientists and industrialists to Korea in the summer of 1952, to study the problem of utilizing electronic devices and principles to the maximum extent, thereby increasing the effectiveness of the individual soldier and reducing the cost of human life.

### ULTRASONICS ENGINEERING

The First Administrative Committee meeting of the Professional Group on Ultrasonics Engineering was held on May 6, 1953 in Washington, D. C.

Members of the committee are: Chairman of the Group: A. L. Lane, Naval Ordnance Laboratory; Vice-chairman, M. D. Fagen, Bell Telephone Laboratories; Secretary, J. Hunter, John Carroll University; and W. G. Cady, California Institute of Technology; W. J. Fry, University of Illinois; Frank Massa, Massa Laboratories; Oskar Mattiat, Clevite-Brush Development Co., P. L. Smith, Naval Research Lab.; W. J. Mayo-Wells, Johns Hopkins Univ.

Committee chairmen are as follows: Paper Procurement and Publications, O. Mattiat; Membership, M. D. Fagen; Sectional Activities, J. Hunter; Finance, P. L. Smith; Legal, W. J. Mayo-Wells.

Plans were made to sponsor a session on ultrasonics engineering at the National Electronics Conference in September.

## Calendar of COMING EVENTS

**IRE-ONR-Univ. of Calif. Symposium on Statistical Methods in Communication Engineering, Berkeley, Calif., August 17-18**

**IRE Western Convention and Electronic Show, Civic Auditorium, San Francisco, Calif., August 19-21**

**International Sight and Sound Exposition and Audio Fair, Chicago, Ill., September 1-3**

**Conference on Nuclear Engineering, University of California, Berkeley, September 9-11**

**National Electronics Conference, Hotel Sherman, Chicago, Ill., September 28-30**

**URSI Fall Technical Meeting, Ottawa, Canada, October 5-8**

**PGUE-Acoustical Society Symposium, Case Institute of Technology, Cleveland, Ohio, October 15-17**

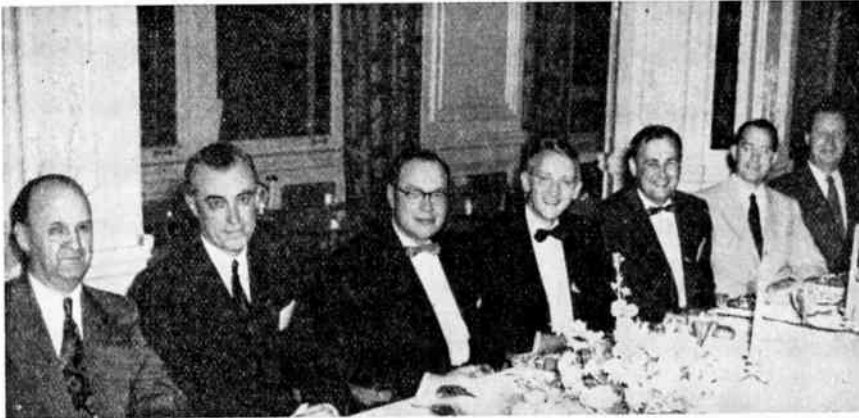
**1953 IRE-RTMA Radio Fall Meeting, Toronto, Ont., October 26-28**

**Conference on Radio Meteorology, University of Texas, Austin, November 9-12**

**Joint IRE-AIEE 6th Annual Conference on Electronic Instrumentation in Medicine and Nucleonics, New York City, November 18-20**



# Institute News and Radio Notes



NATIONAL TELEMETERING CONFERENCE BANQUET

Among those who attended the National Telemetering Conference jointly sponsored by the IRE, AIEE, IAS and ISA were (l. to r.) R. S. Gardner of AIEE; Dr. Harvard Hull of IAS, conference treasurer; D. J. E. Hobson, Stanford Research Institute, banquet speaker; Kipling Adams, General Radio Co.; John Doremus, Allen G. Caldwell Manufacturing Co., conference chairman; W. A. Wildhack of ISA; L. G. Cumming, IRE Technical Secretary.

## Organization for Engineering Unity

The following report to the membership is published at the direction of the IRE Board of Directors.—*The Editor*

For several years, earnest and detailed efforts have been made by a group of engineers broadly representative of leading engineering societies to promote unity in the engineering profession. Their further purpose was to afford both a forum and a spokesman, so to speak, for engineers on matters of such broad scope as might transcend the defined fields of individual engineering societies.

The body chosen in mid-1949 to study these matters, under the general auspices of the Engineers Joint Council and about fifteen collaborating engineering societies (which had appointed their representatives), was known as the "Exploratory Group to Consider the Increased Unity of the Engineering Profession." The IRE was represented on this Exploratory Group.

It was evident at once that any concrete procedures for an increase in the "unity" of the engineering profession were necessarily complex, multi-element matters.

More specifically, three major difficulties were immediately encountered. The first of these may be briefly described as follows. The attractiveness of the broad concept of engineering unity was diminished as soon as an attempt was made to define at least some of the *specific* objectives and procedures of the unity organization. Indeed, up to this time there are some persons who, while sympathetic to the broad concept of engineering unification, find no definite or concrete proposals or aims which seem sufficient at this time to command support. The second difficulty arose from the conflict between a unification based on engineering-society membership and control and a con-

solidation based on individual membership and control, independent of the existing societies. The third problem sprang from varying definitions of the scope and authority of individual engineering societies. Some of these regard themselves as restricted closely to scientific and technical matters. Others wish to go further afield, in some cases impinging on the fields of political, legislative, or even labor-representational activities. Some societies do not regard themselves as authorized to speak for their membership on any but highly technical matters, except perhaps after a special validating vote by the membership. Others take almost the opposite stand as to their right to commit their membership on a wide variety of subjects.

These problems were brought into sharp focus for the IRE by the receipt of an invitation from the Engineers Joint Council (EJC) to join a broadened and modified version of that body planned to function as an engineering unity organization.

One of the objectives of the expanded EJC was the development of sound public policies respecting national and international affairs. This aim could be interpreted as permitting the direct influencing of legislation—a course of action believed to be favored by some in the EJC. Further, a simple majority vote of the Council might be regarded as sufficient to initiate such action. The IRE has consistently refrained, as a matter of established policy, from any such action either as a society or through its Sections.

The new body would also administer, on behalf of the engineering profession, those activities authorized by a majority of the constituent societies of the Council. The implication would seem to be that while the individual engineer is to be represented, only the constituent societies would enjoy

individual membership. The IRE has consistently held to the position that the IRE is not entitled to represent its members as individual members of the engineering profession. Presumably an IRE constitutional amendment would be needed to authorize the IRE Board of Directors thus to represent its membership more widely and to extend that power of representation to another body of its choice.

While the IRE does not take a stand as a society even on technical matters when dealing with outside agencies, it does provide facilities for independent bodies such as the Joint Technical Advisory Committee. This method of operation has proved satisfactory (and is similar to the excellent precedent of the Royal Society, Great Britain, which, throughout its long and distinguished history, has carefully avoided ever taking a position as a society, while assisting wherever possible in the formation and work of any commission established to deal with national problems).

At the March 27, 1953 meeting of the IRE Board of Directors, the Board considered at length the EJC invitation and expressed its viewpoint in the following unanimously approved resolution:

*Whereas*, Our study of the Constitution of the Engineers Joint Council, adopted December 7, 1952, has revealed that acceptance by The Institute of Radio Engineers of the invitation to join the Engineers Joint Council would necessitate abrogation of two basic policies of long standing: one, that the Institute shall not engage directly or indirectly in legislative activity; and the other, that the Institute, as a society, is not entitled to represent its members as individual members of the engineering profession or as a body on social or general professional matters, and shall not, as a society, take a stand even on technical matters; therefore be it

*Resolved*, That, after careful deliberation, the Board of Directors has come to the conclusion that it is not desirable to reverse these policies at this time in order to permit affiliation with the Engineers Joint Council; and be it further

*Resolved*, That, therefore, The Institute of Radio Engineers must regretfully decline the invitation to join the Engineers Joint Council.

However, the Board looked favorably upon co-operative activity with the EJC on any specific problems of mutual interest in which the Institute can engage within the above stated framework. The Board further emphasized that the action taken was believed by it to be in the best interests of the Institute and its members. It should be added that, in the opinion of the Board, a unity organization of the type envisioned could function more appropriately and effectively as an individual membership society rather than as a coalition of professional engineering societies. And, further, the Board directed that the preceding information should appear in the PROCEEDINGS OF THE I.R.E. as a report to the membership



## Professional Group News

### AIRBORNE ELECTRONICS

The Philadelphia Chapter of the Professional Group on Airborne Electronics elected W. W. Felton, Franklin Institute, president; R. J. Esser, Raymond Rosen Engineering Products, vice-president; and C. E. Dolberg, Philco Corp., secretary. At a recent meeting at the Naval Air Development Center in Johnsville, Pa., C. S. Vasaka, engineer with the Center, gave a paper entitled the "Effects of Radio Interference on Airborne Electronics." He discussed the necessity for reduction of radio interference, the methods of reduction, testing, and the test equipment involved.

### ANTENNAS AND PROPAGATION

The new officers and administrative committee of the Professional Group on Antennas and Propagation are: Chairman, P. S. Carter; Vice Chairman, D. C. Ports; Secretary-Treasurer, P. H. Smith; George Sinclair; A. H. Waynick; J. B. Smyth; H. G. Booker; H. A. Finke; J. S. Brown; L. J. Chu; R. B. Jacques; L. C. Van Atta; H. W. Wells.

### AUDIO

The Cincinnati Chapter of the Professional Group on Audio met under the Chairmanship of R. E. Kolo recently at the Hotel Gibson, and Engineering Society Hdqts. G. J. Schulmerich, president of Schulmerich Electronics Inc. spoke about "Carillons." He discussed the characteristics of the tones produced by cast bells and covered the methods used in his carillon bells to secure comparable results. C. A. Maynard, vice president, Indiana Steel Products Co., talked about "Magnetic Structures for Audio and Acoustic Devices." He covered the characteristics of, and magnetic and physical limitations of, permanent magnet materials used in structures for audio and acoustic devices, and the design and application of magnets to such structures.

The newly formed Houston Chapter held an organizational meeting in May at which L. A. Geddes was elected head. D. P. Carlton demonstrated his two latest versions of small folded horns, one with an 8-inch speaker and a tweeter, and other with two 8-inch speakers. (Drawings are available upon request, care of Humble Oil.) He also demonstrated a console with a McIntosh amplifier, Rek-O-Nut turntable, and switching facilities permitting the selection of various output impedances and particular speaker. The PGA tapescript and slides of "A Single Ended Push-Pull Amplifier" by Peterson and Sinclair of General Radio were shown, and Roy Brougher demonstrated a modified version of this type of amplifier. James Hallenburg showed a message repeater. The next meeting will coincide with the beginning of binaural FM broadcasts, probably in August.

The Philadelphia Chapter recently held two meetings in the Edison Building presided over by S. C. Spielman, and W. G. Chancy. Lowell Good, RCA, spoke on "Design Factors for Audio Amplifiers," presenting what performance characteristics are needed for a suitable amplifier and how these

requirements are being met in commercial amplifiers. He covered power, distortion, noise, stability, reliability, and efficiency as they affect satisfactory design. H. H. Scott, president of H. H. Scott, Inc., gave a paper "Component Integration of Sound Reproducing Systems" in which he discussed the over-all problems of high-fidelity audio systems, particularly the contributions of the transducer, amplifier, and the loudspeaker system. He covered the application of dynamic noise suppression to phonographic reproduction from the new low noise records in detail.

### BROADCAST TRANSMISSION SYSTEMS

The Boston Chapter of the Professional Group on Broadcast Transmission Systems met recently at the studios of WCOP with P. K. Baldwin as Chairman. D. W. Bodle of Bell Telephone Labs spoke on "Lightning Protection of Transmitter Plants." Staff members of 15 broadcast stations attended. New officers of the Chapter are Sidney Stadig, WBZ-TV, Chairman; Hollis Gray, WHDH, Vice-Chairman; and Fearing Pratt, N.E. Tel. & Tel., Secretary.

The Chicago Chapter met recently under the Chairmanship of Stephen Bushman; F. M. Dukat, Receiving Tube Division of Raytheon Mfg. Co., was the speaker. In "Some Crystal Application Problems in Radio and Television Receivers," he discussed the use of crystals as low frequency multipliers and uhf mixers, using slides of graphs as illustration. He brought out that video detector performance is affected by the back voltage characteristic of the crystal, the temperature at which the crystal is operating, and the capacity and resistance loading of the crystal upon the detector circuit. Multiplier crystals are similar to video detector crystals, but are chosen for their higher front-to-back resistance ratio and better high frequency characteristics. UHF mixer crystals have a much lower front resistance, lower back voltage range and less capacity than the detector type crystals. Sufficient oscillator current must be injected into the mixer crystal to achieve optimum conversion efficiency. However, the crystal cannot be driven too far in the reverse current direction because of the increase in noise temperature of the crystal. Officers for the coming year are: Chairman, J. T. Williams; Vice-Chairman, K. R. Decho; Secretary, J. F. White.

The Los Angeles Chapter met recently in the Conference Room of the IAS Building with D. E. Foster presiding. A. A. Barco, RCA Labs, spoke on "Developments in the Application of Transistors." At a later meeting E. P. Thias and Robert Eland of Standard Coil Products talked about "An 82-Channel Turret Tuner." Officers for the coming year will be: Chairman, Stanley Cutler, Pacific Mercury TV Mfg. Co.; Vice-Chairman, J. T. McAllister, Hoffman Radio Corp.; and Secretary-Treasurer, A. J. Arman, Stevens Co.

### CIRCUIT THEORY

The Chicago Chapter of the Professional Group on Circuit Theory met at the West-

ern Society of Engineers Building recently under the Chairmanship of L. E. Peppenberg. Speaker of the evening was B. S. Parmet, project engineer with Motorola, Inc., who discussed "The Design of Maximally Flat Amplitude and Time Delay Filters."

### ELECTRON DEVICES NORTH SHORE CHAPTER FORMED

The establishment of a North Shore Chapter of the Professional Group on Electron Devices (Boston Section) has been approved by the Executive Committee of the Institute.

Interested members please contact G. E. Carter, Jr., Bomac Labs., Inc., Salem Road, Beverly, Mass.

### NEW GROUP ON ELECTRONIC COMPONENT PARTS

The need for a professional group concerned with the field of component parts has caused such a group to be established. Officially called the "Electronic Component Parts Professional Group," its interest will be confined to the characteristics, limitations, applications, development, performance, and reliability of component parts. Membership will be open to all IRE members. Engineers interested are invited to join.

Officers of the Group are: Chairman, F. A. Paul, supervisor, reliability group, Northrup Aircraft Co., Hawthorne, Calif.; Vice-Chairman, A. W. Rogers, chief, components and materials branch, Squier Signal Lab., SCEL, Fort Monmouth, N. J.; Secretary-Treasurer, C. G. Walance, Research & Devel. Labs., Hughes Aircraft Co., Culver City, Calif. Administrative committee members are: M. J. Ainsworth, Bendix Corp., 7250 Laurel Canyon Blvd., N. Hollywood, Calif.; J. T. Brothers, components section, Philco Corp., Philadelphia 34, Penn.; J. A. Csepely, Air Arm Div., Westinghouse Electric Corp., Friendship International Airport, Baltimore, Md.; F. B. Haynes, supervisor Electronics Product Service Sect., Glenn L. Martin Co., Baltimore; L. K. Lee, Advanced Techniques Lab., Stanford Research Institute, Stanford, Calif.; H. E. May, tube application co-ordinator, Motorola, Inc., 4545 Augusta Blvd., Chicago 51, Ill.; L. Podolsky, technical asst. to the president, Sprague Electric Co., No. Adams, Mass.; G. Shapiro, Electronics Div., National Bureau of Standards, Washington 25, D. C.; W. G. Tuller, Melpar Electronics, Inc., 452 Swann Ave., Alexandria, Va.

### ENGINEERING MANAGEMENT

The Chicago Chapter of the Professional Group on Engineering Management met recently with F. W. Schor as Chairman. A. W. Graf, patent lawyer, spoke about "Patent Law as it Concerns Employers and Employees." A panel of ten members discussed the subject further with Mr. Graf following his talk.

## TECHNICAL COMMITTEE NOTES

Under the chairmanship of D. C. Ports the **Antennas and Waveguides** Committee met on May 20. There was a discussion of Standards Committee actions on Waveguide terms. The latter part of the meeting was taken up with a discussion of Component definitions.

The **Circuits** Committee convened May 22 under the chairmanship of W. R. Bennett. W. A. Lynch, Chairman of Subcommittee 4.7 reported recommendations made at a meeting of his subcommittee concerning the list of feedback terms Appendix "A" 53 IRE 4. M3. The committee reviewed the above definitions.

The **Electron Devices** Committee convened on May 8 under the chairmanship of G. D. O'Neill. In the absence of R. B. Janes there was no report on Phototube Methods of Test. If the revised phototube definitions are satisfactory to Mr. Janes they will be started on Grand Tour. A report was relayed from Mr. Janes that his subcommittee has considered the latest revised proposals (Storage Tube Definitions) and that nearly all replies are in from a questionnaire sent to interested parties outside the subcommittee.

The **Facsimile** Committee met on May 8 under its new Chairman, Henry Burkhard. The activities of the committee under its former Chairman were reviewed and the following summary was given by J. H. Hackenberg. A general revision of the "1942 Standards on Facsimile: Definitions of Terms" has brought up to date the defini-

tions, which now encompass electronic as well as mechanical scanning techniques. Included are new recording techniques which separate the recording field from the closely related art of television. A list was given of the terms that had been acted upon, revised, and approved in present form by the committee. Also listed were the definitions under discussion but not acted upon. Another item under consideration by the committee is a test chart. On March 6, 1953 it was agreed that essentials of a test chart include four indicators of amplitude or density fidelity, and fifteen which serve to indicate the fidelity of dimension or positioning of the picture elements. A readability chart has been under discussion by the committee and some studies have been made but no definite action taken. The most recent proposal described in the Minutes of March 6, 1953 meeting looks promising, and may supplant the readability chart. After reading the summary of activities the scope of the committee was reviewed.

The **Information Theory and Modulation Systems** Committee met on April 21 under the chairmanship of W. G. Tuller. It was moved, seconded, and passed that the definitions (under consideration by the committee), in agreement with the broader point of view, are on communication theory rather than information theory and should be so headed. The remainder of the meeting was spent in a discussion of the above definitions.

The **Navigation Aids** Committee convened on May 25 under the chairmanship of P. C. Sandretto. Some time was spent discussing the definitions tentatively approved

at the April 27 meeting. Revisions were made in a number of them. Final review of the proposed definitions has now been completed.

On May 11 the **Video Techniques** Committee met under the chairmanship of W. J. Poch. The proposed standard on the Methods of Measurement of Aspect Ratio and Geometric Distortion tentatively approved at the last meeting was reviewed. After several minor corrections it was given final approval for consideration by the Standards Committee by unanimous vote of those present. A. J. Baracket reported that it was the intention of his subcommittee to continue its consideration of Methods of Geometric Distortion with emphasis on effects due to changes in scanning-beam velocity. It is understood that the Subcommittee on Video Signal Transmission is preparing a report on a method of measurement involving the use of a step signal in combination with a super-imposed high-frequency sine-wave. The Chairman reported that L. G. Grignon's paper entitled "Television Video Recording on Film" was returned to the Subcommittee on Utilization with the suggestion that minor revisions be made to reflect the changes in the art since the paper was prepared. The proposed Standards on Methods of Measurement of Pulse Quantities, Part I previously distributed to the committee members was discussed. Definitions approved at the previous meeting were again reviewed. The list of those definitions in the Video Techniques field previously issued in published form were reviewed and approved with a few exceptions.

## Western Electronic Show & Convention\*

CIVIC AUDITORIUM, SAN FRANCISCO, CALIF.—AUGUST 19–21, 1953

Wednesday, 10:00 A.M., August 19

### SESSION I: ELECTRON DEVICES I

*Chairman*, M. Chodorow, Stanford Univ.

- "A 1.8–4 KMC High Gain Wide-Band TWT Amplifier," S. F. Kaisel, L. A. Roberts, and R. P. Lagerstrom, Stanford Univ.
- "A Wide-Band Power Mixer Tube," H. R. Johnson, Hughes Research and Development Laboratories
- "A Wide-Tuning Range Microwave Oscillator/Amplifier," J. L. Putz and W. R. Luebke, Stanford Univ.
- "Helix-Type Backward-Wave Oscillators," D. A. Watkins, Stanford Univ.
- "Cross-Modulation in Traveling-Wave Amplifiers," A. W. C. Nation and J. W. Christie, Univ. of Washington

### SESSION II: COMPUTERS I

*Chairman*, L. D. Stevens, IBM

- "A Series-to-Parallel Data Converter," G. A. Neff, R. L. Sink, and H. E. Burke, Consolidated Engineering Corp.
- "A New Analog-to-Digital Voltage Converter," J. Zweig, California Institute of Technology
- "An Analog-to-Digital Conversion System

\* Sponsored jointly by IRE Region 7 and the West Coast Electronic Manufacturers Association.

- with Printed Decimal Read-Out," J. L. Lindesmith, Clary Multiplier Corp.
- "An Analog-to-Digital Converter," A. D. Scarbrough, Hughes Aircraft Co.
- "The Analyzing Reader," D. H. Shepard, Intelligent Machines Research Corp.

### SESSION III: NOISE AND SIGNAL SPECTRA

*Chairman*, W. W. Harman, Stanford Univ.

- "Instantaneous or Measurable Frequency Spectra," A. D. Watt and V. J. Zurick, National Bureau of Standards
- "The Response of Linear Systems to Non-Gaussian Noise," B. Gold and G. O. Young, Hughes Research and Development Laboratories
- "Linear Detection of Nonstationary Noise-Like Signals," Ralph Deutsch, Hughes Research & Development Laboratories
- "A System of Noise Analysis," S. D. Wannlass and D. M. Jacob, Hughes Research and Development Laboratories

Wednesday, 2:30 P.M., August 19

### SESSION IV: COMPUTERS II

*Chairman*, Torben Meisling, Univ. of California

- "An Improved Reading System for Mag-

netically Recorded Digital Data," Samuel Lubkin, Underwood Corp.

- "Magnetic Materials for Digital Computers," D. R. Brown, Massachusetts Institute of Technology
- "Panel Discussion on the Relative Merits of Different Memory Types," *Moderator*: P. L. Morton, Univ. of California

### SESSION V: AIRBORNE ELECTRONICS

*Chairman*, A. R. Ellis, Stanford Research Institute

- "The Air Navigation Development Board's Program for the Development of the Common System of Air Navigation and Traffic Control," D. K. Martin, Air Navigation Development Board
- "The Measurement of Performance of Airborne Voice-Modulated Communication Systems," E. J. Moore and John Taylor, Stanford Research Institute
- "Corona Interference Reduction by Polarity Discrimination," M. M. Newman, Lightning and Transients Research Institute
- "Magnetic Amplifiers and Their Applications," Victor Boros and David Seddman, Polytechnic Research and Development Co.
- "Airborne Weather Radar for Transport

Aircraft," Richard White, Trans World Airlines

SESSION VI: INSTRUMENTATION I

*Chairman*, D. B. Sinclair, General Radio Co.

"The Application of Counter Techniques to Precision Frequency Measurements," A. F. Boff, Berkeley Scientific Div., Beckman Instruments

"Two Timing-Circuit Innovations," H. B. Brooks, Hughes Aircraft Co.

"Strain Gage Oscillator," E. A. Varallo, Raymond Rosen Engineering Products

"Measurements of Time Jitter in Trains of Video Pulses," J. L. Fitch and R. R. Buss, Stanford Univ.

"A Peak-Reading Vacuum-Tube Voltmeter Which Has a Long Decay Time and is Capable of Measuring the Amplitude of Short Pulses," L. S. Cutler, Gertsch Products

SESSION VII: ELECTRON DEVICES

*Chairman*, T. Moreno, Varian Associates

"Convection Current Noise—Theory and Experiment," S. V. Yadavalli, Univ. of California

"Microwave Oscillator Stability," George Hetland and R. R. Buss, Stanford Univ.

"Air-Coolers for High-Power Vacuum Tubes," A. L. London, Stanford Univ.

"A High-Power High-Gain X-Band Pulsed Amplifier Klystron and Driver Multiplier," L. Zitelli, Varian Associates

"A High-Gain K-Band Amplifier," W. G. Abraham and F. L. Salisbury, Varian Associates

"Operating Behavior of High-Power Pulsed Klystrons," John Jasberg, Stanford Univ.

Thursday, 10:00 A.M., August 20

SESSION VIII: TRANSISTORS

*Chairman*, (to be announced)

"Recovery-Time Measurements on Point-Contact Germanium Diodes," Morgan McMahon, T. E. Firlie, and J. F. Roach, Hughes Aircraft Co.

"A Point-Emitter Junction-Collector Transistor," R. H. Kingston, MIT

"Measurement of the Small Signal Parameters of Transistors," Geoffrey Knight, Jr., R. A. Johnson, and R. B. Holt, Transistor Products, Inc.

"Rapid Determination of Some Electrical Properties of Semiconductors," Luther Davis, Jr., Lawrence Rubin, and W. D. Straub, Raytheon Manufacturing Co.

SESSION IX: ANTENNAS I

*Chairman*, A. S. Dunbar, Dalmo Victor Co.

"Design and Performance of Rotationally Symmetric Feeds for Paraboloidal Reflectors," H. W. Haas, R. W. Dressel, and R. D. Ewing, New Mexico College of Agriculture and Mechanic Arts

"A New Antenna Feed Having Equal  $E$  and  $H$  Plane Patterns," Alvin Chlavin, Hughes Aircraft Co.

"Waveguide Slot Arrays of Large Squint Angle," R. J. Adams and A. M. Lide, Naval Research Laboratory

"The Impedance Properties of Narrow Radiating Slots in the Broad Face of Rectangular Waveguides," Arthur A. Oliner, Polytechnic Institute of Brooklyn

"Principles of Spiral Scanners for Equal Pulse Distribution," J. Richard Huynen, Dalmo Victor Co.

"Boresight Theory for Homogeneous Dielectric Radomes," M. C. Horton, W. E. L. Boyce, and E. O. Hartig, Goodyear Aircraft Corp.

Thursday, 10:00 A.M., August 20

SESSION X: NUCLEAR RADIATION MEASUREMENTS

*Chairman*, H. S. Bright, U. S. Naval Radiological Defense Laboratory  
(Tentative Topics)

"Gamma and Electron Spectrometry with Crystals at High Energy"

"A Discussion of Some Unsolved Instrumentation Problems in Nuclear Physics"

"The Current Status of Radiation Detector Development"

"Neutron Source Standardization"

SESSION XI: SERVOMECHANISMS

*Chairman*, O. J. Smith, Univ. of California

"Nonlinear Control Systems with Random Inputs," R. C. Booton, Jr., MIT

"Comparison of Linear and Nonlinear Servomechanism Response," T. M. Stout, Univ. of Washington

"Time Quantization in a Feedback System," J. F. Waddell and H. D. Morris, Univ. of California

"Stability of Feedback Systems Using a Dual Locus Diagram," Paul Jones, California Institute of Technology

"Geometrical Interpretation of the Response of Linear Systems to Special Inputs," J. R. Moore, North American Aviation

Thursday, 2:30 P.M., August 20

SESSION XII: TRANSISTOR CIRCUITS

*Chairman*, H. M. Zeidler, Stanford Research Institute

"Recent Developments in Transistors," Irving Wolff, RCA

"Transistor Shift Registers," R. H. Baker, I. L. Lebow, and R. E. McMahon, MIT,

"A Point Contact Transistor VHF FM Transmitter," D. E. Thomas, Bell Telephone Laboratories

"A Four-Digit Transistor Accumulator," D. J. Eckl, MIT

"A Transistor Feedback Amplifier for Carrier Frequency Applications," J. C. Lozier and D. D. Cherry, Bell Telephone Laboratories

SESSION XIII: MICROWAVE THEORY & TECHNIQUES

*Chairman*, E. T. Jaynes, Stanford Univ.

"Mode Representations in Open and Closed Uniform Waveguides," Nathan Marcovitz, Polytechnic Institute of Brooklyn

"Applications of Coupled Helices," P. D. Lacy, Hewlett-Packard Co.

"New Applications of Faraday Rotation in Waveguides," A. G. Fox, M. T. Weiss, and S. E. Miller, Bell Telephone Laboratories

"Nonreciprocal Circuits Comprising Ferrite-Loaded Rectangular Waveguides," A. G. Fox, M. T. Weiss, and S. E. Miller, Bell Telephone Laboratories

"The Generation of Electromagnetic Oscillations in the Microwave Region Using

an Adiabatic Kind of Amplification," Gedalia Held, Univ. of California

SESSION XIV: ANTENNAS II

*Chairman*, J. T. Bolljahn, Stanford Research Institute

"Arrays of Closely Spaced Nonresonant Slots," R. J. Stegen and R. H. Reed, Hughes Aircraft Co.

"Diffraction Theory and the Patterns of Suppressed Antennas," George Sinclair, Univ. of Toronto

"Beam-Shaping and Optimum Bandwidth Methods Applied to UHF TV Transmitting Antennas," John Ruze and J. E. Martin, The Gabriel Laboratories

"Voltage Protection of Isolated Cap Aircraft Antennas," R. L. Tanner, Stanford Research Institute

"A Slotted Cylinder Omnidirectional Projector," J. P. Shanklin, Collins Radio Co.

SESSION XV: SERVOMECHANISM EQUIPMENT

*Chairman*, O. J. Smith, U. of Cal.

"A Method of Analysis and Synthesis of Closed-Loop Servo Systems Containing Small Discontinuous Type Nonlinearities," D. T. McRuer and R. G. Halliday

"Optimum Lead-Controller Synthesis in Feedback-Control Systems," L. G. Walters, U. of Cal., Los Angeles

"Predictor Servomechanisms," Lawrence Silva, U. of Cal., Berkeley

"A Complex-Frequency Generator, Yale Barkan, Hughes Aircraft Corp.

"Development of Precision Servo-Controlled Potentiometer-Setting Equipment," L. L. Gordon, Electronic Associated, Inc.

Thursday, 8:00 P.M., August 20

SESSION XVI: COLOR TELEVISION

*Chairman*, W. H. Doherty, Bell Telephone Laboratories

*Speakers:*

W. R. G. Baker, Vice-President, General Electric Co. and Chairman of the National Television System Committee  
Donald G. Fink, Director of Research, Philco Corp., and Chairman, Panel 12 of the NTSC

Friday, 10:00 A.M., August 21

SESSION XVII: AUDIO SYMPOSIUM

*Chairman*, Vincent Salmon, Stanford Research Institute

*Panel:*

"Microphones," W. B. Snow, Western Electro-Acoustic Laboratory

"Recording," F. G. Lennert, Ampex Corp.

"Amplifiers," A. N. Curtis, RCA Victor Division

"Loudspeakers," R. H. Smith, Univ. of Cal.

SESSION XVIII: CIRCUIT THEORY I

*Chairman*, B. J. Bennett, Stanford Research Institute

"The Practical Implication and Applications of Formal Network Theory," D. F. Tuttle, Stanford Univ.

"Design of a Simple Band-Pass Amplifier with Approximate Ideal Frequency Characteristics," W. E. Bradley, Philco Corp.

"Quasi-Distortionless Filter Functions," J. L. Stewart, Univ. of Michigan  
 "Fluctuation Noise Theory as Applied to Circuit Design," T. S. George, Air Force Missile Test Center, Patrick Air Force Base

SESSION XIX: MICROWAVE THEORY & TECHNIQUES II

Chairman, J. R. Whinnery, Univ. of California

"A Microwave Oscillograph," R. C. Honey, Stanford Research Institute  
 "Instrumentation of Microwave Electron Resonance in Magnetic Fields," R. C. Mackey and W. D. Hershberger, Univ. California  
 "An Improved Cross Guide Directional Coupler," H. J. Riblet, Microwave Development Laboratories  
 "Two Novel Types of Waveguide Switches," Amasa Pratt, Century Electronics, Division of Century Metalcraft Corp.  
 "Broad-Banding Circular Polarizing Transducers," D. L. Margerum, Microwave Engineering Co.

SESSION XX: PROPAGATION—GENERAL

Chairman, A. M. Peterson, Stanford Univ.

"Waveguiding on Surfaces with and without Loss," F. J. Zucker, Air Force Cambridge Research Center  
 "A New Solution to the Ionospheric Wave Equation," A. J. Mallinckrodt, The Ralph M. Parsons Co.  
 "Ionosphere Sounding by Cross-Correlation Techniques," P. B. Gallagher and A. M. Peterson, Stanford Univ.  
 "The Long-Distance Horizontal Directivity of a 13.7 MC Antenna," Richard Silberstein, National Bureau of Standards

Friday, 2:30 P.M., August 21

SESSION XXI: PROPAGATION, VHF & UHF

Chairman, J. B. Smyth, U. S. Naval Electronics Laboratory

"Results of Tropospheric Propagation Measurements on Frequencies from 92 to 1046 MC at the Cheyenne Mountain Field Station," A. F. Barghausen and K. O. Hornberg, National Bureau of Standards  
 "Characteristic of an 8.6 mm Radio Transmission Path," C. W. Tolbert and A. W. Straiton, The University of Texas  
 "An Investigation of the Variation of VHF Field Strength Beyond Line-of-Sight," G. H. Keitel and H. M. Swarm, Univ. of Washington  
 "Air-to-Air Propagation—Experimental and Theoretical Results," M. S. Wong, Wright Air Development Center  
 "The Role of Angular Distance in Tropospheric Radio-Wave Propagation," K. A. Norton, National Bureau of Standards  
 "Normal Propagation of Short Radio Waves Well Beyond the Horizon," T. J. Carroll and R. M. Ring, MIT

SESSION XXII: CIRCUIT THEORY II

Chairman, G. L. Matthaei, Univ. of California

"Solving Physical Systems with Very Large Number of Variables in Easy Stages," Gabriel Kron, General Electric Co.  
 "Matrix Analysis of Linear Time-Varying Circuits," L. A. Pipes, Univ. of California and U. S. Naval Ordnance Test Station  
 "Unbalanced RLC Networks Containing Only One Resistance and One Real Transformer," Louis Weinberg, Hughes Research and Development Labs.  
 "An Iterative Method for Network Synthesis," R. E. Scott, MIT and R. L. Blanchard, Transonics, Inc.

SESSION XXIII: INSTRUMENTATION II

Chairman, W. B. Wholey, Hewlett-Packard Co.

"Measurement Problems in VHF-UHF Television Antenna Systems," R. A. Soderman, General Radio Co.  
 "An Auto Impedance Meter for VHF-UHF," John Ebert, Polytechnic Research Development Co.  
 "A Ratiometer," N. L. Pappas, Hewlett-Packard Co.  
 "An Improved Method of Measuring the Current Amplification of Junction-Type Transistors," F. R. Stansel, Bell Telephone Laboratories

SESSION XXIV: AUDIO

Chairman, Roy Long, Stanford Research Institute

"Stereophonic Tape System," R. H. Snyder, Ampex Electric Corp.  
 "Application and Suggestions for Research Concerning Acoustical Problems in Medical Areas," J. K. Hilliard, Altec Lansing Corp.  
 "An Investigation of the Air Chamber of Horn-Type Loudspeakers," Bob H. Smith, Univ. of California  
 "A Simple Calibration Technique for Low Sensitivity Transducers," W. J. Gallo-way, Signal Corps Engineering Laboratories and Univ. of California

Friday, 8:00 P.M., August 21

SESSION XXV: MEDICAL ELECTRONICS

Chairman, A. J. Morris, USN Office of Naval Research

"Area Display by Electronic Mapping, Especially of the Electrical Activity of the Heart," Stanford Goldman, Syracuse Univ.  
 "Electronic Mapping of the Brain," A. R. Tunturi, Univ. of Oregon Medical School  
 "Radioactive Tracer Mapping," H. O. Anger and C. A. Tobias, Donner Laboratory of Medical Physics and the Univ. of California

## IRE People

Isaac L. Auerbach (S'46-M'49-SM'51) has been appointed manager of the Special Electronic Equipment Department of the Burroughs Adding Machine Co. He will primarily be concerned with defense equipment and magnetic development research for the government.



I. L. AUERBACH

Formerly a research engineer, Mr. Auerbach has been engaged in the design of electronic data processing systems and initiated work on magnetic components and circuits. He was responsible for the design of the static magnetic memory system for the ENIAC.

A native of Philadelphia, Mr. Auerbach received the B.S. degree in electrical engineering from Drexel Institute of Technology in 1943. He did graduate work at the Massa-

chusetts Institute of Technology and Harvard University, from which he received the M.S. in applied physics in 1947.

From 1943 to 1946 Mr. Auerbach served as a Navy radar officer, in 1945 assigned to the Naval Research Laboratory for work on IF systems. Prior to joining Burroughs he worked on the BINAC and UNIVAC systems at the Eckert-Mauchly Division of Remington Rand, Inc., and was a tube engineer with the Electronic Tube Corporation.

Mr. Auerbach is chairman of the Philadelphia chapter of the Professional Group on Electronic Computers. He is also a member of Eta Kappa Nu, the American Institute of Electrical Engineers, Association for Computing Machinery, the Scientific Research Society of America, and a registered professional engineer in the state of Pennsylvania.



Robert B. Beetham (S'34-A'36) has been named works manager of the Hicksville, N. Y. plant of Ampere Electronic Corp.

Mr. Beetham had been associated with the Airborne Instrument Laboratory, Mineola, N. Y., since 1949, where he held the positions of executive assistant to the vice president in charge of research and engineering, and since 1951 executive assistant director of research and engineering.



R. B. BEETHAM

Mr. Beetham was born in Jewett, Ohio on July 6, 1904. He received the B.S. degree in electrical engineering from Ohio State University in 1934 and the M.S. in 1936.

Following graduation Mr. Beetham became affiliated with the Collins Radio Company, Ames, Ia. A radio engineer, he eventually became assistant to the president.

Mr. Beetham has served on several IRE committees and is an associate member of the A.I.E. and a member of Eta Kappa Nu.

# IRE People

**Gano Dunn (F'15-L'50)** internationally known engineer and builder and president of the J. G. White Engineering Corporation of New York City, died recently.



GANO DUNN

Mr. Dunn was born in New York City on October 18, 1870. He received the B.S. degree from the College of the City of New York in 1889, and from Columbia University in 1891 the first degree of the first class in electrical engineering awarded degrees in the United States. He later attended RCA Institutes, and held a first-class commercial radio operator's license.

Following graduation, Mr. Dunn joined the Crocker-Wheeler Company and assisted in the design of motors, generators, transformers and other electrical apparatus. He subsequently became chief engineer, vice-president and a director of that company.

Mr. Dunn became associated with the J. G. White Engineering Corporation in 1911 as vice-president in charge of engineering and construction. As president from 1913 on, he directed many outstanding construction projects, among which were 13 transatlantic radio stations, the original Government aviation station at Langley Field, and roads, bridges, power plants, and irrigation systems in Latin America.

Mr. Dunn was elected a director of the Radio Corporation of America in 1938. He was also a director of RCA Communications, Inc., and the National Broadcasting Company. Active in the furtherance of education, he was chairman of the trustees and former president of Cooper Union for the Advancement of Science and Art. He was a member of the Visiting Committee of Harvard Engineering School and former president of the American Institute of Electrical Engineers.

Mr. Dunn was an officer or delegate on many scientific committees and special governmental commissions, including the Science Advisory Board of President Roosevelt. President Hoover offered the directorship of the Bureau of Standards to him. He was asked to consider the secretaryship of the Smithsonian Institution, and twice declined the presidency of the Massachusetts Institute of Technology.

Among the awards presented to Mr. Dunn were the Townsend Harris Medal of the College of the City of

New York, the Thomas A. Edison Medal of the American Institute of Electrical Engineers, the Egleston Medal of Columbia University, Hoover Medal of the National Engineering Societies, Modern Pioneer Award of the National Association of Manufacturers, and the Peter Cooper Medal of the Cooper Union.

Honorary degrees of Mr. Dunn include the D.Sc. from Columbia, Rutgers, Lehigh, and New York Universities, the College of the City of New York, and the LL.D. degree from Bowdoin College, Brunswick, Maine.

Mr. Dunn was honorary secretary for the United States of the Institute of Electrical Engineers and honorary president of the Pan-American Society.

Mr. Dunn was a fellow of the Royal Microscopy Society and the New York Academy of Sciences, and a member of the American Society of Civil Engineers, American Society of Mechanical Engineers, American Academy of Arts and Sciences, American Philosophical Society, Optical Society of America, New York Historical Society, and the New York Zoological Society, Phi Beta Kappa, Sigma Xi, Phi Beta Pi, and Delta Kappa Epsilon.



**George F. Maedel (M'43-SM'43)**, formerly vice president and general superintendent of the RCA Institutes, has been elevated to the presidency of the Institutes.



GEORGE F. MAEDEL

Mr. G. F. Maedel joined RCA Institutes in 1933 as the first instructor of the mathematics department. He transferred to the radio frequency department in 1936, where he became chief instructor in 1940. Mr.

Maedel was appointed assistant superintendent of the Institutes in 1944, and became superintendent in 1947. The next year he was elected to his former position as vice president and general superintendent.

A native of Brooklyn, Mr. Maedel was born there on July 21, 1903. He received the A.B. degree in 1924 and the E.E. degree in 1926 from Columbia University.

Mr. Maedel began his career with the New York Edison Company, where he worked in their planning bureau for a year following graduation. He joined the New York Telephone Company in 1927, to do traffic engineering. From 1931-1933 he headed the Audio Products Engineering Company, where he was concerned with installing public address systems.

Mr. Maedel is a licensed professional engineer in the state of New York.

**Paul N. Bergquist (M'48)**, broadcast consultant, has been appointed field sales representative for broadcast equipment for the RCA Victor Division of the Radio Corporation of America.

Mr. Bergquist was born in Spokane, Wash., on October 8, 1919. He received the B.S. degree in electrical engineering from State College, Pullman, Wash., in 1942. During his college years he was a radio operator for various northwestern radio stations.

In 1942 he joined the U. S. Navy as a radar officer and attended radar school at Harvard University and Massachusetts Institute of Technology. He served as a training and maintenance officer and later as staff radar officer of the Naval Air Advanced Training Command responsible for the training in and maintenance of radar of nineteen Naval Air stations.

After separating from the service in 1946, Mr. Bergquist became a radio engineer with Glen D. Gillett and Associates, later a partner of Gillett and Bergquist.



**Major William S. Dawson (A'49)** has assumed command of the 1300th Student Squadron of the Air Resupply and Communications Service, Mountain Home Air Force Base, Idaho.

Major Dawson recently returned from Japan, where he was Director of Plans and Requirements for 1808th Airways and Air Communications Service Wing. He was responsible for supervision of planning and engineering of communications facilities and electronic navigational aids throughout the Pacific and Korea. He had been Deputy Director until that position was created.

During the past sixteen years Major Dawson has served in military aviation in meteorological and communications assignments such as commanding officer of an AACS Squadron and at the Headquarters of the former Army Air Corps.

Major Dawson is a member of the American Geophysical Union, American Institute of Physics, American Meteorological Society, American Association for Advancement of Science, and the Institute of Aeronautical Sciences.



**J. Walton Colvin (M'51)** has been appointed manager of government sales for the Communication Division of Bendix Radio.

Mr. Colvin joined Bendix in 1942 as a vhf instructor. He successively became technical advisor to the Mediterranean Headquarters of the Air Force from 1944-46, aviation service engineer, and aviation sales engineer. Since 1948 he has been merchandising manager, dealing in Air Force sales.

A native of Somerset, Va., Mr. Colvin was born on December 30, 1914. He is a graduate of the National Radio Institute of Washington, D. C., and Northwestern Institute, Ames, Iowa.

Previous to his association with Bendix Mr. Colvin operated his own radio, electrical sales, and service business.

# IRE People

David E. Cavanaugh (A'46), Aircraft Transformer Corporation, Long Branch, N. J., has been elevated from the position of assistant to chief engineer.

Mr. Cavanaugh was born on September 26, 1919 in North Carolina. He received the B.S. degree in electrical engineering from the Georgia School of Technology, Atlanta, Ga., in 1940.

Following graduation Mr. Cavanaugh worked briefly for the Atlantic Coast Line Railroad Company as a special apprentice before joining the U. S. Army Signal Corps. As a captain Mr. Cavanaugh was concerned with communication of all types and the organization, planning, and training for a signal operation battalion until 1944.

Mr. Cavanaugh joined Bell Telephone Laboratories in 1945. As a member of the power apparatus group he was concerned with small power transformer design and high voltage cathode-ray tube power supplies. He joined the Aircraft Transformer Corporation in 1952.

Mr. Cavanaugh is a member of the AIEE.



Fred W. Albertson (A'33-M'44-SM'49), radio engineer, attorney at law, and partner of Dow, Lohnes and Albertson, Washington, D. C., has been elected president of the Federal Communications Bar Association.



F. W. ALBERTSON

Mr. Albertson was born in Fairgrove, Mich., on September 29, 1908. He received the A.B. degree from the University of Michigan in 1931 and the LL.B. in 1934. He was admitted to the bar in Michigan in

the same year, the District of Columbia in 1935, the Supreme Court of the United States in 1940, U. S. Treasury Department in 1935, Federal Communications Commission, Interstate Commerce Commission, and Securities and Exchange Commission in 1936, and other boards and commissions.

Mr. Albertson has been an amateur radio operator since 1920 and holder of a commercial license since 1925, from which date he did work as chief operator and engineer until 1934. He became a registered professional electrical-communications engineer in the District of Columbia in 1952.

Since 1934 Mr. Albertson has been radio law counsel for numerous radio, telegraph, telephone and broadcast companies and stations, consulting radio engineering firms, and radio manufacturing companies. These include Westinghouse Electric Co., Radio Engineering Laboratories, Inc., Gulf Research and Development Co., Major Edwin H. Armstrong, FM Development Foundation, Paul F. Godley Co., Raymond M. Wilmotte, and others.

Mr. Albertson has been active in IRE activities of the Detroit and Washington Sections and nationally, having served in

various offices of the Washington Section and on the national committees of Public Relations, Awards, and Constitution and By-Laws. He is currently on the Board of Editors and Membership committees.

Mr. Albertson is a member and former president of the Washington Radio Club and the University of Michigan Radio Club (of which he was co-founder). He is a charter member and has held various offices in the Engineers Club of Washington and Federal Communications Bar Association.

Among the other professional societies to which Mr. Albertson belongs are the Academy of Arts and Sciences, the Philosophical Society of Washington, the Radio Pioneers, Delta Theta Pi, American Bar Association, Bar Association of the District of Columbia, and the American Judicature Society.



D. W. Gunn (M'47) has been appointed to the newly created post of assistant general sales manager of the radio and television tube division of Sylvania Electric Products, Inc. He will continue his duties as sales equipment manager.



D. W. GUNN

Mr. Gunn has been with Sylvania since 1931, when he started as a factory engineer in Salem, Mass. In 1936 he became a sales engineer in Chicago, and since then has worked successively as a quality engineer, supervisor of quality control, eastern district sales engineer, east central district sales engineer, and assistant to the general sales manager. He became equipment sales manager in 1951.

Born in New York state in 1907, Mr. Gunn received the B.E.E. degree from Northeastern University, Boston, Mass. in 1929. He then joined the New England Power Co., later the Raytheon Manufacturing Co., Newton, Mass. as a production engineer.



Lawrence A. Hyland (A'29), vice president of Bendix Aviation Corp., has been placed in charge of its engineering program.

Formerly in charge of Bendix research, Mr. Hyland has been a vice president since 1949. He joined Bendix in 1935, when the Radio Research Company which he founded became affiliated with Bendix, and in 1937 became general manager of radio operations, and vice president of Bendix Radio Corp. In 1943 he was elevated to executive engineer of the Aviation Corp.

Mr. Hyland was born in Woodlawn, Nova Scotia on August 26, 1897. In 1917 he joined the U. S. Army, serving as a radio sergeant. In 1920 he transferred to the aviation branch of the U. S. Navy as a chief radioman. He participated in the first blind landing of a flying boat by radio in 1921. He

was given a special discharge in 1926 to become an assistant, later associate radio engineer at the Naval Research Laboratory. Here he first observed and proved the principle of radar detection of aircraft in 1931.

In 1950 Mr. Hyland received the Navy's highest civilian honor, the Distinguished Public Service Award, for his "great service to science and to the welfare of the United States through his early contribution to the development of radar." He is credited with more than 40 inventions, including the radio-shielded spark plug which made possible modern aircraft communications by clearing up interference, the Navy radio wing-loop direction finder, and frequency indicators.

Mr. Hyland is a member of the Guided Missiles Committee of the U. S. Research and Development Board, the Industry and Advisory Board of the U. S. Air Force Arnold Engineering Development Center, the Institute of Naval Engineers, and the Society of Automotive Engineers.



John K. Mitchell (A'40-SM'46) has joined the newly organized Barth Engineering and Manufacturing Co. of Milldale, Conn. as vice president and general sales manager. This company was called the Barth Manufacturing Co. under former ownership.



J. K. MITCHELL

Mr. Mitchell was formerly associated with Sperry Gyroscope Co., Great Neck, L. I. Since 1946 he had been a sales representative, and more recently that company's representative to the U. S. Navy.

Mr. Mitchell was born in East Orange, N. J., on November 10, 1906. He received the B.S. degree in electrical engineering from the Newark College of Engineering in 1936. While serving in the Navy from 1942-45 he attended Bowdoin College's pre-radar course, the Massachusetts Institute of Technology's Radar School and the Naval Research Laboratory's special project school.

Mr. Mitchell then became an anti-jamming officer in the Bureau of Aeronautics, conducted field tests of anti-jamming devices, was an aide to a Navy Liaison officer at the Radio Research Laboratory and Radiation Laboratory in Cambridge, Mass., and finally officer in charge of the Radio Research Navy Office of the Radio Research Laboratory at Harvard University.

Before joining the Navy in 1942 Mr. Mitchell had served from 1923-27 as a radioman in the submarine service. He then worked for a year with the New York Telephone Co. before joining the New Jersey Telephone Co. Until 1938 he held various positions with this company, at which time he became an instructor in electrical engineering at the Newark Technical School.

Mr. Mitchell is a military member of the Society of Naval Engineers.



# Abstracts and References

Compiled by the Radio Research Organization of the Department of Scientific and Industrial Research, London, England, and Published by Arrangement with that Department and the *Wireless Engineer*, London, England

NOTE: The Institute of Radio Engineers does not have available copies of the publications mentioned in these pages, nor does it have reprints of the articles abstracted. Correspondence regarding these articles and requests for their procurement should be addressed to the individual publications, not to the I.R.E.

Acoustics and Audio Frequencies.....	1074
Aerials and Transmission Lines.....	1075
Circuits and Circuit Elements.....	1076
General Physics.....	1078
Geophysical and Extraterrestrial Phenomena.....	1079
Location and Aids to Navigation.....	1080
Materials and Subsidiary Techniques.....	1080
Mathematics.....	1082
Measurements and Test Gear.....	1082
Propagation of Waves.....	1084
Reception.....	1085
Stations and Communication Systems.....	1086
Subsidiary Apparatus.....	1087
Television and Phototelegraphy.....	1087
Transmission.....	1088
Valves and Thermionics.....	1088
Miscellaneous.....	1088

The number in heavy type at the upper left of each Abstract is its Universal Decimal Classification number and is not to be confused with the Decimal Classification used by the United States National Bureau of Standards. The number in heavy type at the top right is the serial number of the Abstract. DC numbers marked with a dagger (†) must be regarded as provisional.

## ACOUSTICS AND AUDIO FREQUENCIES

- 534.2:534.011** 1874  
**An Acoustic Gyrotor**—W. E. Kock. (*Arch. elekt. Übertragung*, vol. 7, p. 106; Feb. 1953. In English.) A device is described which is the acoustic analogue of the microwave gyrotor described by Hogan (1233 of 1952). The required nonreciprocal rotation of the plane of polarization of transverse acoustic waves propagated in a tube is accomplished by rotating a section of the tube at high speed.
- 534.21-13** 1875  
**On Sound Waves of Finite Amplitude**—E. T. Copson. (*Proc. Roy. Soc. A.*, vol. 216, pp. 539–547; Feb. 24, 1953.) An analytical solution of Riemann's equations for the one-dimensional propagation of sound waves of finite amplitude in a gas obeying the adiabatic law  $p = k\rho^\gamma$  is obtained for any value of the parameter  $\gamma$ .
- 534.231** 1876  
**The Sound Field of a Piston Source**—E. W. Guptill. (*Canad. Jour. Phys.*, vol. 31, pp. 393–401; March 1953.) "An exact solution is presented for the sound field between two infinite walls when the source is a piston in one of the walls. A method is also outlined for the case of a source having any amplitude distribution which is a function only of radial distance from the center of the source."
- 534.231** 1877  
**The Acoustic Radiation of the Rectangular Piston Membrane**—H. Stenzel. (*Acustica*, vol. 2, pp. 263–281; 1952. In German.) General formulas are obtained for calculating the sound field immediately in front of the membrane. The adjacent field is calculated by graphical integration. Field contours for square membranes with different dimension/wavelength ratios are shown. General formulas for the radiation impedance are derived; its two components are calculated and represented graphically for

The index to the Abstracts and References published in the PROC. I.R.E., from February, 1952 through January, 1953, is published by the *Wireless Engineer* and may be purchased for \$0.68 (including postage) from the Institute of Radio Engineers, 1 East 79th St., New York, 21 N. Y. As suppliers are limited, the publishers ask us to stress the need for early application for copies. Included with the Index is a selected list of journals scanned for abstracting with publishers' addresses.

membranes with sides in ratio 1, 2, 5 and 10 to 1.

**534.231** 1878

**The Physics of Sound Radiation Pressure**—F. Borgnis. (*Z. Phys.*, vol. 134, pp. 363–376; Feb. 6, 1953.) The radiation pressure of a free beam of a plane compression wave incident normally on a plane obstacle is investigated by means of the hydrodynamic impulse law; this method gives a clear physical idea of the forces on the obstacle. The formulas are derived in terms of both Euler and Lagrange variables. Making use of Brillouin's tensor potential a boundary condition for the beam is derived which takes account of the energy exchange between the beam and the ambient medium; this boundary condition leads to a simple relation between the radiation pressure and the difference of the energy densities on the two sides of the obstacle. As a particular case, the radiation pressure on the boundary surface between two immiscible fluids is considered.

**534.232:534.321.9** 1879

**Ultrasonic Whistles**—A. E. Crawford. (*Research, Lond.*, vol. 6, pp. 106–110; March 1953.) Descriptions are given of generators of resonant-cavity and resonant-wedge type using gas or liquid exciting jets; these are useful for low-power applications such as experiments on ultrasonic propagation in gases, and the emulsification of low-viscosity liquids. Power is provided by a compressor or pump.

**534.241:551.510.52** 1880

**Study of the Echoes of Acoustic Waves in the Stratified Region of the Troposphere**—G. Eckart. (*Acustica*, vol. 2, pp. 256–262; 1952. In French.) Methods of Bremmer and of Schelkunoff are applied to derive wave equations for sound propagation in a stratified atmosphere. The importance of the terms which render the analogy to em wave propagation incomplete (Eckart & Lienard, Jan. 4) is clearly shown.

**534.26** 1881

**On Acoustic Diffraction through an Aperture in a Plane Screen**—J. W. Miles. (*Acustica*, vol. 2, pp. 287–291; 1952. In English.) Generalized Fourier transforms are applied to derive equations for the scattered wave. The aperture impedance is expressed in variational form and compared with the Kirchhoff approximation. Reflection from a disk and diffraction at a circular aperture for the case of oblique incidence are considered. (See also 2686 of 1952.)

**534.3** 1882

**Experimental Study of the Acoustic, Physiological and Psychophysiological Conditions relating to the Aesthetics of Music**—R. Husson. (*Ann. Télécommun.*, vol. 8, pp. 51–72; Feb. 1953.)

**534.32:621.396.619.11** 1883

**Perception of Amplitude Modulations**—H. Ebel. (*Akust. Beihefte*, no. 4, pp. 246–250; 1952.) Modulation at high frequencies is perceptible at modulation levels lower than that required for perception of low-frequency modulation. Amplitude modulations are less discernible in speech and music than in pure tones. Experimental results agree with those of Zwicker (303 of February) and give an indication of the limiting distortion factor of a loudspeaker for agreeable reproduction.

**534.321.9** 1884

**Ultrasonics in Solids**—G. Bradfield. (*Research (London)*, vol. 6, pp. 68–79; Feb. 1953.) Thermal vibrations in solids are discussed in relation to physical constants, and the application of ultrasonic and vhf techniques in elasticity measurements is described. Different forms of BaTiO<sub>3</sub> transducer are shown and applications of ultrasonics in different technical fields are reviewed.

**534.321.9:621.391.6** 1885

**Use of Ultrasonics in Telephony**—L. Pimow. (*Ann. Télécommun.*, vol. 8, pp. 28–30; Jan. 1953.) Measurements have been made of the attenuation of ultrasonic waves propagated in various media, e.g. metal wires, water-filled pipes and air. As a result, equipment has been developed for short-range telephony by means of modulated ultrasonic waves. For two-way operation a suppressed-carrier system may be used; for one-way operation the carrier should be retained. A system is described suitable for conference-room use, with air as the medium of propagation. The carrier-frequency range is 16–100 kc and the radiated power 2–3 W. The receiver is carried on a headband.

**534.44** 1886

**Frequency Analysis of Acoustic Phenomena**—R. Bierl. (*Akust. Beihefte*, no. 4, pp. 225–235; 1952.) The application of a spectral-function diagram derived from the Fourier integral in filter-circuit and integration methods of wave-form analysis is illustrated. Waveforms considered are rectangular and exponential pulses, and sine waves with rectangular and exponential envelopes. The time variation of amplitude and the relative phase of individual frequency components are determined for a limited number of components from the width and position of maxima and the angular velocity of the radius vector of the spectral-function diagram.

**534.6:534.321.2** 1887

**Measurement of Harmonic Intervals of the Musical Scale based on the Subjective Sensation of Consonance**—M. Barkechli. (*Acustica*, vol. 2, pp. 242–250; 1952. In French.)

**534.6:621.395.623** 1888

**The Problem of the Artificial Ear for Cali-**

- brating Telephone Receivers—I. Barducci. (*Arch. elekt. Übertragung*, vol. 7, pp. 155-157; March 1953.) (See Schiaffino, 1814 of 1952.)
- 534.62 1889  
**New Anechoic Chamber of the Technische Hochschule, Karlsruhe**—H. Ebel and P. Maurer. (*Akust. Beihefte*, no. 4, pp. 253-256; 1952.) The design and construction of an anechoic chamber are described. By combining wedge-shaped absorbers and damped Helmholtz resonators an absorption factor of 99% for frequencies down to 160 cps is attained. Total thickness of the wall lagging is 61 cm. Absorption characteristics of the material and of the complete chamber are compared.
- 534.75 1890  
**Contribution to a Scientific Theory of Single-Channel Transmission of Sound (Part 2)**—P. Burkowitz. (*Funk u. Ton*, vol. 7, pp. 10-26; Jan. 1953.) The significance of the amplitude and path-time ratios of reflected and direct sound, and their relation to tonal quality, are discussed (Part 1: 1229 of May).
- 534.771 1891  
**The Békésy Audiometer of the Technische Hochschule, Stuttgart**—W. Kaiser. (*Akust. Beihefte*, no. 4, pp. 235-238; 1952.) Modifications to the audiometer (Békésy, 3325 of 1949), have been made so that threshold intensities throughout the region of audibility may be accurately determined.
- 534.771:534.61 1892  
**The Trend of the Modulation Threshold in the Audible Range**—F. Zwicker and W. Kaiser. (*Akust. Beihefte*, no. 4, pp. 239-246; 1952.) Audiometer methods were used to determine the threshold of perceptibility of loudness and pitch variations of pure tones modulated by a 4-cps tone at different modulation levels. Results for cases of defective and also of normal hearing are discussed.
- 534.84 1893  
**Diffusion in Architectural Acoustics**—W. Furrer and A. Lauber. (*Acustica*, vol. 2, pp. 251-256; 1952. In German.) Analysis of results of measurements shows that the irregularities in the frequency characteristic of a room are not a direct measure of the homogeneity of the sound field, but the mean height of the peaks is a parameter related directly to the "diffusion," or field homogeneity. This parameter has been determined at frequencies around 375 cps and 1650 cps for 11 studios and halls varying in size from 37 m<sup>3</sup> to 20,000 m<sup>3</sup>. Two examples are discussed.
- 534.843 1894  
**Boundary Conditions for the Acoustic Wave Equation**—T. Vogel. (*Acustica*, vol. 2, pp. 281-286; 1952. In French.) The concept of specific normal impedance is discussed in relation to the boundary conditions obtaining for sound propagation in a closed space. Experimental results for a simple case are at variance with this concept. A modified hypothesis is suggested involving two specific impedances, one normal and one tangential to the surface considered.
- 534.843:534.24.001.57 1895  
**Reflection of Sound at Surfaces with Periodic Structure**—E. Meyer and L. Bohn. (*Akust. Beihefte*, no. 4, pp. 195-207; 1952.) The efficacy of uniformly spaced diffusing elements fixed to plane walls has been investigated on small-scale models, using frequencies in the range 15-60 kc. A diffusion index is calculated, which is the ratio of the reflected sound energy outside the 20°-region of the geometrical reflection to the total reflected energy. The dependence of this index on wavelength, width and depth of the projections and angle of incidence of the sound beam, is discussed for projecting elements of semicircular, triangular and rectangular cross-section in front of (a) perfectly absorbing, (b) perfectly reflecting surfaces.
- 534.846.6 1896  
**Measurement of the Reflecting Power of Ceilings, using Ultrasonics**—F. Canac. (*Comp. Rend. Acad. Sci. (Paris)*, vol. 236, pp. 467-469; Feb. 2, 1953.) The effectiveness of ceiling treatments such as hollow panels for controlling the reverberation time of halls is investigated by using small-scale models together with proportionately increased frequencies.
- 621.395.61 1897  
**Sensitivity of Microphones to Stray Magnetic Fields**—L. J. Anderson. (*Trans. Inst. Radio Engrs.*, vol. AU-1, pp. 1-6; Jan./Feb. 1953.) Equipment is described and simple theory is given for (a) comparison of various types of microphone with respect to their sensitivity to hum fields, (b) measurement of hum fields existing in the neighborhood of microphones. Charts show the hum spectra observed in some particular cases.
- 621.395.61:534.612 1898  
**An Experimental Probe Microphone for the Measurement of Sound Pressures**—R. B. Archbold. (*P. O. Elect. Eng. Jour.*, vol. 45, part 4, pp. 145-148; Jan. 1953.) Account of the development of a microphone designed primarily for acceptance tests on telephone apparatus. A long narrow tube is coupled to the diaphragm, and the sensitivity/frequency characteristic is smoothed by introducing a small amount of lamb's wool into each end of the tube.
- 621.395.623.8:621.396.645.371 1899  
**Portable P.A. [public-address equipment]**—E. Griffiths. (*Wireless World*, vol. 59, pp. 201-204; May 1953.) Description of equipment giving an output of 8W with <1% distortion for use in small halls. It includes record player, amplifier, loudspeaker and power pack, the whole contained in two cases of about equal size and weight. The negative-feedback amplifier has arrangements for either single-ended or push-pull input, the latter being more suitable for use with the crystal pickup.
- 621.395.625(083.74):621.396.822 1900  
**Standards on Sound Recording and Reproducing: Methods of Measurement of Noise, 1953**—(Proc. I.R.E., vol. 41, pp. 508-512; May 1953.) Standard 53 IRE 1951.
- 621.395.625.3 1901  
**Print-Through Effect in Magnetic Tape for Sound Recording**—H. J. Tafel. (*Fernmelde- u. Z.*, vol. 6, pp. 17-24; Jan. 1953.) An experimental investigation of printing through, in adjacent windings of rolled tape, in respect of the intensity and permanence of this magnetization. Its dependence on the temperature, and on the duration, frequency and intensity of the original magnetization is assessed.
- 621.395.625.3:534.76 1902  
**A Practical Binaural Recording System**—O. C. Bixler. (*Trans. Inst. Radio Engrs.*, vol. AU-1, pp. 14-22; Jan./Feb. 1953.) Modifications to commercial tape recording and reproducing equipment are described resulting in a simple stereophonic system comprising two microphones and two loudspeakers, each channel using half the tape. Various applications are indicated, including court-room reporting. Broadcasting tests were made by connecting one microphone to an A.M. transmitter and the other to a F.M. transmitter, the listener using A.M. and F.M. receivers simultaneously.
- 621.395.92:621.314.7 1903  
**Transistorized Hearing Aids**—J. D. Fahnestock. (*Electronics*, vol. 26, pp. 154-155; April 1953.) Circuit and performance details are given of various commercially available hearing aids using (a) subminiature valves and transistors or (b) transistors exclusively. Only junction-type transistors are used, with grounded-emitter circuits. Noise level is discussed. Some models have facilities for switching from microphone to a telephone pickup coil.
- 681.84 1904  
**Piezo-electric Crystal Pick-ups**—S. Kelly. (*Jour. Brit. IRE*, vol. 13, pp. 161-170; March 1953.) Bimorph crystal elements are used, usually torsional in the case of Rochelle salt, and always benders in the case of BaTiO<sub>3</sub>. Design methods make use of equivalent electrical circuits. Needle-tip impedance can be reduced to obtain satisfactory tracking at a needle pressure of <5 gm. Frequency response can be levelled from 20 cps to 20 kc, using simple equalizers. Wear and distortion are discussed. Details are given of a two-stylus pickup for 78- and 33<sup>1</sup>/<sub>3</sub>-rpm records.

## AERIALS AND TRANSMISSION LINES

- 621.315.2.015.7 1905  
**Theory of Pulse Technique for Coaxial Cables**—P. Behrend. (*Z. angew. Phys.*, vol. 5, pp. 61-64; Feb. 1953.) Analysis is given for the deformation experienced by rectangular or half-sine-wave pulses traversing a coaxial cable, the transfer function of the cable being assumed to be a subfunction of a Laplace transform. Results are shown in graphs.
- 621.392.21.09 1906  
**Physical Explanation of the Surface Wave on a Dielectric-Coated Line**—P. J. M. Clavier. (*Cables & Trans. (Paris)*, vol. 7, pp. 34-38; Jan. 1953.) The propagation of a surface wave is treated as a series of reflections alternately at the metal surface and the dielectric/air interface. By analogy with waveguide propagation an E<sub>0</sub> mode is defined. Below the limiting frequency for propagation along the line, energy is radiated and the mode analogy is destroyed. The relation between angle of incidence on the reflecting surfaces and the phase and group velocities is illustrated and the variation of the latter as a function of frequency is shown graphically.
- 621.392.26:621.315.61 1907  
**Propagation in Waveguides filled Longitudinally with Two or More Dielectrics**—L. G. Chambers. (*Brit. Jour. Appl. Phys.*, vol. 4, pp. 39-45; Feb. 1953.) Discussion of the propagation of pure TE and TM modes in inhomogeneously filled rectangular and circular waveguides, summarizing the results of research work published since 1943. 16 references.
- 621.396.67 1908  
**An Alternative Method of solving Hallén's Integral Equation and its Application to Antennas near Resonance**—R. King. (*Jour. Appl. Phys.*, vol. 24, pp. 140-147; Feb. 1953.) Hallén's equation is separated into two equations for the in-phase and quadrature-phase current components respectively; these are solved by an iteration method. For values of aerial electrical half-length near odd multiples of  $\lambda/4$ , at least a third-order solution is required for the accurate determination of in-phase current and conductance. Conductance values for a range of radii are evaluated using the third-order formula; comparison with experimental results indicates that for antennas near resonance, just as for very short and very long antennas, account must be taken in the iteration procedure of both the current components.
- 621.396.67 1909  
**Power Gain of Curtain Arrays of Aerials**—P. Hammond. (*Wireless Eng.*, vol. 30, pp. 108-111; May 1953.) The directional concentration of power by systems comprising uniformly spaced antennas carrying equi-phase currents is investigated using the concept of radiation resistance. The field due to an infinitely long filament is first considered and a solution is obtained in terms of Bessel functions of zero order and of the first and second kinds. From this the power output can be determined for a single antenna and for combinations of various numbers of antennas in arrays. For a spacing of about  $3\lambda/4$  between elements, the power gain passes through a maximum, its value being



then about 50% greater than the value for  $\lambda/2$  spacing. This maximum is also obtained for finite-height antennas and for arrays having depth as well as width.

621.396.67:621.315.612.4:621.396.611.4 1910  
Quasi-Degenerated Modes in High- $\epsilon$  Dielectric Cavities—Schlicke. (See 1942.)

621.396.67:621.396.9 1911  
Moulded Plastic Radar Scanners and Stressed Components—(Engineering (London), vol. 175, pp. 28–29; Jan. 2, 1953.) The 14-ft. radar reflector described consists of a sandwich-like construction having outer layers of asbestos-fibre material impregnated with phenolic resin and a resin-impregnated paper-honeycomb core. It is as strong as, stiffer than, and weighs half as much as a reflector made of Al alloy; resistance to weathering is good.

621.396.677 1912  
Reception Diagrams of Rhombic Aerials in a Vertical Plane—J. Dufour. (Tech. Mitt. Schweiz. Telegr.-Teleph. Verw., vol. 31, pp. 65–72; March 1, 1953. In French.) Measurements were made of the received signal strength on the ground, at Châttonnaye, using an airborne transmitter. Results obtained with two slightly different rhombic aerials were compared with the theoretical values for frequencies of 5, 10, 15, 20, 25 and 30 mc. Good agreement was found. There is a strong ground reflection at 6–7 km from the station, giving rise to marked interference for angles of incidence  $< 8^\circ$  from the horizontal.

621.396.677 1913  
A Theory of Plane Reflectors in Microwave Antenna Systems—H. L. Knudsen and M. Andreasen. (Trans. Dan. Acad. Tech. Sci., no. 3, pp. 3–57; 1952.) Values are calculated for the field reflected from an apparently circular reflector illuminated by a point radiator; they differ considerably from results obtained by Aasma. For the case of a finite-size radiator, the calculations are based on the assumption of rectangular radiator and reflector apertures. Curves are presented from which the reflected field and the gain can be read directly or determined by a combination of two readings. Errors introduced by the simplifying assumptions are discussed. Fresnel integrals and related functions are used in the analysis; relevant tables and curves are given.

621.396.677:621.392.26 1914  
Second-Order Beams of Slotted-Waveguide Arrays—H. Gruenberg. (Canad. Jour. Phys., vol. 31, pp. 55–69; Jan. 1953.) Second-order beams due to slot offset have escaped detection because they are not located in the plane containing the waveguide axis, where the radiation pattern is usually measured. The patterns of the second-order beams for a waveguide with staggered slots are analyzed by considering an approximately equivalent arrangement of two parallel linear arrays separated by twice the weighted mean offset. The second-order beams can be suppressed by using (a) an array with all slots aligned and appropriate corrugations in the waveguide wall, or (b) a conventional waveguide array fitted with a horn incorporating a parallel-plate section (3343 of 1952).

621.396.677:621.392.26 1915  
Theory of Waveguide-Fed Slots radiating into Parallel-Plate Regions—L. Lewin. (Jour. Appl. Phys., vol. 24, p. 232; Feb. 1953.) Simpler alternative expressions are derived for integrals introduced in the original paper by Gruenberg (3343 of 1952).

621.396.677:029.62 1916  
Theory of Artificial Slot Antennas—A. Ataman. (Bull. Tech. Univ. Istanbul, vol. 4, pp. 71–89; 1951. In English.) The term "artificial slot" is applied to a radiator comprising a dielectric rod of rectangular cross-section, lying on a conducting surface and having two sides

covered with metal plates between whose upper edges an electric field is established. Such devices are useful for the frequency range 100–300 mc, and may have advantages over a true slotted aerial for use in high-speed aircraft. Analysis is given, treating the arrangement as a uniformly loaded transmission line. A determination is made of the properties of the dielectric required to give satisfactory radiation efficiency; high permeability and low losses are desirable. A numerical calculation is made for a  $\lambda/2$  aerial to operate at 200 mc with a slot width of 2 cm; for a material with a dielectric constant of 10 the slot depth is 0.5 cm.

621.396.677.5:621.318.132 1917  
Receiving Properties of a Wire Loop with a Spheroidal Core—J. R. Wait. (Canad. Jour. Tech., vol. 31, pp. 9–14; Jan. 1953.) The relative gain of a loop antenna with spheroidal core is calculated, assuming core losses to be negligible, an assumption which is justified for ferromagnetic ceramics at frequencies of the order of 200 kc or lower. The magnetic properties of modern ferromagnetic materials are used to good advantage when the spheroid is highly elongated or very much flattened.

#### CIRCUITS AND CIRCUIT ELEMENTS

621.3.011.22/.23:621.315.512 1918  
Internal Alternating-Current Resistance and Reactance of Conductors of Circular Cross-Section—P. M. Prache. (Câbles & Trans. (Paris), vol. 7, pp. 28–33; Jan. 1953.) A numerical table is presented for simple and accurate calculations for solid conductors and for thin or thick tubes. Proximity effect is neglected.

621.3.014/.016:621.3.012.1 1919  
Vector Representation in the Time Plane of Electrical Potential Difference, Current and Power varying Sinusoidally in Time—G. Kouskoff. (Rev. gén. Elect., vol. 62, pp. 86–90; Feb. 1953.) The varying magnitudes are considered, according to a method originally used by Fresnel, as the resultant of two imaginary vectors of equal and constant length, rotating at the same rate in opposite senses. The imaginary plane containing these vectors is called the "time plane." The impedances of a circuit to the two vector components of a sinusoidally varying current are defined, and the method of representing power, i.e. the product of voltage and current, is explained.

621.3.015.7:621.387.4 1920  
A New Pulse-Analyzer Design—C. W. Johnstone. (Nucleonics, vol. 11, pp. 36–41; Jan. 1953.) Description, with detailed circuit diagrams, of a single-channel analyzer which serves as the basic design for multichannel analyzers, details being given of a 10-channel analyzer. Positive pulses are accepted in the amplitude range 3–103 V plus the sum of channel widths. The width and position of the channels can be changed quickly without requiring recalibration. The design is simple and relatively few tubes are required.

621.316.86:537.312.6 1921  
Resistor Temperature Coefficients—F. A. Paul. (Tele-Tech, vol. 12, pp. 52–53, 120; Jan. 1953.) Tests were carried out on four types of pyrolytic-carbon-film resistor and one type of metal-film resistor, several samples of each type, of different resistance ratings, being used. The results obtained for the temperature range from  $-30$  to  $+120^\circ$  C are shown graphically. The temperature coefficients of the carbon-film resistors are considerably lower than those of carbon-composition resistors. The coefficients are negative and much greater than those of wire-wound resistors, though this is not the case for borrocarbon-film resistors [2365 of 1951 (Grisdale et al.)].

621.318.4.011 1922  
Determination of Voltage, Current, and Magnetic Field Distributions together with the Self-Capacitance, Inductance and H.F. Resistance of Single-Layer Coils—A. E. S. Mostafa

and M. K. Gohar. (Proc. IRE, vol. 41, pp. 537–547; May 1953.) A theoretical investigation is made which is applicable to coils of intermediate lengths. The number and magnitudes of the harmonics are calculated, and their effect on the self-capacitance is indicated. Experimental results obtained by other workers support the theoretical results.

621.318.42:538.221 1923  
Ferrite Core Inductors—H. A. Stone, Jr. (Bell Sys. Tech. Jour., vol. 32, pp. 265–291; March 1953.) Design of inductors for communication equipment is considered particularly from the point of view of the best use of the properties of ferrites. Advantages of ferrite compared with metal cores for high-frequency low-power applications include (a) higher Q values, (b) smaller volume, and (c) greater ease of adjustment.

621.318.42:621.311.6 1924  
Miniaturization of Airborne Filter Chokes—W. E. Tanner. (Electronics, vol. 26, pp. 180–183; April 1953.) A calculation chart is given for chokes using 7-mil laminations of 4% Si steel with square stack; use of the chart is illustrated by numerical examples.

621.319.4 1925  
The Power Factor and Capacitance of Mica Capacitors at Low Frequencies—P. R. Mica. (Jour. Sci. Instr., vol. 30, pp. 49–51; Feb. 1953.) Experimental results confirm an empirical law of the form  $af^m$  ( $m$  negative and fractional) for the power factor over the range 1–30 cps at normal temperatures. They also confirm a relation between frequency, power factor and capacitance. Power factors as high as 0.01 have been found at 1 cps, corresponding to increases of nearly 2% in capacitance over the values at higher frequencies.

621.392.2:621.3.015.3 1926  
Calculation of Transient Phenomena in Electrically Short Networks by means of Fourier Integrals—E. Adams. (Öst. Z. Telegr. Teleph. Funk Fernseh. tech., vol. 7, pp. 1–10 and 36–40; Jan./April 1953.) Fourier integrals are applied to the determination of the frequency spectra of (a) periodic functions, (b) nonperiodic functions including step functions. The results are used in discussion of the distortion and initial conditions in short networks to which an impulse voltage is applied.

621.392.5 1927  
Design of Practical Linear Networks with Optimum Signal/Noise Ratios—K. Halbach. (Helv. Phys. Acta., vol. 26, pp. 65–74; Feb. 15, 1953. In German.) A general method is described for the design of networks for which the relation between the input and output signals is represented by linear equations, the frequency spectra of signal and noise being assumed known. The application of the method of analysis in the design of the optimum ionization-chamber amplifier is illustrated, and the signal/noise ratios attainable are compared with those for an RC discriminating network and a delay-line clipping circuit.

621.392.5 1928  
Applications of T Networks—M. Alixant. (Radio Tech. Dig., Éd. franc., vol. 6, pp. 301–316; 1952.) Adaptation of paper by Lavagnino (3032 of 1952) incorporating additional material. 53 references.

621.392.5 1929  
Synthesis of Transfer Functions with Poles Restricted to the Negative Real Axis—L. Weinberger. (Jour. Appl. Phys., vol. 24, pp. 207–216; Feb. 1953.) A procedure for the synthesis of general RC transfer functions by means of unbalanced networks is described. The transfer function need not be minimum-phase, but may have zeros anywhere in the complex plane except on the positive real axis. Use is made of techniques described by Guillemin (2462 of 1949), but the problem is simplified by use also

of a network theorem due to Adler, enabling zero shifting to be performed in two directions from within the total network. In an example worked out, 26 network elements are used, whereas the Guillemin procedure would require 66.

**621.392.5:538.652:546.289** 1930  
**Hall-Effect Modulators and "Gyrators" employing Magnetic-Field-Independent Orientations in Germanium**—W. P. Mason, W. H. Hewitt and R. F. Wick. (*Jour. Appl. Phys.*, vol. 24, pp. 166-175; Feb. 1953.) The application of the Hall effect in Ge to the measurement of magnetic flux has been described previously [Pearson, 3172 of 1948]. Further applications are now described to (a) a product modulator, in which the current corresponding to one signal is passed through the Ge crystal while that corresponding to the other is used to produce the magnetic field, and (b) a circuit element with nonreciprocal transmission properties, or gyrator. In these applications a crystal orientation is used for which the transverse magnetoresistance effects are zero and the variation of the Hall-effect coefficient with flux up to 20,000 gauss is  $\approx 2\%$ . The experimental determination of this orientation is described.

**621.392.52** 1931  
**The Development of the Electrical Filter by K. W. Wagner's Methods**—T. Laurent. (*Arch. elekt. Übertragung*, vol. 7, pp. 126-135; March 1953.) Wagner's method of filter design, which is based on consideration of the filter as a ladder of matched reflection-free sections, is compared with methods developed by Zobel, Cauer and others; it is concluded that the principles laid down by Wagner have lost none of their original validity or usefulness.

**621.392.52** 1932  
**Some Designs of Ladder Filter. Results Obtained and Methods of Calculation**—D. Starynevitch. (*Cables & Trans. (Paris)*, vol. 7, pp. 3-15; Jan. 1953.) The principle of matching half-sections and transforming impedances in designing filters with a minimum number of components is illustrated in two examples: a narrow-band band-pass filter for 612 kc, and a filter with a 4-mc pass band centered on 10 mc. Formulas relating to the transformation of T-type quadrupoles to II-type and vice versa, and to various types of quadrupoles for impedance matching, are collected in appendices.

**621.392.52:[621.392.26<621.315.212** 1933  
**U.H.F. Band-Pass Filters**—J. C. Simon and G. Broussaud. (*Ann. Radioélect.*, vol. 8, pp. 3-19; Jan. 1953.) A direct method is developed for designing waveguide and coaxial-line filters; the characteristics of a 3-cavity filter are calculated. Transverse obstacles comprising sets of thin pins are shown to be better than diaphragms, windows or single pins from the point of view of losses and of manufacture and adjustment. Cavities with  $Q$  values of 100-200 can easily be obtained using four pins of diameter 1-2 mm. Design charts are given, and several types of filter are described and illustrated.

**621.392.52.011.21** 1934  
**Admittance and Transfer Function of a Multimesh Resistance-Capacitance Filter Network**—B. K. Bhattacharyya. (*Indian Jour. Phys.*, vol. 26, pp. 563-574; Nov. 1952.) The impedance function of an  $n$ -mesh RC network is expressed as a recurring continued fraction which is then resolved into the quotient of two polynomials, the admittance function being the reciprocal of this quotient. The transfer function is then determined. The corresponding formulae for an  $n$ -mesh CR network are derived.

**621.392.52.029.64:621.396.611.4** 1935  
**Determination of the Bandwidth of Band-Pass Filters for Centimetre Waves**—E. Lednegg and P. Urban. (*Arch. elekt. Übertragung*, vol. 7, pp. 99-105; Feb. 1953.) Theory developed previously (1115 of 1951) is used to analyze the band-pass-filter operation of an arbitrary

arrangement of coupled cavity resonators. A detailed treatment is given for the system comprising two stagger-tuned coupled resonators.

**621.392.53** 1936  
**Spectrum Equalization**—G. G. Gouriet. (*Wireless Eng.*, vol. 30, pp. 112-123; May 1953.) The transfer characteristics of nearly all forms of linear quadrupoles can be equalized as regards both amplitude and phase by adding to the response function its successive time derivatives or integrals. The method may be applied to systems for which the equivalent passive quadrupole is not realizable, e.g. a scanning aperture. Application of the method to servo-control and television is discussed.

**621.392.54** 1937  
**U.H.F. Magnetic Attenuator**—F. Reggia. (*Radio & Telev. News, Radio-Electronic Eng. Sec.*, vol. 49, pp. 12-14, 24; April 1953.) Construction details and performance curves are given for attenuators of the type previously described (1237 of 1952).

**621.392.54:621.392.26** 1938  
**Cut-Off Attenuators for Waveguide Circuits**—G. Klätte. (*Fernmeldetech. Z.*, vol. 6, pp. 86-89; Feb. 1953.) An equivalent-circuit analysis and report of measurements on short and long cut-off sections providing attenuation respectively less than and greater than 15 db. Beyond a certain length the reduction in attenuation due to reflections at the junction is constant, so that calibration measurements on long sections are unnecessary.

**621.396.6+621.385]:629.13.05** 1939  
**Reliability of Airborne Electronic Components**—B. G. Bromber and R. D. Hill, Jr. (*Proc. IRE*, vol. 41, pp. 513-516; May 1953.) An analysis is made of typical failures. Reliability may be improved by modifications to present-day components and by substitution of less vulnerable elements, such as transistors and magnetic amplifiers.

**621.396.611.1** 1940  
**Forced Oscillations with Nonlinear Restoring Force**—C. Hayashi. (*Jour. Appl. Phys.*, vol. 24, pp. 198-207; Feb. 1953.) Both transient and steady-state oscillations are studied. The original differential equation characterized by a nonlinear term is transformed to the following first-order differential equation:—

$$dy/dx = Y(x, y)/X(x, y).$$

Following Poincaré and Bendixson, the singularities and the integral curves of this equation are discussed, the former being correlated with the steady states and the latter with the transient states of oscillation. The integral curves yield the relation between the initial conditions and the steady-state solutions. Fundamental and subharmonic oscillations of order  $\frac{1}{2}$  are investigated. The theoretical results are compared with measurements made on a circuit containing a saturable iron core; satisfactory agreement is found.

**621.396.611.1** 1941  
**Response of a Series of Resonant Circuits to an Applied E.M.F. whose Frequency is a Linear Function of Time**—J. Marique. (*Ann. Télécommun.*, vol. 8, pp. 43-50; Feb. 1953.) A formula is derived for the response of two or three RLC circuits in series to an e.m.f. of unit amplitude represented by the expression  $e(t) = \exp. j(\omega t + \epsilon^2)$ , where  $\epsilon$  is half the frequency-sweep speed. The fluctuations in the response curve of a single circuit are very much reduced when several circuits are connected in series. The increase of selectivity obtainable is investigated, and frequency-sweep speeds permissible for one, two and three circuits are determined.

**621.396.611.4:621.315.612.4:621.396.67** 1942  
**Quasi-Degenerated Modes in High- $\epsilon$  Dielectric Cavities**—H. M. Schlicke. (*Jour. Appl.*

*Phys.*, vol. 24, pp. 187-191; Feb. 1953.) A theoretical and practical investigation is made of resonators comprising solid circular cylinders composed of materials such as titanates, having permittivities of 2500-10,000, with or without metallization of the surfaces. As a consequence of the high permittivities, cavity-resonator techniques can be used in the vhf range. For cylinders with the ends not metallized, quasi-degenerate TE modes can be realized. Tuning can be effected by inserting magnetic rods or by applying conductive disks externally. A design for an antenna developed from the  $TE_{010}^*$  mode resonator comprises a dielectric spiral coiled round a magnetic rod. Practical disadvantages inherent in these high-permittivity dielectrics are indicated.

**621.396.615:621.316.729** 1943  
**The Method of Analytical Signals. Study of the Synchronization of Amplitude-Limited Oscillators**—J. Daguët. (*Ann. Télécommun.*, vol. 8, pp. 2-10; Jan. 1953.) A method based on that of Ville (1020 of 1950) is used to determine the frequency limits within which synchronization can be effected for a single-tuned self-limiting tube oscillator. The synchronization range is given by  $2\Delta\omega/\omega \leq E_0/QE$ , where  $\Delta\omega$  is the difference between the frequency of the synchronization voltage  $E_0$  and the natural frequency  $\omega$  of the oscillator, and  $E$  is the amplitude of the oscillation in the steady state. The phase angle between the two voltages varies from 0 for  $\Delta\omega=0$  to  $90^\circ$  for  $\Delta\omega=\Delta\omega_{max}$ . A system with wide synchronization range is discussed; this incorporates a phase discriminator whose output, proportional to the phase angle between synchronization and oscillator voltages, is applied to a reactance tube which in turn controls oscillator frequency.

**621.396.615:621.392.4/.5** 1944  
**The Use of Admittance Diagrams in Oscillator Analysis**—H. J. Reich. (*Proc. IRE*, vol. 41, pp. 522-528; May 1953.) A digest of the available information on this technique.

**621.396.615:621.396.822:529.786** 1945  
**Effect of Background Noise on the Frequency of Tube Oscillators. Ultimate Accuracy of Electronic Clocks**—A. Blaquièrre. (*Ann. Radioélect.*, vol. 8, pp. 36-80; Jan. 1953.) Fuller account of work noted previously (2163 of 1952, 968 of April, and back references).

**621.396.615.17** 1946  
**How to design Bistable Multivibrators**—R. Pressman. (*Electronics*, vol. 26, pp. 164-168; April 1953.) The design procedure described is intended to ensure reliable operation in spite of deviations of resistors from nominal values, variations of supply voltage, and deterioration of tube-cathode emission. Formulas are given for determining the appropriate values of coupling capacitance. Triggering networks for dealing with pulses of different amplitude and duration are shown.

**621.396.645** 1947  
**The Effective Bandwidth of Video Amplifiers**—F. Fischer. (*Kunigl. tek. Högsk. Handl., Stockholm*, no. 63, pp. 1-32; 1953.) Expanded version of 3050 of 1952.

**621.396.645:621.396.615.142.2** 1948  
**Fluctuation Noise in a Microwave Superregenerative Amplifier**—T. S. George and H. Urkowitz. (*Proc. I.R.E.*, vol. 41, pp. 516-521; May 1953.) The theory of operation of a superregenerative amplifier is reviewed; Rice's representation of noise current by a Fourier series (2169 of 1945 and back references) is used in the expression for the amplifier output. A study is made of the particular conditions when a reflex klystron is used in the amplifier; expressions are derived for the noise figure in terms of the klystron parameters. The overall noise figure can be reduced by introducing beam current, with its associated shot noise, during the quiescent interval.

- 621.396.645.018.424 1949  
**Calculation of Compensated Wide-Band Amplifiers**—H. Laett. (*Tech. Mitt. schweis. Telegr.-Teleph. Verw.*, vol. 31, pp. 72–80; March 1, 1953. In German and French.) Loss of amplification with increasing frequency, due to the output capacitance of the amplifier tube, is compensated by including inductance in the circuit. Three arrangements are discussed, namely parallel compensation, series compensation and double compensation. Abacs to facilitate calculations are presented.
- 621.396.645.35 1950  
**D.C. Amplifiers with Negative Feedback**—A. Ehmert. (*Z. angew. Phys.*, vol. 5, pp. 24–33; Jan. 1953.) Methods are described for automatically compensating the input impedance of current amplifiers or the input admittance of voltage amplifiers. Details are given of the design and performance of several circuits for measurement purposes, in which very high input impedance with low capacitance is achieved.
- 621.396.654.371:621.317.733 1951  
**The Wien Bridge as a Frequency-Determining Element in Selective Amplifiers**—H. J. Stöhr. (*Funk u. Ton*, vol. 7, pp. 27–33; Jan. 1953.) Analysis of the balance condition in a bridge circuit suppressing the amplifier feedback voltage at a fixed frequency.
- 621.396.662.029.63 1952  
**Coaxial-Cavity Tuning Element for U.H.F.**—(*Radio & Telev. News, Radio-Electronic Eng. Sec.*, vol. 49, pp. 15–16, 30; April 1953.) The design is described of a unit which can be used in television tuners and test instruments for the 470–890 mc band. The unit consists essentially of a metal cylinder with an axial conductor having a gap at the center to form a variable capacitor for tuning. An accurately machined low-loss dielectric tube separates core and cylinder and serves as a close-fitting guide for the tuning plunger. Applications of the unit in a signal generator, a frequency-sweep generator, a wavemeter, and a grid-dip meter are described briefly.
- 621.396.665:621.316.86 1953  
**A.G.C. by Means of Miniature NTC Resistors with Heating Element**—G. H. Schouten. (*Electronic Applic. Bull.*, vol. 12, pp. 33–37; Feb. 1951.) The negative-temperature-coefficient resistors are surrounded by the heating element and enclosed in an evacuated glass tube, the resistor being included in the input circuit of an amplifier and the heating element in the input circuit to obtain efficient a.g.c. Practical circuit details are given and operating characteristics of the NTC resistors are shown graphically.
- 621.397.645.029.62 1954  
**Fundamental Problems of H.F. and I.F. Amplifiers for TV Reception: Part 3—Feedback and Practical Considerations following on the Theory**—A. G. W. Uitjens. (*Electronic Applic. Bull.*, vol. 12, pp. 41–64; Feb. 1951.) A detailed discussion is presented of the effects in television amplifiers of feedback (a) via the cathode-grid capacitance, (b) via the anode-grid capacitance, (c) via the anode-cathode capacitance. The necessary formulas are derived for an amplifying stage in which all three types of feedback are present, so that their interactions can be investigated theoretically. The detailed discussion is, however, confined to systems in which only one form of feedback is present. The theory is illustrated by practical examples in amplifier design.
- 621.392.52 1955  
**Filter Design Data for Communication Engineers**—J. H. Mole. (Book Review.) Publishers: E. & F. N. Spon, London, 252 pp., 63s. (*Wireless Eng.*, vol. 30, pp. 129–130; May 1953.) The book is intended to supplement existing textbooks by providing charts, tables and formulas in convenient form; it is concerned mainly with image-parameter (Zobel) filters.
- GENERAL PHYSICS**
- 530.12 1956  
**The Relativistic Electromagnetic Equations in a Material Medium**—N. W. Taylor. (*Aust. Jour. Phys.*, vol. 6, pp. 1–9; March 1953.) The general relativistic e.m. equations for a material medium are expressed in the form of a single four-vector density equation. The field tensor has six different complex components instead of three, as in the case of a free medium. The classical equations are obtained by separating the real and imaginary parts.
- 530.145:621.314.7 1957  
**Transistors: Theory and Application: Part 2—Energy Levels in Transistor Electronics**—A. Coblenz and H. L. Owens. (*Electronics*, vol. 26, pp. 138–141; April 1953.) A simplified exposition of some of the fundamentals of quantum mechanics relevant to an understanding of transistor operation.
- 530.145.6:537.311.33:621.396.11 1958  
**Some Particular Features of Tropospheric Propagation and their Analogies in Wave Mechanics**—Ortusi. (See 2112.)
- 537.122:621.317.318 1959  
**A Precise Determination of the Charge of the Electron from Shot Noise**—L. Stigmark. (*Ark. Fys.*, vol. 5, pp. 399–426; Oct. 26, 1952.) The electron charge  $e$  is calculated from the shot fluctuations of saturation current in a specially constructed diode connected across a tuned circuit resonant at 600 kc. From precision measurements of circuit parameters and the mean-square value of shot noise, the final result obtained is  $e = (4.797 \pm 0.012) \times 10^{-10}$  esu.
- 537.311.33 1960  
**Electron Spin in Semiconductors**—E. A. Guggenheim. (*Proc. Phys. Soc. (London)*, vol. 66, pp. 121–122; Jan. 1, 1953.) Theory is developed showing that, starting from equilibrium electron distribution expressed in terms of absolute activity, it is possible correctly to take account of electron spin.
- 537.523/.525 1961  
**High-Frequency Discharges in Gases**—G. D. Morgan. (*Sci. Progr.*, vol. 41, pp. 22–41; Jan. 1953.) Discussion of the main characteristics and the mechanism of HF discharges, indicating their practical applications. 70 references.
- 537.525:537.533 1962  
**Field Emission of Electrons in Discharges**—F. L. Jones and E. T. de la Perrelle. (*Proc. Roy. Soc. A*, vol. 216, pp. 267–279; Jan. 22, 1953.) Substantial emission of  $10^4$  to  $10^6$  electrons/second was obtained from cathodes of oxidized Ni and W with electric fields of about 100 kV/cm. By relating this emission to the electric field by the Fowler-Nordheim equation, the effective work function and emitting area of the source of the electrons for oxidized Ni and W were estimated as about 0.5 eV and  $10^{-13}$  cm<sup>2</sup> respectively. These results are discussed.
- 537.533 1963  
**Field Electron Emission and Work Function of Crystal Surfaces**—M. Drechsler and E. W. Müller. (*Z. Phys.*, vol. 134, pp. 208–221; Jan. 20, 1953.) The field close to the surface is determined by measurements on models in an electrolyte tank. Formulas are derived for the density of the field-emission current. These are verified by field-electron-microscope observations on W crystals.
- 537.562:538.122 1964  
**Plasma in a Magnetic Field**—A. Schlüter. (*Ann. Phys., Lpz.*, vol. 10, pp. 422–429; July 15, 1952.) The results obtained by considering plasma (a) from the electron-motion point of view, (b) on the basis of kinetic theory, are discussed and reconciled.
- 537.562:538.56 1965  
**The Relation between Various Types of Plasma Oscillation**—A. Schlüter. (*Ann. Phys. Lpz.*, vol. 10, pp. 418–421; July 15, 1952.) A dispersion relation is derived which applies to plasma oscillations, electron and ion oscillations of the Larmor type and to magnetohydrodynamic waves.
- 538:621.3.01 1966  
**Definition of Magnetic Quantities**—G. Oberdorfer. (*Arch. elekt. Übertragung*, vol. 7, pp. 136–142; March 1953.) A critical examination is made of the nomenclature hitherto used for magnetic quantities, and proposals are made for definitions which fit in with modern ideas without unnecessarily disturbing established usage. Precise definitions are given of field strength, polarization, magnetization, susceptibility and magnetizability.
- 538.221 1967  
**Some Magnetic Properties of Metals: Part 5—Magnetic Behaviour of a Cylindrical System of Electrons for All Magnetic Fields**—R. B. Dingle. (*Proc. Roy. Soc. A (London)*, vol. 216, pp. 118–142; Jan. 7, 1953.) The Schrödinger equation is solved for an electron moving in a uniform magnetic field  $H$ , the boundary of the system being a cylinder with its axis along the direction of the field. Two entirely different types of wave function are possible, one type leading to the small Landau diamagnetism of large systems (Part 1: 2489 of 1952), the other to the larger diamagnetism of small systems (Part 4: 1005 of April). Taking account of the occupied states of both types, the steady contributions to the magnetic susceptibility are determined for low, high and intermediate temperatures.
- 538.221 1968  
**Collective Electron Ferromagnetism: a Generalization of the Treatment and an Analysis of Experimental Results**—K. L. Hunt. (*Proc. Roy. Soc. A (London)*, vol. 216, pp. 103–117; Jan. 7, 1953.) A term involving the fourth power of the magnetization is introduced into Stoner's expression for the energy associated with magnetization. If parameter values are suitably chosen, the properties of Ni show a high degree of coordination, and the magnetization/temperature curves for Ni-Co and Ni-Cu alloys can be interpreted simply.
- 538.3 1969  
**Tentative Theory of Nonlinear Electrodynamics: Part 2**—K. Bechert. (*Ann. Phys., Lpz.*, vol. 10, pp. 430–448; July 15, 1952.) Part 1: 618 of 1951.
- 538.561:537.533/.534 1970  
**Production of Radio Waves by means of the Tcherenkov Effect**—C. A. Klein. (*Ann. Télécommun.*, vol. 8, pp. 38–42; Feb. 1953.) The Tcherenkov effect consists in the emission of em radiation by a particle traveling through a medium with a velocity greater than that of light. The essential results of Frank & Tamm's theory of the effect (*Compt. Rend. Acad. Sci. (URSS)*, vol. 14, pp. 109–114; 1937) are quoted and references given to accounts of experimental verifications of the theory, using electrons and also protons. The possibility of producing em waves in the range between the far infrared and uhf by means of the effect in a narrow channel is discussed. It is concluded that intense sources of em waves should result from the use of powerful beams consisting of packets of electrons. Simple arrangements should suffice for cm and mm waves, but difficulties will certainly be experienced in the case of still shorter waves.
- 538.566:535.42 1971  
**A Rigorous Treatment of the Diffraction of Electromagnetic Waves by a Slit**—R. Müller and K. Westpfahl. (*Z. Phys.*, vol. 134, pp. 245–263; Feb. 6, 1953.) Wave-polarization components parallel to and perpendicular to the slit are considered. An integral equation for the

electric field strength in the slit is found by the method of Levine & Schwinger (83 and 1897 of 1950), and an exact solution is obtained by developing the kernel in a power series of the product of wave number and slit width.) The far-field intensity and the transmission factor of the slit are calculated and compared with the results of Morse and Rubenstein (905 of 1939). The relation of the work to that of Sommerfeld (Vorlesung über theoretische Physik, Bd IV, Optik, §39) and of Groschwitz and Hönl (2183 of 1952) is discussed.

538.566:535.42 1972

**The Three-Dimensional Problem of the Diffraction of Monochromatic Electromagnetic Waves**—D. Z. Avazashvili. (*Compt. Rend. Acad. Sci. (URSS)*, vol. 28, pp. 29–32; Jan. 1, 1952. In Russian.) The distribution of the em field in space for a given distribution of field at a boundary surface is discussed, and conditions are established for the existence of a solution obtained previously (*Trudy Tbilisskovo Matematicheskovo Institutula*, vol. 8, p. 109; 1940).

538.566:621.318.423:621.385.029.6 1973

**The Propagation of Electromagnetic Waves along a Conical Helix with Variable Pitch**—G. Hellgren. (*Chalmers tek. Högsk. Handl.*, no. 130, 13 pp.; 1953.) Theoretical analysis. Expressions are derived for the reflection coefficient, which may be practically zero, and for the impedance characteristics.

538.63 1974

**Galvanomagnetic Effects in Conductors**—D. K. C. MacConald and K. Sarginson. (*Rep. Progr. Phys.*, vol. 15, pp. 249–274; 1952.) A review of the Hall effect and magnetoresistance in conductors, with primary reference to metals (including ferromagnetic materials); semiconductors are mentioned briefly. A physical survey of the whole field is first made; in the second part a more mathematical treatment is given of some of the major problems involved. Over 60 references.

538.632 1975

**Hall Effect**—O. Lindberg. (*Proc. I.R.E.*, vol. 41, p. 507; May 1953.) Correction to paper noted in 713 of March.

538.652 1976

**Magnetostriction**—E. W. Lee. (*Sci. Progr.*, vol. 41, pp. 58–77; Jan. 1953.) Discussion of magnetostriction phenomena in single crystals and in multicrystal materials. Three effects are distinguished: (a) form effect, (b) "forced" magnetostriction, (c) spontaneous linear magnetostriction.

#### GEOPHYSICAL AND EXTRATERRESTRIAL PHENOMENA

523.5:621.396.9 1977

**On the Nature of the Decay of a Meteor Trail**—J. Feinstein. (*Proc. Phys. Soc. (London)*, vol. 65, p. 741; Sept. 1, 1952.) Critical discussion of the theories of Kaiser and Closs (1108 of 1952) and of Greenhow (2493 of 1952).

523.5:621.396.9 1978

**On the Decay of Radio Echoes from Meteor Trails**—T. R. Kaiser and J. S. Greenhow. (*Proc. Phys. Soc. (London)*, vol. 66, pp. 150–151; Feb. 1, 1953.) Discussion shows that observed phenomena are explicable by the theories of Kaiser and Closs (2208 of 1952) and of Greenhow (2493 of 1952). Many points of disagreement between observation and Feinstein's theory (1885 of 1951 and 1977 above) are noted.

523.5:621.396.9 1979

**An Experimental Study of Radio Reflections from Meteor Trails**—R. L. Closs, J. A. Clegg and T. R. Kaiser. (*Phil. Mag.*, vol. 44, pp. 313–324; March 1953.) The dependence of the echoes on the polarization of the incident wave has been investigated and the existence of resonance scattering with transverse polarization verified.

523.72 1980

**Thermal Theories of the High-Intensity Components of Solar Radio-Frequency Radiations**—J. H. Piddington. (*Proc. Phys. Soc. (London)*, vol. 66, pp. 97–104; Feb. 1, 1953.) Thermal theories of the origin of enhanced RF radiation from regions which occasionally attain brightness temperatures of  $10^{10}$  deg K or more are discussed. None of the theories is found capable of explaining the available observational data. It is concluded that all three radiation components are generated by the ordered (nonthermal) motion of electrons.

523.72:523.746 1981

**A Method of Analysis of the Directivity of Solar Radio Emission from Sunspots**—T. Takakura. (*Nature (London)*, vol. 171, p. 445; March 7, 1953.)

523.72:531.758:523.745 1982

**An Estimate of the Density and Motion of Solar Material from Observed Characteristics of Solar Radio Outbursts**—H. K. Sen. (*Aust. Jour. Phys.*, vol. 6, pp. 67–72; March 1953.) Theory previously given by Feinstein and Sen (104 of 1952) is extended and applied to the observations made in Australia by Wild and McCready (1629 of 1951) and by Wild (1630, 2169 and 2170 of 1951) of the spectra of solar RF outbursts in the range 70–130 mc. The dispersion equation, involving the velocity of solar material erupting into a static corona and the temperatures and densities of the material and of the corona, enables the velocity of the material to be estimated as about 500 km/s, with a particle density of about  $10^9/\text{cm}^3$ .

523.74/.75:[550.38+551.510.5 1983

**Solar and Terrestrial Relationships**—D. H. McIntosh. (*Meteor. Mag. (London)*, vol. 82, pp. 11–15; Jan. 1953.) The general problem of the relation between solar activity on the one hand and meteorological, geomagnetic and ionospheric phenomena on the other is reviewed, with special reference to an account by Scherhag (*Wetterkarte*, No. 74, March 14, 1952) of events which he interprets as being related to an intense solar eruption on Feb. 24, 1952. No such flare has been reported. It is concluded that no clear evidence has yet been given of a direct relation between solar phenomena and meteorological effects.

523.746"1952.10/.12" 1984

**Provisional Sunspot-Numbers for October to December, 1952**—M. Waldmeier. (*Jour. Geophys. Res.*, vol. 58, p. 112; March 1953.)

538.122:523 1985

**The Origin of Magnetic Fields in Moving Plasma**—L. Biermann. (*Ann. Phys., Lps.*, vol. 10, pp. 413–417; July 15, 1952.) Discussion indicates that diffusion effects produce sufficiently large emf's in rotating masses of ionized gas to account for the existence of solar and stellar magnetic fields.

550.372:621.396.11 1986

**Effect of a Large Dielectric Constant on Ground-Wave Propagation**—Wait and Campbell. (See 2113.)

550.38"1952.10/.12" 1987

**Cheltenham [Maryland] Three-Hour-Range, Indexes K for October to December, 1952**—R. R. Bodle. (*Jour. Geophys. Res.*, vol. 58, p. 112; March 1953.)

550.385"1952.07/.12" 1988

**Principal Magnetic Storms [July–Dec. 1952]**—(*Jour. Geophys. Res.*, vol. 58, pp. 113–115; March 1953.)

550.386 1989

**International Data on Magnetic Disturbances, Third Quarter, 1952**—J. Bartels and J. Veldkamp. (*Jour. Geophys. Res.*, vol. 58, pp. 109–111; March 1953.)

551.510.3:535.325 1990

**The Constants in the Equation for Atmos-**

**pheric Refractive Index at Radio Frequencies**—E. K. Smith, Jr. and S. Weintraub. (*Jour. Res. Nat. Bur. Stand.*, vol. 50, pp. 39–41; Jan. 1953.) The formula for scaled-up refractivity  $N$  for air is  $N = (K_1/T)[p + K_2(c/T)]$ , where  $K_1$ ,  $K_2$  are constants. The value proposed for  $K_1$  is derived from recent reliable microwave and optical measurements of the refractive index of dry air by Barrell (*Jour. Opt. Soc. Amer.*, vol. 41, pp. 295–299, 1951, Birnbaum *et al.* (1426 of 1951) and Essen and Froome (1371 of 1952), after adjustment to allow for an average amount of  $\text{CO}_2$  in the composition of the air.  $K_2$  is derived from two other constants obtained from measurements of the dielectric constant of water vapour by Birnbaum and Chatterjee [2269 of 1952 (please note additional author)]. A table of values of the constants used by various workers from 1933 to 1952 is given, with comments on discrepancies.

551.510.52 1991

**The Geographical and Height Distribution of the Gradient of Refractive Index**—B. R. Bean. (*Proc. I.R.E.*, vol. 14, pp. 549–550; May 1953.) Charts are presented of the February and August distributions of the effective earth's radius factor over the U.S.A., and of the vertical distribution of refractive-index gradient for warm, temperate and cold climates.

551.510.535 1992

**Long-Delay Ionospheric Echoes at 150 kc**—J. J. Gibbons, R. L. Schrag and A. H. Waynick. (*Nature (London)*, vol. 171, pp. 444–445; March 7, 1953.) A report of results obtained at Pennsylvania State College Ionosphere Research Laboratory, using a vertical-incidence pulse transmitter with 2-MW peak power. Recordings with a 5-min exposure were made every half hour from 2000 to 0400 L.M.S.T. of the signals received on an antenna system suitable for receiving circularly polarized waves. Three records, obtained on November 9, 1952, showed an isolated echo corresponding to a reflection height of about 900 km. The echo only appeared on the records of the extraordinary wave. Similar records were obtained on two subsequent nights. Possible explanations of these long-delay echoes are considered; they may be due to reflections from a region above the height of maximum ionization of the  $F_2$  region.

551.510.535 1993

**On the Comparative Increases of the  $F_1$  and  $F_2$  Ionizations from Sunspot Minimum to Sunspot maximum**—M. Ghosh. (*Jour. Geophys. Res.*, vol. 58, pp. 41–51; March 1953.) The proportionate increase of ionization, from the epoch of sunspot minimum to sunspot maximum, is not the same for the  $F_1$  as for the  $F_2$  layer, being of the order of 1.6 for the former and 3.0 for the latter. Assuming (a) the F region to be due to ionization of atomic oxygen, (b) an increase in temperature with height above the  $F_1$  maximum, (c) an effective recombination coefficient decreasing rapidly with height, calculations are made for three different ionosphere models, the results being in each case in satisfactory agreement with observations.

551.510.535:523.78 1994

**Effect of the Solar Eclipse of 25th February 1952 on the Ionosphere E Layer in Equatorial Africa**—S. Estrabaud. (*Compt. Rend. Acad. Sci. (Paris)*, vol. 236, pp. 833–835; Feb. 23, 1952.) A report and discussion of observations of E-layer critical frequencies at Bangui. The critical frequency of the  $E_2$  layer decreased suddenly at the commencement of the eclipse and was soon masked by that of the  $E_1$  layer. A graph of the observed values of  $f_oE$  shows that the effects of the eclipse were certainly perceptible some 5 to 20 minutes before the first contact. An explanation of the observed effects is based on the assumption of two solar regions more active than the rest, one in the corona near the western edge of the disk, the other near the eastern edge.

- 551.510.535:537.29+538.69 1995  
**Electromagnetic Effects in the Ionosphere: Effects of Crossed Constant-Magnetic and Alternating-Electric Fields**—R. Jancel and T. Kahan. (*Compt. Rend. Acad. Sci. (Paris)*, vol. 236, pp. 788–790; Feb. 23, 1953.) The effect of the crossed fields on the distribution of the velocities of the free electrons in an ionized gas is studied by means of the general equation of Boltzmann, collisions between electrons being assumed negligible. The result obtained includes, as particular cases, those of Druyvestyn (1930 Abstracts, p. 350 and 1700 of 1935), Chapman and Cowling (The Mathematical Theory of Nonuniform Gases) and Margenau (3246 of 1946).
- 551.510.535:551.55:621.396.9 1996  
**A Study of Winds in the Ionosphere by Radio Methods**—J. H. Chapman. (*Canad. Jour. Phys.*, vol. 31, pp. 120–131; Jan. 1953.) Report of an investigation made using Mitra's method (96 of 1950). The measurements were made in Ottawa, and later in Montreal, and covered a period of a year. At a nominal height of 110 km (E layer) the speed of the wind showed a mean daily variation of approximately half-day period and about 40 m/s amplitude. This variation can be explained on the basis of tidal oscillations in the atmosphere. A variation corresponding to lunar atmospheric tides has also been detected at this level. The winds in the F region appear to increase in speed with increase of magnetic activity; this effect is not observed in the E region except during severe ionospheric disturbances.
- 551.510.535:551.594.12 1997  
**A Procedure for the Determination of the Vertical Distribution of the Electron Density in the Ionosphere**—L. A. Manning. (*Jour. Geophys. Res.*, vol. 58, pp. 117–118; March 1953.) Comment on 409 of February (Kelso).
- 551.510.535:621.3.087.4 1998  
**An Ionosphere Recorder for Low Frequencies**—J. C. Blair, J. N. Brown and J. M. Watts. (*Jour. Geophys. Res.*, vol. 58, pp. 99–107; March 1953.) Based on HF recorder design, this beat-frequency instrument covers the range 50 kc–1 mc and uses a single-loop antenna about 350 ft long by 150 ft high. Sample records are reproduced.
- 551.594.5 1999  
**Radio Measurements and Auroral Electron Densities**—P. A. Forsyth. (*Jour. Geophys. Res.*, vol. 58, pp. 53–66; March 1953.) Simultaneous recordings of 56- and 106.5-mc echoes from auroral clouds were made at Saskatoon. A large number of echoes at 56 mc were found for which there were no corresponding echoes at 106.5 mc, and the echo amplitude ratio for the two frequencies varied widely. Critical reflections from small volumes of intense ionization seem the most probable explanation of these observations, where intense auroral displays are concerned. This would involve electron densities of the order of  $10^9/\text{cm}^3$  in small volumes of the aurora for periods of time short in comparison with the duration of the display.
- 551.594.5+523.5+551.510.535:621.396.9 2000  
**Long-Duration Echoes from Aurora, Meteors, and Ionospheric Back-Scatter**—D. W. R. McKinley and P. M. Millman. (*Canad. Jour. Phys.*, vol. 31, pp. 171–181; Feb. 1953.) A report of radar echoes of unusual types observed in the course of the Ottawa meteor-research program. 20- $\mu$ s pulses with a peak power of 200–400 kW were radiated on a frequency of 33 mc. Some of the echoes were correlated with visual observations of aurora. The extremely long duration (9 min to over 30 min) of some meteor echoes was probably caused by abnormal ionospheric conditions. Weak semipermanent echoes (duration up to or over 1 hour) are attributed to reflection at vertical or near-vertical incidence from irregularities in the lower ionosphere, possibly the same as those responsible for the long-range propagation reported by Bailey *et al.* (2581 of 1952).
- LOCATION AND AIDS TO NAVIGATION**
- 621.396.9 2001  
**High-Quality Radar Picture Display Unit**—R. T. Petruzzelli. (*Tele-Tech*, vol. 12, pp. 54–57, 102; Jan. 1953.) A description is given, with block diagrams, of equipment providing television pictures of the PPI display of airport-surveillance radar, Type ASR-2, together with mapping and df information. Two independent channels, each terminating in its own 12-in. display unit, enable different areas round the airport to be monitored. A 30-in. display for plotting purposes is also provided. The conversion from the PPI display to standard 525-line 30-frame television scan is effected by means of the graphicon storage tube [1539 of May—Dyall *et al.*]. The display control consoles include all controls for the radar set normally found on the original radar indicator. The plotting display console has no control over the radar set and can merely switch its mixer amplifier to accept the signals from either of the two channels.
- 621.396.9 2002  
**A Special Type of Pulse Modulation for the Transmission of Radar Pictures (Sampling)**—E. Roessler. (*Fernmeldetechn. Z.*, vol. 6, pp. 78–79; Feb. 1953.) The principles of a sampling system for bandwidth reduction are described. See 1921 (Otto) and 3430 (McLucas) of 1952. It is proposed to introduce, in German, the term "Durchmusterung" for this sampling process.
- 621.396.9:[551.578+551.594.22] 2003  
**Frontal Precipitation and Lightning Observed by Radar**—J. S. Marshall. (*Canad. Jour. Phys.*, vol. 31, pp. 194–203; Feb. 1953.) Patterns obtained by radar methods at wavelengths of 3.2 cm and 10.7 cm are shown and discussed. Observations in vertical section were made by scanning at angles of elevation up to 30°.
- 621.396.9:551.578.1 2004  
**Radar Observations of Rain from Non-freezing Clouds**—R. S. Styles and F. W. Campbell. (*Aust. Jour. Phys.*, vol. 6, pp. 73–85; March 1953.) A detailed account, with photographs of typical displays, of results obtained with airborne radar equipment.
- 621.396.9:621.396.65.029.64 2005  
**Remote Display of Radar Pictures**—R. F. Hansford and G. J. Dixon. (*Wireless World*, vol. 59, pp. 218–222; May 1953.) Description of the Decca Radar Link, Type 2, designed for transmission of information from a radar site to a distant point where it can again be displayed on a radar indicator without loss of detail. The wavelength used is about 9 cm, and the transmitter power 0.5 W. Negative a.m. is used for the video signals and positive modulation on a time basis for the synchronizing pulses and bearing information. The transmitter RF unit is housed in a watertight box mounted behind the paraboloid antenna on an 80-ft mast. The transmitter tube is a v.m. Heil-type tube. A similar antenna arrangement is used with the receiver, which has a reflex-klystron local oscillator. Full test facilities are included. Reliable transmission is provided over a distance up to 20–30 nautical miles. Repeater stations may be interpolated in the link.
- 621.396.9:621.396.67 2006  
**Moulded Plastic Radar Scanners and Stressed Components**—(See 1911.)
- 621.396.9:778.5 2007  
**Cinematographic Recording of Panoramic Radar Images**—M. J. de Cadenet. (*Ann. Télécommun.*, vol. 8, pp. 19–27; Jan. 1953.) A method developed by the C.N.E.T. in France for recording television images is adapted. A detail description is given of camera equipment with servomechanism for synchronizing camera operation with antenna rotation.
- 621.396.93.088 2008  
**More on Direction Finders**—H. G. Hopkins. (*Proc. I.R.E.*, vol. 41, pp. 548–549; May 1953.) Comment on 142 of 1952 (Hansc). It is recommended that the term 'unwanted' should be reserved for the component which introduces errors when the direction finder is operated on a uniform unobstructed site. The proposed distinction between primary and secondary instrumental polarization errors is also criticized.
- 621.396.932/933 2009  
**Decca Charts**—H. C. Freiesleben. (*Telefunken Ztg*, vol. 26, pp. 49–53; Jan. 1953.) A detailed description is given of the method of computing Decca curves in which the differences of the distances of a number of points on the earth's surface from the transmitters are first calculated, the points corresponding to round values of the differences being then found by interpolation.
- 621.396.933 2010  
**Radio Navigation and Air Traffic Safety Measures**—O. J. Selis. (*Tijdschr. ned. Radio-geenoot.*, vol. 18, pp. 59–87; March 1953.) A survey of present methods and trends both for en-route navigation and for approach and landing, with special reference to installations in Holland.
- MATERIALS AND SUBSIDIARY TECHNIQUES**
- 533.5 2011  
**Methods of Obtaining High Vacua by Ionization**—H. Schwarz. (*Le Vide*, vol. 7, pp. 1262–1266; Nov. 1952.) Analysis shows that no true pumping effect can be obtained with a simple d.c. discharge. In the system described a ring-shaped anode has a potential of 2kV or more and a second annular electrode beyond it is at cathode potential. Four outlet tubes fitted with auxiliary electrodes are spaced around the anode. A weak magnetic field imparts a helical motion to the electrons beyond the anode. Pressures lower than  $5 \times 10^{-6}$  mm Hg are obtained.
- 535.212:546.482.21 2012  
**Study of the Infrared Photoluminescence of Copper-Activated Cadmium Sulphide**—E. Grilhot and P. Guintini. (*Compt. Rend. Acad. Sci. (Paris)*, vol. 236, pp. 802–804; Feb. 23, 1953.) The photoluminescence of CdS-Cu comprises a band in the infrared between 0.7 and 1.4  $\mu$ , with a maximum at 1.02  $\mu$ .
- 535.215:546.817.221 2013  
**The Photovoltaic Effect in Natural Lead Sulphide**—R. Lawrance. (*Aust. Jour. Phys.*, vol. 6, pp. 124–125; March 1953.) Correction to paper abstracted in 1930 of 1952.
- 535.215.2:546.28 2014  
**Long-Wavelength Infrared Photoconductivity of Silicon at Low Temperatures**—B. V. Rollin and E. L. Simmons. (*Proc. Phys. Soc. (London)*, vol. 66, pp. 162–168; March 1, 1953.)
- 535.215.3:538.639 2015  
**Theory of the Photomagnetolectric Effect**—P. Aigrain and H. Bulliard. (*Compt. Rend. Acad. Sci. (Paris)*, vol. 236, pp. 595–596; Feb. 9, 1953.) An approximate theory is developed which assumes the charge carriers of the two different types in semiconductors to have equal mobilities and which gives values of the photomagneto-electric potential difference in good agreement with the experimental results reported by Kikoin and Noskow (Abstracts, p. 507; 1934).
- 535.215.3:538.639:546.289:548.55 2016  
**Experimental Results on the Photomagnetolectric Effect**—P. Aigrain and H. Bulliard. (*Compt. Rend. Acad. Sci. (Paris)*, vol. 236, pp. 672–674; Feb. 16, 1953.) Measurements were made on small plates, 0.1 to 1 mm thick, cut from single crystals of Ge of various degrees of purity, the illuminated face being in



general well polished chemically. Various methods of measurement are described. The results obtained confirm the theory previously given (2015 above).

535.343+535.32 2017

Inter-relation between Optical Constants for Lead Telluride and Silicon—T. S. Moss. (*Proc. Phys. Soc. (London)*, vol. 66, pp. 141-144; Feb. 1, 1953.)

535.343 2018

The Optical Constants of Lead Sulphide, Lead Selenide and Lead Telluride in the 0.5-3- $\mu$  Region of the Spectrum—D. G. Avery. (*Proc. Phys. Soc. (London)*, vol. 66, pp. 134-140; Feb. 1, 1953.)

535.343:546.23 2019

The Optical Absorption and Reflection of Amorphous and Hexagonal Selenium—J. Stuke. (*Z. Phys.*, vol. 134, pp. 194-207; Jan. 20, 1953.) Measurements were made on thin layers, using wavelengths between 300 and 1200  $\mu$ , at temperatures in the range  $-180^{\circ}$  C to  $+100^{\circ}$  C. At the transformation from the amorphous to the hexagonal form the absorption constant increases over the whole of the wave-range investigated. For hexagonal Se a strong absorption band is observed at 2.2 eV. The absorption and reflection measurements show good agreement.

535.343+537.312.5:546.817.221 2020

Absorption Spectra of Lead Sulphide at Different Temperatures—W. Paul and R. V. Jones. (*Proc. Phys. Soc. (London)*, vol. 66, pp. 194-200; March 1, 1953.)

535.37 2021

Induced Conductivity in Luminescent Powders: Part 2—A.C. Impedance Measurements—H. Kallmann, B. Krauer and A. Perlmutter. (*Phys. Rev.*, vol. 89, pp. 700-707; Feb. 15, 1953.) A.C. impedance changes induced by ultraviolet, infrared, X-ray and  $\gamma$ -ray irradiation of (Zn:Cd)S powders agree with the results previously obtained with d.c. (Kallmann and Kramer, 3438 of 1952.)

535.37:546.472.21 2022

The Influence on the Luminescence of ZnS Phosphors of Lattice Defects caused by Pounding—I. Broser and W. Reichardt. (*Z. Phys.*, vol. 134, pp. 222-224; Jan. 20, 1953.) An investigation is made of the reduction of luminescence of ZnS-Cu phosphors as the fineness of the material increases. Formulas derived are discussed in relation to theories of radiationless transitions.

535.37:546.472.21 2023

Optical Measurements on Electroluminescent Zinc Sulphide—J. F. Waymouth. (*Jour. electrochem. Soc.*, vol. 100, pp. 81-84; Feb. 1953.) Results of measurements of absorption and emission spectra are reported.

535.37:546.472.21 2024

On the Nature of Fluorescent Centers and Traps in Zinc Sulphide—H. A. Klasens. (*Jour. electrochem. Soc.*, vol. 100, pp. 72-80; Feb. 1953.) The impurity levels in the energy diagram of a ZnS phosphor are considered to be localized  $S^{2-}$  levels lifted above the filled  $S^{2-}$  band due to the presence of monovalent positive or trivalent negative activator ions in the lattice. Electron traps are formed similarly by the replacement of S ions by monovalent negative ions or of  $Zn^{2+}$  ions by trivalent positive ions. The emission characteristics of ZnS phosphors seem to be more a property of the lattice than of the activator.

537.224 2025

Plastic Electrets—H. H. Wiedner and S. Kaufman. (*Jour. Appl. Phys.*, vol. 24, pp. 156-161; Feb. 1953.) Previously proposed explanations of the electret mechanism are discussed and measurements on specimens made of plexiglas, lucite and nylon are reported. The experimental results support the view that

there exist two decaying polarizations of opposite sense due to ionic migration (a) within the dielectric and (b) across the electrode/dielectric interface (see Gross, 4055 of 1944.)

537.226 2026

Variation with Time of the Dielectric Properties of Ferroelectric Ceramics—D. M. Kazarnovski. (*Zh. tekh. Fiz.*, vol. 22, pp. 553-558; April 1952.) A report of observations covering a period of three years. It appears that the dielectric constant of ferroelectric ceramics decreases with the time; methods for stabilizing it are discussed.

537.226.2:546.212-16 2027

Anisotropy of the Dielectric Constant of Ice—F. Humbel, F. Jona and P. Scherrer. (*Helv. Phys. Acta*, vol. 26, pp. 17-32; Feb. 15, 1953. In German.) Dielectric constant  $\epsilon$  and loss angle  $\delta$  were measured as a function of temperature and frequency for square plates cut from large single crystals. The difference between the values of  $\epsilon$  for directions parallel and perpendicular to the  $c$ -axis decreases with temperature decrease. The variation of  $\epsilon$  and  $\delta$  with frequency is similar to that found for polycrystalline ice.

537.311.33 2028

Theory of Mixed Semiconductors—O. Madelung and H. Welker. (*Z. angew. Phys.*, vol. 5, pp. 12-14; Jan. 1953.) For simple  $n$ - or  $p$ -type semiconductors the carrier concentrations and mobilities can be easily found from the measured values of conductivity and Hall coefficient. For mixed semiconductors further measurements are required; the thermoelectric power and the variation of the resistance with the strength of an applied magnetic field are suitable properties for this purpose. Formulas relating the various parameters are discussed. The Hall coefficient depends on the strength of the magnetic field and may change its sign at high field strength.

537.311.33 2029

A Conductive Ceramic for Microwave Applications—(*Eng. (London)*, vol. 195, p. 363; March 6, 1953.) "Caslode" is the name given to a semiconductor with a dielectric constant of about 20 and a loss angle between  $10^{\circ}$  and  $20^{\circ}$  at a wavelength of 3.2 cm, suitable for use without water-cooling as a dummy load in waveguides.

537.311.33 2030

Semiconductor Properties of the Systems K-Sb, Cs-Sb, K-In and Cs-In—R. Suhrmann and C. Kangro. (*Naturwissenschaften*, vol. 40, pp. 137-138; Feb. 1953.) Graphs are given which show (a)  $\log \chi$  for K-Sb compounds with varying proportions of K from 0 to 100%, (b)  $\log \chi$  plotted against  $1/T$  for values of  $1/T$  in the range  $3-9 \times 10^{-3}$  for the compounds  $Cs_3Sb$  and  $K_3Sb$ ,  $\chi$  being the specific conductivity and  $T$  the absolute temperature. For intrinsic semiconduction, the energy levels in  $K_3Sb$ ,  $KSb$  and  $Cs_3Sb$  are respectively 0.79, 0.88 and 0.56 eV. For lattice-defect semiconduction, the levels are 0.23 and 0.16 eV respectively for  $K_3Sb$  and  $Cs_3Sb$ . For K-In and Cs-In compounds also, the temperature coefficient of resistance is negative; for  $Cs_2In_3$  the resistance drops by a factor of about  $10^4$  between  $83^{\circ}$  and  $287^{\circ}$ K, the corresponding drop for  $K_3In$  being only from 82 to 37.7 $\Omega$ .

537.311.33:546.27.03 2031

Study of the Properties of Boron—J. Lagrenaudie. (*Jour. Phys. Radium*, vol. 14, pp. 14-18; Jan. 1953.) Continuation of work noted in 1696 of June. Conductivity measurements at temperatures up to  $700^{\circ}$  C yield a value of about 1.28 eV for the intrinsic energy. The material should be useful for thermistors. Thin layers are transparent in the infrared, with an absorption electric threshold at a wavelength near  $1\mu$ . Only very weak rectifying effects were observed; measurements on single crystals are required before conclusions can be reached

about the practical possibilities of the material for rectifiers.

537.311.33:546.289 2032

A Thermoelectric Study of the Electrical Forming of Germanium Rectifiers—M. Kikuchi and T. Onishi. (*Jour. Appl. Phys.*, vol. 24, pp. 162-166; Feb. 1953.) Experimental methods described by Granville and Hogarth (161 of 1952) were applied. Remarkable improvements in the  $I/V$  characteristics were obtained by applying appropriate alternating forming voltages. Using  $n$ -type crystals, the thermoelectric current observed on the etched surface was converted by the forming from  $n$ -type to  $p$ -type. The dependence of the thermo-emf on the contact pressure is greatly increased by the forming. The results indicate that a substance with relatively high resistivity and  $p$ -type thermo-emf is formed between the point contact and the Ge surface.

537.311.33:546.289 2033

Plastic Deformability of Germanium at Relatively High Temperatures—L. Graf, H. R. Lacour and K. Seiler. (*Z. Metallkde*, vol. 44, pp. 113-114; March 1953.) Experiments on single crystals of purity  $>99.999\%$  are reported. At temperatures  $>600^{\circ}$  C plastic deformation without time lag was obtained. The appearance of slip lines indicates that an actual lattice translation occurs. Variation of resistivity caused by heat treatment is greatly reduced if the specimens are simultaneously subjected to plastic deformation. See also 1403 of May (Gallagher).

537.311.33:546.289 2034

Pressure-Welded  $p$ - $n$  Junctions in Germanium—R. G. Shulman and D. M. Van Winkle. (*Jour. Appl. Phys.*, vol. 24, p. 224; Feb. 1953.) A mechanically strong weld is obtained by applying local pressure at the surfaces to be joined. Pressures of about 100 kg/cm<sup>2</sup> are obtained with moderate forces by making the contact area extremely small; this is achieved by making one contact surface optically flat and the other of controlled roughness. Characteristics of junctions prepared by this process are shown; their HF response is better than that of units prepared by drawing or diffusion.

537.311.33:546.289:621.396.822 2035

Shot Noise in Germanium Filaments—R. H. Mattson and A. van der Ziel. (*Jour. Appl. Phys.*, vol. 24, p. 222; Feb. 1953.) The correctness of the noise formula previously derived (Herzog and van der Ziel, 1936 of 1952) is verified by further measurements of greater accuracy over an extended frequency range.

537.311.33:546.817.221 2036

Transistor Action and Related Phenomena in Lead Sulphide Specimens from Various Sources—C. A. Hogarth. (*Proc. Phys. Soc. (London)*, vol. 66, pp. 216-220; March 1, 1953.) Examination of a large number of specimens of PbS has indicated a maximum free-carrier concentration at  $290^{\circ}$ K of  $2 \times 10^{17}/\text{cm}^3$  if transistor action is to be found. This leads to a value of 0.65 eV for the width of the forbidden band at  $290^{\circ}$ K. Transistor action was only observed in  $p$ -type specimens and was always associated with good rectification and a strong photovoltaic effect.

537.311.33:546.817.221 2037

The Electronic Band Structure of PbS—D. G. Bell, D. M. Hum, L. Pincherle, D. W. Sciama and P. M. Woodward. (*Proc. Roy. Soc. A (London)*, vol. 217, pp. 71-91; March 24, 1953.) The cellular method is used to determine electronic wave functions of the Bloch type for PbS.

537.311.33:621.314.632 2038

The Theory of Solid Rectifiers—A. I. Gubanov. (*Zh. tekh. Fiz.*, vol. 22, pp. 381-393; March 1952.) A theory is proposed based on the assumption that the barrier layer is a thin semiconducting layer with a conductivity of the

- type opposite to that of the main body of the rectifier. From a solution of the Poisson's and diffusion equations the current/voltage characteristic of the rectifier is determined. A numerical example is given for the case of a  $\text{Cu}_2\text{O}$  rectifier; the theoretical curve for the dependence of the rectifier resistance on voltage shows good agreement with experimental curves.
- 537.311.33:621.396.822** 2039  
**Noise in Semiconductors at Very Low Frequencies**—B. V. Rollin and I. M. Templeton. (*Proc. Phys. Soc. (London)*, vol. 66, pp. 259-261; March 1, 1953.) Previous measurements by Kronenberger (2879 of 1951) showed that down to frequencies of about 0.2 cps the mean-square noise voltage per unit bandwidth is inversely proportional to the frequency  $f$ . A method is described by which measurements on pyrolytic carbon resistors have been made at much lower frequencies. The noise is recorded on slow-running magnetic tape, which is then joined to form a closed loop. The loop is run through the pickup head at normal speed and the noise spectrum analyzed with a standard type of AF wave analyzer. By varying the recording speed, measurements were made for frequencies from  $10^{-4}$  to 10 cps. The results obtained show that even at the lowest frequency the  $1/f$  law is still obeyed fairly closely. A special arrangement is described for obtaining the amplification necessary for recording the noise voltages at the very low frequencies used.
- 537.311.33:621.396.822** 2040  
**Shot Noise in Semiconductors**—A. van der Ziel. (*Jour. Appl. Phys.*, vol. 24, pp. 222-223; Feb. 1953.) A calculation is made of the shot noise generated in a semiconductor by dc, assuming that the numbers of free electrons and holes fluctuate independently, and the average drift path is short compared with the length of the specimen. An examination is made of the special cases of electron conductors, mixed conductors, intrinsic semiconductors in which electrons and holes disappear by surface trapping, and intrinsic semiconductors in which electrons and holes disappear only by recombination.
- 538.221** 2041  
**Magnetic After-Effects associated with Initial Permeability and Barkhausen Jumps**—R. Feldtkeller and G. Sorger. (*Arch. elekt. Übertragung*, vol. 7, pp. 79-87; Feb. 1953.) A discussion of the Jordan, Richter and Ewing effects observed in relaxation processes in ferromagnetic materials; the first two are associated with the initial permeability and the last is associated with the Barkhausen jumps. The Richter and Ewing effects both depend on the diffusion of foreign atoms.
- 538.221** 2042  
**Applications and Properties of Ferroxcube**—(*Electronic Applic. Bull.*, vol. 13, p. 80; May 1952.) Correction to paper noted in 750 of March.
- 538.221** 2043  
**Ferrites**—A. Fairweather, F. F. Roberts and A. J. E. Welch. (*Rep. Progr. Phys.*, vol. 15, pp. 142-172; 1952.) A description is given of the physical and chemical structure of ferrites, and of their preparation, with an outline of Néel's theory of ferromagnetism and of the Kramers-Anderson theory of super-exchange spin coupling. Possible mechanisms which may account for the observed rather steep fall of permeability with increase of frequency, and for the associated energy absorption, are discussed. The dielectric properties of ferrites, of interest in HF applications, are considered. The observed very strong dispersion and absorption may be interpreted in terms of the inhomogeneous microphysical structure of the sintered material, which is known to be sensitive to the oxygen content and heat treatment. The very-low-frequency dielectric absorption may be due to adsorbed moisture. The semiconducting properties are discussed briefly. Over 150 references.
- 538.639:538.245** 2044  
**On the Temperature Dependency of Magneto-resistance Effect of Iron Single Crystal**—Y. Gondo and Z. Funatogawa. (*Jour. Phys. Soc. (Japan)*, vol. 7, pp. 41-43; Jan./Feb. 1952.)
- 538.652:548.55** 2045  
**Measurement of Magnetostriction in Single Crystals**—R. M. Bozorth and R. W. Hamming. (*Phys. Rev.*, vol. 89, pp. 865-869; Feb. 15, 1953.) A simplified procedure is given for determining the five magnetostriction constants of a ferromagnetic single crystal of the cubic type.
- 539.153:537.311.1** 2046  
**The Band Structure of Metals**—G. V. Raynor. (*Rep. Progr. Phys.*, vol. 15, pp. 173-248; 1952.) The development of the electron theory of metals is briefly reviewed and the electronic structures of a selection of monovalent and polyvalent metals are surveyed, Na and Cu being discussed in detail. Difficulties arising in connection with the calculation of electronic interactions, particularly in the case of divalent and trivalent metals, are discussed. The nature of transitional metals is considered in detail. The possibility of extending the theory to alloys is discussed, particularly for alloys based on Cu and on Ni. Over 80 references.
- 546.321.85-842:548.0(537+539.32)** 2047  
**The Properties of  $\text{KH}_2\text{PO}_4$  below the Curie Point**—H. M. Barkla and D. M. Finlayson. (*Phil. Mag.*, vol. 44, pp. 109-130; Feb. 1953.) Report of an investigation of the dielectric, piezoelectric and elastic properties of  $\text{KH}_2\text{PO}_4$  crystals at temperatures down to  $20^\circ\text{K}$ . A second transition occurs at a temperature about  $60^\circ$  below the Curie point ( $122^\circ\text{K}$ ), and marks the onset of a steep rise of coercive field with decreasing temperature. A qualitative domain theory is presented to account for the main features of the ferroelectric state in  $\text{KH}_2\text{PO}_4$ .
- 546.321.85-842:548.73** 2048  
**X-Ray Analysis of the Ferroelectric Transition in  $\text{KH}_2\text{PO}_4$** —B. C. Frazer and R. Pepinsky. (*Acta Cryst., Camb.*, vol. 6, part 3, pp. 273-285; March 10, 1953.) Report of detailed investigation of the tetragonal structure at  $4^\circ$  above the transition temperature of  $122^\circ\text{K}$ , and of the orthorhombic structure  $6^\circ$  below this temperature.
- 546.821:538.632** 2049  
**The Hall Effect in Titanium**—G. W. Scovill. (*Jour. Appl. Phys.*, vol. 24, pp. 226-227; Feb. 1953.) Preliminary report of measurements made by a dc method at a temperature of about  $100^\circ\text{C}$ .
- 547.476.3:537.226** 2050  
**The Effect of Electric Field on the Domain Structures in Rochelle Salt**—M. Marutake. (*Jour. Phys. Soc. (Japan)*, vol. 7, pp. 25-29; Jan./Feb. 1952.)
- 549.212:537** 2051  
**The Electrical Properties of Graphite**—G. H. Kinchin. (*Proc. Roy. Soc. A*, vol. 217, pp. 9-26; March 24, 1953.) Report of measurements made, over a wide range of temperatures, of the Hall coefficient and resistivity of a range of multicrystal graphites with different crystal sizes and of a single crystal of Travancore graphite.
- 621.315.61:621.793:669.21/.23** 2052  
**The Production and Testing of Precious-Metal Coatings on Insulating Materials**—A. Keil and G. Offner. (*Fernmeldelech. Z.*, vol. 6, pp. 73-77; Feb. 1953.) Methods of metallizing the surfaces of plastics and ceramics are outlined and suitable methods of assessing the properties of such coatings, particularly as regards resistivity, adhesion and soldering, are suggested.
- 621.315.612.4:546.431.824-31** 2053  
**Transition Energy and Volume Change at Three Transitions in Barium Titanate**—G. Shirane and A. Takeda. (*Jour. Phys. Soc. (Japan)*, vol. 7, pp. 1-4; Jan./Feb. 1952.)
- 621.315.616:547-128†** 2054  
**Silicones—and Insulation**—(*Elect. Times*, vol. 123, pp. 47-49; Jan. 8, 1953.) Illustrated note of applications of silicone rubber as sheathing and insulating tape.
- 621.315.616.1** 2055  
**Electrical Properties of Rubber**—J. Granier. (*Compt. Rend. Acad. Sci. (Paris)*, vol. 236, pp. 786-788; Feb. 23, 1953.) Experiments are described which show that the dc conductance and the dielectric constant and loss angle at 1 kc of rubber decrease considerably when the material is subjected to increasing compressional, tensile, or shearing forces with resulting distortion. When the material is compressed in a cavity which prevents distortion, little or no change is observed in the dielectric constant and loss angle. An explanation of these results is suggested.
- 778.37** 2056  
**Isotransport Camera for 100,000 Frames per Second**—C. D. Miller and A. Scharf. (*Jour. Soc. Mot. Pict. Telev. Eng.*, vol. 60, pp. 130-144; Feb. 1953.) Description of equipment developed by the Battelle Memorial Institute and available for loan to other research organizations.

## MATHEMATICS

**621.392.5:538.652:681.142** 2057  
**Magnetostrictive Sonic Delay Line**—H. Epstein and O. Stram. (*Rev. Sci. Instr.*, vol. 24, pp. 231-232; March 1953.) Description of a recirculating storage unit using a thin-wall Ni tube as the magnetostrictive element, with suitable transducer coils enclosed in ferrite cups whose length is adjusted to correspond to the half wavelength of a 600-kc vibration in the Ni tube. Experimental delay lines giving delays of  $100\mu\text{s}$  and  $800\mu\text{s}$  have been constructed. Operational characteristics are listed.

**681.142** 2058  
**High-Speed Product Integrator**—A. B. Macnee. (*Rev. Sci. Instr.*, vol. 24, pp. 207-211; March 1953.) A method of using a high-speed analogue computer to evaluate product integrals is described.

**681.142** 2059  
**Resistance Network Analog Computer**—(*Tech. News Bull. Nat. Bur. Stand.*, vol. 37, pp. 19-21; Feb. 1953.) Description of a computer of the type developed by Liebmann (1954 of 1950 and 2839 of 1952).

**681.142** 2060  
**The Electronic Discrete Variable Computer**—S. E. Gluck. (*Elec. Eng., N. Y.*, vol. 72, pp. 159-162; Feb. 1953.) Outline description of the EDVAC, a binary computer having a mercury-delay-line storage system of large capacity. See also 434 (Goodman) and 1357 (Gray) of 1952.

**681.142:538:221** 2061  
**Ferrites Speed Digital Computers**—D. R. Brown and E. Albers-Shoenberg. (*Electronics*, vol. 26, pp. 146-149; April 1953.) The use of ferrite toroids in storage units of the matrix type [2258 of 1952] (Papian) leads to increased speed and reliability of operation. Differences in the hysteresis curves required for storage and for switching purposes are discussed. A pulse method of testing the toroids is described. A particular Mg ferrite (MF-1118) used at the M.I.T. has a saturation flux density of 2000 gauss and a coercivity of 1.5 oersteds.

## MEASUREMENTS AND TEST GEAR

**535.32:538.56.029.64** 2062  
**The Refractive Indexes of Water Vapour, Air, Oxygen, Nitrogen, Hydrogen, Deuterium and Helium**—L. Essen. (*Proc. Phys. Soc. (London)*, vol. 66, pp. 189-193; March 1953.) The method described by Essen and Froome (1707 of 1951) was used in measurements at 9.2 kmc.

The results for water vapour, air, O<sub>2</sub> and N<sub>2</sub> agree with the values previously found at 24 kmc. The values for H<sub>2</sub> and D<sub>2</sub> are respectively 2% and 3% higher than the calculated values of Ishiguro *et al.* (*Proc. Phys. Soc. (London)*, vol. 65, pp. 178-187; March 1, 1952.)

621.3.018.41(083.74) 2063

**The Microwave Frequency Standard**—L. J. Rueger and A. E. Wilson. (*Radio & Telev. News, Radio-Electronic Eng. Sec.*, vol. 49, pp. 5-7, 41; March 1953.) An account is given of standardized equipment at the National Bureau of Standards for providing a calibration service for frequencies from 300 mc to 40 kmc, and of developmental equipment to extend the range to 75 kmc. The standard microwave frequencies are derived directly from one of the stable 100-kc crystal oscillators maintained by the N.B.S. Harmonic frequencies at 10-mc intervals are provided up to 5 kmc, at 50-mc intervals to 25 kmc, and at 250-mc intervals to 40 kmc, the gaps being bridged by means of a precision variable-frequency oscillator. Frequency meters are calibrated under conditions as close as possible to those of normal use. Details are given of the methods adopted.

621.3.018.41(083.741.): [621.314.7+621.396.611.21] 2064

**Precision Transistor Oscillator**—(*Tech. News Bull. Nat. Bur. Stand.*, vol. 37, pp. 17-19; Feb. 1953.) A frequency standard contained in a tube of length 7 in. and diameter 1½ in. is described. It comprises an oscillator using a Type-2517 junction transistor, a high-precision 100-kc GT-cut quartz-crystal unit [see Griffin, 1083 of April] and a long-life Hg cell. The transistor in an earthed-emitter circuit produces an output of 0.8V across a tuned circuit connected to the collector electrode. The crystal driving current is taken from the junction of two capacitors forming an attenuator between the collector and earth. Performance is comparable to that of a standard valve oscillator. (For another account, see *Electronics*, vol. 26, pp. 206, 214; May 1953.)

621.317.32.087.4 2065

**The Suitability of the "Fixed Level" Recording Method for Propagation Research**—G. Borč and W. Rappaport. (*Fernmeldetechn. Z.*, vol. 6, pp. 33-36; Jan. 1953.) The design of an u.s.w. field-strength recorder is outlined. Its principle is that described by Ferrari (*A.E.G. Mitt.*, vol. 41, pp. 299-302; Nov./Dec. 1951), a pulse being generated whenever the integral of the measured quantity over a specified time reaches a fixed level. The average interval between pulses is inversely proportional to the mean amplitude of the measured quantity. A method of evaluating the maximum error is illustrated. By means of a subsidiary relay-operated circuit, the number and duration of short-period fluctuations above and below a fixed level can be recorded.

621.317.335.3:537.226.2/3 2066

**A Standing-Wave Method for Measuring Electromagnetic Absorption in Polar Liquids at Frequencies of the Order  $3 \times 10^9$  cps**—V. I. Little. (*Proc. Phys. Soc. (London)*, vol. 66, pp. 175-184; March 1, 1953.) Description of a simple method, with typical results for the absorption coefficient and dielectric constant of water and of dioxan with small admixtures of water and of ethyl alcohol.

621.317.335.3.029.64 2067

**New Method of Measurement of the Complex Dielectric Constant of Solids and Liquids at Centimeter Wavelengths**—J. Le Bot and S. Le Montagner. (*Compt. Rend. Acad. Sci. (Paris)*, vol. 236, p. 469-471; Feb. 2, 1953.) A Method is described which requires only very small quantities of the material under test. Solid samples in the form of rods, or liquid samples contained in thin-walled glass tubes are arranged as shunt elements transverse to the larger sides of a rectangular waveguide. Using a short-circuited waveguide section and fixed

detector, the positions of a movable piston are found for minimum readings with and without the sample. From the piston displacement and the values of the minima the admittance of the shunt is determined and hence, by means of simple formulas, the dielectric constant of the sample is calculated.

621.317.335.3.029.64 2068

**Results of Measurements of Dielectric Constants at 9500 mc by a New Method**—S. Le Montagner and J. Le Bot. (*Compt. Rend. Acad. Sci. (Paris)*, vol. 236, pp. 593-594; Feb. 9, 1953.) Using the method previously described (2067 above, Le Bot and Le Montagner) measurements were made on polyethylene, plexiglas and nonpolar and polar liquids, including water. Results are tabulated and compared with figures obtained by other workers. The sensitivity of the method is such that the addition of even 1% of water to pure dioxan is clearly detectable.

621.317.335.3.029.64 2069

**The Theory of Measurements of Dielectric Constants at Centimeter Wavelengths**—N. V. Kotosonov. (*Zh. Tekh. Fiz.*, vol. 22, pp. 530-536; March 1952.) A general formula (6) is derived for the reflection coefficient of a two-layer dielectric filling a waveguide. From this, assuming that the second layer is air, another formula (7) is derived for the reflection coefficient for any position of the sample in the waveguide. Two methods for measuring the dielectric constant of layers of liquid and solid dielectrics are proposed and optimum conditions of measurement are established.

621.317.336.015.7:621.315.212 2070

**The Response to Television and Testing Pulses of Cables with Nonuniform Characteristic Impedance**—H. Kaden. (*Arch. elekt. Übertragung*, vol. 7, pp. 157-162, 191-198; March/April 1953.) The effect of the nonuniformities is that the cable output corresponding to a step-voltage input is distorted into a tailing-off form. The tail is due to (a) double internal reflections and (b) reflections at the cable ends in combination with single internal reflections. Effect (a) is proportional to the product of the nonuniformity function and its second derivative; it varies linearly with time for short cables and exponentially for long cables. Effect (b) depends on the first derivative of the nonuniformity function; it varies as the square root of the time for short cables and exponentially for long cables. Methods are described for measuring the nonuniformity function and its first and second derivatives; pulses of alternate polarity are used. The correlation range of the nonuniformities is determined; the smaller its value, the longer is the pulse tail. The relation between the autocorrelation function of the nonuniformities and the frequency spectrum of the reflected pulse is discussed in an appendix.

621.317.34.029.63.64 2071

**Measurement of the Centimeter-Wave Propagation Coefficient of Quadripoles**—W. Klein. (*Fernmeldetechn. Z.*, vol. 6, pp. 25-33; Jan. 1953.) Methods of measuring the attenuation and phase coefficients of linear passive quadripoles at centimeter wavelengths are described. Limits are defined within which the node-displacement method of Weissfloch (711 of 1943) is applicable to low-loss quadripoles. Transmission characteristics of a 4-cavity filter for 2.03 kmc, with a 30-mc pass band, are shown. The determination of input impedance from the s.w.r. and the open- and short-circuit impedances is illustrated, with reference to the Smith diagram for the above filter and for a travelling-wave-valve helix.

621.317.341:621.315.212.2 2072

**Measurement of the Attenuation of Coaxial Lines (from 1 to 4000 mc)**—H. Jassin. (*Câbles & Trans.*, vol. 7, pp. 16-27; Jan. 1953.) Three measurement techniques are described: (a) frequencies up to 40 mc, use of a HF bridge; (b) 50-400 mc, comparison of output powers of dif-

ferent lengths of identical line (for equal inputs); (c) above 500 mc, measurement of standing-wave ratios. Typical attenuation/frequency curves for rigid and for flexible lines are shown.

621.317.35 2073

**A Highly Selective Frequency-Spectrum Analyzer**—H. Lange. (*Nachr. Tech.*, vol. 2, pp. 471-473, 476; Dec. 1952.) Description and circuit details of an instrument for frequency analysis in the range 30 cps-20 kc. A frequency is selected by adjustment of a 60-80-kc Colpitts oscillator. The difference-frequency signal derived is applied successively to two differential bridge circuits each containing a 60-kc crystal. Amplitudes of 20 mV-100 V can be measured; at 1 V, maximum error is about 1%.

621.317.4.029.5:538.221 2074

**High-Frequency Calibration of Magnetic Materials**—(*Engineer (London)*, vol. 195, pp. 329-330; Feb. 27, 1953.) A brief account of National Bureau of Standards methods for determining the RF permeability and loss factor of ferrites and iron powders in the frequency range 50 kc-30 mc. The primary calibration standard is a nonmagnetic coaxial line of variable length and high dimensional accuracy; the magnetic characteristics of a sample are determined from measurements of the lengths of line required to give the same value of inductance with and without the sample inserted. A secondary standard rugged enough to be used in a factory production line is an RF permeameter with a transformer comprising a reference toroid acting as primary and a short coaxial line acting as secondary.

621.317.7:621.396.82 2075

**Aircraft Radio-Interference Measurements**—M. M. Newman, R. C. Schwantes and J. R. Stahmann. (*Elect. Eng., N. Y.*, vol. 72, pp. 36-40; Jan. 1953.) A double-beam high-speed oscillograph suitable for measurements of either atmospheric or man-made noise is described. One channel has a 10 mc amplifier, the other a 0.1-250 mc distributed-type wide-band amplifier. A 25-kV intensification potential is provided to facilitate photography of the trace. Two methods for more rapid noise analysis are briefly mentioned.

621.317.715 2076

**A Moving-Coil Galvanometer of Extreme Sensitivity**—K. Copeland, A. C. Downing and A. V. Hill. (*Jour. Sci. Instr.*, vol. 30, pp. 40-44; Feb. 1953.) The galvanometer movement is strongly overdamped, but the short natural period of the coil compensates for this, and full deflection is reached in a few seconds. The very light Cu coil, wound on a Cu frame, is suspended by flat CdCu wires kept taut by two flat-rolled springs, a construction facilitating careful balancing. Hill's photoelectric deflection amplification method (3175 of 1948) is used. Tests show that the mean of 7 readings is reasonably certain to be accurate to within  $4 \times 10^{-11}$  A under normal laboratory conditions.

621.317.715 2077

**The Brownian Fluctuations of a Coupled Galvanometer System**—A. V. Hill. (*Jour. Sci. Instr.*, vol. 30, pp. 44-45; Feb. 1953.) When two galvanometers are coupled by a photocell and amplifier combination, the fluctuations of the primary instrument are reduced by the inertia and damping of the second. A formula is derived for the rms value of the fluctuations observed on the second galvanometer and is applied to calculations for particular cases.

621.317.725 2078

**A High-Resistance Direct-Voltage Valve Voltmeter with a Measurement Range of -500 to +500V**—A. Ehmert and R. Mühleisen. (*Z. angew. Phys.*, vol. 5, pp. 43-47; Feb. 1953.) The instrument described has an input impedance of about  $5 \times 10^{12} \Omega$  and an input capacitance of about 0.3 pF; it is suitable for measurements of current down to about  $10^{-12}$  and determinations of capacitance down to 0.1 pF. The calibration



curve is practically linear, the slope being 125  $\mu\text{A}/500\text{V}$ . The equipment is mains operated, and is compensated against mains voltage fluctuations.

621.317.725:621.396.645 2079

**An Electrometer Valve Voltmeter of Wide Range**—A. W. Brewer. (*Jour. Sci. Instr.*, vol. 30, pp. 91–92; March 1953.) A dc voltmeter with a range of +500V and a rapid response suitable for atmospheric-electricity measurements is obtained by modifying Farmer's circuit (3337 of 1942) so that the electrometer valve and the associated ordinary valve both act as cathode followers, two further ordinary pentodes being used as "tail valves."

621.317.76.029.63:621.396.615.14 2080

**U.H.F. Grid-Dip Meter**—A. E. Hylas and W. V. Tyminski. (*Electronics*, vol. 26, pp. 175–177; April 1953.) Oscillators for the frequency range 390–1000 mc are discussed. This range lies above that of self-oscillation of the valve used, and is attained by means of series-capacitance tuning as described by Pettit (2452 of 1950). The capacitance is distributed to form a balanced circuit, thus providing a maximum-current point on the probe at a location which remains fixed as the oscillator is tuned.

621.317.799:621.396.822.029.64 2081

**Noise Comparator for Microwaves**—J. J. Freeman. (*Radio & Telev. News, Radio-Electronic Eng. Sec.*, vol. 49, pp. 11, 49; March 1953.) Secondary standards of noise power used at the National Bureau of Standards consist of klystrons or fluorescent tubes; these are calibrated in terms of the noise power of a matched load at a known temperature by means of a "noise bridge" which is a modified form of Dicke's radiometer (475 of 1947). The method of calibration is described, with details of the microwave switch, quarter-wave plate and waveguide transducer used for calibration at 9 kmc.

621.395.625(083.74):621.396.822 2082

**Standards on Sound Recording and Reproducing: Methods of Measurement of Noise, 1953**—(Proc. I.R.E., vol. 41, pp. 508–512; May 1953.) Standard 53 IRE 19 S1.

621.396.622.6:621.317.3 2083

**Testing U.H.F.-TV Mixer Crystals**—N. DeWolf. (*Electronics*, vol. 26, pp. 156–160; April 1953.) To evaluate the effect of Ge-crystal mixers on the over-all noise figure of receivers, the conversion loss and noise temperature must be determined. For simplicity, the wide-band conversion loss as defined by Torrey and Whitmer (2989 of 1948) is adopted. Laboratory equipment is described consisting essentially of an UHF receiver adapted for the measurement of conversion loss, noise temperature and RF and IF crystal admittances. Local-oscillator frequency is 900 mc and the IF is 30 mc. A Wollaston wire bolometer is used for the output-measurements. A complete set of measurements can be made in 5 min. Simpler AF methods for production testing are also described.

534.321.9.001.8:532.574 2084

**Electronic Flowmeter**—(*Tech. News Bull. Nat. Bur. Stand.*, vol. 37, pp. 30–31; Feb. 1953.) The principle of the instrument described is the phase comparison of ultrasonic waves before and after transmission over a fixed distance in a fluid. Transmitter and receiver are identical magnetostriction or piezoelectric transducers, and their connections to the phase meter are interchanged periodically by a rotary commutator or electronic switch. The difference between the two phase shifts is a measure of the flow velocity. Applications include the measurement of air currents and of slow or rapid flow of fluids in pipes.

534.321.9.001.8:538.652:534.232 2085

**A High-Frequency Reciprocating Drill**—E. A. Neppiras. (*Jour. Sci. Instr.*, vol. 30, pp. 72–73; March 1953.) A high-Q magnetostriction

transducer is used in conjunction with a step-up velocity transformer to produce intense vibrations at a low ultrasonic frequency, for drilling or cutting hard brittle materials. See also 1988 of 1952 (Kuris).

538.56.029.63:534.222.2 2086

**Reflection of Microwaves by Explosion-Wave Fronts**—B. Koch. (*Compt. Rend. Acad. Sci. (Paris)*, vol. 236, pp. 661–663; Feb. 16, 1953.) A sharp discontinuity of the electron density of the medium occurs at the front of an explosion wave. Measurements of the velocity of such a wave have been made by means of the Doppler effect for 23-cm waves reflected from the wave front. The mean value of the velocity thus determined is about 3.5% greater than that given by classical methods. A possible explanation of the discrepancy is given.

621.316.7 2087

**Processes in Regulating Systems with Time Delay**—K. Kùpfmüller. (*Arch. elekt. Übertragung*, vol. 7, pp. 71–78; Feb. 1953.) An investigation is made of the processes consequent on a disturbance of equilibrium in static and astatic systems. Rules for optimum design are derived.

621.38.001.89:621.95 2088

**Electronic Prevention of Drill Breakage**—(*Engineering (London)*, vol. 175, pp. 278–279; Feb. 27, 1953.) To prevent breakages when drilling deep holes in Al, a device is used which reverses the drill when the torque exceeds a given amount. The torque-control unit consists essentially of an unbalanced Wheatstone-bridge circuit in which the galvanometer is replaced by the grid circuit of a valve.

621.384.6 2089

**Ion Optics in Long High-Voltage Accelerator Tubes**—M. M. Elkind. (*Rev. Sci. Instr.*, vol. 24, pp. 129–137; Feb. 1953.)

621.384.611 2090

**Phase Stability of the Microtron**—C. Henderson, F. F. Heymann and R. E. Jennings. (*Proc. Phys. Soc. (London)*, vol. 66, pp. 41–49; Jan. 1, 1953.) The permissible variation in energy or magnetic field for stable acceleration in an electron cyclotron is calculated and the results are discussed in relation to resonant-cavity design.

21.384.611/612 2091

**Perturbations in the Magnetic Deflector for Synchro-cyclotrons**—K. J. Le Couteur. (*Proc. Phys. Soc. (London)*, vol. 66, pp. 25–32; Jan. 1, 1953.)

621.384.612 2092

**The Proton Synchrotron at Birmingham University**—(*Engineer (London)*, vol. 195, pp. 271–274, 305–307; Feb. 10 and 27, 1953.) Outline description of design and construction. See also 700 of 1951 (Hibbard).

621.384.612 2093

**A 35-Million-Volt Synchrotron**—O. Wernholm. (*Ark. Fys.*, vol. 5, Parts 5/6, pp. 565–580; Oct. 26, 1952.) Description of the construction and operation at the Royal Institute of Technology, Sweden, of a synchrotron producing an electron beam with energies continuously variable from 3 to 35 MeV.

621.385.833 2094

**Potential and Field of a Cylindrical Electrostatic Lens with Three Slits**—M. Laudet. (*Cah. Phys.*, pp. 73–80; Jan. 1953.) Analysis for a system comprising three pairs of half-planes at different potentials.

621.385.833 2095

**An Electrostatic Single Lens permitting Rigorous Calculation**—P. Schiske. (*Nature (London)*, vol. 171, pp. 443–444; March 7, 1953.)

621.385.833 2096

**Determination of the Trajectory of an Electron by Successive Differentiations**—É. Du-

rand. (*Compt. Rend. Acad. Sci. (Paris)*, vol. 236, pp. 471–473; Feb. 2, 1953.)

621.385.833 2097

**Astigmatism of Electron Lenses**—S. Leisegang. (*Optik, Stuttgart*, vol. 10, pp. 5–14; 1953.)

621.385.833 2098

**Investigation of the Asymmetry of [electron] Lenses with Magnetic Pole-Pieces using Rays with Slightly Subtelescopic Paths [im schwach unterteleskopischen Strahlengang!]**—F. Lenz and M. Hahn. (*Optik, Stuttgart*, vol. 10, pp. 15–27; 1953.)

621.385.833 2099

**A Simple Approximate Formula for the Field Distribution along the Axis of Magnetic Electron Lenses with Unsaturated Pole-Pieces**—H. Bremner. (*Optik, Stuttgart*, vol. 10, pp. 1–4; 1953.)

621.385.833 2100

**The Adjustment of Spherically Corrected Electron-Optical Systems**—R. Seeliger. (*Optik, Stuttgart*, vol. 10, pp. 29–41; 1953.)

621.385.833 2101

**Special Construction Features of an Electrostatic [electron] Microscope for the Laboratory**—H. Bethge. (*Optik, Stuttgart*, vol. 10, pp. 137–142; 1953.)

621.385.833:538.221 2102

**Remanence in Soft-Iron Circuits of Magnetic Electron Lenses**—B. v. Borries, F. Lenz and G. Opfer. (*Optik, Stuttgart*, vol. 10, pp. 132–136; 1953.)

621.385.833:621.311.6 2103

**High-Frequency High-Voltage Equipment for [electron] Microscope with Intermediate Accelerator**—S. Panzer. (*Optik, Stuttgart*, vol. 10, pp. 107–111; 1953.)

621.387.42 2104

**Factors influencing the Life of Self-Quenching Counters**—S. S. Friedland and H. S. Katzenstein. (*Rev. Sci. Instr.*, vol. 24, pp. 109–112; Feb. 1953.)

621.387.424 2105

**Ethylene and Ethyl Alcohol as Quenching Agents in External-Cathode Geiger Counters**—R. L. Chasson and M. L. MacKnight. (*Rev. Sci. Instr.*, vol. 24, pp. 212–213; March 1953.)

621.387.424 2106

**Construction of Maze-Type Counters [with external cathode], and their Characteristics from 0° to 50° C**—R. Favre and C. Haenny. (*Helv. Phys. Acta*, vol. 26, pp. 53–64; Feb. 15, 1953. In French.)

621.387.464 2107

**A Method of Increasing the Effective Resolution of Scintillation Counters**—K. G. Standing and R. W. Peelle. (*Rev. Sci. Instr.*, vol. 24, pp. 193–195; March 1953.)

## PROPAGATION OF WAVES

538.566 2108

**Higher-Order Approximations in Ionospheric Wave Propagation**—C. O. Hines. (*Jour. Geophys. Res.*, vol. 58, pp. 95–98; March 1953.) Feinsein's results (2608 of 1950), though mathematically correct, are not directly applicable to the physical problem for which they were intended. Similar treatment, but assuming real solutions only, is here developed. Certain results previously obtained, in particular those concerning resonance, are found for certain orders of approximation, but the general validity of the approach is found to be doubtful.

621.391.3 2109

**The Fields of an Electric Dipole in a Semi-infinite Conducting Medium**—J. R. Wait and L. L. Campbell. (*Jour. Geophys. Res.*, vol. 58, pp. 21–28; March 1953.) Expressions for the electric and magnetic fields at all points inside the conductor are developed in terms of Thom-

son's functions, the approximations made implying frequencies  $< 100$  kc and observation of the fields at distances much less than the free-space wavelength. Curves are shown plotting each field against a parameter involving conductivity, angular frequency and radial distance from the source. An example for for 30-kc propagation in sea water is worked out.

621.396.11 2110

**Ionospheric Storm-Warning Services. Assessment of their Value**—C. M. Minnis. (*Wireless Eng.*, vol. 30, pp. 103–108; May 1953.) It is suggested that the usefulness of a set of forecasts should be measured in terms of their economic value for a communication system. A figure of merit is derived which expresses the increase in economic value resulting from use of a set of forecasts. This figure includes a parameter representing the effects of ionospheric disturbances and depending also on the type of system operated and on the geographic location of the circuit; its value is unity for a perfect set of forecasts.

621.396.11 2111

**Theoretical Curves for Resonance Interaction between Electromagnetic Waves Incident Vertically on the Ionosphere**—M. Motzo. (*Nuovo Cim.*, vol. 9, pp. 213–219; March 1, 1952.) Bailey's theory of gyro-interaction (9 of 1939) is extended to the case of vertical incidence. The curves obtained in this case have only a single resonance peak.

621.396.11:530.145.6:537.311.33 2112

**Some Particular Features of Tropospheric Propagation and their Analogies in Wave Mechanics**—M. Ortusi. (*Ann. Radioelect.*, vol. 8, pp. 81–95; Jan. 1953.) Classical theory of tropospheric propagation is summarized, and the limits within which it is valid are discussed. The problem is shown to be mathematically analogous to that of determining particles trajectories in wave mechanics. The waves associated with the electron and hole aspects of the elementary particle are shown to correspond with particular cases of propagation in Gamow and Eckersley modes. The analogy is developed by comparing the form of a potential barrier separating solid media with the refractive-index profile for an atmospheric column including an inversion layer. The discussion indicates the manner in which holes are created inside barrier layers.

550.372.621.396.11 2113

**Effect of a Large Dielectric Constant on Ground-Wave Propagation**—J. R. Wait and L. L. Campbell. (*Canad. Jour. Phys.*, vol. 31, pp. 456–457; March 1953.) Curves are plotted showing variation of field strength with distance from transmitter for values of ground dielectric constant ranging from 2 to 200, assuming a value of  $0.1 \times 10^{-4}$  emu for the ground conductivity. Vertically polarized radiation of frequency 200 kc is assumed. At great distances from the transmitter, high values of dielectric constant give rise to great increase of field strength.

621.396.11:551.510.535 2114

**Magneto-ionic Multiple Splitting determined with the Method of Phase Integration**—W. Pfister. (*Jour. Geophys. Res.*, vol. 58, pp. 29–40; March 1953.) The method used involves a first-order W.K.B. approximation with an integration path in the complex plane. The propagation constant is represented on a four-sheeted Riemann surface corresponding to up-going and down-coming waves of ordinary and extraordinary types of polarization. The branch points connecting the sheets represent the reflection points or the coupling points. When suitable integration paths around the branch points are chosen, five fundamental magneto-ionic components are found. Numerical calculations for moderate magnetic latitude based on an ionosphere model with Chapman distribution of electrons and exponential decrease of collision frequency are made and the results

presented in curves showing virtual height and absorption for the five components found.

621.396.11:551.510.535 2115

**Ionosphere Critical Frequencies at Oblique Incidence**—H. Poverlein. (*Z. angew. Phys.*, vol. 5, pp. 15–19; Jan. 1953.) The dependence of muf on the inclination of the geomagnetic field and on the direction of wave propagation is investigated on the basis of previously prepared graphs showing (a) the ratio of critical frequency at vertical incidence to that at oblique incidence, as a function of angle of incidence, and (b) the ratio of critical frequency without magnetic field (identical with that of the ordinary ray in the E-W plane) to that of the ordinary ray in the plane of the magnetic meridian, also as a function of the angle of incidence. For low frequencies (0.75 mc) the latter ratio has a rather high value at the magnetic equator.

621.396.11.029.55 2116

**Observations at Calcutta of Pulses Transmitted from Delhi**—S. S. Baral and A. K. Saha. (*Indian Jour. Phys.*, vol. 26, pp. 521–538; Nov. 1952.) An account of observations during November 1950 and May–June 1951 of transmissions at frequencies of 17.74 and 21.7 mc. Possible modes of propagation are discussed; it is concluded that the signals are received by single reflection from the  $F_2$  layer and that multiple reflections from the  $F_2$  layer or single reflections from the E and  $F_1$  layers are not involved. The signal attenuation in the Delhi-Calcutta path is estimated and the results are tabulated. Statistical analysis of the fluctuations of the received signals indicates greater stability for the lower ordinary ray than for the upper ordinary (Pedersen) ray.

621.396.11.029.55 2117

**Extended-Range Radio Transmission by Oblique Reflection from Meteoric Ionization**—O. G. Villard, Jr., A. M. Peterson, L. A. Manning and V. R. Eshleman. (*Jour. Geophys. Res.*, vol. 58, pp. 83–93; March 1953.) Tests show that communication can be maintained between low-power stations approximately 1200 km apart at frequencies around 14 mc when no detectable F-, E- or sporadic-E-layer reflections are taking place. The average signal level is 10 db above noise level, and the signal appears to come from the direction of the transmitter, a continual small shift suggesting that there is no single point of reflection. Tests involving three transmission paths of differing lengths were made to determine total duration of discernible meteor-trail echoes. Results showed increased echo durations over oblique paths and thus support the theory that the signals are obliquely reflected from diffuse meteor trails.

621.396.11.029.62/.63 2118

**Graphs relating to the Propagation of Ultra-short Waves between Points within Visible Range**—L. Sacco. (*Poste e Telecomunicazioni*, vol. 21, pp. 55–71; Feb. 1953.) Various graphs are presented for facilitating design calculations for usw and microwave links, and for determining the best wavelength from the point of view of efficiency and stability of operation in relation to meteorological and geographical factors.

621.396.11.029.62:551.510.535 2119

**Scattering of 56-mc Radio Waves from the Lower Ionosphere**—P. A. Forsyth, B. W. Currie and F. E. Vawter. (*Nature (London)*, vol. 171, pp. 352–353; Feb. 21, 1953.) Radar records made during 1952 at Saskatoon show persistent scatter echoes with a diurnal and seasonal variation. Similar observations at Ottawa by McKinley and Millman on 33 mc are also mentioned (see 2000 above.)

621.396.812.3 2120

**Some Studies on Random Fading Characteristics**—R. B. Banerji. (*Proc. Phys. Soc. (London)*, vol. 66, pp. 105–114; Feb. 1, 1953.) Critical examination of the theory of random signals reflected from the ionosphere indicates

that the velocity distribution of fading is independent of the power spectrum of the reflected wave. The effect produced on the velocity distribution of fading by superposing a steady signal on a randomly fading wave is found to be small, resulting in only a very slight increase of the velocity of fading. An alternative method is given for determining the autocorrelation function of the fading pattern, from which the power spectrum of the reflected wave can be derived by inverse Fourier transformation. This provides an alternative method of determining the velocity of drift of ionospheric irregularities.

## RECEPTION

621.396.62 2121

**The Design of a Comparator A.M./F.M. Broadcast Receiver**—F. H. Beaumont. (*Jour. Brit. Inst. Radio Eng.*, vol. 13, pp. 131–148; March 1953.) Discussion of the design of a superheterodyne receiver to meet a specification drawn up by the BBC for making subjective comparisons of AM and FM transmissions in the frequency band 87.5–95 mc. The choice of circuits for RF amplifier, frequency changes, IF amplifier, detector, discriminator, noise limiters and AF stages is dealt with in detail.

621.396.62:621.396.664 2122

**An Automatic-Scanning Receiver for Radio Monitoring**—F. J. M. Laver, F. M. Billinghurst and F. J. Lee. (*P. O. Elect. Eng. Jour.*, vol. 45, Part 4, pp. 149–153; Jan. 1953.) The tuning frequency of a sensitive communication receiver is swept over a predetermined band of width up to 1 mc once every two minutes by means of a drive unit mechanically coupled to the tuning spindle. A continuous permanent record is obtained on electrosensitive paper of all signals received above a given strength in any desired frequency band between 4 and 27.5 mc.

621.396.62:621.396.812 2123

**Highly Stable Receiver for Space Waves**—G. Bartels. (*Nachr. Tech.*, vol. 3, pp. 28–29; Jan. 1953.) For investigations of the lower ionosphere, field-strength measurements are made on long-wave transmissions over paths of some hundreds of kilometers. A simple 4-valve receiver is used comprising HF stage, mixer with quartz-controlled oscillator, IF amplifier and crystal detector, and dc valve voltmeter bridge with recording instrument. The sensitivity is about 0.3 mV/m for full-scale deflection of a 1 mA/150 mV instrument.

621.396.621:621.396.822:519.272 2124

**The Detection of Weak Signals by Correlation Methods**—P. Rudnick. (*Jour. Appl. Phys.*, vol. 24, pp. 128–131; Feb. 1953.) Comparison of an autocorrelation system with a conventional detection system comprising band-pass filter, rectifier and low-pass filter indicates that for the same detection threshold the former system has to be far more complex. An alternative system involving multiplication of the incoming signal by a local sinusoidal signal is shown to be closely parallel to the conventional system.

621.396.621.029.55:621.396.822 2125

**Dependence of the Signal/Noise Ratio of Short-Wave Receivers on the Input Voltage**—K. Fischer. (*Telefunken Ztg.*, vol. 26, pp. 43–48; Jan. 1953.) In receivers with agc it is preferable, so far as signal/noise ratio is concerned, for the gain control to be effected in the later stages, but from the point of view of cross modulation the regulation should be effected at the receiver input. In order to determine the best compromise between these conflicting requirements, experiments were carried out with circuit arrangements in which the gain control could be applied to different groups of valves. With such arrangements cross-modulation can be reduced with an accompanying reduction of the signal/noise ratio, or the latter increased at the expense of cross-modulation sensitivity, so

that the optimum circuit for particular conditions can be adopted.

621.396.621.54 2126  
**Problems concerning Tracking Calculations in the Superheterodyne**—J. Mohrmann. (*Funk u. Ton*, vol. 7, pp. 1-9; Jan. 1953.) Critical discussion of tracking methods, underlining errors and omissions involved. See also 2323 of 1952.

621.396.621.54:621.396.822 2127  
**Noise Factor and its Relation to the Sensitivity of a Superheterodyne Receiver with Crystal Mixer**—E. Willwacher. (*Telefunken Ztg*, vol. 26, pp. 33-42; Jan. 1953.) Noise factor is defined and a formula is derived for the noise factor of a series arrangement of  $n$  quadripoles, each of which may add to the input noise. Analysis is presented for a mixer stage, an equivalent circuit being utilized. The results enable the optimum sensitivity of a superheterodyne receiver to be calculated. Numerical calculations are in good agreement with experimental values.

621.396.622.6:621.317.3 2128  
**Testing U.H.F.-TV Mixer Crystals**—De-Wolf. (See 2083.)

621.396.622.71 2129  
**Calculation of the Efficiency and Damping of Diode Detectors**—H. H. van Abbe. (*Electronic Applic. Bull.*, vol. 13, pp. 65-71; May 1952.) See 1195 of April.

621.396.662.029.63 2130  
**Automatic Tuning Devices in Microwave Receivers**—G. Voigt. (*NachrTech.*, vol. 2, pp. 456-459; Dec. 1952.) The principles of an automatic system are described whereby the mean IF is maintained at the center frequency of the demodulation characteristic. The control voltage is derived from the dc component of the discriminator. Methods of correcting for frequency fluctuations (a) up to  $\pm 250$  kc, (b) up to 0.5-1 mc, are outlined.

621.396.828 2131  
**Eliminating Interference caused by Railway Systems fed with Single-Phase Current at 15 kV**—J. Meyer de Stadelhofen. (*Tech. Mitt. Schweiz. Teleph Verw.*, vol. 31, pp. 33-52; Feb. 1, 1953. In French.) Report of investigations made by the Swiss Post Office and Swiss Railways to determine the extent of radio interference caused by the electric traction system and to find means for reducing it. As regards the Sottens, Beromünster and Monte Ceneri stations, operating in the frequency range 500-800 kc, the interference can be reduced to 1/10-1/30 of its original value by simple means.

621.396.828 2132  
**A "Codan" for A.M. Receivers**—J. B. Rudd. (*Proc. I.R.E. (Australia)*, vol. 14, pp. 33-40; Feb. 1953.) The "Codan" (carrier-operated-devices-anti-noise) is an auxiliary circuit device which selects a wanted carrier out of noise at an IF stage by means of a narrow-band filter and operates a relay to open the audio circuit. It can operate with signal/noise ratios  $> 1$ . A practical unit is described which uses a double-heterodyne process and a band-pass delay line to overcome the effects of frequency drift. Performance figures are given.

621.396.828:621.327.43 2133  
**Suppression of Radio Interference from Fluorescent Lamps over the Frequency Range 150 kc-1.5 mc**—J. Meyer de Stadelhofen. (*Tech. Mitt. Schweiz. Telegr.-Teleph Verw.*, vol. 30, pp. 239-248; Aug. 1, 1952. In French and German.) RF processes in fluorescent-lamp circuits are analyzed. For satisfactory suppression of interference, both a mains filter and a screen round the tube are essential. The ballast coil should be arranged symmetrically and should have low-capacitance windings. Measurement results indicate that interference can be reduced to a tenth of its original value, even in unfavorable circumstances, using simple means.

## STATIONS AND COMMUNICATION SYSTEMS

621.39.001.11 2134  
**Symposium on Information Theory, London, September 1950**—(*Trans. I.R.E.*, PGIT-1, 208 pp.; Feb. 1953.) Full report of the proceedings at the symposium noted in 984 of 1951 (Jackson).

621.39.001.11 2135  
**The Information Content of an Electromagnetic Signal**—D. Gabor. (*Arch. elekt. Übertragung*, vol. 7, pp. 95-99; Feb. 1953.) The amount of information that can be extracted from the signal by means of a valve is limited by (a) spontaneous fluctuations of the signal, (b) shot effect, and (c) a phenomenon resulting from the quantum nature of the em field, in accordance with which an electron interchanging energy with the signal field affects the phase of the field by an indeterminate amount, even when the resultant energy exchange is zero. The amount of information obtainable by simultaneous measurement of amplitude and phase is thus of an order no greater than would be obtained by means of an ideal photon counter, which is insensitive to phase changes. See also 208 of 1951.

621.39.001.11 2136  
**Optimum Linear Shaping and Filtering Networks**—R. S. Berkowitz. (*Proc. I.R.E.*, vol. 41, pp. 532-537; May 1953.) Analysis is made to derive the optimum transfer characteristics for the transmitter and receiver of a linear communication system, assuming power levels and over-all distortion to be fixed. Formulas are derived based on two different criteria, namely (a) the mean-square value of the receiver-output noise component, and (b) the probability that the receiver-output-noise component exceeds a given value at least once during a given observation period. The choice of criterion appropriate in a particular case depends on the mechanism by which the receiver output is converted into information.

621.392.001.11 2137  
**Analytical Signals with Limited Spectrum: Part 2**—J. A. Ville. (*Câbles & Trans.*, vol. 7, pp. 44-53; Jan. 1953.) Applications of the theory developed previously (1020 of 1950) are made to the determination of the relation between phase change and attenuation in a linear network as a function of frequency and to analysis of the limiting distortion compensation practicable in the presence of noise. The synthesis of a signal by superposition of  $\cos^2$ -type signals (2933 of 1951) is related to the problem of resolution of a signal by means of Shannon's formula; the synthesis can be simplified by referring signals of the  $\sin t/t$  type to  $\cos^2$ -type signals by suitable regrouping of terms. See also 1177 of April (Jouguet).

621.394.324 2138  
**Progress in Teleprinter Technique**—K. Reche. (*Elektrotech. Z., Edn. A*, vol. 74, pp. 4-10; Jan. 1, 1953.) Recent developments resulting in faster, more certain and more economical operation are described, with details of typical equipment.

621.396.029.6:621.396.8:519.2 2139  
**Problems of U.S.W. Coverage**—F. von Rautenfeld and H. W. Fastert. (*Tech. Hausmitt. NordwDtsch. Rdfunks*, vol. 5, pp. 9-17; Jan./Feb. 1953.) Methods previously considered for determining the effective service area of a vhf transmitter [213—Gressmann and Kaltbeitzler, and 214—Grosskopf, of January] are illustrated by detailed calculations for the fm transmitters at Lingen and Nordhelle, 156 km apart, for both co-channel and adjacent-channel operation. See also 197 of January (Bangen and Fastert).

621.396.43+621.396.65:621.397.26 2140  
**The State of Development of Directional Radio Equipment and the Planning of Directional Radio Links in the German Federal Re-**

public—K. O. Schmidt. (*Fernmeldetech. Z.*, vol. 6, pp. 51-58; Feb. 1953.) Illustrated review of features of television relay equipment and multichannel fm and ppm telephony systems.

621.396.619.13:621.396.41 2141  
**Calculation of the Distortion of a Frequency-Modulated Wave**—J. P. Vasseur. (*Ann. Radioelect.*, vol. 8, pp. 20-35; Jan. 1953.) Formulas are derived which are applicable for calculating both the distortion due to variation with frequency of the delay produced by an amplifier, and that due to the superposition on the main signal of echo signals caused by reflection in aerial feeders, etc. The analysis applies to both low and high modulation rates and to both single-frequency and composite signals. In multiplex systems frequency distortion may give rise to cross-talk; a formula due to Lewin (986 of 1951) is used to calculate the magnitude of this effect for the case of slow modulation.

621.396.619.16 2142  
**Pulse Distributors**—H. Oberbeck. (*Telefunken Ztg*, vol. 26, pp. 23-32; Jan. 1953.) In multichannel PM systems, different types of equipment for distributing the pulses to the various channels are required according to the type of modulator and demodulator used. Descriptions are given of the basic principles and special features of various types of pulse distributor, detailed accounts of which have been published previously.

621.396.65 2143  
**Radio-Telephone Link between Turkey and the West**—(*Engineer (London)*, vol. 195, p. 363; March 6, 1953.) Brief details of transmitter and receiver installations at Ankara providing a new radiotelephone link with Western Europe and the U.S.A., and an extension of existing radiotelegraph facilities.

621.396.65:621.396.41:621.396.619.24 2144  
**Single-Sideband Multichannel Operation of Short-Wave Point-to-Point Radio Links: Part 1—General Survey**—W. J. Bray and D. W. Morris. (*P. O. Elect. Eng. Jour.*, vol. 45, part 3, pp. 97-103; Oct. 1952.) The principles of ssb working are outlined, its advantages are pointed out and the basic techniques used for multichannel telegraphy and telephony are described.

621.396.65:621.396.61/62 2145  
**Single-Sideband Multichannel Operation of Short-Wave Point-to-Point Radio Links: Part 2**—Owen and Ewen. (See 2175.)

621.396.65:621.396.619.16 2146  
**Transmission Performance Figures for Directional PPM Systems**—P. Barkow. (*Fernmeldetech. Z.*, vol. 6, pp. 2-11; Jan. 1953.) Tests have been conducted on PPM systems operating in Germany. Performance figures are compared with CCIF specifications based on data for carrier-current systems. Noise figures of equipment for long-distance and local traffic are analyzed and the permissible noise levels throughout a communication chain are discussed in relation to transmitter power, receiver sensitivity and bandwidth.

621.396.65:621.397.6 2147  
**The Decimeter-Wave Beam Radio Equipment FREDA I**—Behling, Brühl and Willwacher. (See 2160.)

621.396.712+621.396.712:621.396.66 2148  
**Transmitting and Monitoring Stations of the NWDR**—(*Tech. Hausmitt. NordwDtsch. Rdfunks*, vol. 5, pp. 18-21; Jan./Feb. 1953.) A list is given of the NWDR medium-wave, sw, usw and television transmitting stations, as at 1st January 1953, with details of height above sea level, frequency, type of modulation, power, type of aerial, programme, and date of commencing operation. The equipment of the monitoring stations at Wittsmoor, Hamburg and Norderney is also listed.

621.396.72.029.62 2149  
Transmitter and Studio for Private USW Stations—Tetzner. (See 2178.)

### SUBSIDIARY APPARATUS

651-526 2150  
Synthesis of Servomechanisms by Root Locations—D. W. Russell and C. H. Weaver. (*Elec. Eng., N. Y.*, vol. 72, p. 41; Jan. 1953.) Summary only.

621.311.6 2151  
The Cockcroft-Walton Voltage-Multiplying Circuit—E. Everhart and P. Lorrain. (*Rev. Sci. Instr.*, vol. 24, pp. 221-226; March 1953.) The original circuit (see *Proc. Roy. Soc. A*, vol. 136, p. 619; 1932) is studied by considering it as a transmission line. Losses are examined, and formulas are developed for the voltage efficiency for a given size of capacitor and number of stages. Two modifications to improve voltage efficiency are discussed; the first is the use of a loading coil at the hv end of the line, the other is the inclusion of inductors in series with each of the capacitors.

621.311.62 2152  
Improved Variable Power Supply—W. Crevston. (*Radio & Telev. News*, vol. 49, pp. 42, 115; April 1953.) A modification of Walker's circuit (3562 of 1952) is described which provides direct-voltage outputs from 50 to 300 V, together with heater supplies. Inherent regulation is as good at 50 V as at 300 V.

621.314.632 2153  
Hermetically Sealed Magnesium Copper-Sulfide Rectifiers—M. Gamble. (*Elec. Mfg.*, vol. 48, p. 132; Oct. 1951.) Short note on the construction methods used for this type of rectifier, which has an operating range from  $-70^{\circ}$  to  $+200^{\circ}$  C or higher.

621.314.632/.634 2154  
Advanced Developments in Metallic Rectifiers—W. F. Bonner and F. J. Oliver. (*Elec. Mfg.*, vol. 48, pp. 128-133, 288; Oct. 1951.) Discussion of improvements relative to higher operating voltage, smaller size, operation at high and at low temperatures, and higher efficiency, largely resulting from requirements of the Services. Se rectifiers are particularly considered.

621.314.671 2155  
New Rectifier Tube for Extremely High Power and Voltage Levels—T. H. Rogers. (*Elec. Eng., N. Y.*, vol. 72, pp. 51-56; Jan. 1953.) This tube has a Th-W filament with catenary configuration and a cylindrical anode of Ta coated with W powder. Its characteristics are: anode dissipation rating, 1.5 kW; peak current rating, 10A; maximum peak inverse voltage, 110 kV.

621.315.616:621.355.2 2156  
Microporous Thermoplastic Separators for Lead Acid Batteries—(*Engineer (London)*, vol. 195, pp. 386-387; March 13, 1953.) Brief account of the manufacture and properties of "Porvic," a PVC sheet material. A similar account is given in *Plastics*, vol. 18, pp. 104-106; April 1953.

621.355.2 2157  
Addition Agents for Negative Plates of Lead-Acid Storage Batteries: Part 2—Pure Organic Compounds—E. J. Ritchie. (*Jour. Electrochem. Soc.*, vol. 100, pp. 53-59; Feb. 1953.) The best results were obtained with carbohydrates and some of the homologous phenolic compounds.

### TELEVISION AND PHOTOTELEGRAPHY

621.317.336.015.7:621.315.212 2158  
The Response to Television and Testing Pulses of Cables with Nonuniform Characteristic Impedance—Kaden. (See 2070.)

621.397.26:621.396.65]†621.396.43 2159  
The State of Development of Directional

Radio Equipment and the Planning of Directional Radio Links in the German Federal Republic—Schmidt. (See 2140.)

621.396.65 2160  
The Decimetre-Wave Beam Radio Equipment FREDA I—H. Behling, G. Brühl and E. Willwacher. (*Telefunken Zig.*, vol. 26, pp. 4-22; Jan. 1953.) The name FREDA signifies "frequenzmodulierte Dezimeteranlage." The equipment is designed for the Hamburg-Cologne link, the operating frequency being 1755  $\pm$  n.60 mc for the different channels. A description is given, with block diagrams, of the arrangements at the terminal transmitting and receiving stations and at a relay station. Details of the construction of the transmitter HF oscillator, mixer and amplifier stages are illustrated by photographs. Modulator and demodulator schematic circuit diagrams are given and performance data are summarized. Transmitter power is 5 W and the gain of the 3-m parabolic reflector, with dipole feed, relative to an elementary dipole, is 1060. Signal/noise ratio for the television channel is good.

621.397.335 2161  
Synchronization and Pulse Technique in Television—J. Günther. Correction slip inserted in Nov./Dec. issue of *Tech. Hausmitt. NordwDtsch. Rdfunks* gives a corrected diagram for Fig. 1 of paper abstracted in 1153 of April.

621.397.5:535.623 2162  
Recent Advances in Color Television—F. W. de Vriener. (*Tijdschr. ned. Radiogenoot.*, vol. 18, pp. 105-112; March 1953. In English.) Systems and apparatus developed in the USA are discussed.

621.397.61/.62 2163  
Storage and Picture-Difference Methods in Television Reception—F. Schröter. (*Arch. elekt. Übertragung*, vol. 7, pp. 63-70; Feb. 1953.) Use of a storage method at the receiver eliminates the need to transmit "redundant" information, i.e. signals corresponding to picture points which have undergone no change since the previous scan. A description is given of a particular type of storage tube using a 2-3- $\mu$  thick insulating target with a mesh-type anode on the scanned face and a mesh-type photocathode on the other face. Such a tube can provide a flicker-free picture of good brightness with a frame frequency of 16 per second. For use in converting pictures brought by line to a broadcasting station, the tube can be modified by including the photocathode in a Farnsworth-type dissector arrangement. Reception by this method combines satisfactorily with transmission by picture-difference methods using two-speed scanning, leading to a substantial reduction of the required bandwidth and transmitter power.

621.397.61 2164  
Television Camera Equipment of Advanced Design—L. L. Pourciau. (*Jour. Soc. Mot. Pict. Telev. Engs.*, vol. 60, pp. 166-180; Feb. 1953.) Descriptions are given of the servo circuits and mechanical design features of a television camera chain in which lens selection and focus are remotely controlled. Special emphasis is laid on convenient grouping of controls.

621.397.61:621.396.619.23 2165  
Spiral-Beam Tube Modulates 1 kW at UHF—Cuccia. (See 2188.)

621.397.61(494) 2166  
Justification of the Choice of the Döle as Site for a Television Transmitter—H. Laett and J. Dufour. (*Tech. Mitt. schweiz. Telegr.-TelephVerw.*, vol. 30, pp. 264-270; Sept. 1, 1952.) (In French.) See 246 of January (Laett).

621.397.611.2 2167  
Some New Aspects of the Construction and Application of the Image Iconoscope—H. Bruining. (*Le Vide*, vol. 7, pp. 1248-1255; Nov. 1952.) Recent improvements in design are de-

scribed, including the use of (a) a close-mesh grid in front of the photocathode to eliminate ion spots, (b) an L-type cathode in the electron gun. A focusing system providing variable magnification is discussed. Methods of target stabilization are noted.

621.397.62 2168  
Application of the ECL80 and EQ80 Tubes in Flywheel Synchronization Circuits—A. Boekhorst, P. D. van der Knapp and P. A. Neeteson. (*Electronic Appl. Bull.*, vol. 13, pp. 72-80; May 1952.) Full details are given of two practical arrangements. The first uses a Type-ECL80 triode-pentode in the phase discriminator circuit and effects comparison between pulses at incoming synchronizing frequency and local line-timebase frequency; the second uses a Type-EQ80 enneode and effects comparison between pulses at incoming synchronizing frequency and a sawtooth voltage at local line frequency. Additional features for suppressing the effects of interference on the synchronization are described.

621.397.62 2169  
Television Converter—C. A. Marshall. (*Wireless World*, vol. 59, pp. 223-226; May 1953.) Detailed description of a frequency-converter unit for use with nontunable television receivers. The particular values of circuit components given are for adapting a Channel-1 receiver (45mc vision, 41.5 mc sound) to Channel-3 reception (56.75 mc vision, 53.25 mc sound), but the general design is not restricted to these channels.

621.397.62:535.88 2170  
Special Problems in Television Large-Picture Installations—E. Schwartz. Correction slip inserted in the Nov./Dec. issue of *Tech. Hausmitt. NordwDtsch. Rdfunks* gives a corrected diagram for Fig. 1 of paper abstracted in 1168 of April.

621.397.621.2:621.385.832 2171  
Transfer Characteristics and Mu Factor of Picture Tubes—K. Schlesinger. (*Proc. I.R.E.*, vol. 41, pp. 528-532; May 1953.) The characteristics of television-receiver-tube guns are analyzed, taking account of the variation with grid voltage of the active cathode area. The value of gamma lies between 2.4 and 2.5 for various structures, while the value of the amplification factor is strongly influenced by changes in system parameters. The theoretical results were verified experimentally.

621.397.645.029.62 2172  
Fundamental Problems of H.F. and I.F. Amplifiers for TV Reception: Part 3—Feedback and Practical Considerations following on the Theory—Uitjens. (See 1954.)

621.397.82 2173  
Television Reception and Interference—W. Werner. (*Tech. Hausmitt. NordwDtsch. Rdfunks*, vol. 5, pp. 1-8; Jan./Feb. 1953.) Methods are suggested for reducing interference from cw signals which produce effects in the IF band, and also from impulse voltages. Radiation from the deflection system of the receiver or tube and from the receiver local oscillator is discussed, practical methods of measuring it are noted and means found effective in reducing it are described. Screening of the picture tube to reduce X-ray emission is also mentioned.

621.397.82 2174  
A Combining Unit for Superimposing Two Television Pictures on the Same Cathode-Ray Tube—D. Wray. (*P. O. Elec. Eng. Jour.*, vol. 45, Part 4, pp. 172-174; Jan. 1953.) Apparatus is described by means of which another waveform can be combined with the television signal without loss of synchronism. The effect on the picture of various types of interference can be simulated. The delay occurring in a long-distance looped television transmission system is evidenced by the displacement between the two pictures observed simultaneously when the signal generated at the transmitter is combined

with that received after travelling round the loop.

### TRANSMISSION

621.396.61/.62 2175

**Single-Sideband Multi-Channel Operation of Short-Wave Point-to-Point Radio Links: Part 2**—F. C. Owen and A. B. Ewen. (*P. O. Elect. Eng. Jour.*, vol. 45, Part 4, pp. 154–159; Jan. 1953.) The present equipment is an improved form of that previously described [2395 of 1948—Bray *et al.*]; it generates a low-power independent-sideband signal comprising two 6-kc channels, one on each side of a reduced-level 3.1-mc pilot carrier, suitable for application to the final modulator and power-amplifier stages of a sw transmitter. Alternatively a single-channel dsb signal can be generated. The associated monitor receiver is designed to accept signals from the transmitter drive unit at 3.1 mc or from the power-amplifier stages at radiation frequency. Part 1: 2144 above (Bray and Morris).

621.396.61.026.446.029.53:621.396.97 2176

**Megawatt A.M. Broadcast Transmitter**—J. O. Weldon. (*Tele-Tech.*, vol. 12, pp. 50–51; 116; Jan. 1953.) Illustrated description of equipment comprising two identical 500-kW transmitters whose outputs are combined to feed 1 MW to the aerial system. Four Machlett 250-kW Type-ML5682 tubes are used in the power amplifier of each transmitter, with four more in the output stage. Grid-bias modulation of the first Type-ML5682 tube is effected by means of four Type-805 tubes in parallel constituting the output stage of the AF amplifier. Operating characteristics in the frequency range 540–1600 kc were found consistently good.

621.396.619.11 2177

**The Impulse Modulator**—H. Moss. (*Jour. Brit. I.R.E.*, vol. 13, pp. 150–159; March 1953.) A highly linear amplitude modulator is achieved by using a negative-feedback circuit in which the tube anode current is arranged to be as nearly as possible proportional to the anode voltage and applying rectangular on-off switching pulses to the tube grid at carrier frequency, the modulating voltage being applied to the anode. The modulated RF output is taken from a resonant load in series with the tube. 100% depth of modulation can be obtained without requiring residual carrier neutralization. Harmonic distortion, modulation efficiency and linearity, and the influence of pulse mark/space ratio, are discussed.

621.396.72.029.62 2178

**Transmitter and Studio for Private USW Stations**—K. Tetzner. (*Funk-Technik (Berlin)*, vol. 8, pp. 132–133; March 1953.) Brief description of commercially produced equipment for use in local broadcasting stations owned by cultural institutions etc. in Germany. Transmitter powers range from 50 W to 250 W, the operating frequency being near 100 mc. Studio equipment to satisfy basic requirements is outlined.

### VALVES AND THERMIONICS

546.289:621.314.632 2179

**Evaporated Point-Contact Rectifiers**—E. G. Roka, C. H. Jackson and R. P. Ulrich. (*Jour. Appl. Phys.*, vol. 24, pp. 228–229; Feb. 1953.) A study has been made of the effect on a Ge rectifier of replacing the "whisker" contact by a contact comprising a very small area of evaporated silver. A significant improvement of the rectifying properties is observed. If the rectifier with whisker contact is subjected to alternating pulses of amplitude about 30V, the reverse resistance is thereby increased and the substitution of the evaporated contact then produces no improvement.

546.289:621.385.2 2180

**Negative Resistance in Germanium Diodes**—J. Kauke. (*Radio & Telev. News, Radio-Electronic Eng. Sec.*, vol. 49, pp. 8–10; April 1953.) Ge diodes show negative-resistance effects at values of the reverse voltage somewhat higher than the rated continuous-working

voltage. Applications of such effects in the production of a swatooth-wave oscillator, a sine-wave oscillator, a lock-in circuit and a voltage divider are described.

621.383.27:621.387.464 2181

**Photomultipliers Particularly Suitable for counting Scintillations**—É. Morilleau, H. Dor-mont and R. Champeix. (*Compt. Rend. Acad. Sci. (Paris)*, vol. 236, pp. 474–476; Feb. 2, 1953.) Various measures adopted to obtain improved performance are indicated. Curved reflector-type Cu dynodes coated with Cs are used. By focusing the emission from the cathode on to a very small first dynode a low value of background noise is achieved together with constant gain and optical screening of the cathode.

621.385:621.396.615.142 2182

**Influence of the Lorentz Force on Space-Charge Waves in Electron Beams**—J. Labus. (*Arch. elekt. Übertragung*, vol. 7, pp. 88–94; Feb. 1953.) For a beam of infinite diameter there are two possible values of phase velocity of the space-charge waves. When the formula is modified to take account of finite beam diameter, an infinite number of values of phase velocity are found. On taking into account the effect of the Lorentz force on the motion of the electrons, the formula obtained is very little different from that for the infinite-diameter beam, and gives values of phase velocity nearly independent of beam diameter and nearly equal.

621.385.029.6 2183

**Travelling-Wave Tubes**—R. Kompfner. (*Rep. Progr. Phys.*, vol. 15, pp. 275–327; 1952.) The historical development of traveling-wave tubes is described and a simple theory of their operation is outlined. More complete theory due to Pierce is sketched which permits calculation of the effects of attenuation, of non-synchronous velocities, and of space charge. Recent developments in the helix-type traveling-wave tube are described, such as Brillouin focusing of electron streams in axial magnetic field and noise characteristics of electron streams. Various types of traveling-wave tube are described and their special features are discussed. Wherever possible, attempts have been made to explain the modes of operation of the various types in simple physical terms. Over 140 references.

621.385.032.216:537.533.8 2184

**Changes in Secondary and Thermionic Emission from Barium Oxide during Electron Bombardment**—J. Woods and D. A. Wright. (*Brit. Jour. Appl. Phys.*, vol. 4, pp. 56–61; Feb. 1953.) Further experiments on BaO films (see 895 of March) are reported. Changes in secondary emission after 15–30 min bombardment depend on the film thickness and are due to a reduction process forming an excess of metal within the oxide. Thermionic emission also varies with thickness and there is a close correlation between the two types of emission in respect of decay and recovery effects.

621.385.1:621.396.822 2185

**Noise in Gas Discharges**—A. van der Ziel. (*Jour. Appl. Phys.*, vol. 24, pp. 223–224; Feb. 1953.) Comment on 2670 of 1950 (Parzen and Goldstein) indicating that to make the noise-power formula there derived valid for all frequencies the term corresponding to shot noise requires modification. The theory of shot noise in semiconductors (2040 above) is applied. The revised formula indicates that the shot noise is much greater at low than at high frequencies.

621.396.615.141.2 2186

**A 3 cm-Magnetron for Beacons**—G. A. Espersen and B. Arfin. (*Philips tech. Rev.*, vol. 14, pp. 87–94; Sept./Oct. 1952.) (See 3184 of 1951.)

621.396.615.141.2 2187

**New Magnetron Oscillator with Interdigital Circuit**—A. Leblond, O. Doehler and R.

Warnecke. (*C. R. Acad. Sci. (Paris)*, vol. 236, pp. 55–57; Jan. 5, 1953.) The oscillatory system of a multislot magnetron can be considered as a section of a line with periodic structure closed on itself [see 1543 of May—Leblond *et al.*]; with such a system, in order to avoid the sudden frequency jump on passing from one oscillation mode to another, the phase velocity of the fundamental wave of the delay line constituted by the oscillatory system should be of opposite sign to the group velocity, and the dispersion should be relatively low. A suitable interdigital structure satisfying these requirements is described with which a peak HF output of 300 kW on 11-cm wavelength has been obtained from a tube operated with peak anode voltage of 22 kV, peak anode current 26A and magnetic field 2,700 gauss.

621.396.619.23:621.397.61 2188

**Spiral-Beam Tube Modulates 1 kW at UHF**—C. L. Cuccia. (*Electronics*, vol. 26, pp. 130–134; April 1953.) A modified form of the electron-beam coupler tube previously described (2975 of 1949) is used as a television modulator in the 800 mc frequency range. Modulation is performed by means of five auxiliary electron beams in the output cavity; a 50-V modulator grid swing can control power output over a range of 98% of maximum (300W with a beam voltage of 750V). The device has good linearity, a bandwidth of 5 mc and a transfer efficiency of 50%.

621.396.622.63 2189

**Conductivity of and Flicker Effect in Crystal Detectors**—N. Nifontoff. (*Onde élect.*, vol. 33, pp. 58–61; Jan. 1953.) See 1037 of April and back references.

621.396.622.63:546.28 2190

**Silicon Crystal Detectors**—J. M. Mercier and R. P. Musson-Genon. (*Onde élect.*, vol. 33, pp. 40–57; Jan. 1953.) An account of the methods of manufacture of Si detectors adopted by the Compagnie Française Thomson-Houston and of their characteristics and use as mixers in uhf circuits. (See also, Mercier, 2070 of 1951.)

### MISCELLANEOUS

025.45:621.3 2191

**Work of the 3rd Meeting of the International Electrical Engineering UDC Committee and the 1st Meeting of the Telecommunications Subcommittee of the International Federation for Documentation**—C. Frachebourg. (*Tech. Mitt. schweiz. Telegr.-Teleph. Verw.*, vol. 31, pp. 30–31; Jan. 1953. In French.) Brief note of the proceedings, with proposed revised classifications for the sections on antennas and radar.

621.38/.39:[002+026+025.45 2192

**Radio and Electronic Engineering Literature**—(*J. Brit. I.R.E.*, vol. 13, pp. 65–75; Jan. 1953.) A report prepared by the Technical Committee of the British Institution of Radio Engineers as a guide to the main sources of information on modern developments including abstracting services, Government publications, library facilities, patents, etc. A brief explanation is given of the working of the Patent Office Library and of the UDC (Universal Decimal Classification) system as applied to radio and electronic engineering.

621.39(083.74/.75) 2193

**Standardization and Telecommunications**—R. Goret. (*Ann. Telecommun.*, vol. 8, pp. 11–18; Jan. 1953.) An account is given of the structure and operation of the commission set up in France in 1945 to study the standardization of telecommunications equipment. Specifications established by the commission are listed and discussed.

621.396 2194

**Radio Progress during 1952**—(Proc. I.R.E., vol. 41, pp. 452–507; May 1953.) A review including over 1000 references to world literature. Material is arranged under the headings indicated in 2404 of 1952, with additional sections on Feedback Control Systems and on Magnetics.